TH 1720

METALLOGENY AND ASSOCIATED ALTERATION OF GOLD OCCURRENCES, BOUSQUET TOWNSHIP, NORTHWESTERN QUEBEC

Documents complémentaires

Additional Files





Licence



License

Cette première page a été ajoutée
au document et ne fait pas partie du
rapport tel que soumis par les auteurs.

Énergie et Ressources naturelles
Québec

METALLOGENY AND ASSOCIATES ALTERATION OF GOLD OCCURRENCES BOUSQUET TOWNSHIP NORTHWESTERN QUEBEC

GILDAR J. ARSENEAU

~~1978~~ 1995

1H 1720

METALLOGENY AND ASSOCIATED ALTERATION OF GOLD OCCURRENCES, BOUSQUET TOWNSHIP NORTHWESTERN QUEBEC

Gildar J. Arseneau

QE
364.2
M37
A781
1995
QFO

T-4401

QE
364.2
M37
A481
1995
QFD

METALLOGENY AND ASSOCIATED ALTERATION OF GOLD OCCURRENCES, BOUSQUET TOWNSHIP, NORTHWESTERN QUEBEC

RESSOURCES NATURELLES
BIBLIOTHÈQUE
QUÉBEC

by

Gildar J. Arseneau

T-4401

A thesis submitted to the faculty and the Board of Trustees of the Colorado School of Mines in partial fulfillment of the requirements for the degree of Doctor of Philosophy (Geology).

Golden, Colorado

Date [illegible]

Signed: [illegible]
Gildar Joseph Arseneau

Approved: [illegible]
Dr. Richard W. Hutchinson
Thesis Advisor

Golden, Colorado

Date May 10, 1995

[illegible]
Dr. Roger M. Slatt
Professor and Head,
Department of Geology and
Geological Engineering

ABSTRACT

Gold mineralization in Bousquet Township of northwestern Quebec occurs in sheared Archean felsic to mafic volcanic and intrusive rocks of the Blake River Group. Eleven significant gold occurrences occur along a five kilometre strike length, four of the occurrences are presently being mined and the others remain sub-economic. Each occurrence is characterized by a specific host rock, ore type and alteration assemblage. Production from existing mines exceeds 5 million Troy ounces and present total reserves for the area are estimated at 4.3 million ounces. Gold mineralization occurs both as pyritic bodies and as quartz-dominated veins. Various previous studies have interpreted the gold mineralization to have originated by syngenetic, epigenetic syn-tectonic, epigenetic post-tectonic and multi-stage syngenetic followed by epigenetic overprinting processes.

The chemical characteristics of the rocks of the volcanic sequence exhibit many similarities to those of comparable rocks from modern day plate tectonic environments. Major element analyses of the Blake River Group volcanic rocks indicate bimodal volcanism similar to that associated with tensional tectonic environments, and their trace elemental and rare earth element characteristics are compatible with those of mafic rocks from back-arc basin environments. However, the tectonic discrimination diagrams for these rocks also suggest differences of unknown significance in tectonic regimes and mantle chemistry from Archean time to the present. Trace element ratio diagrams further distinguish subtle differences between rocks of units 2 and 6, therefore discounting an earlier interpretation of north facing stratigraphy on the southern limb of a major syncline in the southern part of the Blake River Group.

Alteration mineral assemblages associated with the eleven gold occurrences change from the base to the top of the volcanic sequence from iron and carbonate minerals at the

base to manganese-rich minerals at the top for occurrences hosted in mafic rocks, and from a quartz-sericite assemblage to an andalusite-muscovite assemblage for felsic hosted occurrences.

A detailed synthesis of the metallogeny of the Blake River Group in Bousquet Township, developed from this study, suggests that the generative hydrothermal system evolved through time along with the volcanic members of a cyclical volcanic succession. This evolutionary change progressed from a deep water exhalative system of unfocused discharge that predominated in mafic pillowed flows, upward to a shallow water system of focused discharge in poorly consolidated, felsic volcaniclastic debris. This prolonged hydrothermal system resulted in minor gold and pyrite enrichment in the base of the sequence and in the formation of auriferous massive sulfide deposits at the top. The presence of the poorly consolidated volcaniclastic debris or sediment was essential for the formation and preservation of the sulfide deposits on the sea floor. Progressive and prolonged "leaching" of the occurrences in the lower volcanic cycles by the continuing hydrothermal activity may, in part, account for the lower grade and size of the former when compared to those near the top of the sequence.

Metamorphism and deformation remobilized gold and base metals into discordant, cross-cutting auriferous-pyritic veins, and auriferous, millimetre-scale fractures that are important in most of the occurrences. Manganiferous garnet- and andalusite-bearing alteration assemblages associated with gold mineralization on the Bousquet property represent metamorphosed equivalents of prior, sea floor alteration of mafic and felsic rocks respectively. Paragenetic sequences at the Bousquet No. 2 Mine are indicative of plastic deformation and flowage of sulfide minerals under confining stress, and reflect late, superimposed metamorphic processes rather than primary genetic ones.

The economic gold concentrations in Bousquet Township resulted from multiple processes each acting at different times upon products of earlier processes during the prolonged volcanic and tectonic evolution of the volcanic rocks of the Blake River Group.

TABLE OF CONTENTS

Page

ABSTRACT iii

LIST OF FIGURES ix

LIST OF TABLES xiv

ACKNOWLEDGEMENTS xv

Chapter 1. INTRODUCTION 1

1.1 General Statement 1
1.2 Purpose and Objectives of Study 1
1.3 Location and Access 2
1.4 Physiography and Bedrock Exposure 2
1.5 Exploration and Mining History 4
1.6 Previous work 7
1.7 Method of Investigation 8

Chapter 2. REGIONAL GEOLOGY OF ABITIBI GREENSTONE BELT 9

2.1 Introduction 9
2.2 Stratigraphy 9
2.3 Structure 10
2.4 Metamorphism 10

Chapter 3. GEOLOGY OF STUDY AREA 14

3.1 Introduction 14
3.2 Kewagama Group 14
3.3 Blake River Group 16

3.3.1 Unit 1 16
3.3.2 Unit 2 17
3.3.3 Unit 3 17
3.3.4 Unit 4 22

3.3.5 Unit 5 26
3.3.6 Unit 6 30

3.4 Cadillac Group 30
3.5 Mooshla Intrusive Complex 32

3.5.1 Quartz Diorite 34
3.5.2 Porphyritic Quartz Diorite 34
3.5.3 Trondhjemite 38
3.5.4 Mafic Dikes 38

3.6 Diabase Dikes 42
3.7 Structure 42
3.8 Metamorphism 44

Chapter 4. GEOLOGY OF GOLD OCCURRENCES 50

4.1 Introduction 50
4.2 # 6 Occurrence 50
4.3 # 5 Occurrence 53
4.4 Westwood Occurrence 53
4.5 Doyon Mine Occurrence 54

4.5.1 Main Zone 56
4.5.2 # 1 Zone 56
4.5.3 West Zone 59

4.6 # 4 Occurrence 62
4.7 Warrenmac Occurrence 64
4.8 Bousquet No. 1 Mine Occurrence 64

4.8.1 # 3 Zone 68
4.8.2 # 2 Zone 73
4.8.3 # 1 Zone 74

4.9 Bousquet No. 2 Mine Occurrence 74

4.9.1 Massive Zone 75
4.9.2 Fringe Zone 79

4.10 Mooshla A Occurrence 83

4.11 Other Occurrences 83

Chapter 5. METAMORPHISM AND ALTERATION 84

5.1 Introduction 84
5.2 Alteration of Mafic Volcanic Host Rock 85

5.2.1 Chloritoid 85
5.2.2 Ankerite-Muscovite 86
5.2.3 Garnet 86

5.3 Alteration of Felsic Volcanic Host Rock 92

5.3.1 Quartz-Sericite 92
5.3.2 Andalusite-Muscovite 93

5.4 Alteration of Intrusive Host Rock. 94

5.4.1 Siliceous Core 94
5.4.2 Phyllic Alteration 95
5.4.3 Propylitic Alteration 95

5.5 Summary 101

Chapter 6. GEOCHEMISTRY OF BLAKE RIVER GROUP. 102

6.1 Introduction 102
6.2 Major Element Analyses 103
6.3 Trace Element Analyses 107
6.4 Rare Earth Element Analyses 115
6.5 Fluid Inclusion Data 119
6.6 Geochronology 122
6.7 Summary 122

Chapter 7. SYNTHESIS OF THE GENETIC EVOLUTION AND METALLOGENY OF BLAKE RIVER GROUP. 124

7.1 Introduction 124

7.2 Genetic Evolution of Blake River Group 125

7.2.1 Cycle 1 126
7.2.2 Cycle 2 127
7.2.3 Cycle 3 128
7.2.4 Mooshla Intrusion 130
7.2.5 Metamorphism 130
7.2.6 Deformation 131

7.3 Modern Analogues 133

7.4 Recommendations for Further Work 135

7.5 Recommendations for Exploration 135

Chapter 8. CONCLUSIONS 137

REFERENCES CITED 140

APPENDIX 1 Major Element Analyses of the Rocks of the Blake River Group 153

APPENDIX 2 Trace Element Analyses of the Rocks of the Blake River Group 161

APPENDIX 3 Electron Microprobe Analyses of Garnets from the Blake River Group 168

LIST OF FIGURES

Figure 1. Location Map 3

Figure 2. Location of mineralized zones on the Bousquet property 6

Figure 3. Structural setting of Blake River Group 12

Figure 4. Geology of Doyon and Bousquet properties 15

Figure 5. Photograph of pillow basalt from unit 1 18

Figure 6. AFM plot for the rocks of unit 1 19

Figure 7. Total alkali versus silica plot for the rocks of unit 1 20

Figure 8. AFM plot for the rocks of unit 2 21

Figure 9. Total alkali versus silica plot for the rocks of unit 2 21

Figure 10. Photograph of heterolithic blocky tuff member of unit 3 23

Figure 11. Photograph of blocky tuff member from north wall of Doyon pit 24

Figure 12. AFM plot for the rocks of unit 3 25

Figure 13. Total alkali versus silica plot for the rocks of unit 3 25

Figure 14. Photomicrograph of mylonitic texture of sericite schist of unit 4 27

Figure 15. AFM plot for the rocks of unit 4 28

Figure 16. Total alkali versus silica plot for the rocks of unit 4 28

Figure 17. AFM plot for the rocks of unit 5 29

Figure 18. Total alkali versus silica plot for the rocks of unit 5 29

Figure 19. AFM plot for the rocks of unit 6 31

Figure 20. Total alkali versus silica plot for the rocks of unit 6 31

Figure 21. CIPW normative classification of the rocks of the Mooshla intrusion 33

Figure 22. Modal classification of the rocks of the Mooshla intrusion 33

Figure 23. Photograph of spotted trondhjemite 36

Figure 24. Photograph of intrusive breccia between trondhjemite and porphyritic quartz diorite 37

Figure 25. Photomicrograph of mymerkitic texture in trondhjemite 39

Figure 26. Photomicrograph of sericite-filled fractures in trondhjemite 40

Figure 27. Photomicrograph of altered trondhjemite 41

Figure 28. Photomicrograph of post-deformational biotite in mafic dike of the Mooshla intrusion 43

Figure 29. Photomicrograph of kink crenulation of S_1 schistosity 45

Figure 30. Photomicrograph of epidote and calcite alteration in mafic rocks of the Blake River Group 47

Figure 31. Photomicrograph of large tabular andalusite porphyroblast partly altered to kaolinite and diaspore 48

Figure 32. P-T diagram of peak metamorphic conditions at the Bousquet No. 2 Mine 49

Figure 33. Schematic stratigraphic correlation diagram of rocks of the Blake River Group, Bousquet and Doyon properties 52

Figure 34. Photomicrograph of gold grain occurring with calcite and quartz 57

Figure 35. Photograph of irregular massive pyrite lenses in sericite schist of unit 4 58

Figure 36. Photomicrograph of recrystallized nematoblastic pyrite, # 1 zone, Doyon Mine 60

Figure 37. Photograph of narrow zoned quartz-pyrite vein in porphyritic quartz diorite 61

Figure 38. Photograph of massive pyrite vein in altered trondhjemite 63

Figure 39. Photograph of fine-grained-banded rock from # 4 occurrence on Bousquet Property 65

Figure 40. Photomicrograph of garnetiferous footwall rock from Warrenmac occurrence 66

Figure 41. Typical plan view of the orebody at the Bousquet No.1 Mine 69

Figure 42. Photograph of manganiferous garnet rock from Bousquet No. 1 Mine 71

Figure 43. Photomicrograph of altered andalusite porphyroblast from Bousquet No. 1 Mine 72

Figure 44. Simplified section view of massive zone at Bousquet No.2 Mine 76

Figure 45. Photograph of siliceous, pyrite-chalcopyrite stockwork from Massive zone 77

Figure 46. Photograph of upper contact of complex main massive sulfide body with hanging wall andalusite schist 78

Figure 47. Photograph of breccia from central portion of massive sulfide body 80

Figure 48. Photomicrograph of subhedral pyrite with interstitial bornite, chalcopyrite and gold 81

Figure 49. Typical plan view of Bousquet No.2 Mine 82

Figure 50. Photomicrograph of garnet from the footwall of the # 3 zone at the Bousquet No. 1 Mine 88

Figure 51. Photomicrograph of anhedral garnet from trondhjemite 89

Figure 52. Average FeO variation of garnet grains 90

Figure 53. Average MnO variation of garnet grains 90

Figure 54. FeO variation in garnet grains with 400 micron radii 91

Figure 55. MnO variation in garnet grains with 400 micron radii 91

Figure 56. Photomicrograph of rock from siliceous alteration core of trondhjemite 96

Figure 57. Photograph of phyllic alteration with pyrite veinlets 97

Figure 58. Photograph of altered quartz diorite 99

Figure 59. Photograph of blocky tuff member from unit 3 altered to chlorite and epidote 100

Figure 60. Histogram of silica content of the volcanic rocks of the Blake River Group 104

Figure 61. Major oxide variations plotted against silica for the volcanic rocks of the Blake River Group 105

Figure 62. Major oxide variations plotted against silica for the rocks of the Mooshla intrusion 106

Figure 63. Four oxide ratio-ratio diagram for the rocks of the Mooshla intrusion 108

Figure 64. Three oxide ratio-ratio diagram for the rocks of the Mooshla intrusion 108

Figure 65. Ti-Y-Zr diagram for basaltic rocks of the Blake River Group 110

Figure 66. Ti-Zr diagram for basaltic rocks of the Blake River Group 111

Figure 67. Ti-Y-Zr diagram of average values for basaltic rocks of the Blake River Group 113

Figure 68. Ti-Zr diagram of average values for basaltic rocks of the Blake River Group 113

Figure 69. Spidergram of average values for basaltic rocks of the Blake River Group 114

Figure 70. (Zr/Y)/Zr ratio for the felsic volcanic rocks of units 2 and 6 116

Figure 71. (Zr/Ti)/Ti ratio for the felsic volcanic rocks of units 2 and 6 116

Figure 72. Three element ratio-ratio diagram for the rocks of the Mooshla intrusion 117

Figure 73. Four element ratio-ratio diagram for the rocks of the Mooshla intrusion 117

Figure 74. Spidergram normalized to NMORB values for the rocks of the Mooshla intrusion 118

Figure 75. Chondrite normalized REE distribution of the basaltic rocks of the Blake River Group 120

LIST OF TABLES

Table 1. Production and mineral inventory of gold occurrences in Bousquet Township 5

Table 2. Volcanic stratigraphy of Southern Abitibi Belt 11

Table 3. Modal proportions (volume %) of minerals of the Mooshla Intrusive Complex 35

Table 4. Stratigraphic location of Gold occurrence with mineralized zones 51

Table 5. Total reserves of mineralized zones of the Doyon Mine 55

Table 6. Total reserves of mineralized zones of the Bousquet No. 1 Mine 67

ACKNOWLEDGEMENTS

The writer wishes to express his appreciation to the many individuals and organizations that have supported this project. I would like to thank my advisory committee, Dr. Richard Hutchinson, Dr. Graham Closs, Dr. Gregory Holden, Dr. John Emerick, and Dr. James McNeil. In particular, I would like to thank my advisor, Dr. Richard Hutchinson for organizing and supervising this study. Also special thanks are due to Phillip Walford for enduring the often tedious politics associated with the organization of this project. Thanks to Daniel Doucet, Marc Arpin, Andre Bourget of the Bousquet Complex and Lise Chenard and Christian Massicotte of the Doyon Mine for their help in organizing field support, access to the mines and stimulating geological discussions. Thanks to the geological technicians at Doyon for chauffeuring me through the underground workings. Thanks to John Drexler for his help in securing time on the microprobe at University of Colorado and for his supervision of the analyses.

Financial support of this research was provided by Lac Mineral Limited, now Barrick Gold Corporation, and a fellowship from the Dean of Research of the Colorado School of Mines, their help is gratefully acknowledged.

Finally, I thank my son Francis for ensuring that I was never late for class by waking at six every morning, and my wife Catherine for exceptional moral support and faith.

Chapter 1
INTRODUCTION

1.1 General Statement

Gold mineralization in Bousquet Township occurs in Archean felsic to mafic volcanic and intrusive rocks. Eleven significant gold occurrences occur along a five kilometre strike length, four of the occurrences are presently being mined and the others remain sub-economic at present gold prices. Each occurrence is hosted by a unique rock and alteration assemblage. The regional stratigraphic, tectonic and structural settings of the gold occurrences and their possible inter-relationships are not well determined. Genetic hypotheses for the economic gold concentrations in Bousquet Township include syngenetic, epithermal syn-tectonic, epithermal post-tectonic and multi-stage syngenetic with epigenetic overprinting processes.

1.2 Purpose and Objectives of Study

The purpose of this research is to investigate and determine the regional metallogenic relationships between the Bousquet No. 1, the Bousquet No. 2 and the Doyon gold mines and to resolve the controversy over the younging direction of the volcanic rocks of the Blake River Group in Bousquet Township in northwestern Quebec. Specifically, the study aims to describe the geology and alteration assemblages found at the Doyon mine, the Warrenmac and Westwood occurrences and incorporate the findings with previous studies carried out at the Dumagami Mine and at the Bousquet No. 1 and No. 2 mines in order to develop a comprehensive metallogenic synthesis for the district.

This study documents the stratigraphic relationships between the mineralized horizons that occur in Bousquet Township on the Bousquet and Doyon mining properties in order to determine whether any stratigraphic controls are partly responsible for the

location of the gold mineralization in the area.

The study also describes and compares the wall rocks and alteration at each gold occurrence in order to determine the most useful factors in recognizing new mineral deposits within Bousquet Township, and within similar greenstone environments.

1.3 Location and Access

The study area is located in Bousquet Township of northwestern Quebec, Canada. The area is approximately 600 kilometres north of Montreal on highway 117 and lies halfway between the towns of Rouyn-Noranda and Val D'Or. The map area occupies the northwestern part of Bousquet Township and is bounded to the east by highway 395, to the west by highway 393, and to the north and south by the Doyon and Bousquet property limits (Figure 1). The study area is limited to the Bousquet and Doyon mining properties formerly held by Lac Minerals Limited which is now controlled by Barrick Gold Corporation of Toronto.

Access to the study area is by paved highway for the perimeter of the area and by dirt roads maintained by the property owners. Most of the study area is covered with a 100 metres spaced, north-south, cut grid which facilitates access to the central parts of the map area.

1.4 Physiography and Bedrock Exposures

The study area has the characteristic relief of the Canadian Shield and taiga ecosystem. Most of the area is comprised of small, semi-barren hills less than 50 metres high, separated by low-lying, generally swampy terrain. The entire area is covered with black spruce mixed with white birch and aspen on the hillsides and spruce with alder in the low-lying area. The Bousquet river divides the area approximately on the Bousquet - Doyon property boundary lines. Outcrop exposure is restricted to the higher elevations on the hilltops or on access road cuts. General exposure is less than 5 percent of the

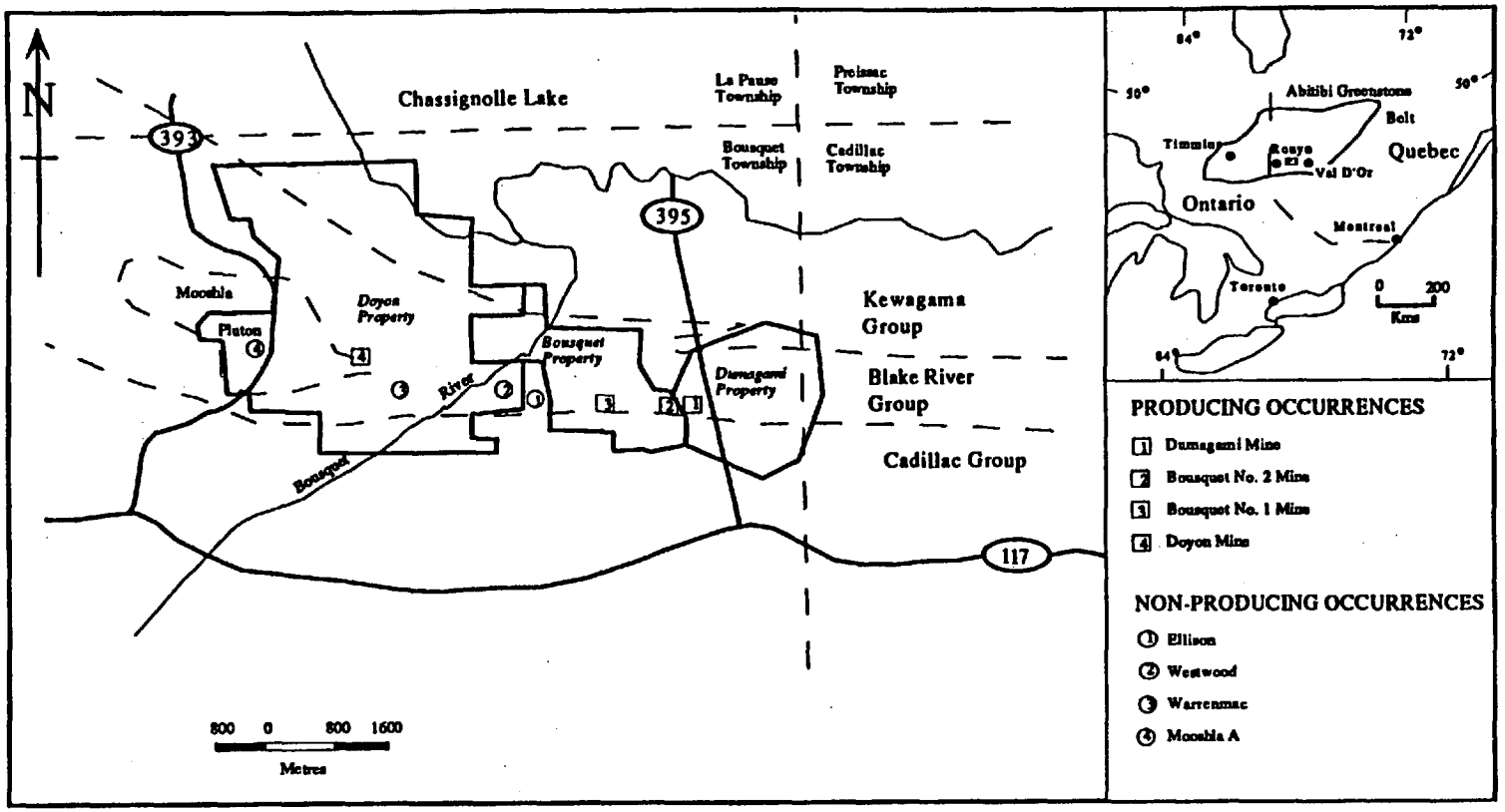


Figure 1. Location Map (After Stone, 1988 with modifications).

entire area but locally bedrock exposure can approach 100 percent at higher elevations on hilltops.

1.5 Exploration and Mining History

The study area includes four mines producing gold from three separate orebodies. Significant gold concentrations also occur at the nearby Ellison, Westwood, Warrenmac and Mooshla A occurrences as well as on the Bousquet No. 1 property (Figure 1). Production from the existing and past mines exceeds 5 million oz., and present reserves for the area are estimated at 4.3 million oz., (Table 1).

Gold mineralization was first discovered in the Bousquet area in the early 1930's on the MicMac, Westwood and Warrenmac properties (Stone, 1988). The first production of gold was from the Mooshla Mine during the early 1940's when 4400 tons of ore with an average grade of 0.78 Troy ounce per ton (oz/ton) were mined (Savoie et al., 1986). Gold mineralization was found on the Bousquet No. 1 property in 1937 when the #4, #5 and # 6 mineralized occurrences were located but the deposit remained sub-economic until the #1, #2 and # 3 zones were found in 1975 (Figure 2). The Mine currently produces 53,000 ounces of gold from an average mill head grade of 0.21 oz/ton and has a current mineral inventory of 2.2 million tons with an average grade of 0.21 oz/ton (Lac Minerals Limited, Annual Report 1993).

The Doyon #1 zone was discovered in 1976 by La Societe Quebecoise d'Exploration Miniere (SOQUEM) and Silverstack. Lac Minerals took control of Silverstack Limited in 1977 and discovered the Main and West zones. The mine began operation as an open pit on the #1 and Main zones in 1980 and was subsequently converted to an underground mine in 1988. The Doyon Mine now produces an excess of 240,000 Troy ounces annually and has current reserves of 10 million tons with an average grade of 0.18 oz/ton (The Northern Miner, August 19, 1994).

Dumagami Mines Limited first discovered gold on the ground immediately east

Table 1. Production and mineral inventory of gold occurrences in Bousquet Township.

Occurrence	Production (oz)	Reserves (tons)	Grade (oz/t)	Contained ounces	Source
Mooshla A	3,432	--	--	--	1
Doyon	3,000,000	10,000,000	0.18	1,800,000	2
Warrenmac	--	100,000	0.16	16,000	3
Westwood	18	--	--		4
Ellison	--	861,000	0.16	137,760	4
Bousquet 1	700,000 *e	2,274,500	0.21	477,645	3
# 6	--	--	0.03		5
# 5	--	3,459,800	0.06	207,588	5
# 4	--	196,400	0.13	25,532	6
Bousquet 2	764,300	7,600,000	0.19	1,444,000	3
Dumagami	672,000 e	2,000,000 e	0.14	280,000	4
Total	5,139,750	26,491,700	0.16	4,388,525	

* includes production from # 5 occurrence
e estimate

Sources:
1) Savoie et al., (1986).
2) The Northern Miner (1994)
3) A.Bourget, pers. comm., (1995)
4) Marquis et al., (1990)
5) Valliant (1981)
6) Tourigny et al., (1992)

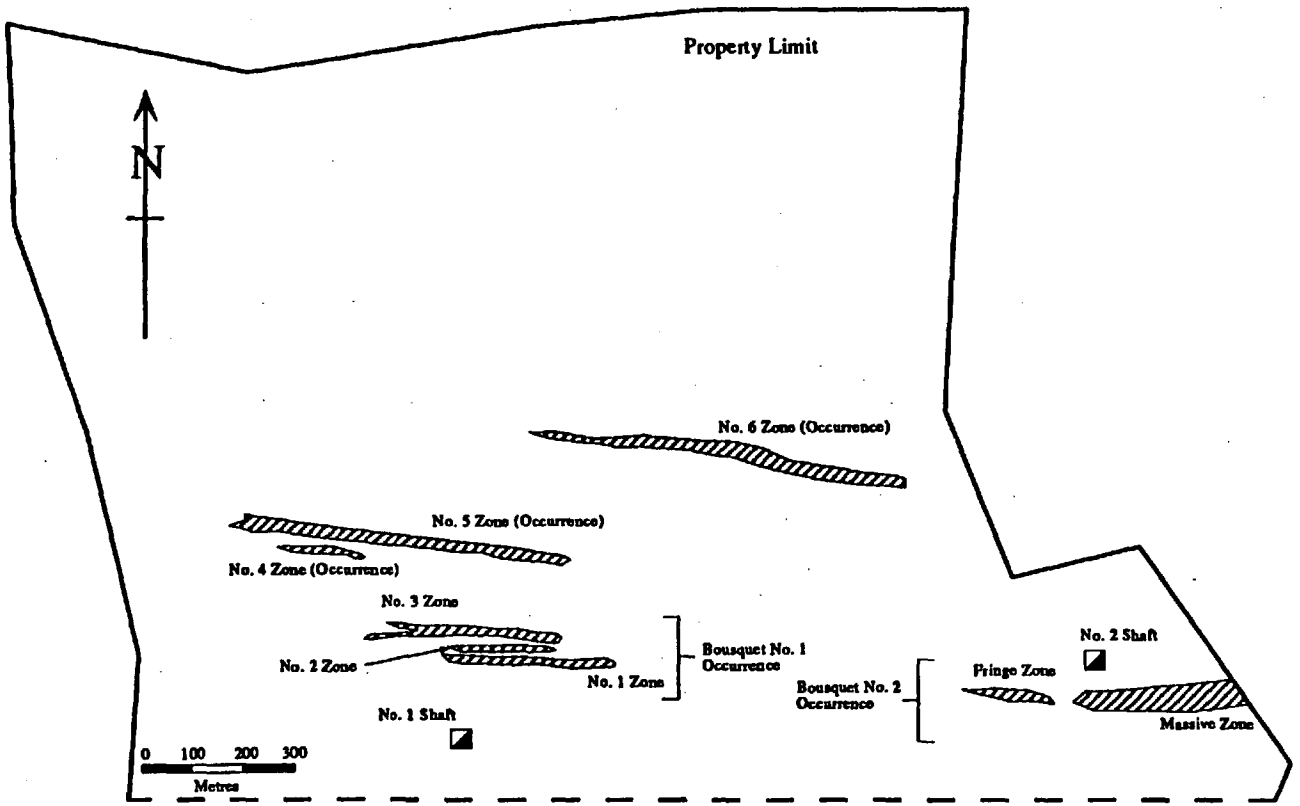


Figure 2. Location of mineralized zones on the Bousquet property.
(After Valliant, 1981 with modifications)

of the study area in 1963 and, through an exploration drilling campaign, in 1985 discovered an orebody which straddles the Dumagami-Bousquet property boundary. Drilling by Lac Minerals extended the ore body down dip on the Bousquet side to outline 5.2 million tons of ore grading 0.25 oz/ton gold and 0.71 percent copper. This ore body is referred to as the Bousquet #2 on the Barrick property and as the Laronde ore body on the Dumagami property.

The Ellison prospect was discovered in 1970 by Yorbeau Resources where they outlined some 750,000 tons of 0.16 oz/ton gold in three separate mineralized horizons (Stone, 1988). The Ellison prospect is now controlled by Republic Goldfields Limited and was not accessible for sampling during the course of this research.

In August 1994, American Barrick Resource Limited made a successful bid for all the outstanding shares of Lac Minerals Limited and now controls both the Doyon and Bousquet properties. After the take-over, American Barrick changed its name to Barrick Gold Corporation, and are the current owners of the deposits.

1.6 Previous Work

The geology of Bousquet Township was first described by Bancroft (1911) and Wilson (1913) but it was not until Gunning (1937, 1941) that the stratigraphy and structure of the area were properly documented. More recently, the area was described in detail by Dimroth et al., (1982, 1983a, b), Gelinas and Ludden (1984), Hubert et al., (1984), Imreh (1976) and Ludden and Hubert (1986).

Detailed studies of the gold mineralization at the Bousquet No. 1 Mine have been carried out by Valliant (1981), Valliant and Barnett (1982), Bateman (1984), Tourigny (1988), Tourigny et al., (1988), and Tourigny et al., (1992). The Bousquet No. 2 deposit was described by Tourigny et al., (1993), Teasdale (in progress), and indirectly by Marquis (1990) and Marquis et al., (1992). The geology of the Doyon Mine was briefly described by Filion et al., (1976) and Savoie et al., (1991). Regional studies describing

the metamorphism and structural setting of the area were carried out by Stone (1988) and Tourigny (1984) respectively.

1.7 Method of Investigation

The descriptive geological work in this study is a compilation of previous work combined with the author's own field work during the summers of 1993 and 1994. Work for this study included field mapping of the area and the collection of representative samples from each rock unit, by the author, in order to establish a reference with the previous work by Valliant (1981), Bateman (1984), Tourigny (1988), Stone (1988) and Teasdale (in progress). During the field mapping, each gold occurrence was mapped and sampled in detail.

Some 395 samples were collected from surface exposures, underground workings and exploration drill core. These samples fully represent all the host igneous rocks and associated alteration halos of each gold occurrence. The samples were analyzed for major and trace elements by X-Ray Fluorescence at X-Ral Laboratories in Toronto.

For this study, the author mapped the underground workings at the Doyon mine at 1:2000 to identify major rock and alteration types associated with the gold mineralization at this mine. Selected areas within the mine were mapped at 1:250 in order to associate alteration type with gold grade for each rock type. Mapping of alteration types was supplemented with the description of 58 thin and polished sections and some 100 microprobe analyses of garnet crystals which were carried out using a JOEL 8600 Superprobe at the University of Colorado at Boulder. Ten double polished thin sections were prepared for a fluid inclusion study of the mineralized veins from the Doyon mine. All data analyses were carried out by the author at the Colorado School of Mines.

Chapter 2
REGIONAL GEOLOGY OF ABITIBI GREENSTONE BELT

2.1 Introduction

The study area is within the southwestern portion of the Archean Abitibi greenstone belt, a 750 kilometres long by 250 kilometres wide belt of structurally deformed and metamorphosed lava flows, volcaniclastic rocks, chemical and clastic sedimentary rock and syn- to post-tectonic granitoid batholiths. The greenstone belt is part of the Superior Structural Province and is bounded to the north by the Quetico Sub-Province, to the west by the Kapuskasing Sub-Province and by the rocks of the Grenville Province to the east and southeast (Card, 1990). Radiometric U/Pb age determinations on zircons throughout the Abitibi belt yield ages from 2,740 - 2,680 Ma (Feng et al., 1992; Corfu et al., 1989; Jensen, 1985).

Many base and precious metal deposits have been located within the meta-volcanic rocks of the Abitibi belt. These deposits have contributed greatly to the development and growth of the communities of Timmins and Kirkland Lake, Ontario as well as Noranda, Val D'Or, Matagami and Chibougamau, Quebec.

2.2 Stratigraphy

The volcanic rocks of the Abitibi belt are multi-cyclical and range from tholeiitic basaltic or ultramafic komatiitic flows at the base of each cycle to calc-alkaline rhyolitic flows and pyroclastic units near the top (Thurston et al., 1985). Each cycle is characterized by bimodal volcanism. Based on lithologic and geochemical controls the Abitibi greenstone belt is divided into a Northern Volcanic Zone and a Southern Volcanic Zone (Ludden et al., 1986; Ludden and Hubert, 1986). The meta-volcanic rocks of

Bousquet Township are within the Southern Volcanic Zone. Dimroth et al., (1982) divided the Southern Volcanic Zone into three separate volcanic cycles which they termed Lower Supergroups I and II and Upper Supergroup. The Rocks of the three Supergroups are further assigned to five different volcanic centers (Table 2). Rocks of the study area belong to the Upper Supergroup of the Lake Abitibi volcanic center, and are assigned to the Blake River Group.

2.3 Structure

The major structural features of the Southern Volcanic Zone of the Abitibi belt are easterly plunging, steeply dipping, isoclinally folded synclinoriums intruded by granitic diapirs. The synclinoriums of meta-volcanic and meta-sedimentary rocks are separated by west-northwest, east-southeast and east-west-trending faults defining lozenge shaped blocks that are stratigraphically and structurally independent of one another (Jensen, 1985; Hubert and Ludden, 1986). A penetrative cleavage is developed in all rocks parallel to the major east-west structural breaks.

The Larder Lake - Cadillac break is one of these major east-west trending structural faults and can be traced eastward from Kirkland Lake, Ontario through Cadillac, Quebec and to the Grenville front. It passes only one kilometre south of the study area (Figure 3).

2.4 Metamorphism

The supracrustal rocks of the Abitibi belt have been regionally metamorphosed to lower to middle greenschist facies with local amphibolite grade developed near the contact with younger granitic intrusions (Jolly, 1978). Primary volcanic and sedimentary structures are generally well preserved throughout the greenstone belt except near the major structural breaks where the rocks have been pervasively altered to carbonate minerals intermixed with fine white mica and chlorite. In sharp contrast to this low grade

Table 2. Volcanic stratigraphy of Southern Abitibi Belt.

	Timmins South	Timmins North	Lake Abitibi	Quebec	Kirkland Lake
UPPER SUPERGROUP					Timiskaming Gp.
	Upper Tisdale Gp.		Blake River Gp.	Blake River Gp.	Blake River Gp.
	Middle Tisdale Gp.		Kinojevis Gp.	Kinojevis Gp.	Kinojevis Gp.
	Lower Tisdale Gp.	Lower Tisdale Gr.	Stoughton-Roquemaure Gp.	Malartic Gp.	Larder Lake Gp.
				Lois Fm.	
LOWER SUPERGROUP II	Porcupine Gp.	Kidd Creek Rhyolite	Hunter Mine Gp.		Skead Gp.
					Catherine Gp.
					Wabewawa Gp.
					Pacaud Gp.
LOWER SUPERGROUP I	Upper Deloro Gp.				
	Middle Deloro Gp.				
	Lower Deloro Gp.				

Source: Jensen (1985)

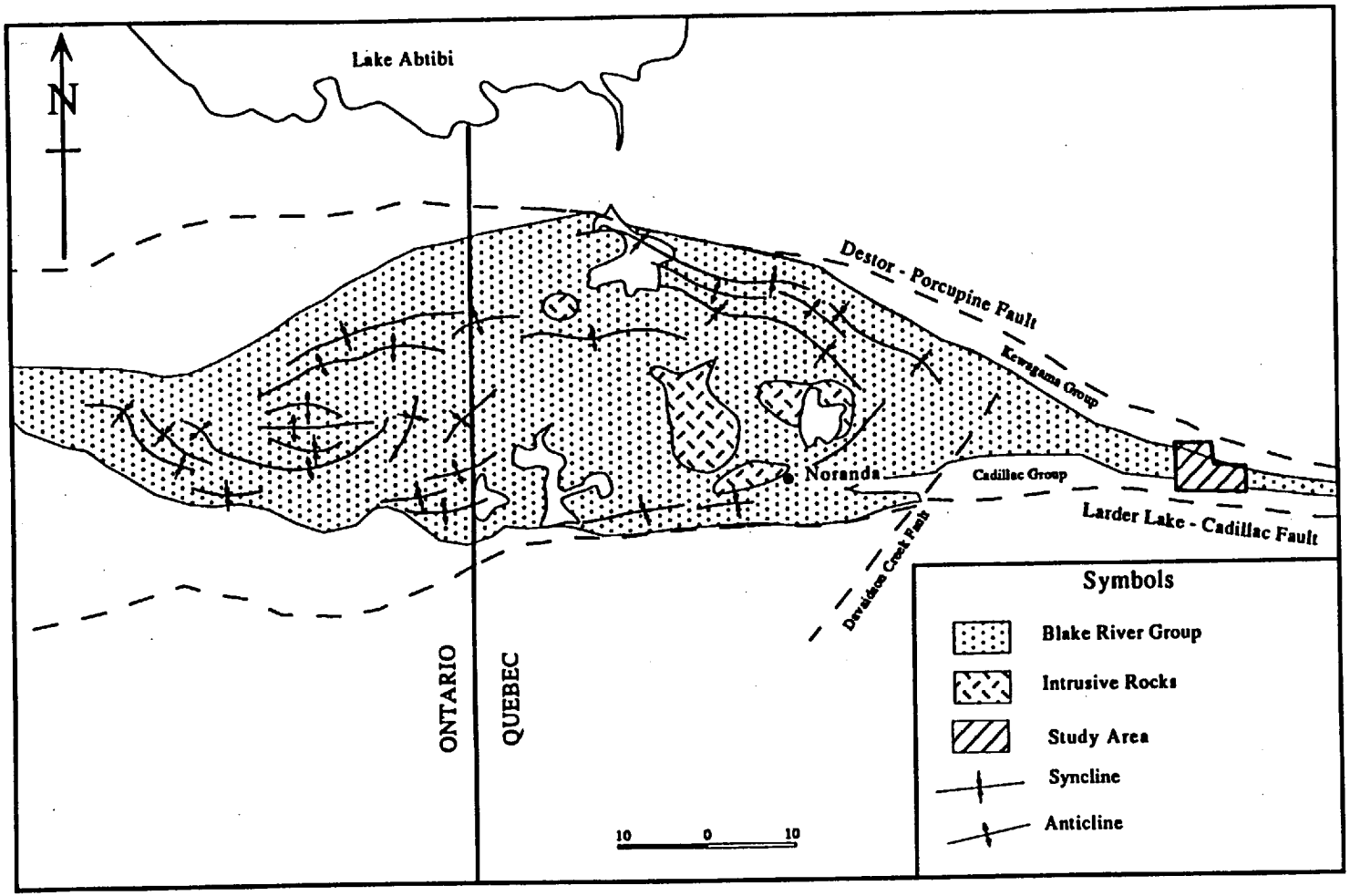


Figure 3. Structural setting of Blake River Group. (After Jensen, 19895)

metamorphism in the greenstone belts, the surrounding rocks have been metamorphosed to granitic gneiss of upper amphibolite grade (Card, 1990).

In this study, the prefix "meta" which applies to all rocks described will be omitted for brevity, but, readers are reminded that all rock units have been metamorphosed to at least lower greenschist facies.

Chapter 3
GEOLOGY OF STUDY AREA

3.1 Introduction

Bousquet Township is underlain in the north by the sedimentary rocks of the Kewagama Group, through its central parts by volcanic and volcaniclastic rocks of the Blake River Group and by the sedimentary rocks of the Cadillac Group in its southern portions. The volcaniclastic rocks of the Blake River Group have been intruded by the intrusive rocks of the Mooshla complex in the western part of the Doyon property (Figure 4). The volcanic sequence is in fault contact with the sedimentary rocks of the Kewagama Group to the north, and its contact with the Cadillac Group to the south is an unconformity. All mappable units strike east-west and dip steeply to the south. Several northeast-trending Proterozoic diabase dikes cut the Archean sequence.

3.2 Kewagama Group

The Kewagama Group underlies the northernmost part of the study area on the Doyon Property and consists mainly of argillite, siltstone and greywacke. Primary sedimentary structures are well preserved and include graded bedding, small scours and oblique stratification. These structures indicate younging directions towards both north and south (Stone, 1988). Rocks of the Kewagama Group are composed of volcanic rock fragments and fine-grained quartz and feldspar crystals (Dimroth et al., 1983a; Stone, 1988). The contact between the Kewagama and the Blake River Group is not exposed but follows a linear depression some 30 metres wide which is generally interpreted to represent the Lake Parfouru fault, a sub-parallel structure to the Destor-Porcupine fault (Savoie et al., 1986; Tourigny, 1984; Tourigny et al., 1987; Figure 3).

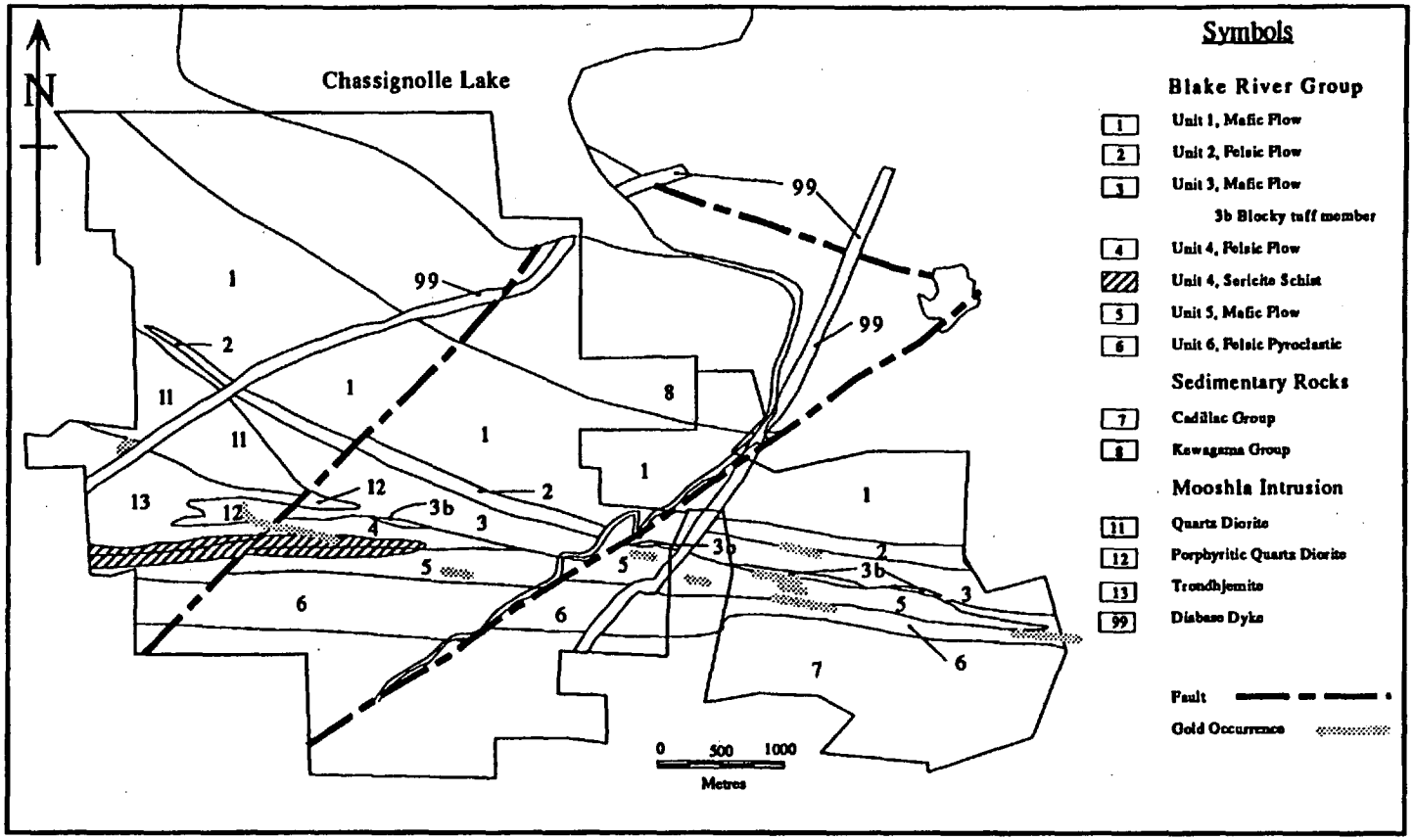


Figure 4. Geology of Doyon and Bousquet Properties. (From Savoie, 1990, and this study).

3.3 Blake River Group

Rocks of the Blake River Group range from tholeiitic to calc-alkaline basalt, and andesite with felsic volcanic and volcaniclastic strata. In Bousquet Township, the Blake River Group has been divided from the base to the top into six mappable units representing three volcanic cycles. The units are simply termed 1 through 6 on the Bousquet - Doyon property (Savoie et al., 1991). Each cycle consists of a mafic member at the base and a felsic one at the top. The proportion of mafic to felsic components in each cycle changes from the base of the Blake River Group to the top with the lower cycle consisting mostly of mafic components and the upper cycle consisting of lesser mafic but mostly felsic volcanic rocks. The volcanic units generally strike east - west and dip steeply to the south. Volcanic stratigraphy is assumed to young to the south because of pillows found near the base of the Blake River Group in unit 1 of cycle 1 and the metal zonation of the ore deposits within the volcanic sequence.

Terminology of volcanic rock used in this study is that of LeBas et al., (1986) which is based on whole rock analyses of fresh rock recalculated to 100 percent without CO_2 and H_2O content. In order to assure that the samples selected were minimally affected by hydrothermal alteration, the alteration index of Ishikawa et al., (1976) was calculated for each analyzed sample:

$$A.I. = [MgO+K_2O/MgO+K_2O+Na_2O+CaO]X100$$

All samples with an A.I. greater than 50 were excluded from the database and do not appear in any classification diagrams in this study. The Ishikawa alteration index is believed to be reliable for most mafic to felsic volcanic suites (LaFleche et al., 1992a; Hashiguchi et al., 1983; Date et al., 1983).

3.3.1 Unit 1

Unit 1 has a minimum thickness of 1000 metres and marks the base of the Blake River Group and its lowest cycle. The unit consists of thick sequences of basaltic

pillowed and massive lava flows intruded by gabbroic sills and dikes. Individual flows are 5 to 30 metres thick. Pillows are well preserved, only slightly flattened and range in size from 0.5 to 1 metre in diameter (Figure 5). The pillows are very fine-grained, non-porphyritic and chloritic with selvages of fine-grained epidote and chlorite usually less than 3 to 5 cm thick. The rocks are tholeiitic and most are of basaltic or basaltic andesite in composition (Figures 6, 7). Near the base of unit 1, pillows indicate that stratigraphic top is to the south. The contact between units 1 and 2 appears conformable.

3.3.2 Unit 2

Unit 2 is a very continuous body of quartz porphyritic rhyolite with an average thickness of 60 m. It is very uniform and does not appear to change significantly in composition or thickness over 10 kilometres of strike length. It contains up to 30 percent euhedral phenocrysts of quartz 1 to 3 mm long in a fine-grained matrix of quartz and fine white mica and epidote. Because of its narrow width and lateral continuity, it has been suggested that unit 2 could not be a flow (Savoie et al., 1986). However, it is intercalated with thin pillowed flows less than a metre thick near the # 6 occurrence on the Bousquet property. Furthermore, lapilli and blocks have been identified within this unit (Valliant, 1981; Stone, 1988). The rocks are calc-alkaline rhyolite in composition (Figures 8, 9). This unit marks the top of cycle one. Similarities between this unit and unit 6 at the top of cycle 3 prompted previous workers to interpret that these two units were one and the same, but disposed respectively on the north and south limbs of a syncline (Bateman, 1984; Eliopoulos, 1983).

3.3.3 Unit 3

Unit 3 overlies unit 2 on the Doyon Property but it has not previously been recognized on the Bousquet Property (Savoie et al., 1986, 1991; Tourigny, 1988; Stone, 1988). It has a minimum thickness of 30 metres on the Doyon Property and forms



Figure 5. Photograph of pillow Basalt from unit 1. Note fine-grained epidote selvage. Handle on hammer is 30 cm.

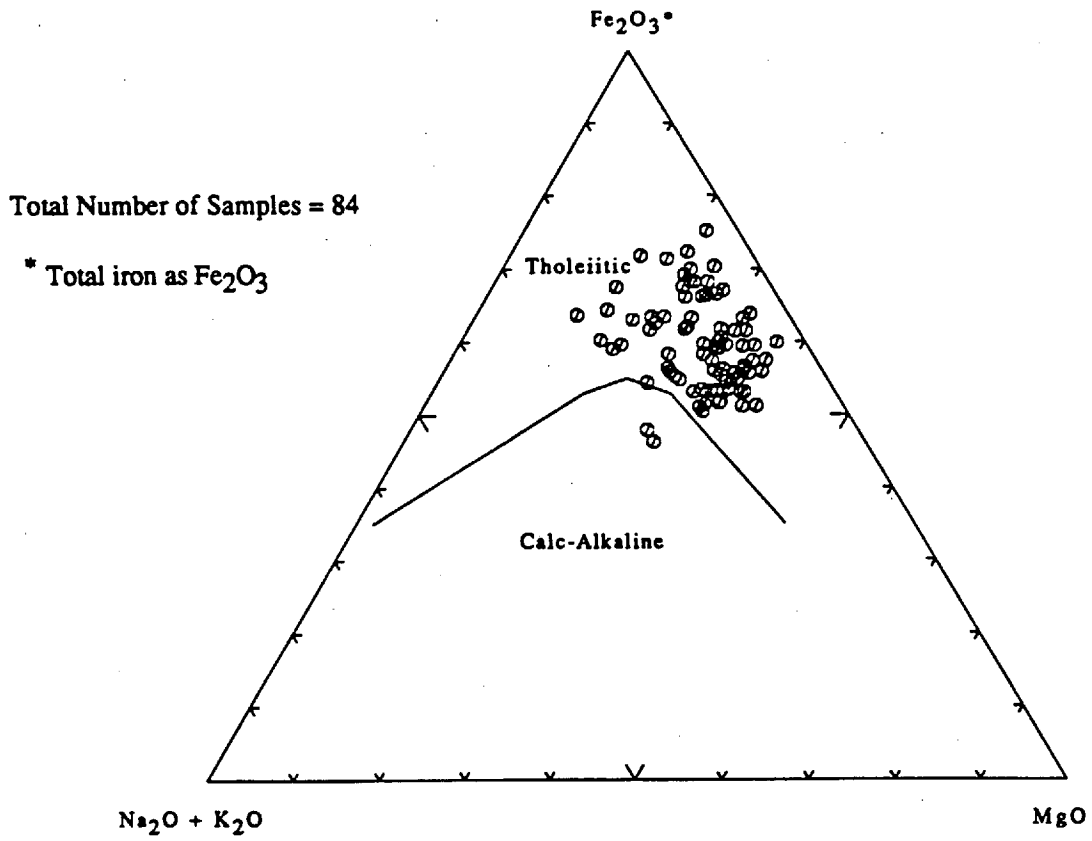
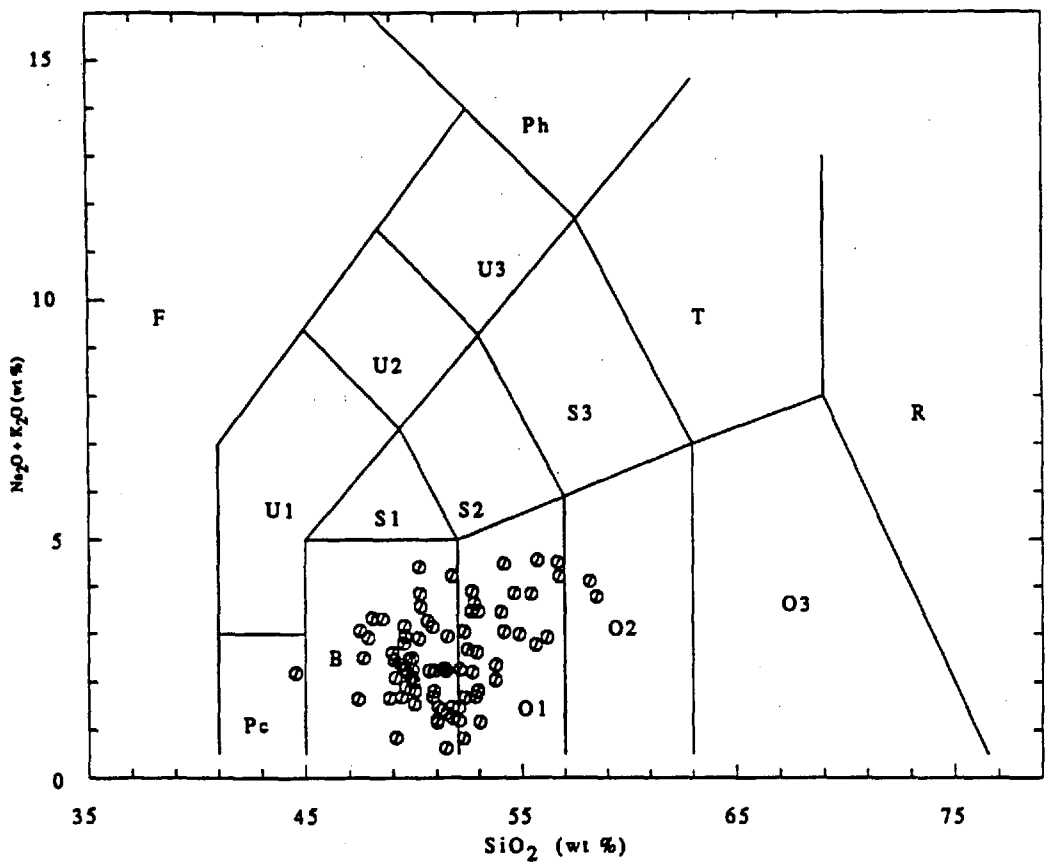


Figure 6. AFM Plot for the rocks of unit 1 (Irvine and Baragar, 1971).



Symbols

Pc	Picrobasalt	S2	Basaltic tracyandesite
B	Basalt	S3	Trachyandesite
O1	Basaltic Andesite	T	Trachyte
O2	Andesite	U1	Basanite
O3	Dacite	U2	Phonotephrite
R	Rhyolite	U3	Tephriphonolite
S1	Trachybasalt	Ph	Phonolite
		F	Foidite

Figure 7. Total alkali versus silica plot for the rocks of unit 1 (LeBas et al., 1986)

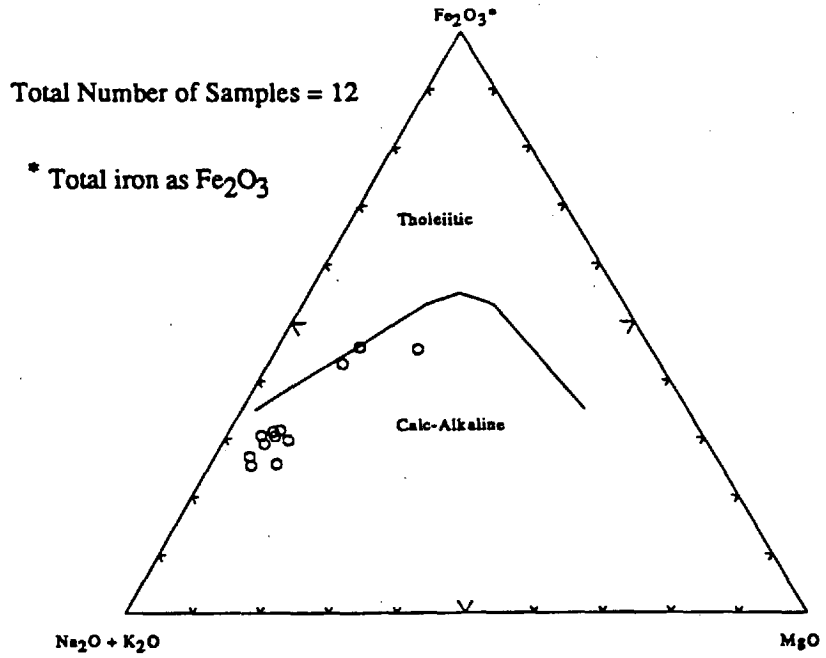


Figure 8. AFM Plot of the rocks of unit 2 (Irvine and Baragar, 1971).

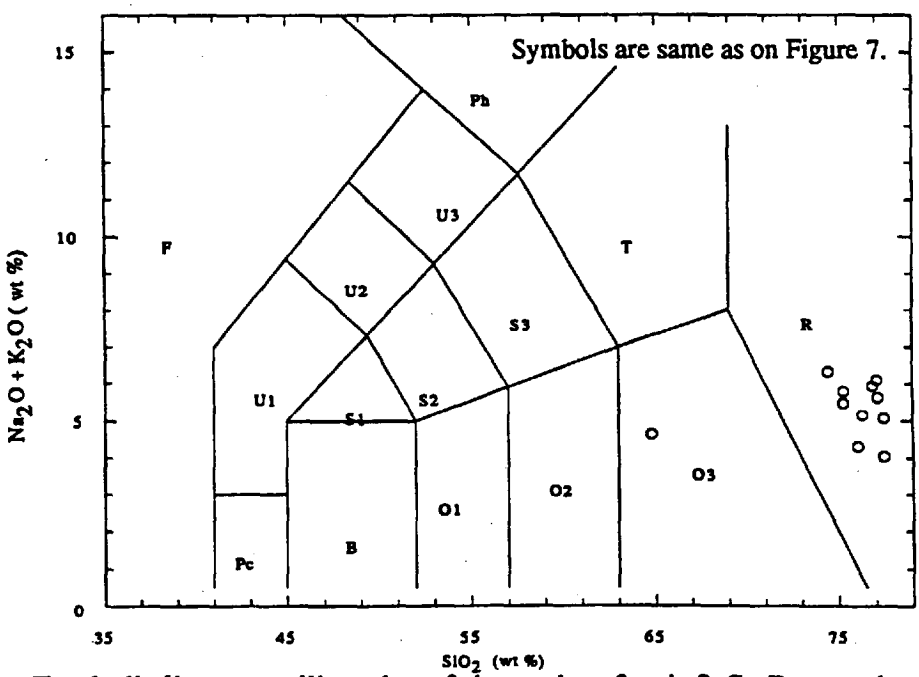


Figure 9. Total alkali versus silica plot of the rocks of unit 2 (LeBas et al., 1986)

the base of the second volcanic cycle. This unit consists of fine-grained basaltic flows and tuffaceous horizons near the base and a thin blocky tuff of intermediate composition near the top. The flows are pillowed to massive and pervasively chloritized. Younging direction could not be determined from the pillow shapes because they have been strongly deformed and stretched parallel to the regional foliation.

The blocky tuff member that marks the top of unit 3 is exposed on the north wall of the main pit on the Doyon Property. This member is an heterolithic volcaniclastic rock with coarse fragments ranging from 1 up to 50 cm in maximum dimension. The fragments are sub-rounded to lenticular, amount to 30 percent of the rock volume and range in composition from chloritized andesite to quartz-feldspar porphyry and pumice (Figure 10). In the vicinity of the Doyon pit, the pumice fragments have been completely altered to epidote, clinozoisite and calcite (Figure 11).

A discontinuous horizon of blocky tuff identified during field mapping of the Bousquet Property during the course of this study is identical to the blocky tuff member of unit 3 of the Doyon Property. This discontinuous horizon is therefore interpreted as the lateral extension of the blocky tuff member of unit 3 on the Doyon Property (Figure 4).

Rocks of unit 3 range in composition form tholeiitic basalt to calc-alkaline dacite (Figures 12, 13). Unit 3 is overlain by unit 4 on the Doyon Property and directly by unit 5 east of the Doyon pit where unit 4 is absent. The unit is cut by the intrusions of the Mooshla Complex to the west.

3.3.4 Unit 4

Unit 4 is exposed only at the Doyon Mine, where it is a narrow band of strongly foliated and sericitized felsic, volcaniclastic rocks some 60 metres thick. These rocks are comprised of a fine-grained matrix of quartz, fine white mica, feldspar and calcite with up to 30 percent quartz as phenocrysts. This unit marks the top of cycle two, and



Figure 10. Photograph of heterolithic blocky tuff member of unit 3. Note sub-rounded feldspar porphyry clast in foreground and flattened pumice fragments above hammer handle. Handle on hammer is 30 cm.



Figure 11. Photograph of blocky tuff member from north wall of Doyon pit. Note pumice fragments selectively replaced by epidote. "Nokin" lens cap for scale.

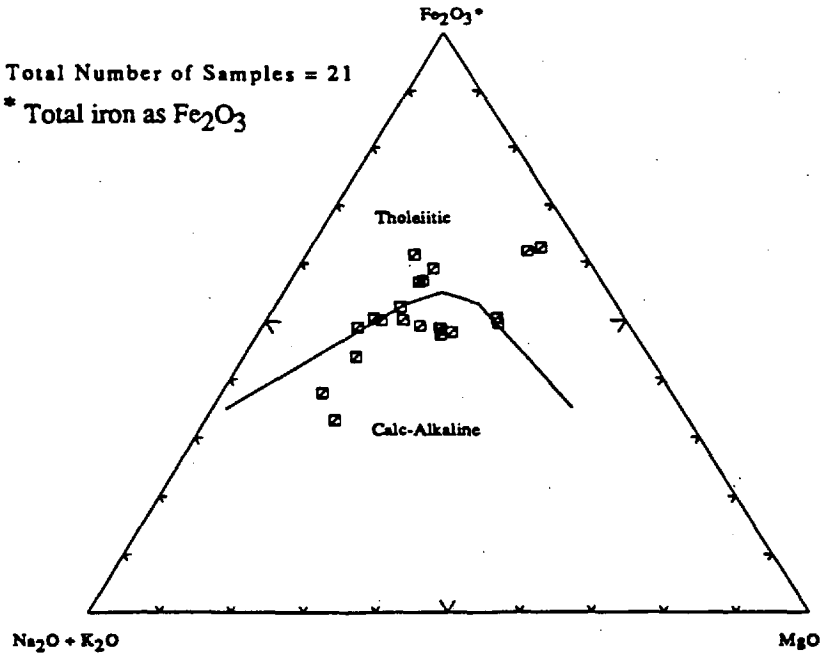


Figure 12. AFM plot for the rocks of unit 3 (Irvine and Baragar 1971).

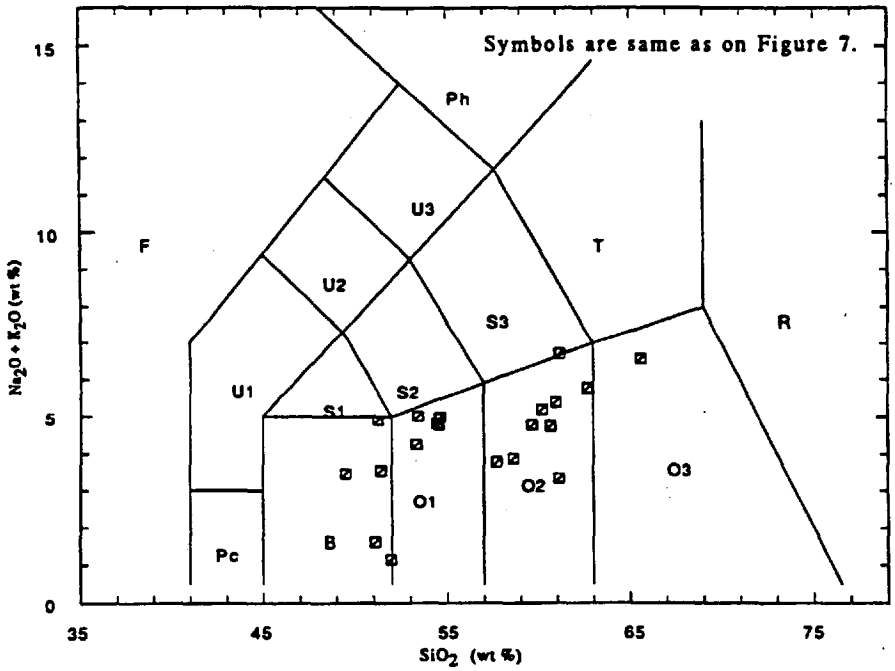


Figure 13. Total alkali versus silica plot for the rocks of unit 3 (LeBas et al., 1986)

contains 1 to 3 percent disseminated pyrite elongated parallel to the foliation. Its central portion is a blocky tuffaceous rock which grades laterally into a finer-grained tuff toward the margins of the unit (Savoie et al., 1986). Unit 4 pinches out laterally to the east near the Bousquet river and is cut to the west and down dip by the Mooshla intrusions. The upper contact of unit 4 with unit 5 is gradational through a 100 metre wide quartz-sericite schist. This was previously interpreted as a separate unit of the Blake River Group (Savoie et al., 1992) or as a large shear zone (Stone, 1988). Field work in this study indicates that the sericite schist was generated by metamorphism and deformation of an hydrothermal alteration halo formed during the emplacement of the Mooshla Complex. The sericite schist has a gradational contact with the underlying, relatively unaltered felsic volcanic rocks of unit 4 and its central portion displays evidence of cataclastic deformation (Figure 14).

Rocks of unit 4 are mostly rhyolitic and calc-alkaline, although the sericite schist member is characterized by a marked decrease in MgO which moves its analyses into the tholeiitic field on the AFM diagram (Figures 15, 16).

3.3.5 Unit 5

Unit 5 has a maximum thickness of 100 metres on the Doyon Property (Savoie et al., 1991) and forms the base of the third and uppermost volcanic cycle on the property. It directly overlies unit 3 on the Bousquet Property and unit 4 near the Mooshla Intrusive Complex (Figure 4). Rocks of unit 5 are pillowed flows intercalated with mafic to intermediate tuffaceous horizons. As a whole, these rocks are physically and chemically indistinguishable from those of unit 3 (Appendix 1, Figures 12, 13, 17 and 18). However, unit 5 contains no blocky pyroclastic flows and has some distinctive garnetiferous horizons associated with gold mineralization (Valliant, 1981; Bateman, 1984; Savoie et al., 1986). In contrast, no garnetiferous horizons are known in unit 3. Unit 5 is host to the # 4 and 5 occurrences on the Bousquet Property. Chemically, the

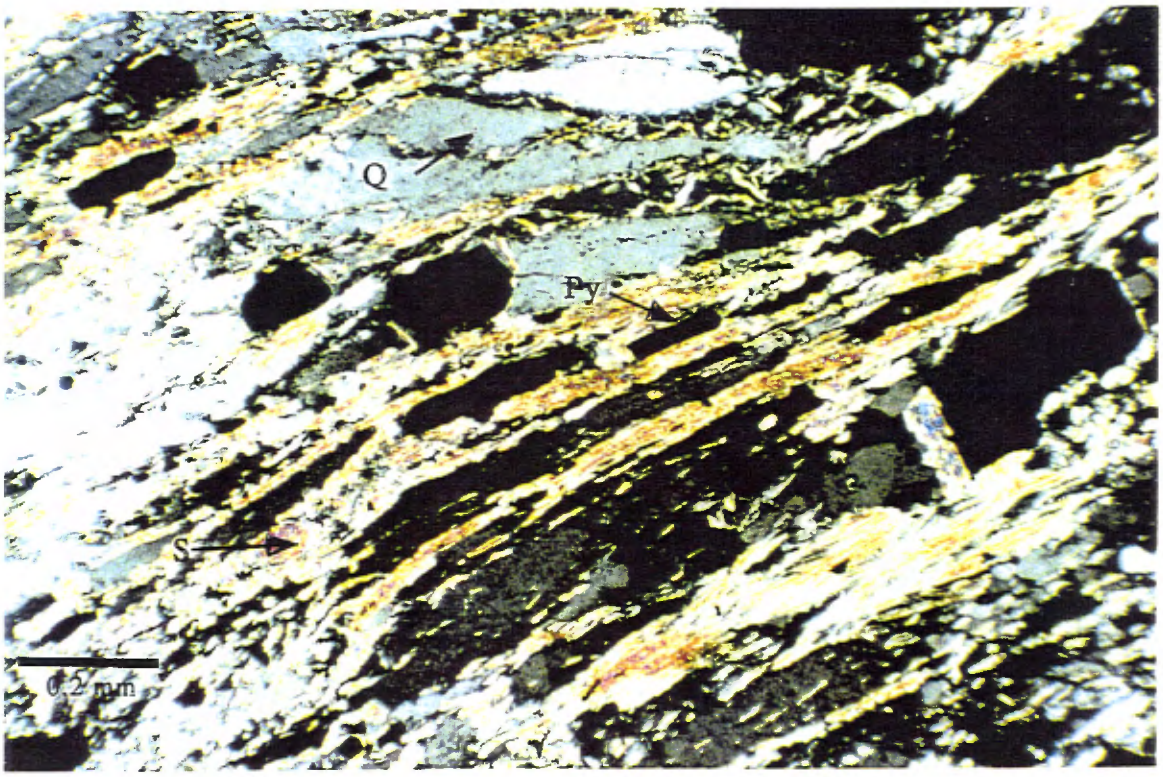


Figure 14. Photomicrograph of mylonitic texture in sericite schist of unit 4. Note quartz and pyrite elongated parallel to foliation. Sample 93-103. Transmitted light, crossed polars, 75X. Q = quartz, Py = pyrite, S = sericite.

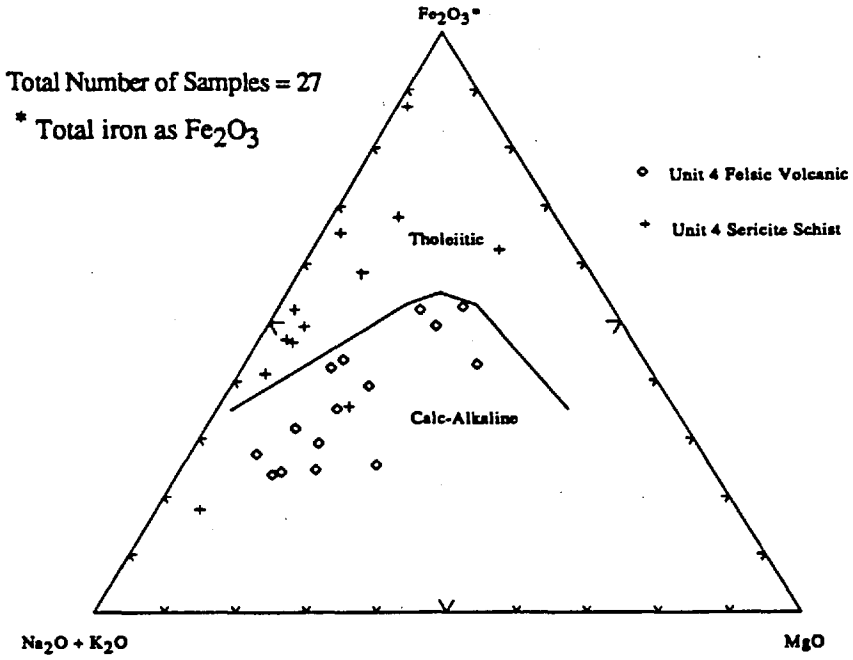


Figure 15. AFM plot for the rocks of unit 4 (Irvine and Baragar, 1971).

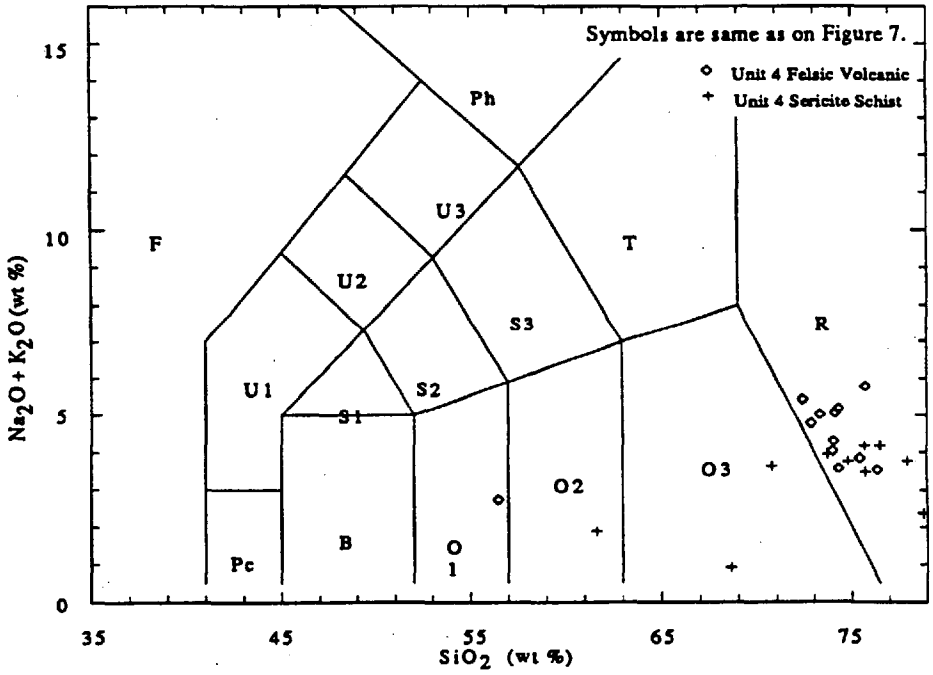


Figure 16. Total alkali versus silica plot for the rocks of unit 4 (LeBas et al., 1986)

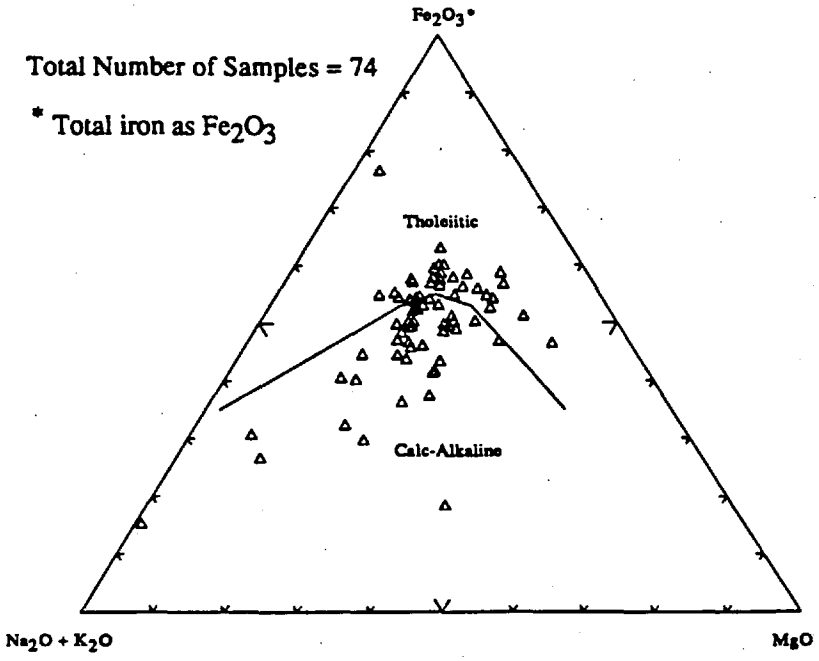


Figure 17. AFM plot for the rocks of unit 5 (Irvine and Baragar, 1971)

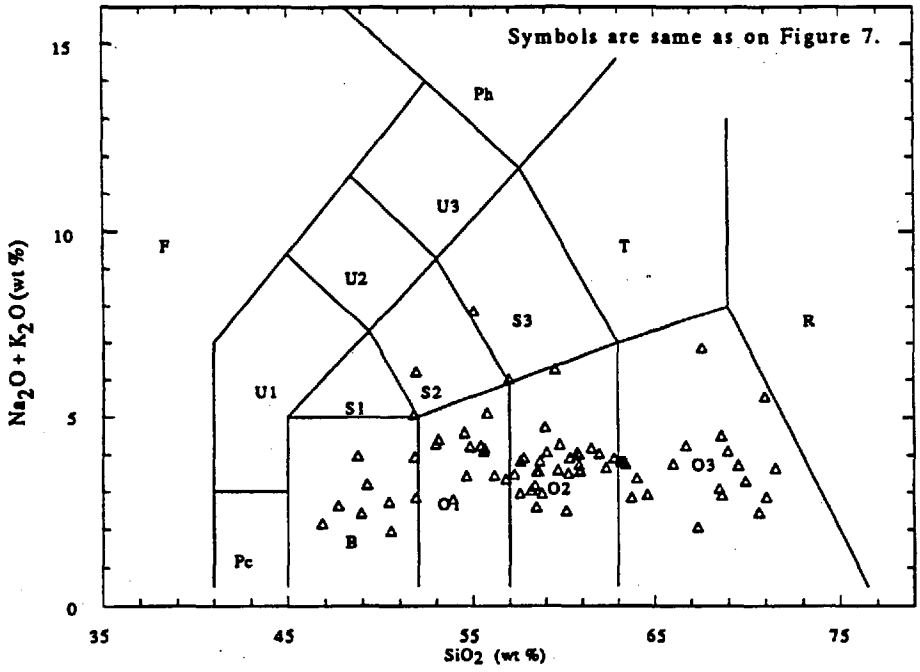


Figure 18. Total alkali versus silica plot for the rocks of unit 5 (LeBas et al., 1986)

rocks are tholeiitic to calc-alkaline in composition and range from basalt to dacite (Figures 17, 18).

3.3.6 Unit 6

Unit 6 consists of a sequence of fine-grained to blocky rhyolitic tuff. It is less than 60 metres thick on the Bousquet Property and exceeds 200 metres in thickness on the Doyon Property. The proportion of blocky tuff to ash tuff decreases rapidly to the west and east of the study area (Stone, 1988). This unit marks the top of the third volcanic cycle, and of the Blake River Group in the study area. The rocks are calc-alkaline and rhyolitic in composition (Figures 19, 20). They consist of 20 % fine-grained quartz phenocrysts less than 3 mm in length in a matrix of quartz, fine white mica, and plagioclase, with minor biotite. This unit is host to the Bousquet No. 1 and No. 2 Mines.

The upper contact of unit 6 with the sedimentary rocks of the Cadillac Group is marked by a 30 to 40 cm wide pyrrhotitic-pyritic-graphitic shear about 1 metres below the volcano-sedimentary contact. The contact between the rocks of unit 6 and those of the Cadillac Group has been interpreted as the Dumagami fault (Tourigny et al., 1988). However, in the vicinity of the Bousquet No. 1 and No. 2 mines the contact is not faulted and appears to be an unconformity.

3.4 Cadillac Group

Argillite and greywacke are the most prominent sedimentary rock types of the Cadillac Group but beds of sandstone, siltstone, conglomerate, iron formation and minor basaltic flows are also present in significant amount (Stone, 1988). Beds dip steeply to the south, graded bedding and cross stratification indicate younging directions both to the north and south, suggesting that the Group is isoclinally folded.

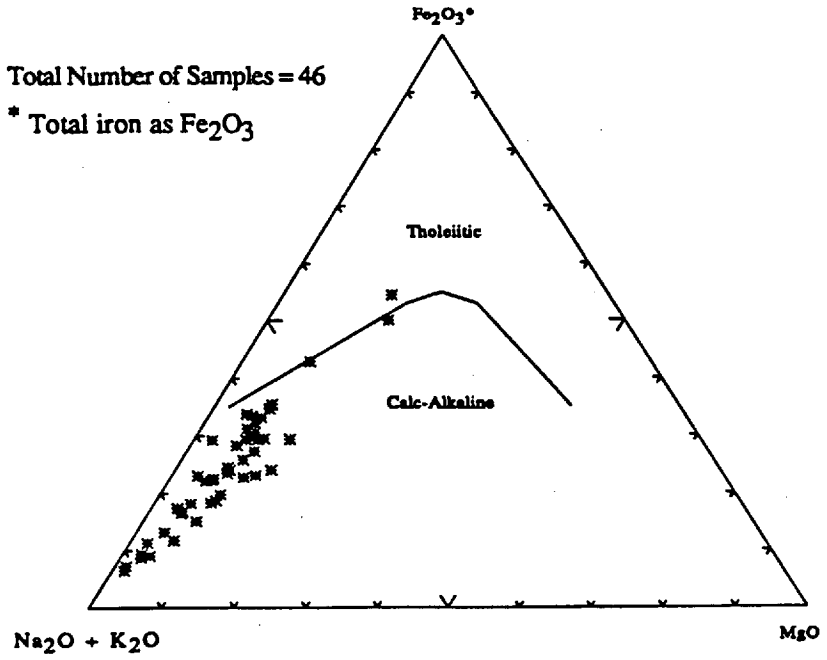


Figure 19. AFM plot for the rocks of unit 6 (Irvine and Baragar, 1971)

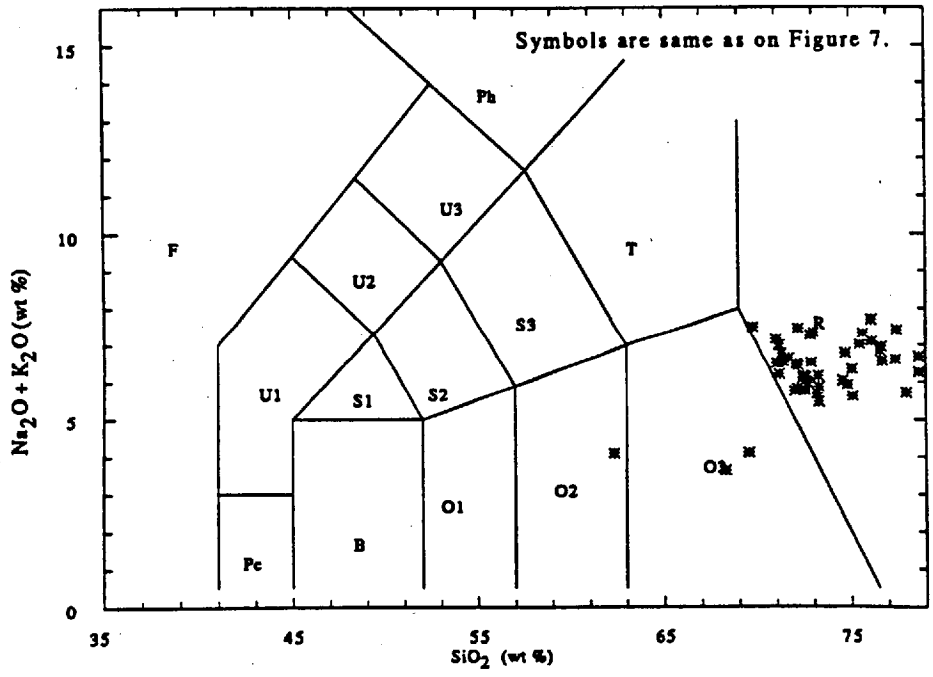


Figure 20. Total alkali versus silica plot for the rocks of unit 6 (LeBas et al., 1986)

3.5 Mooshla Intrusive Complex

The Mooshla Complex is a multi-phase sill-like body 1.5 kilometres wide and 4 kilometres long. The intrusion was emplaced in the central portion of the Blake River Group in the western part of the Doyon Property. Contact metamorphic effects due to the emplacement of the Complex are minor to non-existent for most of the intrusion but a 100 metre wide sericite schist is developed on the southern contact of the intrusion. The intrusion is interpreted to be co-magmatic with the felsic rocks of the Blake River Group (Valliant and Hutchinson, 1982).

Classification of igneous rocks is based on the texture of the rock combined with the modal volume proportion of quartz, plagioclase and potassium feldspar, according to the IUGS classification as proposed by Streckeisen (1976). Alternatively, igneous rocks are classified using various chemical diagrams usually derived from CIPW normative calculations or chemical analyses of major oxide components (Carmichael et al., 1974). Langshur (1990), classified the different phases of the Mooshla intrusion according to the IUGS classification and identified four discrete phases; a cumulate gabbro, a quartz diorite, a tonalite and a leuco tonalite.

The tonalite is not mineralogically distinguishable from the quartz diorite. Modal proportions indicate that the tonalite does consistently contain more quartz than the quartz diorite and petrological studies indicate that the rock is coarser-grained and more equigranular than the latter. The leuco tonalite chemically resembles a trondhjemite and has similar modal proportions to the quartz diorite (Figures 21, 22).

In the study area, three discrete phases of the Mooshla intrusion were recognized, a quartz diorite, a porphyritic quartz diorite and a trondhjemite. These correspond to Langshur's (1990) tonalite, quartz diorite and leuco tonalite respectively. The cumulate gabbro crops out west of the Doyon property and was not observed during field mapping.

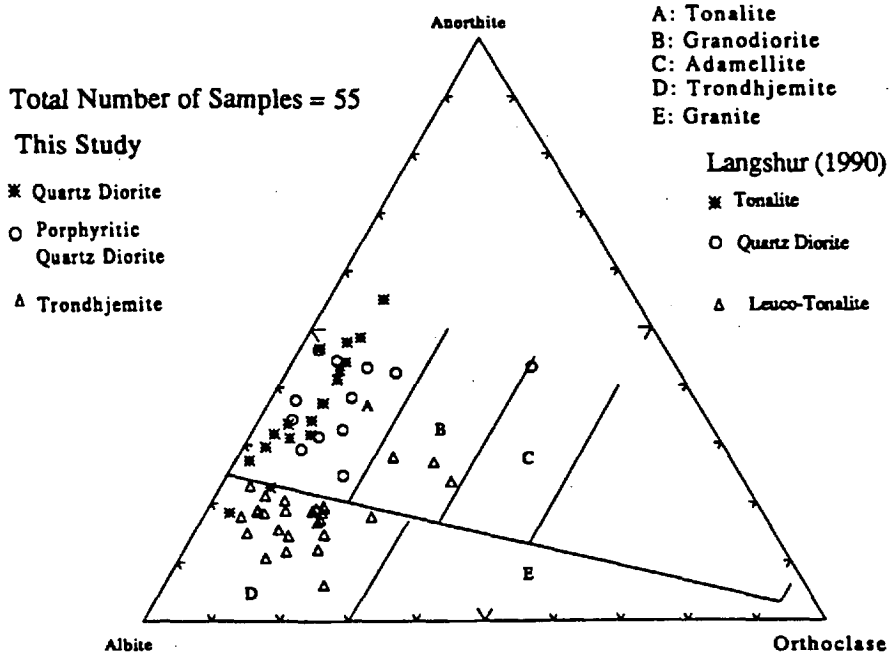


Figure 21. CIPW normative classification of the rocks of the Mooshla intrusion (Barker, 1979).

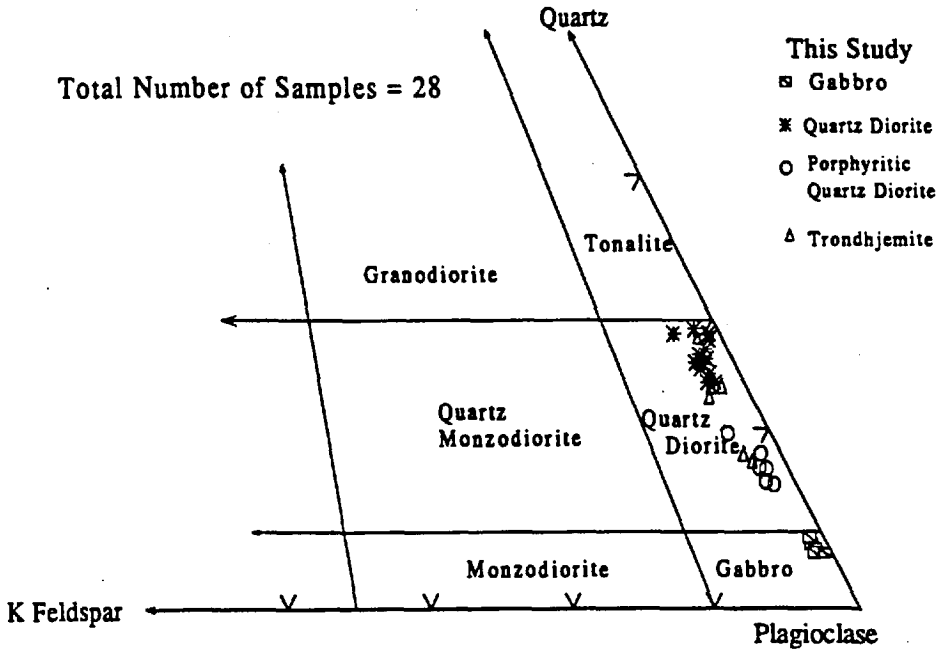


Figure 22. Modal classification of the rocks of the Mooshla intrusion (Streckeisen, 1976).

3.5.1 Quartz Diorite

Medium-grained hypidiomorphic quartz diorite occupies the northern and western part of the Mooshla Intrusion. The rock is essentially composed of plagioclase feldspar, chlorite, biotite, with 15 to 20 percent quartz and minor amounts of epidote, muscovite and calcite as alteration products (Table 3).

Plagioclase grains are subhedral, 13 to 20 mm in length, display Carlsbad twinning and have an anorthite content ranging from 5 to 26 percent (Langshur, 1990). The grains are saussuritized giving them a yellowish green appearance in hand specimen. Quartz is present as fine, anhedral grains interstitial to the feldspar and the amphibole grains. Amphibole grains are altered to chlorite and biotite along grain boundaries and cleavage planes. The amphibole ranges in composition from actinolitic hornblende to magnesio-hornblende (Langshur, 1990). Accessory minerals include epidote, apatite, magnetite, pyrite and zircon.

3.5.2 Porphyritic Quartz Diorite

A lens of porphyritic quartz diorite occupies the southern portion of the intrusion. This lens is entirely enclosed in the trondhjemite, has a maximum thickness of 200 metres at the surface and pinches out about 500 metres below surface. This rock is chemically very similar to the quartz diorite but texturally, is highly variable. Grain size is fine to medium with saussuritized plagioclase phenocrysts 10 to 15 mm in length. The rock consists of altered, anhedral feldspar phenocrysts in a fine-grained matrix of quartz, fine white mica (sericite) and chlorite with minor calcite, epidote, and pyrite. This rock has been intruded by the trondhjemite and in part has been digested by the latter, yielding a characteristic spotted texture (Figure 23). In places, an intrusive breccia is developed at its contact with the trondhjemite (Figure 24).

Table 3. Modal proportion (volume %) of minerals of the Mooshla Intrusive Complex.

	Quartz diorite	Porphyritic quartz diorite	Trondhjemite
Numbers of samples	17	6	5
Quartz	8 to 20	5 to 10	10 to 15
Plagioclase	50 to 60	40 to 50	50 to 65
Amphibole	0 to 10	15 to 25	0
Biotite	0 to 8	0 to 10	0 to 10
Chlorite	5 to 20	20 to 30	5 to 15
Muscovite	0 to 5	5 to 20	2 to 8
K-Feldspar	0 to 5	0 to 3	0 to 5
Average grain size (mm)	15	7	10

Data from Langshur (1990) and this study.



Figure 23. Photograph of spotted trondhjemite. Note chloritic blebs and fragment of porphyritic quartz diorite in upper corner of sample on the left. Ch = chlorite, Fg = fragment.



Figure 24. Photograph of intrusive breccia between trondhjemite and porphyritic quartz diorite. Note elongated porphyritic quartz diorite in whitish trondhjemite. Hammer handle is 30 cm.

3.5.3 Trondhjemite

Volumetrically, trondhjemite is the second largest member of the Mooshla Complex, and occupies the central and southern portion of the pluton. The rock is medium- to fine-grained and appears whitish grey in outcrop, and for this reason, has been given the field name alaskite by prospectors and mine geologists. Langshur (1990) identified this rock as leuco tonalite because of its similar modal composition to the quartz diorite, but chemically and petrographically it is very different from the quartz diorite and can best be described as a trondhjemite (Figures 21, 22). The rock consists of euhedral plagioclase crystals 5 to 6 mm long in a matrix of quartz, feldspar and chlorite. Feldspar exhibits good albite twinning and has an anorthite content of 30 to 35 percent. Chlorite is pleochroic light to dark green and is an alteration product after biotite. Quartz and feldspar are intergrown in a myrmekitic texture (Figure 25). The trondhjemite is cut by a set of micro-fractures parallel to the regional foliation. The fractures are filled with muscovite, and quartz appears to have been recrystallized along the wall of the fracture zones (Figure 26).

The trondhjemite intruded both the quartz diorite and the porphyritic quartz diorite as evidenced by the intrusive breccia at the contacts with the latter and by dikes of trondhjemite in the former (Stone, 1988). In the vicinity of the Doyon mine, the trondhjemite is altered to a quartz, sericite, pyrite rock (Figure 27). This altered trondhjemite is the host rock for the West zone of the Doyon mine.

3.5.4 Mafic Dikes

Several mafic dikes less than 10 metres wide cut the trondhjemite in the underground working at the Doyon mine. These are black to dark green, aphanitic to very fine-grained. Mineralogically, the rock consists of a fine-grained aggregate of quartz, feldspar, chlorite, white mica, biotite and calcite. Chlorite and muscovite are aligned parallel to the regional fabric.

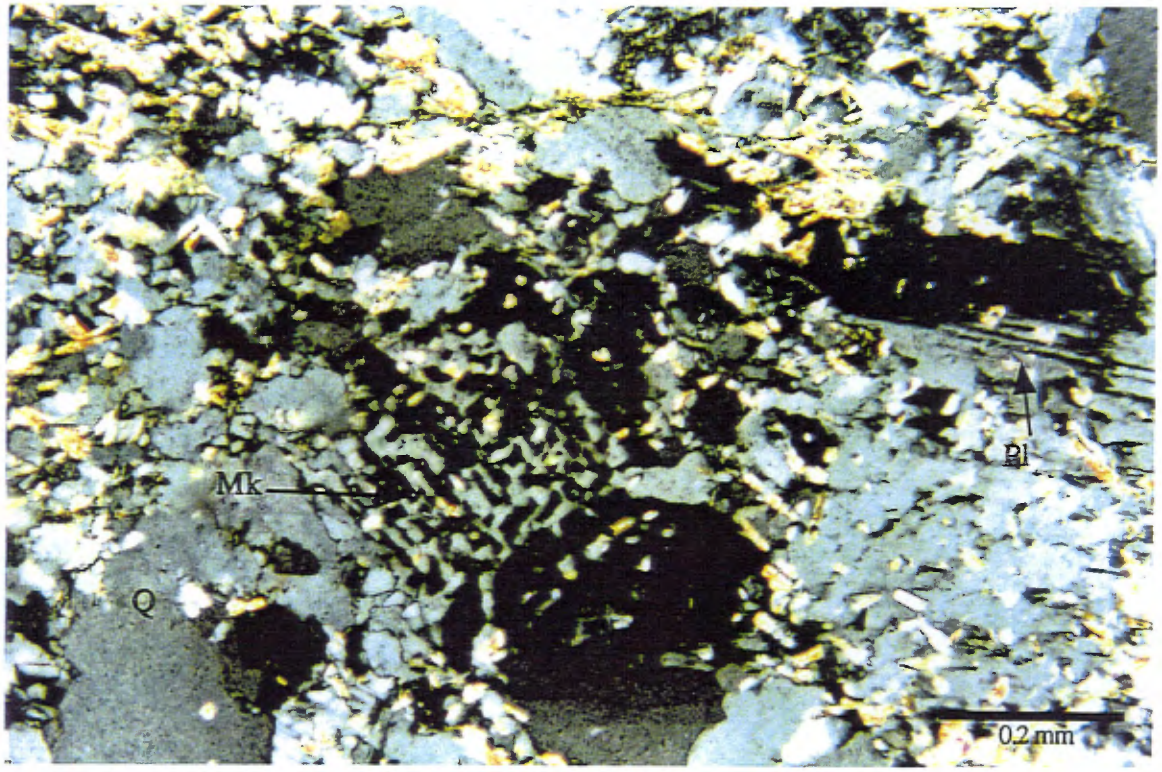


Figure 25. Photomicrograph of myrmekitic texture in trondhjemite. Sample 93-89. Transmitted light, crossed polars. 100X. Pl = plagioclase, Q = quartz, Mk = myrmekite.

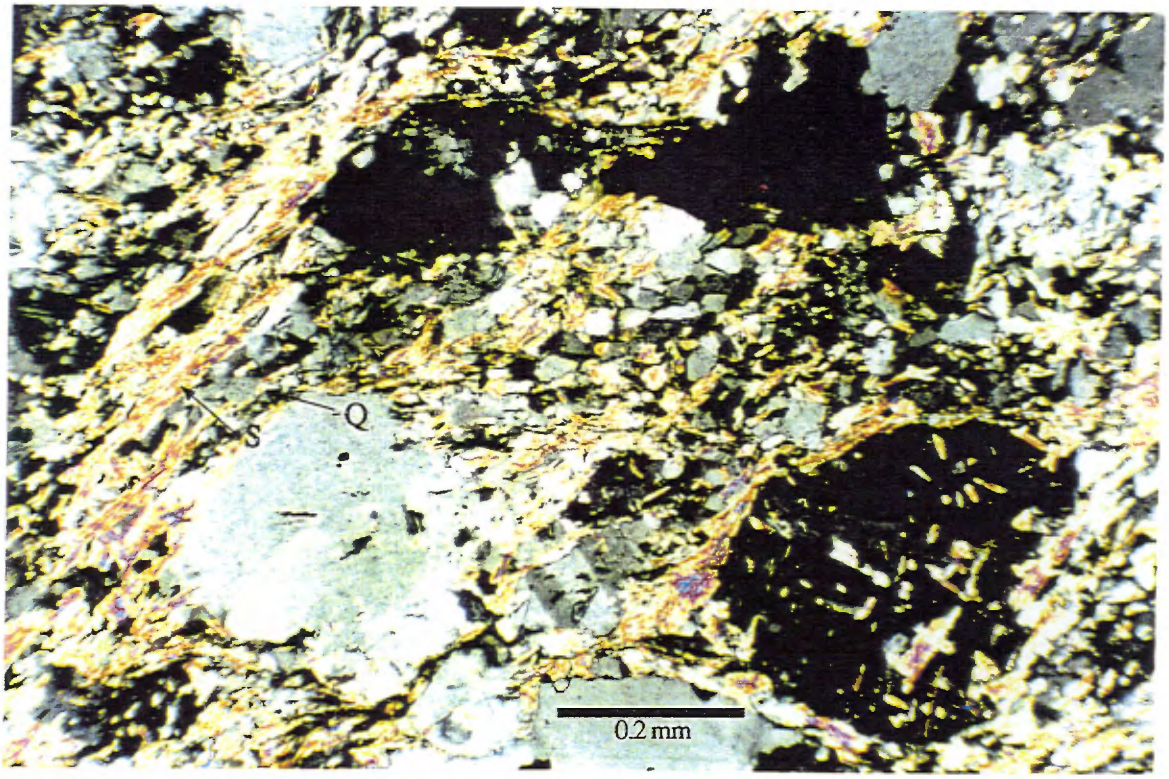


Figure 26. Photomicrograph of sericite-filled fractures in trondhjemite. Note re-crystallized quartz grains on fracture walls. Sample 93-100. Transmitted light, crossed polars, 100X. Q = quartz, S = sericite.

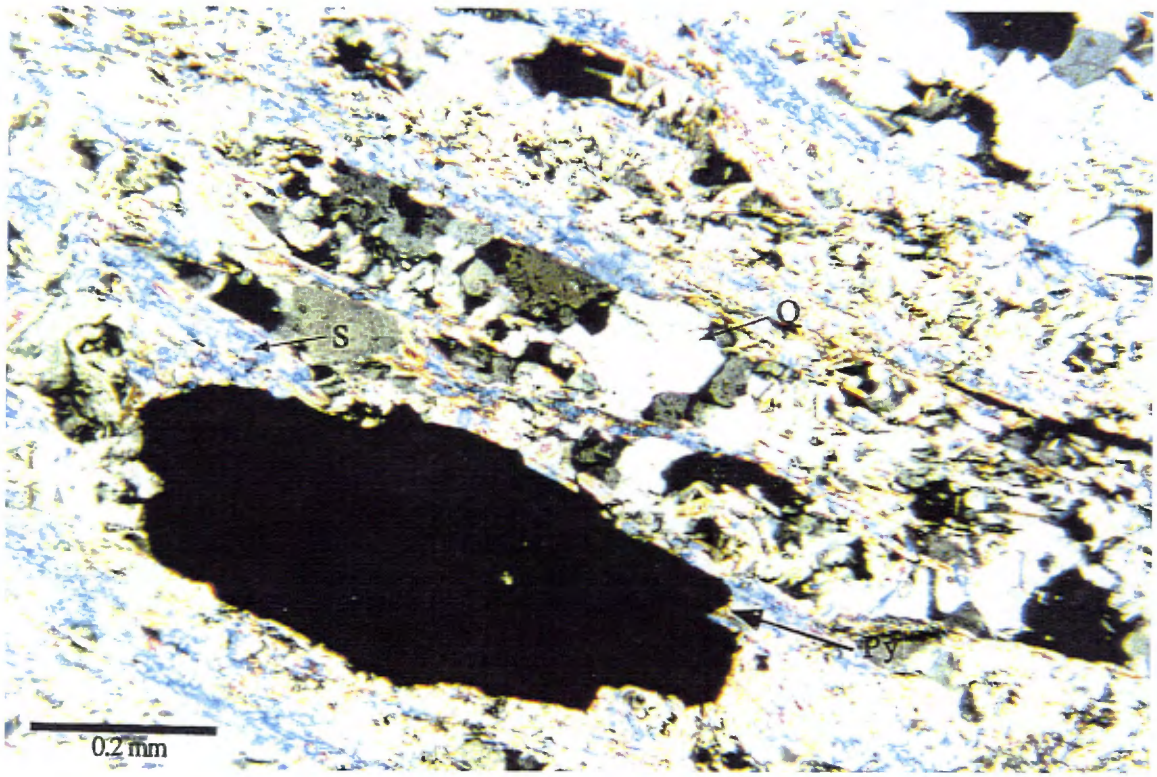


Figure 27. Photomicrograph of altered trondhjemite. Note quartz sericite and pyrite all aligned parallel to regional foliation. Sample 93-31. Transmitted light, crossed polars, 100X. Q = quartz, S = sericite, Py = pyrite.

Calcite is ubiquitous and appears to be post deformational (Figure 28). The dikes are un-mineralized and post-date gold mineralization. They are, however, displaced by later, complex faults indicating that some deformation is post-mineralization at the Doyon mine.

3.6 Diabase Dikes

Several northeast-trending, vertical Proterozoic diabase dikes intrude the Archean volcano-sedimentary rocks. These dikes are only weakly altered, with the augite being replaced by amphibole and the plagioclase saussuritized. The rock exhibits prominent ophitic texture and is commonly plagioclase-porphyritic (Stone, 1988). The diabase dikes have a strong magnetic response and contain abundant accessory magnetite. The dikes are post-gold mineralization and have been displaced right laterally by later faults.

3.7 Structure

All rocks of the area exhibit a penetrative foliation that strikes east-west and dips steeply to the south. This schistosity is deflected around the Mooshla intrusion and is generally parallel to the intrusive contacts (Savoie et al., 1990). Tourigny (1988) divided the rocks of Blake River Group in Bousquet Township into two separate structural domains. Units 1 and 2 of the first volcanic cycle belong to structural domain 1 while units 3 to 6 of the second and third cycles belong to structural domain 2. Rocks of domain 1 were interpreted as representing a relatively undeformed, south-facing sequence of basaltic flows and felsic pyroclastic rocks. Rocks of domain 2 were interpreted as representing a 500 metre wide zone of deformation, consisting of schist and mylonite in fault contact with each other. No lithological correlation was assumed to be possible within the rocks of domain 2 (Tourigny, 1988). Mapping for this study is not in agreement with these observations.

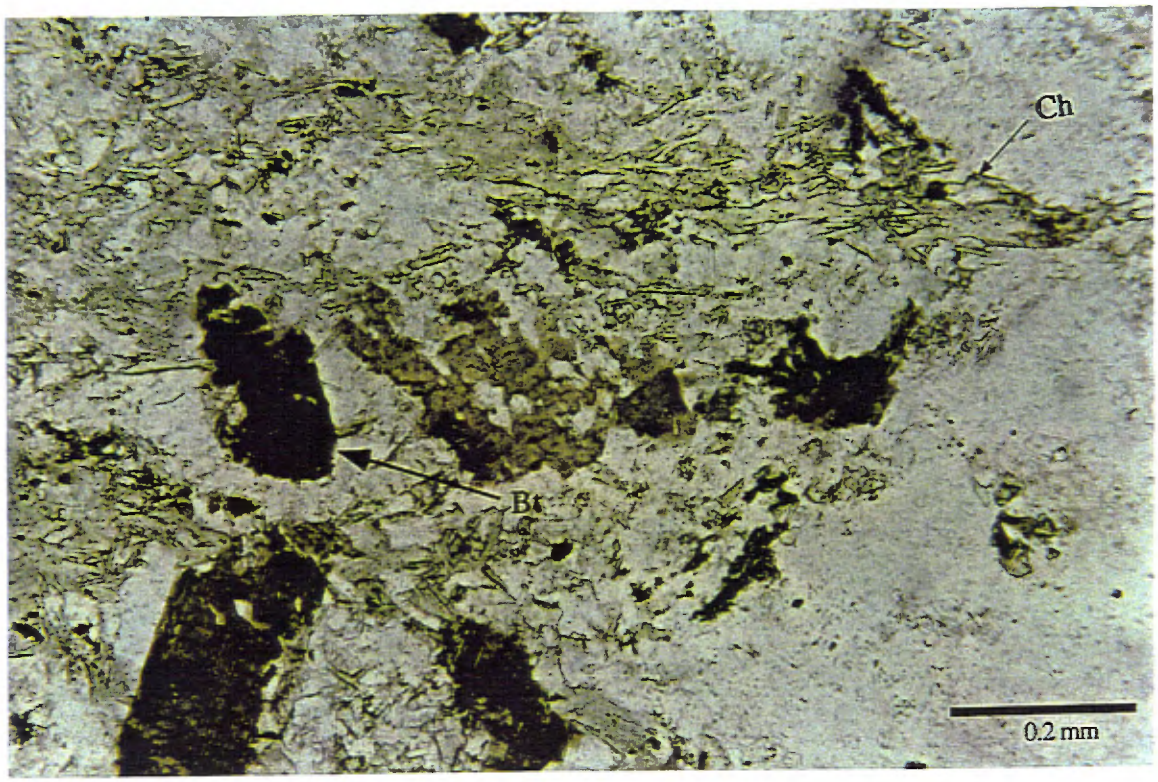


Figure 28. Photomicrograph of post-deformational biotite in mafic dike of the Mooshla intrusion. Note regional foliation indicated by alignment of chlorite grains. Sample 94-07. Transmitted light, plane polarized, 100X. Bt = biotite, Ch = chlorite.

Current mapping instead, indicates that the rocks of the Blake River Group have been folded into a single, south-facing homocline. Although no major folds are recognized, several minor folds and crenulation of S_1 were observed (Figure 29). Deformation appears more intense in the rocks of units 3 to 5, where stratigraphic polarity cannot be definitely determined, but the structural deformation in unit 6 is similar to that of the rocks of units 1 and 2 of structural domain 1. Although deformation is intense in units 3 to 5, the volcanic stratigraphy can still be recognized. Pillowed flows and volcaniclastic horizons are traceable over the entire map area. Strain and shearing appear to have been focused along east-west-trending, anastomosing faults. Units 3 and 5 appear to have been strongly affected by the deformation, but movement of the fault block is not discernable across faults, and geological contacts appear unaffected by the deformation. Two distinct sets of lineations are present on the fault plane; an earlier lineation plunges 50 to 60 degrees west while the later lineation is sub-horizontal.

The entire area is cut by the younger, northeast-trending Doyon and Bousquet River faults. The latter fault has an apparent horizontal displacement in the order of 250 metres (Savoie et al., 1990) but displacement on the former is not fully understood although it is probably of similar magnitude.

3.8 Metamorphism

All rocks of the Blake River Group have been metamorphosed to upper greenschist facies (Jolly, 1978; Stone, 1988). The typical mineral assemblage in the mafic volcanic rocks includes chlorite, garnet, biotite and white mica. Hornblende, oligoclase and biotite are present in rocks of unit 1 and in the quartz diorite of the Mooshla intrusion (Marquis et al., 1990). The assemblage of hornblende, oligoclase, biotite, and clinozoisite suggests that prograde metamorphism attained the greenschist-amphibolite transition with temperature of 440 ± 25 °C, as calculated by Stone (1988) from the plagioclase-amphibole geothermometer (Spear 1980). Epidote, clinozoisite and calcite are all

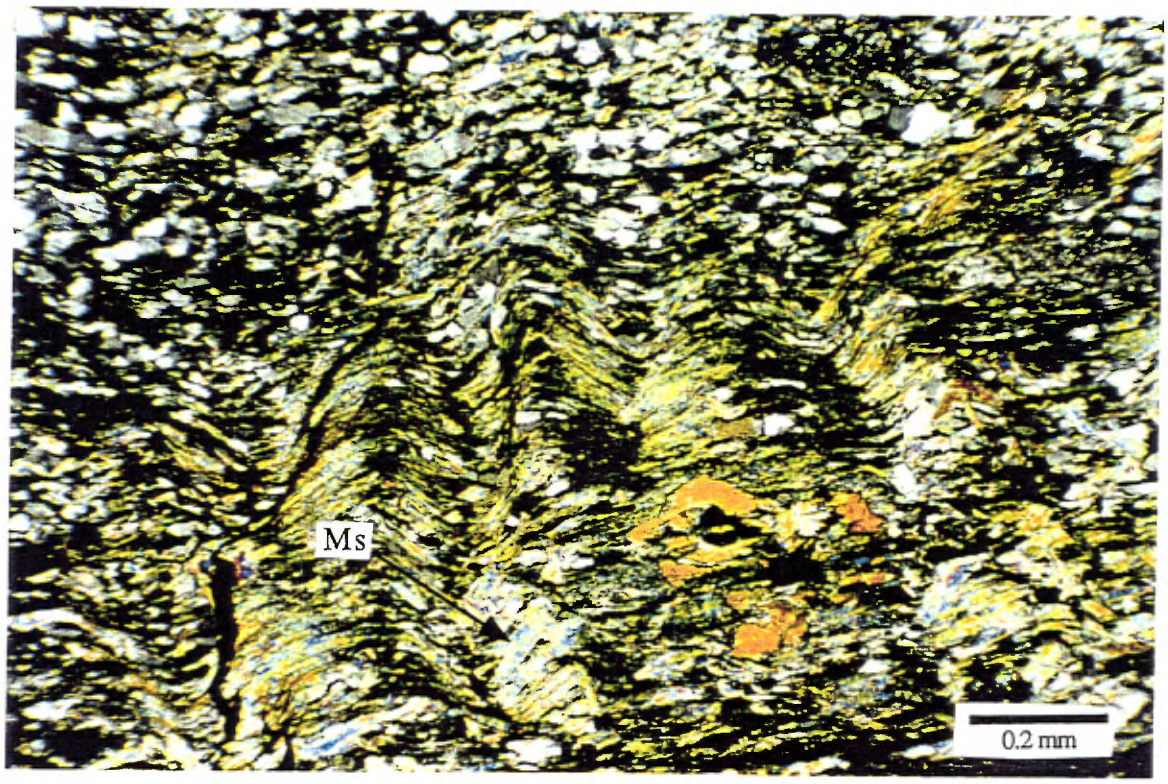


Figure 29. Photomicrograph of kink crenulation of S_1 schistosity. Sample 93-81. Transmitted light, crossed polars, 75X. Ms = muscovite

common accessory minerals and together amount to 20 percent of the rock volume (Figure 30).

Felsic units of the Blake River Group are characterized by intense sericitization near the Mooshla intrusion and by the presence of andalusite porphyroblasts on the Bousquet Property (Figure 31). The presence of andalusite indicates that pressure was less than 3.8 kbar (Holdaway, 1971). The assemblage of andalusite, chlorite, oligoclase and the ductile behavior of the country rock suggest that maximum prograde metamorphism was achieved between 400 to 450 °C and pressures of 2 to 3.8 kbars (Marquis et al., 1990, Figure 32).

Retrograde reactions have partially replaced primary metamorphic minerals. Biotite is partially replaced by chlorite, hornblende is rimed by actinolite and andalusite is replaced by kaolinite and diaspore.

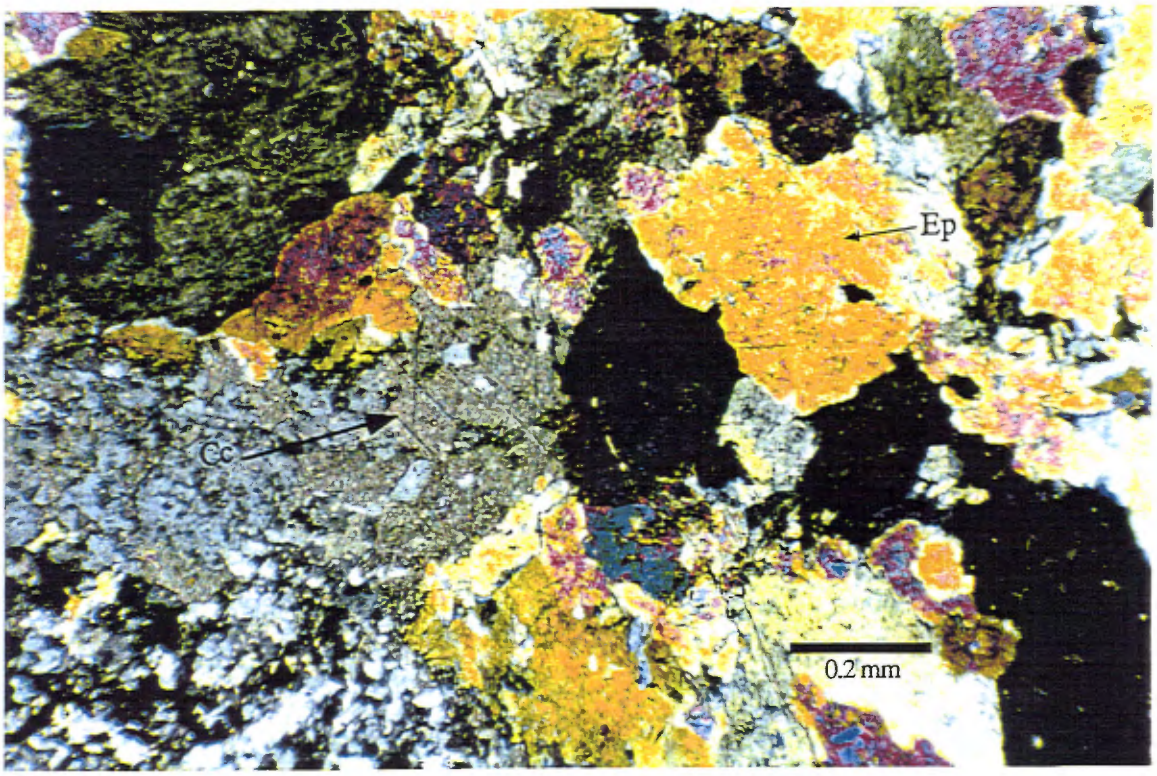


Figure 30. Photomicrograph of epidote and calcite alteration in mafic rocks of the Blake River Group. Sample 93-47 from unit 3. Reflected light crossed polars, 75X. Ep = epidote, Cc = calcite.

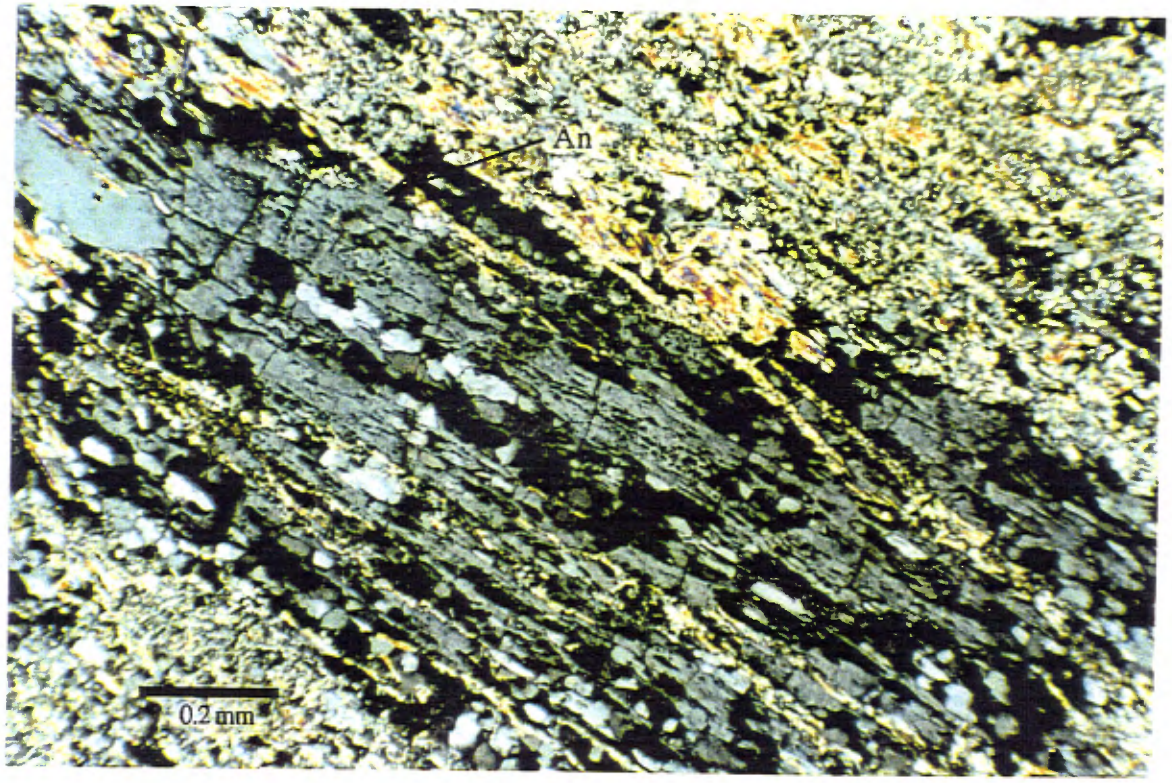


Figure 31. Photomicrograph of large tabular andalusite porphyroblast partly altered to kaolinite and diaspore. Sample 94-93, unit 5 Bousquet No. 1 mine. Reflected light crossed polars, 75X. An = andalusite

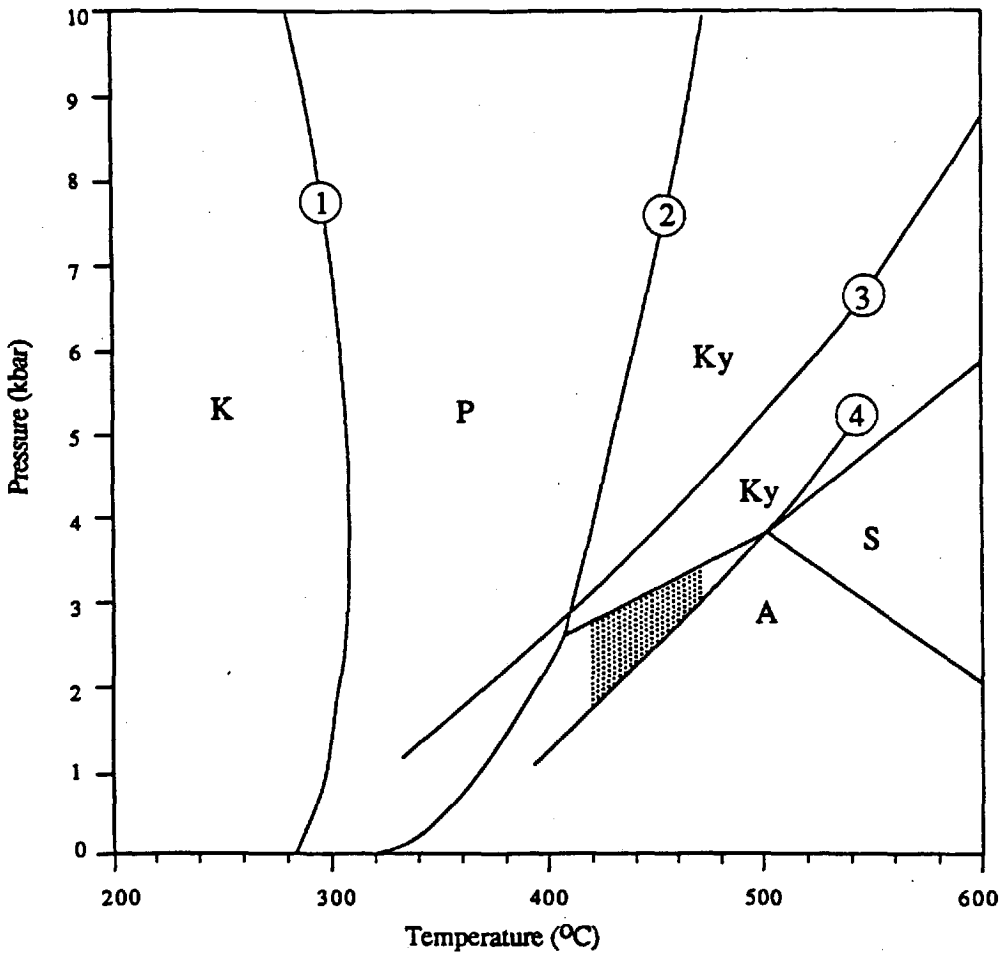


Figure 32. P-T diagram of peak metamorphic conditions at the Bousquet No 2 Mine. (Marquis et al., 1990 with modifications). A: andalusite; K: kaolinite; Ky: kyanite; P: pyrophyllite; S: sillimanite.

1) Kaolinite = Pyrophyllite + H_2O (Hemley et al., 1980)

2) Pyrophyllite = Andalusite + Quartz + H_2O (Hemley et al., 1980)

3) Oligoclase in reaction (Maruyama et al., 1983)

4) Chlorite out reaction (Maruyama et al., 1983)

Invariant point from Holdaway (1971)

Chapter 4
GEOLOGY OF GOLD OCCURRENCES

4.1 Introduction

A total of eleven gold occurrences are located within the study area, each consists of one or more mineralized zones (Table 4). Four of these occurrences are being mined while the others remain sub-economic at the present gold price. Two occurrences, the Ellison and Dumagami, are not described because they were not accessible for sampling or mapping. Each occurrence is characterized by a specific host rock, ore type and alteration assemblage. To develop a comprehensive metallogenic hypothesis, each occurrence with its corresponding mineralized zones, or ore is described in its stratigraphic position from lowest in the north to highest in the south, and east to west as outlined in Table 4 and figure 33.

4.2 # 6 Occurrence

The # 6 occurrence is within a shear at the upper contact between units 2 and 3 on the Bousquet property (Figure 33). The occurrence is 700 metres long, 10 to 15 metres wide and has an average gold grade of 0.03 oz/ton but no substantial reserves (Valliant, 1981). Its western part is within the quartz porphyritic rock of unit 2 whereas its eastern part is in the mafic pyroclastic rock of unit 3 (Tourigny and Hubert, 1986). The occurrence consists of three sub-parallel, semi-concordant, discontinuous, zones 1 to 2 metres wide of 10 to 30 percent disseminated pyrite and pyrrhotite with lesser amounts of magnetite and sphalerite. All zones strike 095° and dip 80° south (Valliant, 1981).

These three mineralized zones have similar texture and mineralogy, except that sphalerite and magnetite, which are present in trace amounts in the lower two zones are

Table 4. Stratigraphic location of gold occurrences with mineralized zones.

Occurrence	Zones	Host Units	Volcanic Cycle
# 6 (Bousquet Property)	3 zones	2-3	1-2
# 5 (Bousquet Property)	1 zone	3-5	2-3
Westwood	2 zones	3-5	2-3
Ellison*	Zone C	3-5	2-3
	Zone B	5	3
	Zone A	6	3
Doyon Mine	Main Zone	4	2
	# 1 Zone	4-5	2-3
	West Zone	Mooshla	N/A
# 4 (Bousquet Property)	1 zone	5	3
Warrenmac	1 zone	5-6	3
Bousquet No. 1 Mine	# 3 Zone	6	3
	# 2 Zone	6	3
	# 1 Zone	6	3
Dumagami Mine*	Massive Zone	6	3
	South Zone	6	3
Bousquet No. 2 Mine	Massive Zone	6	3
	Fringe Zone	6	3
Mooshla A	1 zone	Mooshla	N/A

* Not included in current study.

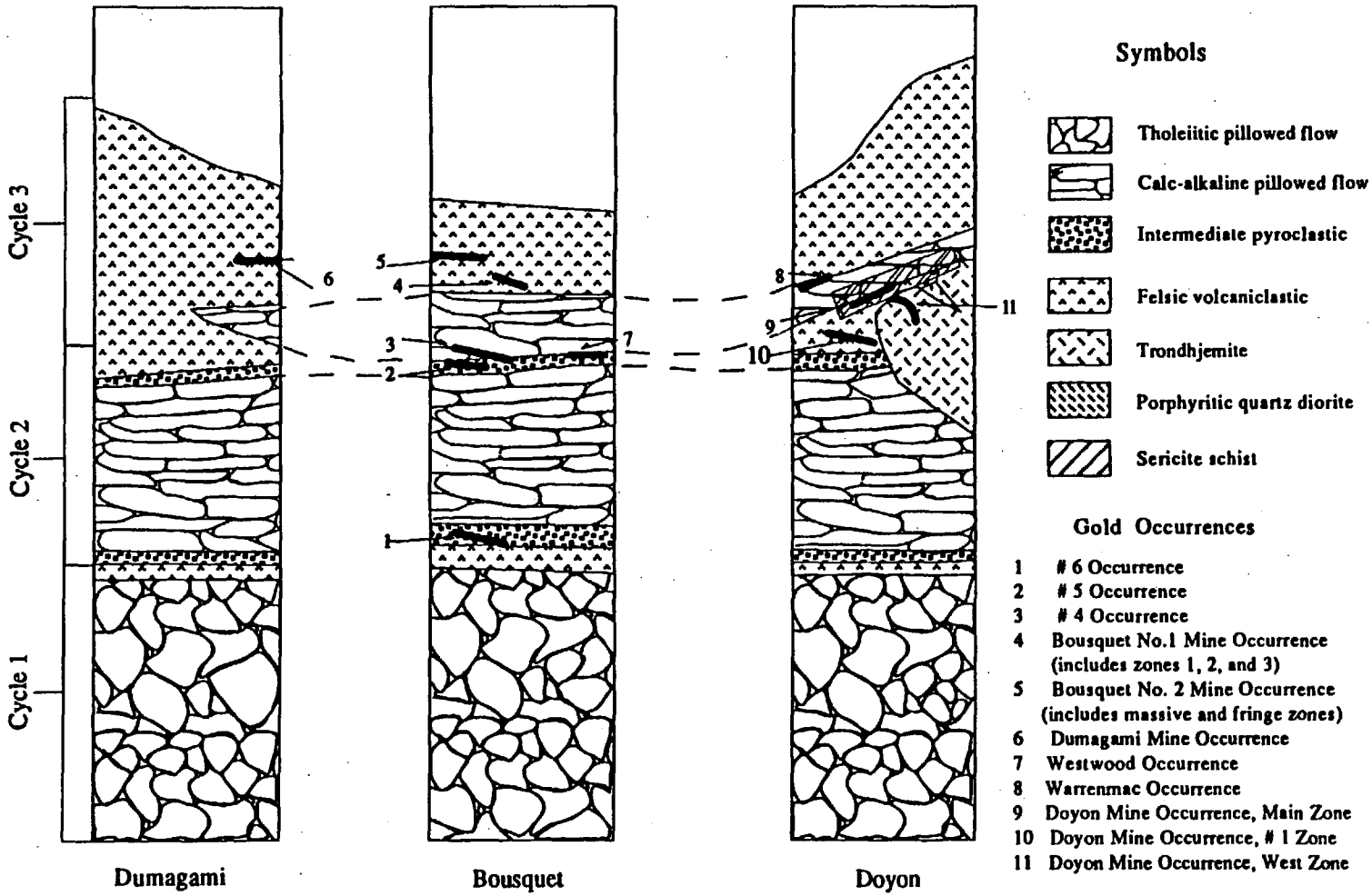


Figure 33. Schematic stratigraphic correlation diagram of rocks of the Blake River Group, Bousquet and Doyon properties.

thus at the same stratigraphic position as the # 5 occurrence (Figure 33). It consists of several trenches, now mostly covered with overburden and debris and, a 60 metres-deep vertical shaft with 300 metres of lateral development (Gunning, 1941). No significant reserves have been outlined. Gold is associated with two narrow, strongly sheared, carbonatized and chloritized zones in a fine-grained, mafic tuffaceous rock and with a boudinaged quartz vein. Sulfide minerals consist of finely disseminated euhedral pyrite and chalcopyrite Pyrite occurs as disseminations and as mm-scale bands sub-parallel to the foliation. Chalcopyrite is finer-grained and occurs with pyrite and with late carbonate minerals. Footwall to the occurrence is a blocky tuff that is identical to the blocky tuff located north of the # 5 occurrence on the Bousquet property.

4.5 Doyon Mine Occurrence

The Doyon Mine is the largest and most profitable gold deposit in the study area. Past production exceeds 3 million oz. and present reserves are 10 million tons averaging 0.18 oz. gold per ton, accounting for a total of some 4.8 million oz. of gold. The Doyon occurrence includes three mineralized zones, all of minable grade; the Main, the # 1 and the West zones (Table 5). The mine began operation as an open pit in 1980 to exploit the # 1 zone. Underground development began in 1983 to exploit the Main and West zones. Operations are now solely underground, and currently developed to a depth of 650 metres. Plans are to deepen the shaft 1,000 metres to access the downward extension of the West zone orebody (The Northern Miner, August, 1994).

The Main zone is hosted in the felsic volcanic rocks of unit 4 of the second volcanic cycle. The # 1 zone is hosted in the sericite schist at the contact between units 4 and 5, and the West zone is hosted by the Mooshla intrusion. Each mineralized zone is distinguished by a unique ore type. All ore zones dip steeply south and plunge 55° to the west (Savoie et al., 1986).

Table 5. Total reserves of mineralized zones of the Doyon Mine.

Zone	Reserves (tons)	Grade (oz/ton)
Main	6,000,000	0.15
# 1	1,000,000	0.16
West	3,000,000	0.25
Total	10,000,000	0.18

Source: Savoie et al., (1990).

4.5.1 Main Zone

The Doyon Main zone is 900 metres long, 5 to 60 metres wide and extends from surface to depths below the lowest level of the mine. Gold mineralization is hosted in several sub-parallel, en-echelon, semi-concordant quartz-pyrite-chalcopyrite layers 2 to 60 cm wide. The larger layers can be traced for tens of metres and strike 105° with a 55° dip to the south. The zone is semi-concordant with the regional foliation and truncated by a complex system of anastomosing faults which strike 80° to 100° north (Savoie et al., 1990). The zone is for the most part, hosted by the felsic rocks of unit 4. However, its western end is enclosed within the mafic volcanic rocks of unit 3 and its eastern end is terminated against the sericite schist at the contact of units 4 and 5.

The layers consist essentially of 60 to 70 percent white, recrystallized quartz, 20 to 25 coarse euhedral pyrite and 3 to 5 percent chalcopyrite. Calcite and chlorite are common accessories. Native gold occurs at pyrite grain boundaries or remobilized along with calcite and quartz in late fractures (Figure 34). Gold grains are microscopic to several mm in size. Chalcopyrite is hypidioblastic and interstitial to pyrite or in fractures within pyrite grains. Accessory minerals include calaverite, petzite, altaite, chalcocite, sphalerite and galena (Guha et al., 1982).

Below the 5-1 level of the mine (300 metres below surface), the Main zone is hosted by the trondhjemite phase of the Mooshla intrusion.

4.5.2 # 1 Zone

The Doyon # 1 zone is 180 metres long and 10 to 15 metres wide. Because of poor host rock competency, this zone was mainly mined from the open pit, but a few underground stopes were developed in the sericite schist. Gold is associated with irregular, semi-concordant lenses of semi-massive pyrite 5 to 20 cm wide (Figure 35). The pyritic lenses are sub-parallel to the regional foliation but generally dip 10 to 15° more steeply than the foliation of the host rock. The pyritic lenses consists of 80 to 90

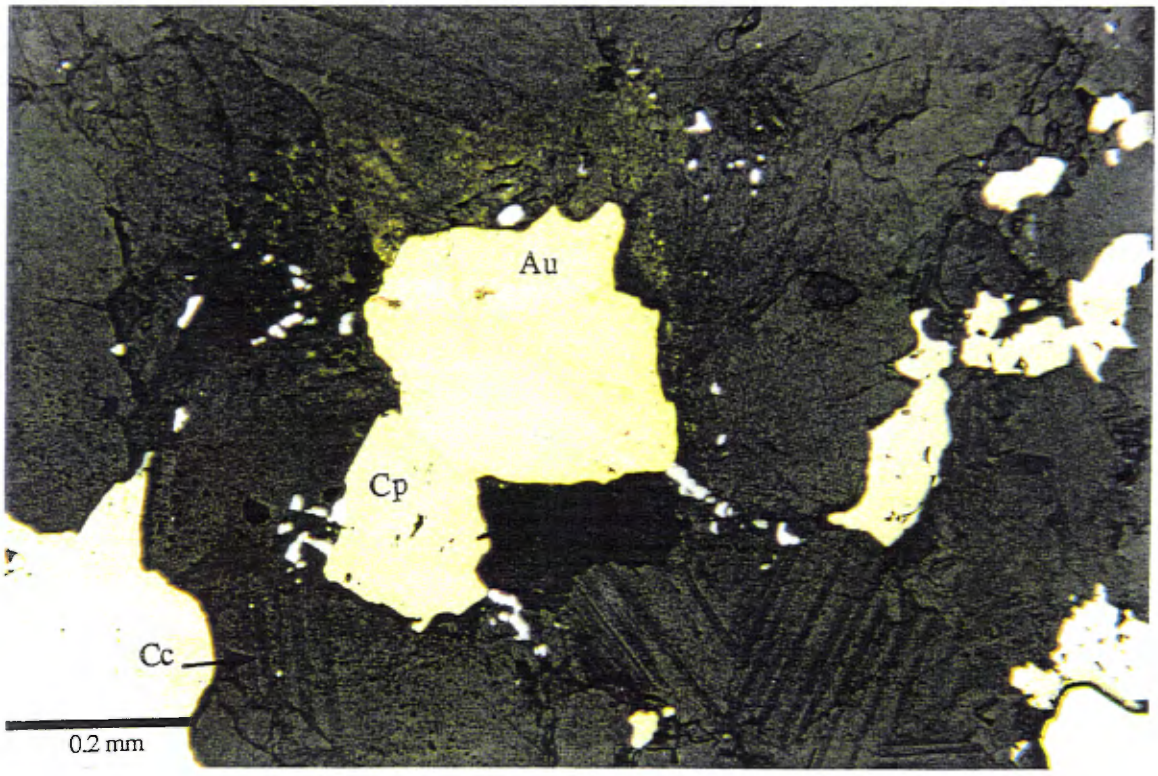


Figure 34. Photomicrograph of gold grain occurring with calcite and quartz. Sample 94-14. Reflected light, 100X. Py=pyrite, Cc=calcite, Au=gold, Cp = chalcopyrite.

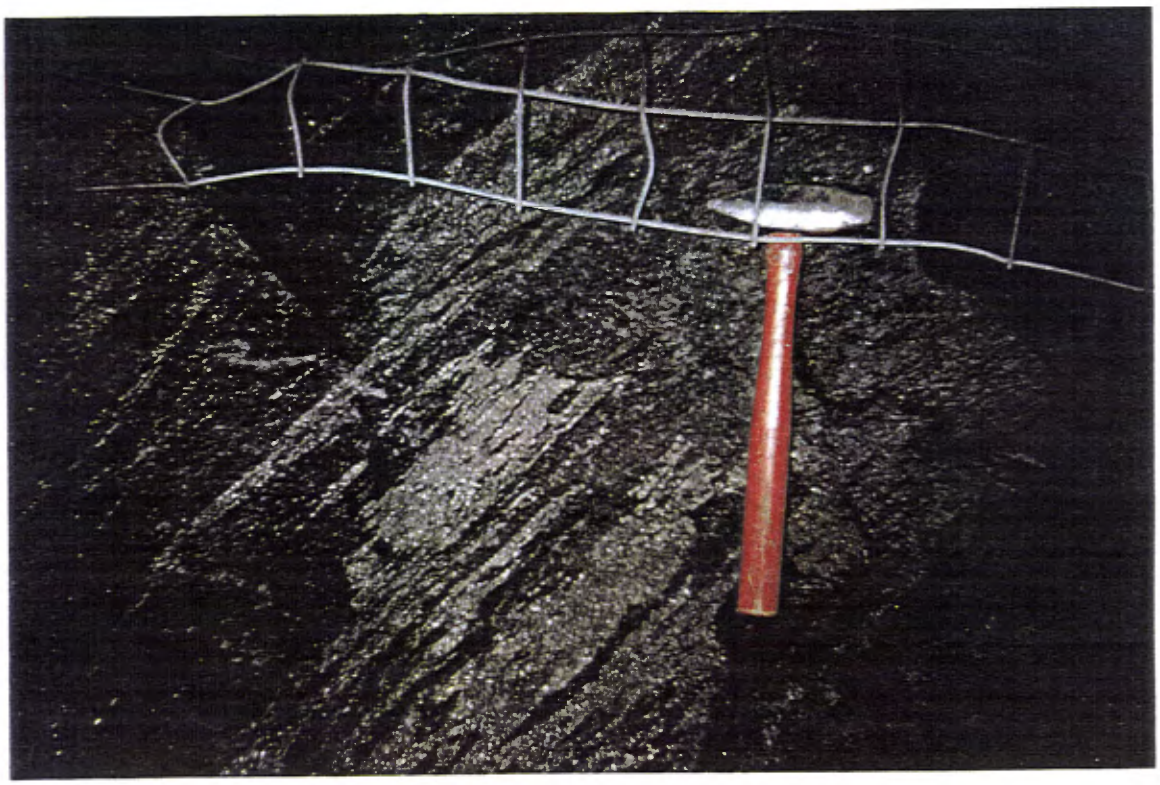


Figure 35. Photograph of irregular massive pyrite lenses in sericite schist of unit 4. Note discontinuous and sub-parallel nature of pyrite concentrations. Handle on hammer is 30 cm.

percent elongated, re-crystallized pyrite with minor amounts of chalcopyrite and pyrrhotite. Aggregates of pyrite are intergrown with quartz and chlorite, and many pyrite grains exhibit pressure shadows of muscovite. Some pyrite has been recrystallized in long, nematoblastic grains sub-parallel to the foliation (Figure 36). Chalcopyrite and pyrrhotite occur as finer, disseminated grains in a matrix of pyrite, quartz and muscovite. Although not observed during this study,rare grains of sphalerite, galena and arsenopyrite occur in the # 1 zone (Guha et al., 1982; Savoie et al., 1986). Gold is distributed along quartz-pyrite grain boundaries, and in cleavage planes of the micaceous minerals. Telluride minerals are very rare (Guha et al., 1982).

4.5.3 West Zone

The West zone is 600 metres long and approximately 75 metres wide and hosted in the Mooshla intrusion west of the Doyon fault (Savoie et al., 1990). Although not therefore part of the stratigraphic sequence, the zone is best described here for continuity with the other zones at the Doyon mine. The zone consists of varying types and combinations of veins.

From the surface to a depth of 350 metres, the zone is in the porphyritic quartz diorite, below that level, it is in the trondhjemite. Within the former, vein mineralogy and morphology are similar to those in the Main zone, except that veins of the West zone strike north-northwest to north-south and dip steeply to the west. Individual veins are 15 to 60 cm wide and traceable for ten's of metres. Some veins consist of massive pyrite, but most contain quartz, pyrite, chalcopyrite, sphalerite, carbonate and chlorite. Visible gold is common and gold content is proportional to the amount of chalcopyrite present. Veins are occasionally zoned with pyritic walls and a quartz-carbonate-rich core, but this zoning is crude and discontinuous (Figure 37). Pyrite grains are usually euhedral and coarse, up to 5 mm in maximum dimension. Chalcopyrite is fine-grained, surrounds the pyrite grains or forms inclusions in the euhedral pyrite. Gold occurs as small grains with

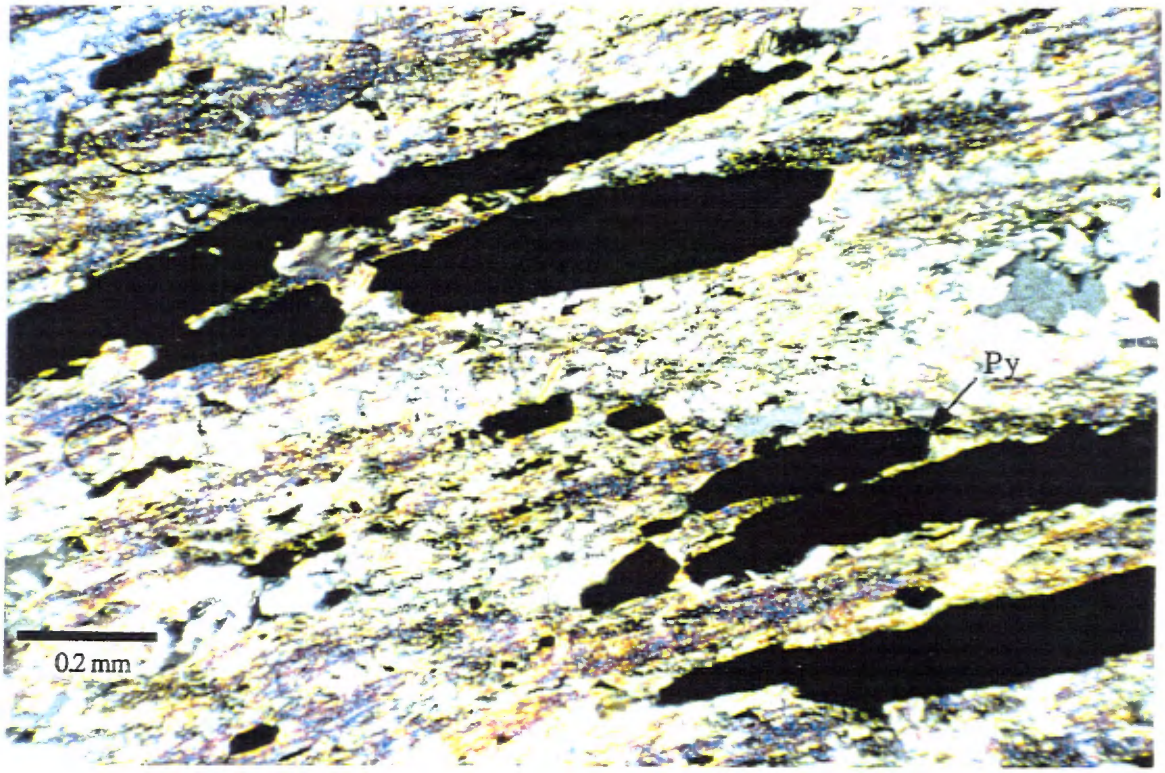


Figure 36. Photomicrograph of recrystallized nematoblastic pyrite # 1 Zone, Doyon Mine. Sample 93-103. Py = pyrite. Transmitted light, crossed polars, 75X.

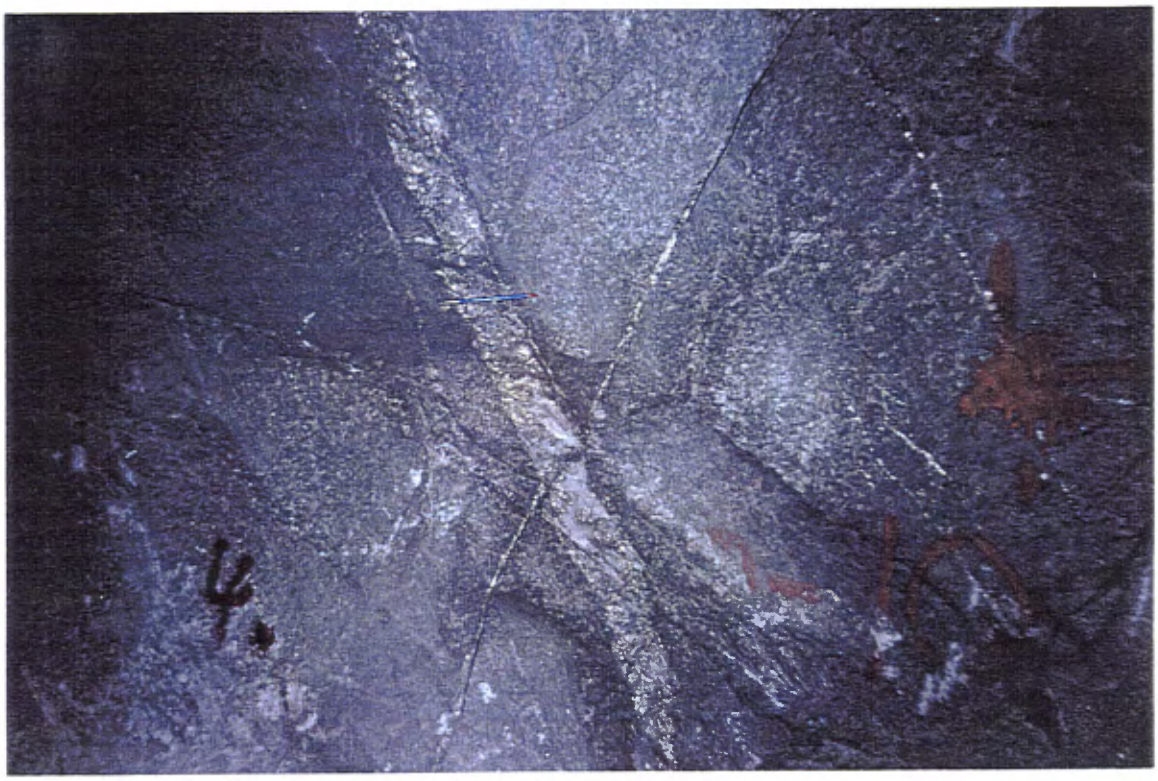


Figure 37. Photograph of narrow, zoned quartz-pyrite vein in porphyritic quartz diorite. Note crude zonation with highest pyrite concentration occurring near the vein walls next to pencil. 7-3 Level M10 vein. Pencil is 15 cm long.

the chalcopyrite or as large ones with calcite and quartz. Near the veins, the host rock is altered to a light brown or tan color. This alteration envelope is sericitic and has a well developed schistosity. Alteration halos are usually less than 60 cm wide regardless of vein thickness.

Veins in the trondhjemite are similar mineralogically to those in the quartz diorite, and in unit 4 but their morphology is quite different. Veins in trondhjemite are small, less than 10 cm wide, and most are traceable for only a few metres. Most veins consist of equal amounts of pyrite and quartz with 3 to 5 percent chalcopyrite, although some are of massive pyrite (Figure 38). Visible gold is also abundant and local grades in excess of 1 oz/ton are common.

The host trondhjemite is altered to a quartz-sericite-pyrite schist, and all igneous textures have been destroyed. Narrow quartz-pyrite veins are almost ubiquitous throughout the altered trondhjemite but are gold-bearing only where the host quartz-pyrite-sericite has more than 10 percent disseminated pyrite. The narrow gold-bearing veins are grouped in a minable zone that trends north-south and dips west, but within the zone, individual veins strike and dip in several directions. The veinlets when mined, have a uniform gold content of 0.25 oz/ton which makes them the richest ores in the Doyon Mine. As the mine progresses deeper, the narrow body of veinlet ore becomes a more important ore type and will probably soon be the largest source of gold production (L. Chenard, pers. comm.).

4.6 # 4 Occurrence

The # 4 occurrence is within the mafic volcaniclastic rocks of unit 5, 20 metres south of the # 5 occurrence, on the Bousquet property. It is a single mineralized zone 150 metres long and 2 metres wide that strikes parallel to the # 5 occurrence. Its reserves are calculated at 196,400 tons averaging 0.13 oz/ton gold. The occurrence is hosted in a fine-grained, banded rock consisting of dark green material intermixed with light brown



Figure 38. Photograph of massive pyrite vein in altered trondhjemite. Note disseminated pyrite in wall rock. Level 4-0, Doyon Mine, West zone. Red tip on pencil is 1.5 cm long.

aphanitic layers. The darker bands are chlorite-biotite-calcite-rich whereas the lighter colored bands are muscovite-quartz-ankerite-bearing (Figure 39).

Sulfide minerals include pyrite and minor chalcopyrite both as disseminations and veinlets oblique to the foliation. Minor pyrrhotite and magnetite are present within the mineralized zone. Native gold occurs in fractures in pyrite, at grain boundaries and in fractured quartz or with calcite (Tourigny, et al., 1989). Micaceous minerals are aligned parallel to the foliation and quartz is re-crystallized to a granoblastic texture.

4.7 Warrenmac Occurrence

The Warrenmac occurrence is situated between the Doyon Mine and the Bousquet River. It is a single mineralized zone within the mafic volcaniclastic rocks of unit 5, at or near their contact with the overlying unit 6. Current reserves are 100,000 tons grading 0.16 oz/ton gold. Gold is associated with a lens of massive pyrite-chalcopyrite-sphalerite up to 3 metres thick. Footwall of the lens of massive sulfide is a distinctive garnetiferous, chloritic mafic rock (Figure 40). The hanging wall is a siliceous, intermediate to felsic volcaniclastic rock. Away from the massive sulfide, the contact between the footwall garnetiferous and the hanging wall siliceous volcaniclastic rocks is both faulted and interdigiting. Gold content within the massive sulfide lens is associated with highest copper content.

4.8 Bousquet No. 1 Mine Occurrence

The Bousquet No. 1 Mine consists of three separate, heavily mineralized zones situated in fault-bounded blocks, at or near the contact between units 5 and 6, of the third and uppermost cycle, approximately 100 metres south of the # 4 occurrence. The three zones are closely spaced and, in the central parts of the mine, were mined as one single orebody. Since 1979, the mine has produced approximately 700,000 oz of gold and current reserves indicate that an additional 475,000 ounces could be produced (Table 6).



Figure 39. Photograph of fine-grained-banded rock from # 4 occurrence on Bousquet Property. Note the banding outlined by the alternating chloritic and ankeritic layers.

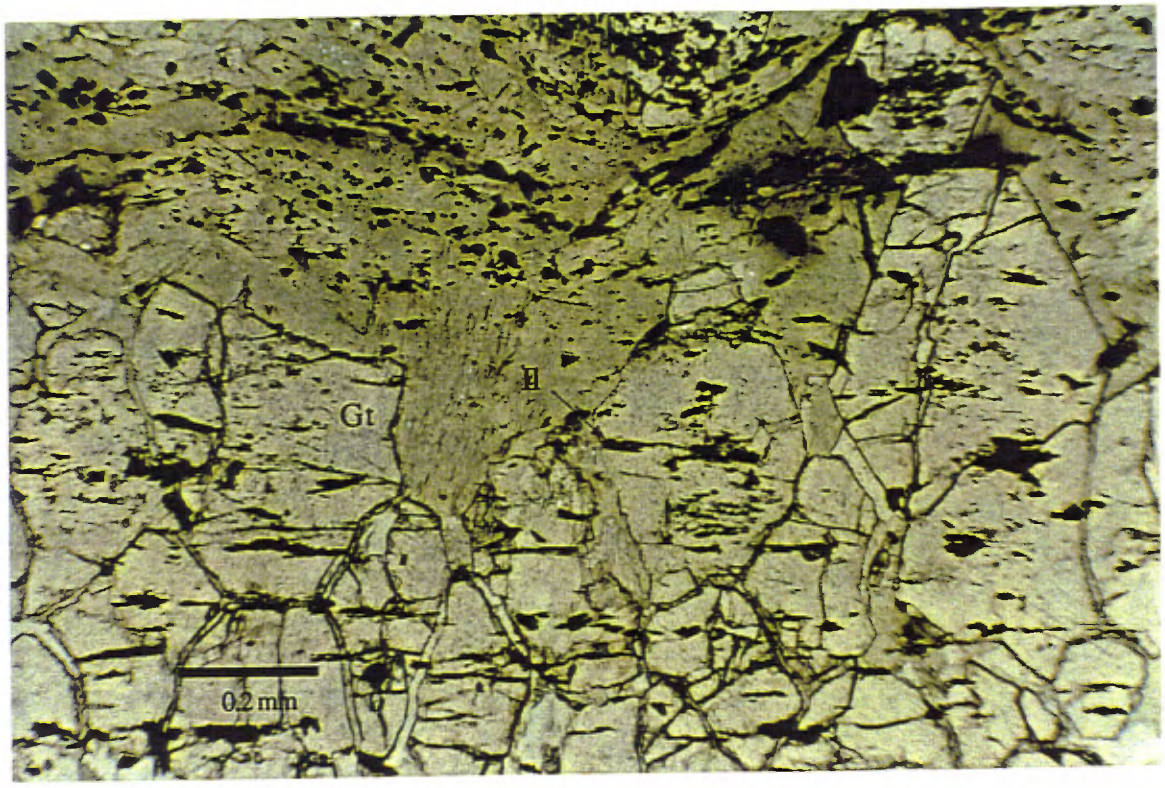


Figure 40. Photomicrograph of garnetiferous footwall rock from Warrenmac occurrence. Note linear inclusions of ilmenite in garnets. Sample 93-80. Gt = garnet, Il = ilmenite. Transmitted light 75X.

Table 6. Total reserves of mineralized zones of the Bousquet No. 1 Mine.

Zone	Reserves (tons)	Grade (oz/ton)
# 3	1,966,712	0.23
# 2	126,100	0.16
# 1	181,700	0.17
Total	2,274,512	0.21

Source: M. Arpin (pers. comm., 1995)

Stratigraphic relationships at the Bousquet No. 1 Mine have been interpreted as a homoclinal sequence younging to the south (Gunning, 1941; Valliant, 1981; Valliant and Hutchinson, 1982; Stone, 1988). Others have interpreted the sequence to lie on the south limb of a syncline, and the stratigraphic section to young to the north (Eliopoulos, 1983; Bateman, 1984). Work by Tourigny and Hubert (1986), and Tourigny (1988) indicates that faulting was the principal factor in controlling the current distribution of rock types, and that stratigraphic facing could not be inferred. Results of field mapping during this study are in agreement that reverse faulting and shearing played a major role in the present distribution of lithologic types at Bousquet No.1, nevertheless, the overall stratigraphic relationship of unit 6 overlying unit 5 is maintained along strike throughout the mine. The overall sequence is interpreted as younging to the south, and the stratigraphic ordering of the mineralized zones in the Bousquet No. 1 Mine is therefore # 3, # 2, and # 1 zones.

4.8.1 # 3 Zone

Geology and alteration of the important # 3 zone have been the focus of several studies (Valliant, 1981; Bateman, 1984; Tourigny, 1988). This zone is 3 to 15 metres wide, extends for 600 metres along its east-west strike, dips steeply south and plunges 65° west. Its thick central and eastern parts are mined out, but mining continues to the west of 6800E, where the zone bifurcates into a northern and a southern lens (Figure 41). Over 80 percent of the reserves at Bousquet No. 1 Mine are within this zone.

East of 6800E, the ore is light grey in color, aphanitic and very siliceous. It consists of alternating quartz, muscovite and pyrite in concordant, mm to cm wide bands defining a good layering. Pyrite is the most abundant sulfide and accounts for nearly 30 percent of the rock volume. It occurs as euhedral, disseminated grains 3 to 5 mm in diameter and as mm wide concordant bands of nearly massive, recrystallized pyrite. Plagioclase in the zone has been replaced by white mica, and quartz is recrystallized to

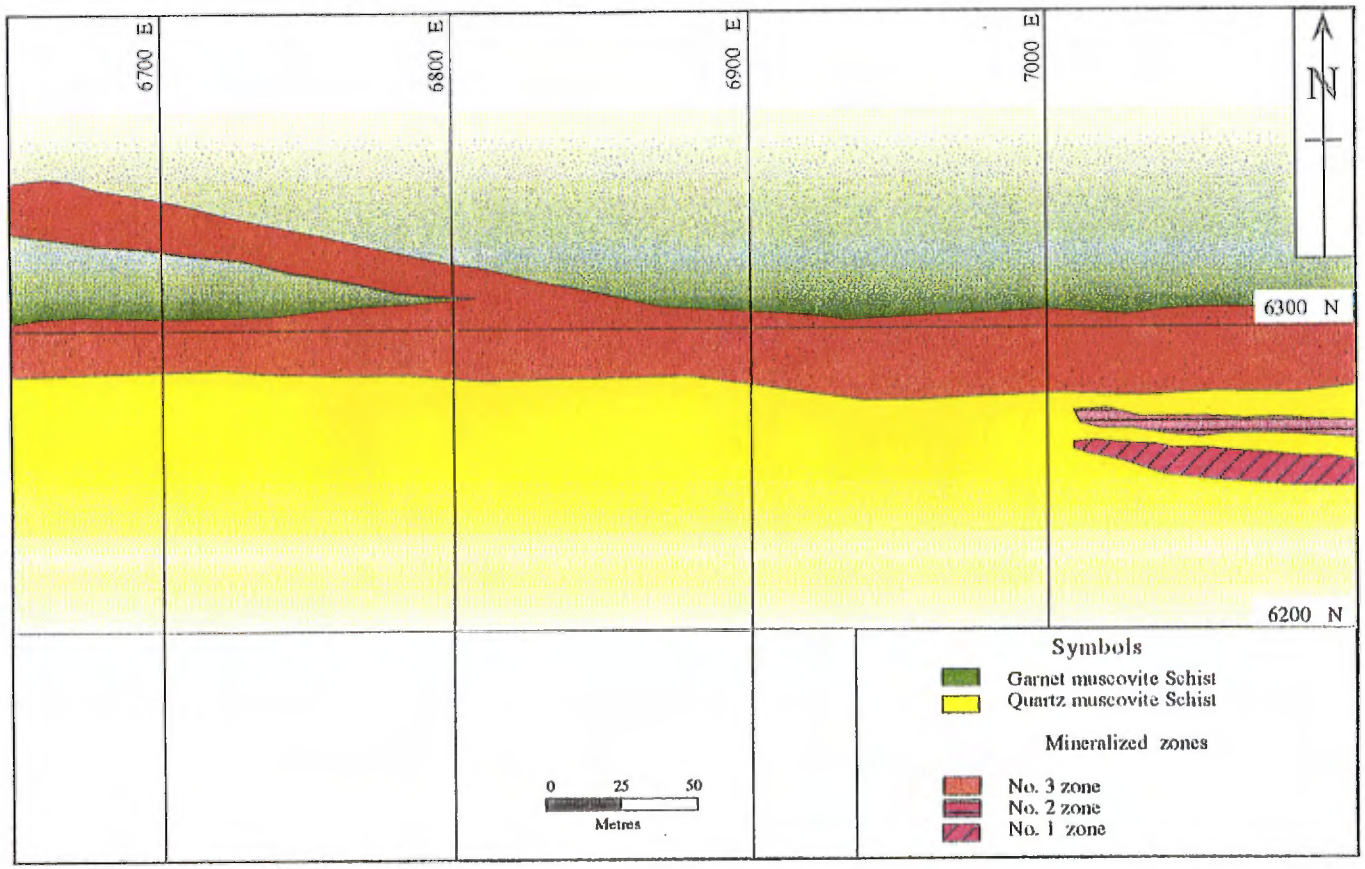


Figure 41. Typical plan view of the orebody at the Bousquet No. 1 Mine. Level 3-0 (180 m beow surface). (After Bateman, 1984, with modifications).

a granoblastic polygonal texture (Tourigny et al., 1989b).

Ore minerals include chalcopyrite, altaite, petzite, sphalerite and native gold (Gauthier, 1977). Gold forms 5 to 20 micron grains on silicate grain boundaries, on mica cleavage planes or as inclusions and fracture fillings in pyrite (Stone, 1988). Spectacular sheets of native gold several centimetres in diameter coat mm-scale fractures that cut the regional foliation at high angles. Chalcopyrite forms small, anhedral, disseminated grains interstitial to pyrite, and inclusions within pyrite grains. Sphalerite is a trace component throughout the zone but is concentrated in a discontinuous, semi-concordant, 10 cm wide band near the footwall contact of the zone (Valliant, 1981).

The footwall rocks of the # 3 zone are a distinctive manganiferous garnet-bearing mafic schist. This rock is aphanitic, dark green to black, 1 to 10 metres thick, and extends along strike beyond the mineralized zone (Valliant, 1981). The amount of garnet in the footwall and the thickness of garnet-bearing rock are proportional to the pyrite and gold content of the ore zone (Valliant and Barnett, 1982). The rock consists of alternating, mm-scale, quartz-rich and muscovite-chlorite rich bands that contain up to 25 percent porphyroblasts of pink garnet 3 to 5 mm in diameter (Figure 42). Calcite, ilmenite, apatite and chlorite are also present in minor amounts. The garnetiferous mafic schist is in fault contact with the ore-bearing quartz-sericite schist, and laterally grades into a fine-grained mafic tuff of unit 5.

The hanging wall of the # 3 zone is a dark grey, andalusite-bearing schist. This rock is 1 to 3 metres thick and extends for 500 metres along strike beyond the mineralized zone. Laterally, the andalusite schist grades into a fine-grained, felsic volcaniclastic rock of unit 6. Mineralogically, the andalusite schist consists of 15 to 20 percent andalusite poikiloblasts, up to 1 cm in diameter, altered to a fine-grained aggregate of diaspore and kaolinite, within a muscovite-quartz-rich matrix (Figure 43). The matrix consists of 40 to 50 percent granoblastic, polygonal quartz with



Figure 42. Photograph of manganiferous garnet rock from Bousquet No. 1 Mine Sample 94-74. Note pink garnet porphyroblasts in aphanitic chloritic matrix. Gt = garnet.

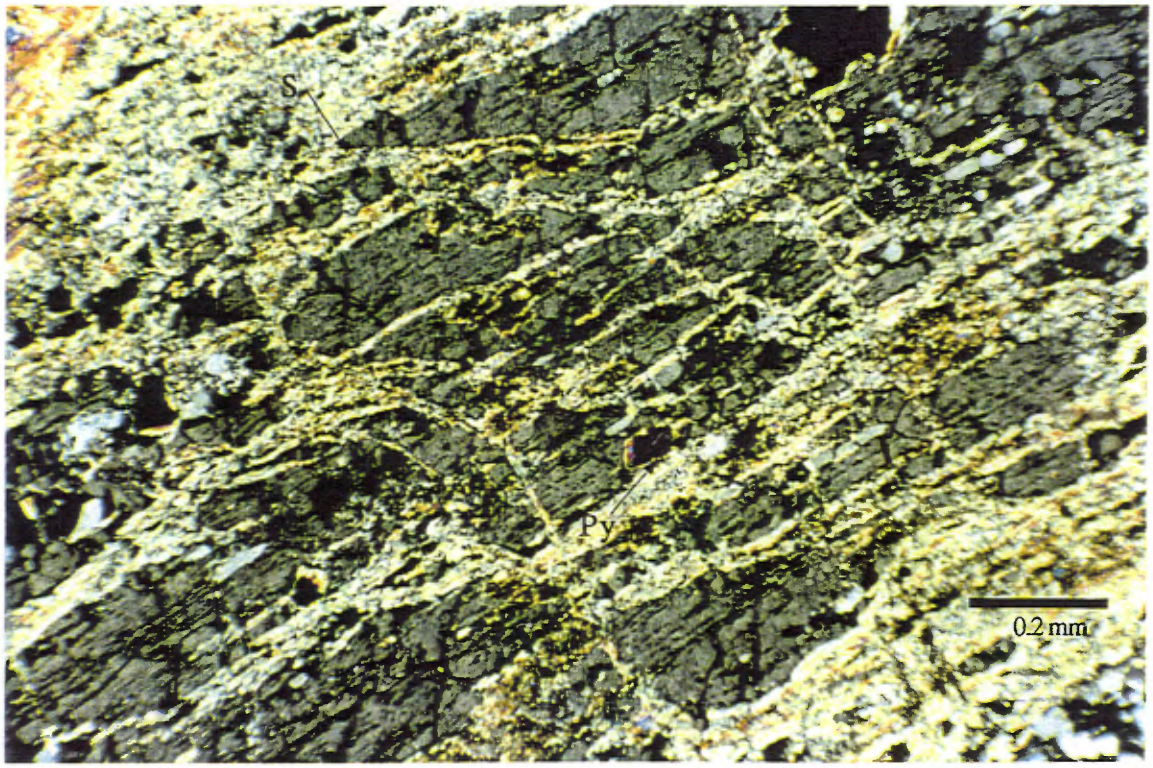


Figure 43. Photomicrograph of altered andalusite porphyroblast from Bousquet No. 1 Mine. Note sericite in fractures and fine inclusions of pyrite. Py = pyrite, S = sericite. Sample 94-40. Transmitted light, crossed polars 75X.

20 to 30 percent lepidoblastic muscovite, pyrophyllite and minor kyanite (Bateman, 1984). Disseminated, euhedral pyrite comprises up to 15 percent of the rock. Apatite and rutile are accessory minerals.

West of 6800E, gold mineralization is hosted in two lenses of quartz-sericite rock, 1 to 2 metres wide, separated by a 10 metre-wide band of chloritized mafic rock containing less than 5 percent disseminated pyrite, the rock is garnetiferous near the footwall of both lens and identical in composition to the garnetiferous rock east of 6800E. Both mineralized lenses contain similar sulfide minerals in the central portion of the zone, east of 6800 E. However, the northern lens is hosted in a felsic schist that lacks andalusite, whereas the host rock of the southern lens are similar to those of the central portion.

4.8.2 # 2 Zone

This zone is 4 metres wide, extends for 200 metres along its east-west strike, dips steeply south, and lies 10 metres statigraphically above the # 3 zone. It is hosted in a strongly sheared, light brown to buff colored quartz-sericite-andalusite schist containing 5 to 10 percent disseminated pyrite. A 10 to 15 cm wide boudinaged, smoky quartz "layer" usually marks the lower contact of the zone. The footwall rocks are sheared, chloritic, siliceous, felsic volcaniclastic rock with 3 percent disseminated pyrite. These rocks are in fault contact with the hanging wall andalusite schist of zone 3. The hanging wall rocks are similar to the rocks that host the mineralization. Sulfide minerals, pyrite, chalcopyrite, sphalerite and minor pyrrhotite occur both as disseminations and in mm-scale, discordant to semi-concordant, discontinuous layers. Gold occurs as micron sized grains as inclusions in chalcopyrite.

4.8.3 # 1 Zone

The # 1 zone is the southernmost zone at the Bousquet No. 1 Mine, it is 3 metres wide, extends for 380 metres along its east-west strike and lies 5 metres stratigraphically above the # 2 zone. It consists of a 2 to 3 metre-wide quartz-sericite-andalusite rock identical to that of the # 2 zone. The hanging wall rocks are a dark to light brown, chloritic, andalusite schist that contains minor sphalerite in discordant veinlets.

Sulfide mineralogy consists of discordant and semi-concordant chalcopyrite and pyrite bands 1 to 2 cm wide. Gold is associated with chalcopyrite along with minor amounts of sphalerite and gudmundite (Tourigny et al., 1989a).

4.9 Bousquet No. 2 Mine Occurrence

The Bousquet No.2 Mine has produced over 750,000 oz of gold since it began production in 1990 after its discovery by drilling the down-plunge extension of the previously known Dumagami occurrence. It has combined total reserves of 7.6 million tons averaging 0.19 oz/ton gold, 0.4 oz/ton silver and 0.47 percent copper (A. Bourget, pers. comm., 1995). The geology and mineralogy of the deposit have been the focus of several recent research papers, (Tourigny et al., 1993; Marquis et al., 1992; Teasdale et al., 1995; Teasdale, in progress) hence only a brief description of the geology is included here.

This important occurrence includes two separate mineralized zones, named massive and fringe by the mine geologists. The massive zone consists of a well-zoned, complex massive sulfide body and siliceous stockwork mineralization. The fringe zone consists of disseminated and stringer pyritic mineralization. Both zones are hosted in felsic pyroclastic rocks of unit 6 that are altered to an andalusite-muscovite rock. The andalusite-bearing schist is in fault contact with a garnetiferous-quartz-sericite schist in the footwall and a garnetiferous-chlorite schist in the hanging wall. All contacts dip steeply south and strike east-west.

4.9.1 Massive Zone

Over 80 percent of the current reserves are within the massive zone which consist of a well zoned pyritic, massive sulfide orebody that extends 275 metres along its east-west strike, 1,000 metres down dip and is 5 and 20 metres thick. It is composed of five distinct segments including, from footwall to hanging wall, a footwall lens of massive pyrite, a siliceous, pyrite-chalcopyrite stockwork, a complex main body of massive pyritic sulfide, a layer containing discordant chalcopyrite veinlets, and a concordant layer of sphalerite-rich bands all of them gold bearing (Figure 44).

The lower contact of the footwall lens is a fault that marks the lower limits of the orebody (Tourigny et al., 1993). The footwall lens of massive sulfide lens consists of 95 to 98 percent recrystallized pyrite and is 30 to 60 cm wide with only minor chalcopyrite, bornite and sphalerite. The lens is slightly oblique to the foliation of its host andalusite schist and has sharp upper and lower contacts. A siliceous rock that contains 20 to 30 percent pyrite-chalcopyrite in a stockwork of mm-wide veinlets overlies the footwall lens (Figure 45). Gold occurs in the siliceous stockwork as micron-sized grains at pyrite grain boundaries, and at triple junctions of recrystallized pyrite grains (Tourigny et al., 1993). The siliceous stockwork grades upward into the complex body of massive sulfide that forms the main part of the orebody.

The complex main massive sulfide body is tabular, 1 to 5 metre wide, oriented parallel to the foliation, and of both massive and brecciated layers. Individual massive pyritic layers are 0.2 to 1.5 metres wide, contain 95 percent recrystallized pyrite and 2 to 5 percent bornite, with minor chalcopyrite. The contact between layers of massive pyrite and the overlying rock is very sharp and commonly sheared (Figure 46). Within the massive sulfide body, pyrite is recrystallized and granoblastic. Bornite, with chalcopyrite and tennantite, is interstitial to the pyrite grains and occupies fractures in both pyrite and quartz, and these are perpendicular to the regional foliation. A 1 to 2 metre-wide, discontinuous breccia occupies the central portion of the complex massive

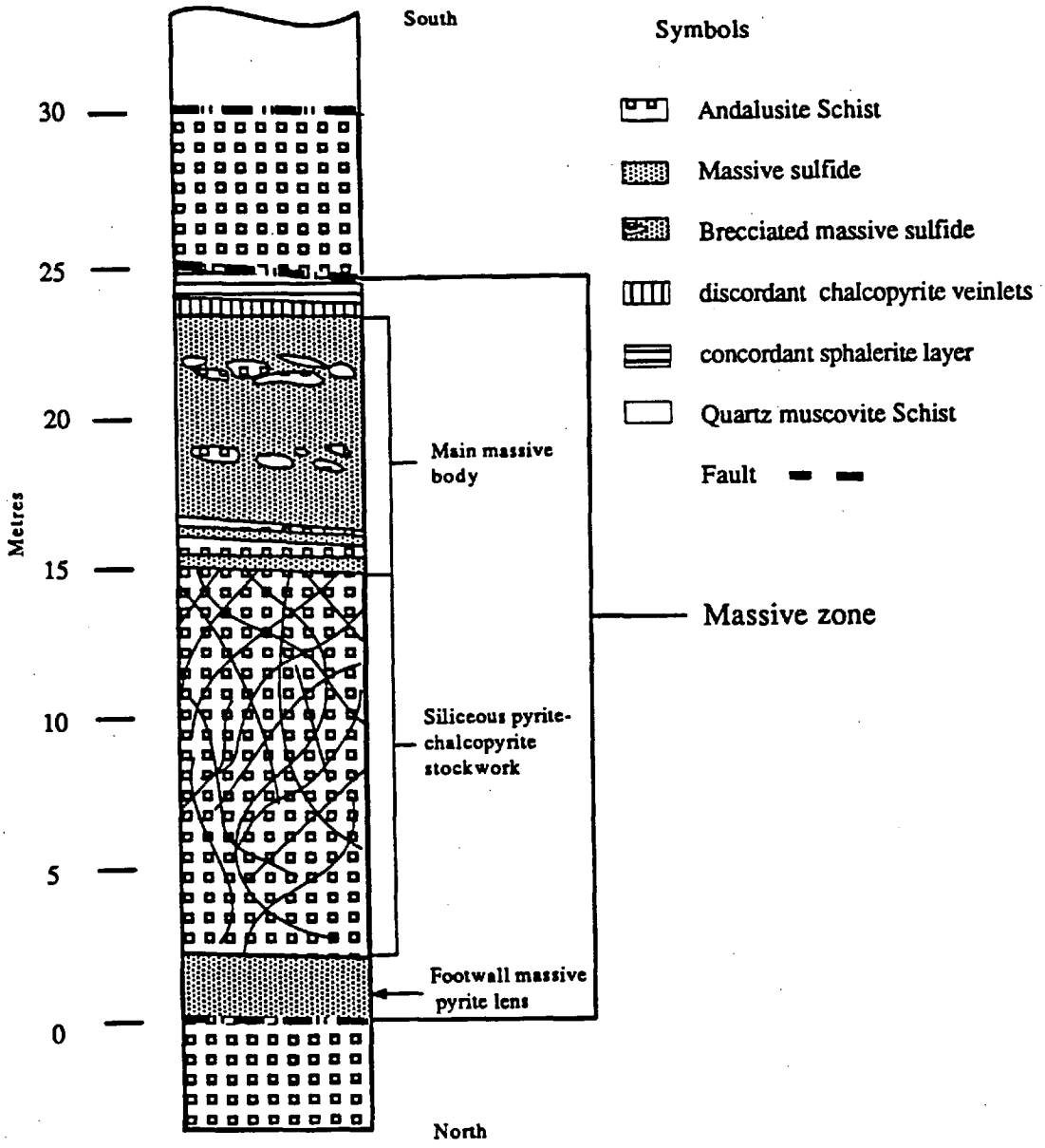


Figure 44. Simplified section view of massive zone at Bousquet No. 2 Mine.



Figure 45. Photograph of siliceous, pyrite-chalcopyrite siliceous stockwork from massive zone. Sample 94-42. Note light blue color of andalusite schist indicative of pervasive silicification.

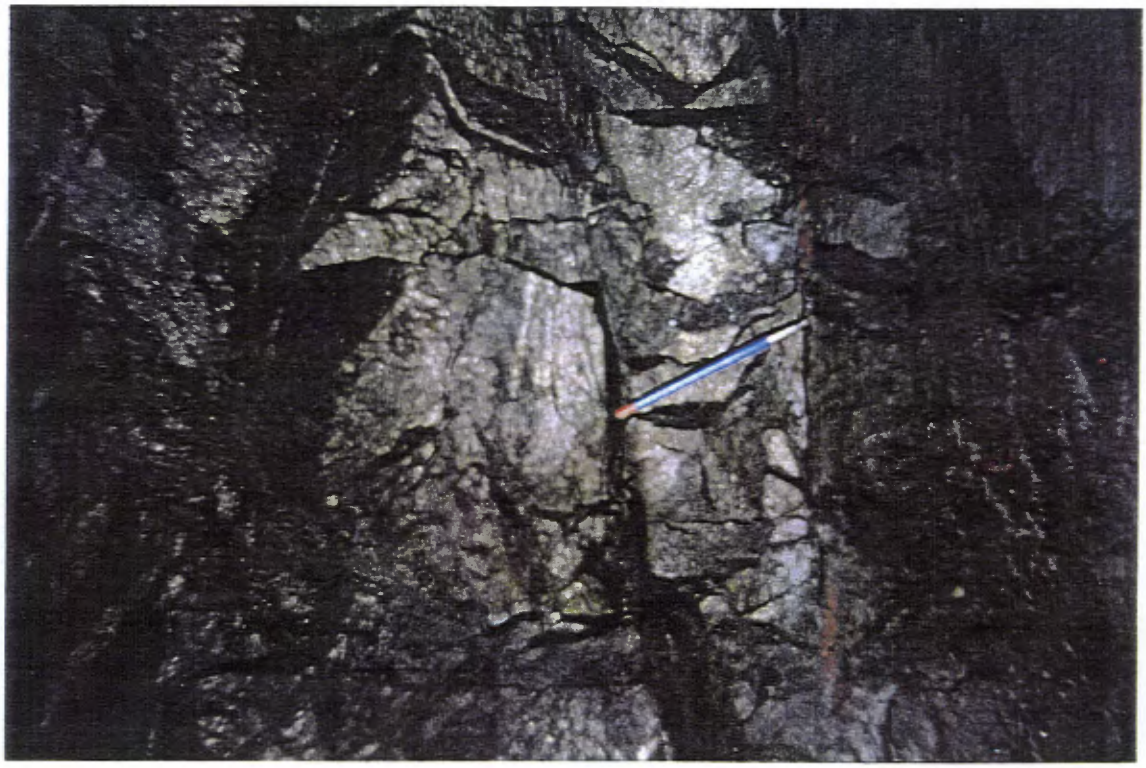


Figure 46. Photograph of upper contact of complex main massive sulfide body with hanging wall andalusite schist. Pencil is 15 cm long.

sulfide body. Included fragments in the breccia are mostly andalusite schist and range in size from a few cm up to 1 metre in length. The fragments of andalusite schist are matrix-supported, aligned and flattened parallel to the foliation (Figure 47). Some fragments of quartz-porphyritic rhyolite are also present, but account for less than 20 percent of the fragment population. Pyrite constitutes the matrix and 40 to 60 percent of the rock volume, but locally the breccia is fragment-supported, and pyrite is less than 20 percent. Bornite, along with chalcopyrite and gold, is highest at the boundaries between lenses of this breccia and flanking massive sulfide. Gold occurs in mm-scale fractures in pyrite and silicate minerals, as inclusions within pyrite or interstitial to recrystallized pyrite (Figure 48). Arsenopyrite, altaite, clausthalite, colusite, hessite, mawsonite, petzite, calaverite, renierite, and tellurobismuthite have also been reported (Tourigny et al., 1993; Brosnahan, 1992). The upper contact of the complex main massive sulfide body is marked by a 5 to 10 cm-wide graphitic schist or shear. The rock overlying the graphitic schist is a strongly foliated, grey andalusite schist, with 5 to 10 percent mm-scale, discordant pyrite-chalcopyrite veinlets. These form an anastomosing network that gives a brecciated appearance to the host andalusite schist. The segment containing the discordant chalcopyrite veinlets is absent in the western part of the orebody, but is up to 3 metres thick at the eastern property boundary (Figure 49). Overlying the segment of discordant chalcopyrite veinlets is a 2 to 3 metre-wide layer containing mm-scale, concordant seams of honey-colored sphalerite, galena and pyrite. Locally, the seams account for 10 percent of the rock volume. The upper contact of the sphalerite-bearing layer is faulted against the rhyolitic tuff of unit 6.

4.9.2 Fringe Zone

The Fringe zone occurs approximately 50 metres east of the massive zone (Figure 49). It contains combined reserves of 2.25 million tons with an average grade of 0.12 oz/ton gold and 0.03 percent copper. It is 1 to 2 metres wide, consists of 10 to 15

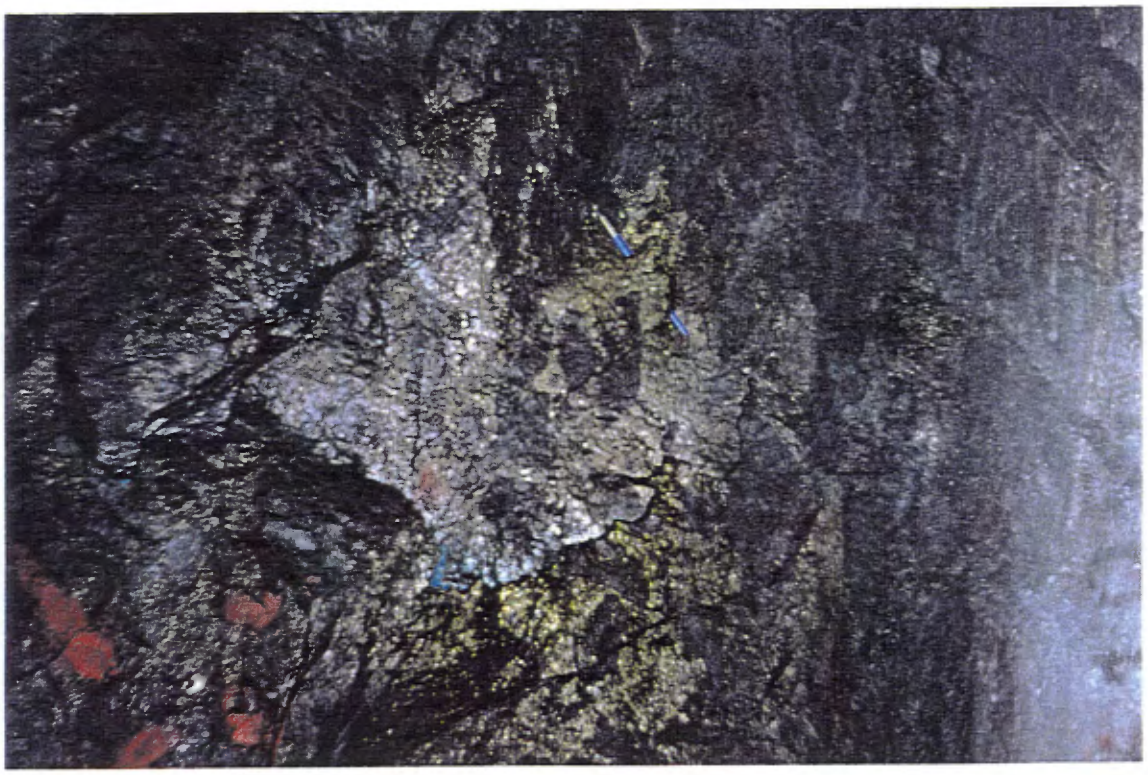


Figure 47. Photograph of breccia from central portion of complex main massive sulfide body. Note alignment of andalusite schist fragments. Note blue azurite staining from oxidation of bornite. Pencil is 15 cm long.

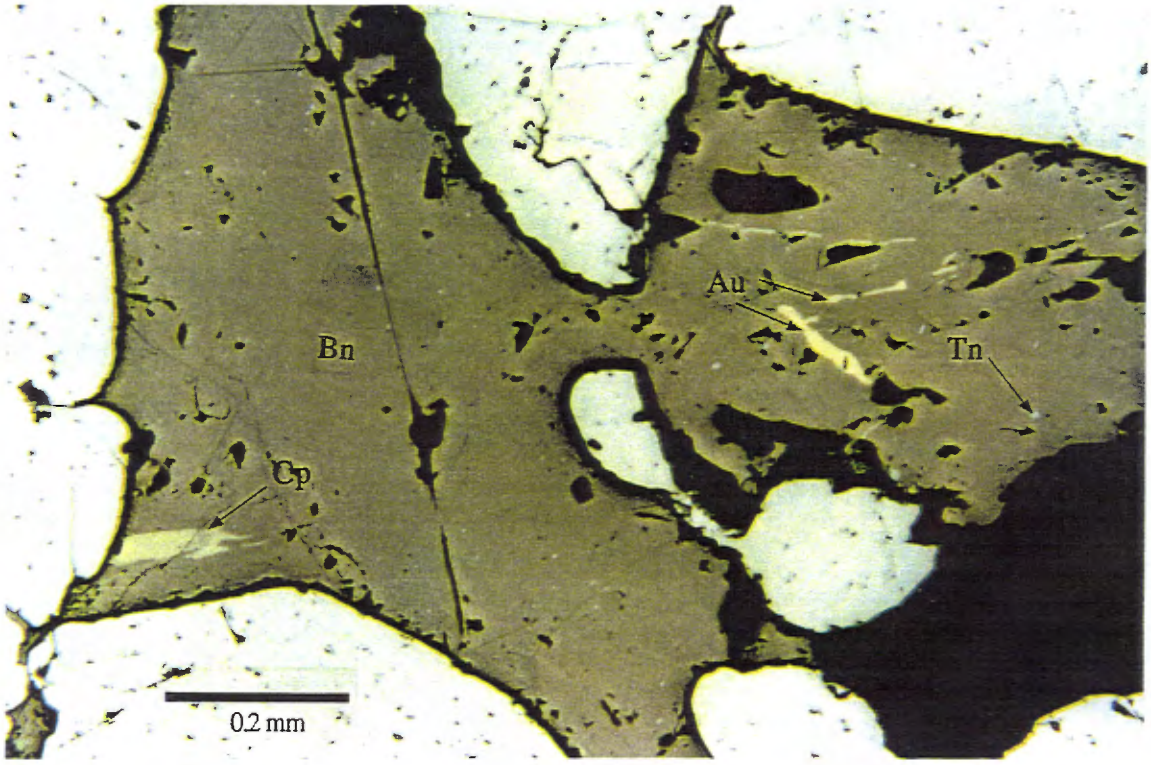


Figure 48. Photomicrograph of subhedral pyrite with interstitial bornite chalcopyrite and gold. Bn = bornite. Cp = chalcopyrite, Tn = tennantite, Au = gold. Sample 94-46. Reflected light 100X.

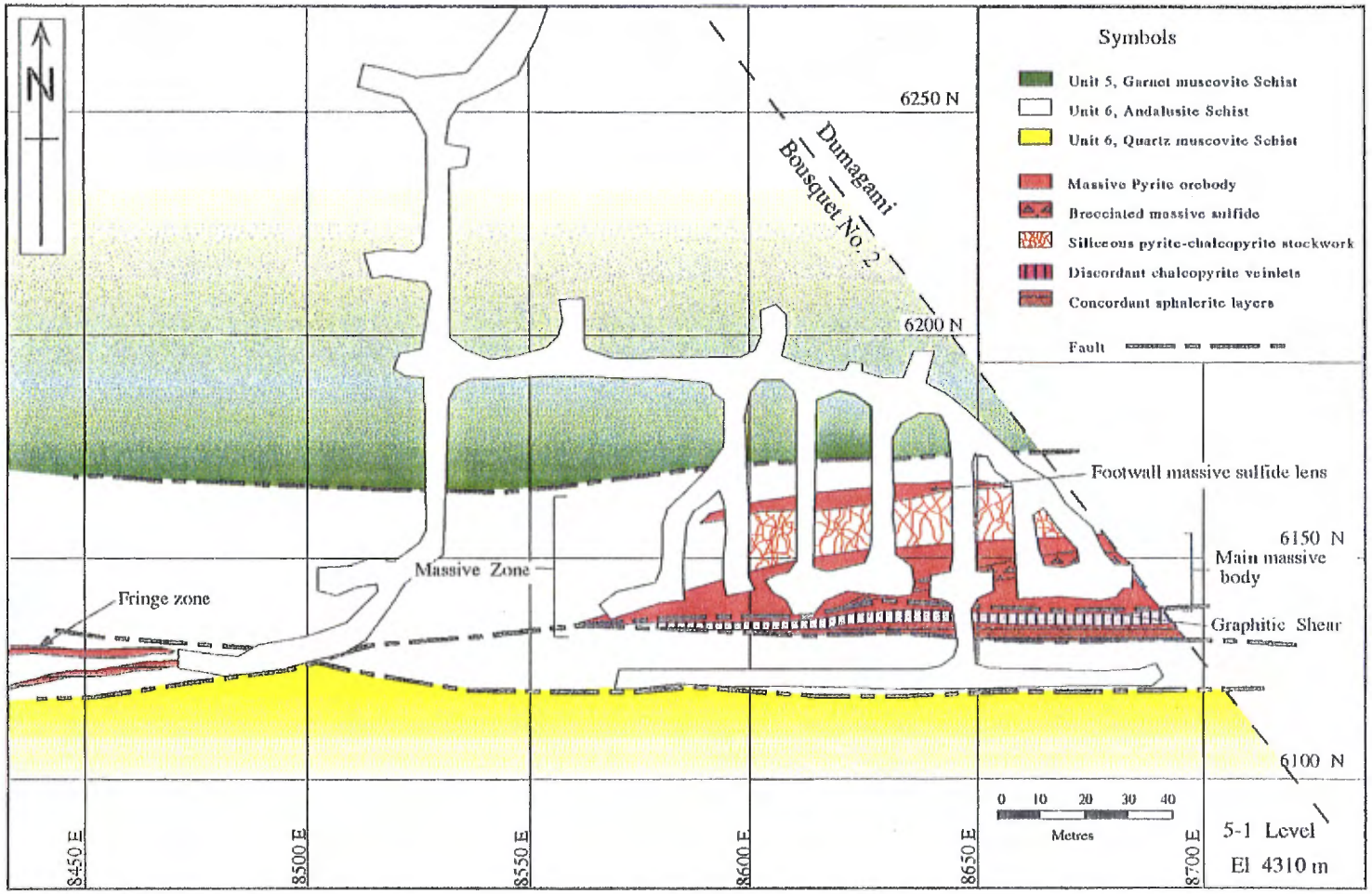


Figure 49. Typical plan view of Bousquet No. 2 mine. Note faulted relationship of fringe zone with the massive zone. Level 5-1, 650 m below surface.

percent disseminated, euhedral pyrite as well as several foliation parallel pyritic seams 5 to 10 cm wide. The mineralization occurs within sheared andalusite schist near the faulted contact of the overlying rhyolitic tuff. No mineralization occurs however in the rhyolitic tuff unit.

4.10 Mooshla A Occurrence

The Mooshla A occurrence is within the trondhjemite of the Mooshla intrusion, and produced the first gold in the area. The occurrence was explored with a vertical shaft to a depth of 120 metres and some 4,900 tons were extracted to yield 3,863 oz of gold (Valliant and Hutchinson, 1982). Gold mineralization was associated with coarse, euhedral pyrite and minor chalcopyrite in milky, quartz-tourmaline veins less than 50 cm wide that were oriented north-northwest (Gunning, 1941). Drilling by Lac Minerals failed to outline significant reserves or lateral continuity (A. Savoie, pers. comm., 1994).

4.11 Other Occurrences

Although not part of this research, several significant gold occurrences are present within a few kilometres along strike to west of the study area. These occurrences are within the Blake River Group and include, from east to west, the Ellison occurrence, the past producer Mic Mac mine and the current producing Mouska mine. The Ellison occurrence includes three separate gold zones termed A, B, and C. The A is similar to zone 3 at Bousquet No. 1 whereas zones B and C may correlate with the # 4 and # 5 occurrences respectively (Stone, 1988). The Mouska and Mic Mac occurrences lie within unit 1 and consist mainly of quartz-pyrite-pyrrhotite veins (A. Savoie, pers. comm., 1993).

The Dumagami Mine occurrence lies east of the study area. The mine has estimated reserves of 2 million tons of 0.14 oz/ton gold (Marquis et al., 1990). The mineralization at this occurrence is the up-dip continuation of that of the Bousquet No. 2 mine.

Chapter 5
METAMORPHISM AND ALTERATION

5.1 Introduction

The rocks of the Blake River Group have been regionally metamorphosed to upper greenschist facies which has altered their original rock chemistry and mineralogy. Furthermore, retrograde reactions towards lower greenschist facies have also affected the area (Marquis et al., 1990). Notwithstanding, the original rock with primary structures is often well preserved and protoliths are often easily identifiable (Tourigny et al., 1992; Stone; 1988; Savoie et al., 1991). Hydrothermal alteration, associated with all gold occurrence, is metamorphism involving high fluid to rock ratios by which the minerals of a protolith are converted to more stable ones (Barnes, 1979). Therefore, hydrothermal alteration of similar protoliths by fluids of similar composition and temperatures should yield similar alteration products.

Gold occurrences in the study area occur in altered mafic volcanic rocks, felsic volcanic and pyroclastic rocks and within the intrusive rocks of the Mooshla complex. Most occurrences are at or near the contact between mafic and felsic volcanic protoliths. Previous workers, (Marquis et al., 1990; Savoie et al., 1986; Tourigny et al., 1988), suggested that gold concentrations in Bousquet Township resulted from the precipitation of auriferous metamorphic fluids in dilatant zones. If this hypothesis is correct, the associated alteration of occurrences hosted in similar protoliths ought to be similar. The study of metamorphism and alteration products is therefore best carried out by comparing those occurrences that are in similar inferred protoliths from the stratigraphic base to top, and west to east.

5.2 Alteration of Mafic Volcanic Host Rock

The # 6 gold occurrence, is hosted in mafic volcaniclastic rocks of unit 3, the # 5, the # 4, the Ellison, the Warrenmac, and the Westwood occurrences are all hosted in mafic tuffaceous rocks of unit 5. Furthermore, the volcaniclastic rocks of unit 5 form the footwall of the # 3 zone at the Bousquet No. 1 mine. Regional metamorphism to greenschist facies of mafic rocks resulted in the assemblage of chlorite + albite + calcite + zoisite (Spear, 1993). Hydrothermal alteration associated with the several gold occurrences in these mafic host rocks resulted in mineral assemblages that are unique and restricted to the rocks spatially associated with the mineralization. Furthermore the assemblages change from a chloritoid-ankerite assemblage in mafic rocks at the base to a manganiferous garnet-muscovite assemblage in comparable mafic rocks near the top of the volcanic succession.

5.2.1 Chloritoid

Chloritoid with chlorite and ankerite occurs in the hanging wall rocks of the # 6 occurrence where it locally accounts for up to 25 percent of the rock (Tourigny and Hubert, 1986). Minor chloritoid, usually as inclusions in manganese garnet, also occurs in the footwall wall rocks of the # 3 zone at Bousquet No. 1 mine. Chloritoid at the # 6 occurrence occurs as 2 mm long, polysynthetically twinned, poikiloblasts, and has low MnO but as much as 28 weight percent Fe_2O_3 (Stone, 1988). The grains are oblique to the general foliation and appear to postdate deformation. Chloritoid in the footwall of the # 3 zone contains 4.5 to 5.2 weight percent MnO but only 17 to 20 percent Fe_2O_3 (Bateman, 1984).

5.2.2 Ankerite-Muscovite

The # 5, # 4, Westwood and Ellison occurrences are all associated with an ankerite-muscovite±magnetite alteration assemblage which is characterized by a light

brown to dark green, thinly-banded, fine-grained tuffaceous or volcanic flow rock. The light brown bands are 1 to 2 cm wide and consist of fine-grained muscovite, with ankerite and minor magnetite. Magnetite grains are pseudomorphed by ankerite. Pyrite is present as euhedral grains and as discordant micro veinlets. Muscovite grains are aligned with the foliation, and ankerite forms interstitial grains and fillings in vugs with quartz. Dark green bands consist of chlorite, calcite, fine-grained quartz and muscovite.

5.2.3 Garnet

Garnetiferous rock is present in the footwall of the Warrenmac occurrence, Bousquet No. 1 and the Bousquet No. 2 Mines. Garnets also occur in the trondhjemite of the Mooshla intrusion and are considered here for comparison. Much emphasis has been placed on the presence of garnet-bearing rocks in the study area because of their elevated MnO content and the known association of manganese with massive sulfide deposits that were formed in a syn-depositional sea floor environment (Wonder et al., 1988; Spry and Wonder, 1989).

At the Bousquet No 1. Mine, manganese garnet-bearing rocks in the footwall of the # 3 zone have been interpreted as representing the metamorphosed equivalent of original, sea floor manganese nodules (Valliant, 1981). Bateman (1984) cited the concentration of manganese-rich garnets in the footwall as evidence for an overturned and northward-younging sequence in the Blake River Group in the vicinity of the gold occurrence.

For this study, garnets were collected for microprobe analyses from the footwall of the Warrenmac occurrence, the Bousquet No. 1 and 2 Mines, as well as from the trondhjemite of the Mooshla intrusion at the Doyon Mine. The results are presented in Appendix 3.

At the Warrenmac occurrence, garnets grains are euhedral and appear fresh. The ilmenite and pyrite inclusions within the grains are linear and parallel to the foliation.

The garnetiferous rock at the Bousquet No. 1 Mine has been studied in detail (Valliant, 1981; Valliant and Barnett, 1982; Bateman, 1982; Stone, 1988) consequently, in this study, only a few samples were collected from the footwall of the # 3 zone to establish a basis for comparison. This garnetiferous rock is symmetrically in distributed and grades laterally in both directions into a fine-grained, chloritic, mafic tuffaceous rock. The garnets are orange to pink, 0.4 to 2 mm in diameter and comprise up to 20 percent of the rock volume. Here, the grains of garnet are euhedral to subhedral, with straight to sigmoidal inclusion trails, indicating a syn-to post-tectonic growth (Figure 50). Inclusions are of manganiferous ilmenite, pyrite, quartz, chloritoid and minor apatite. The garnet-bearing rock is anomalous in manganese content, 1.6 to 3.0 weight percent, compared to 0.1 to 0.25 weight percent in the mafic tuffaceous rock along strike (Stone, 1988). Garnets from the footwall of the No. 2 Mine appear similar to those at the Bousquet No. 1. Mine.

Garnets in rocks of the Mooshla intrusion are associated with sericite in altered trondhjemite and are anhedral with serrated edges. These garnets appear to occupy the sites of sericite, and crystal growth appears to have been restricted by the availability of alumina (Figure 51).

Garnets from all occurrences exhibit compositional zoning, with manganese rich-core and iron-rich rims. The grains are of the almandine-spessartine solid solution series with an average of 21 weight percent MnO in the core and 15 weight percent in the rims (Appendix 3). Garnet grains from all occurrences range in size from 50 to 1200 microns. To assess differences in garnet zonation from all occurrences, two different tests were carried out. First, all core, mid-grain and rim analyses, were averaged for each occurrence regardless of grain size (Figures 52, 53), and second, multiple analyses were carried out on equal sized grains of 400 micron radius (Figures 54, 55). Both tests indicate similar zonation patterns which are consistent with normal iron-manganese fractionation during garnet growth below the staurolite-garnet isograd (Tracy et al., 1976; Yardley, 1977).

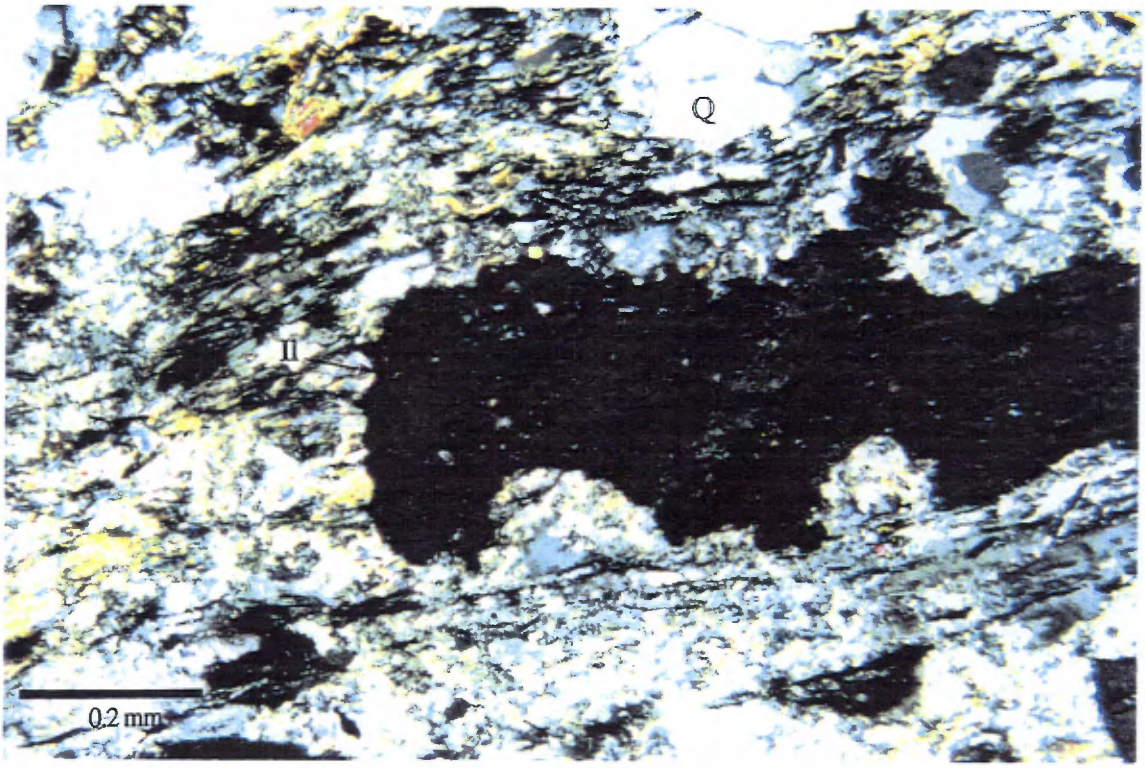


Figure 50. Photomicrograph of garnet from the footwall of the # 3 zone at the Bousquet No. 1 Mine. Note parallel inclusion trails of ilmenite. Sample 94-74. Q = quartz, Il = ilmenite Transmitted light, crossed polars, polars are at 86 degrees to show internal structure of garnet grains. 100X.

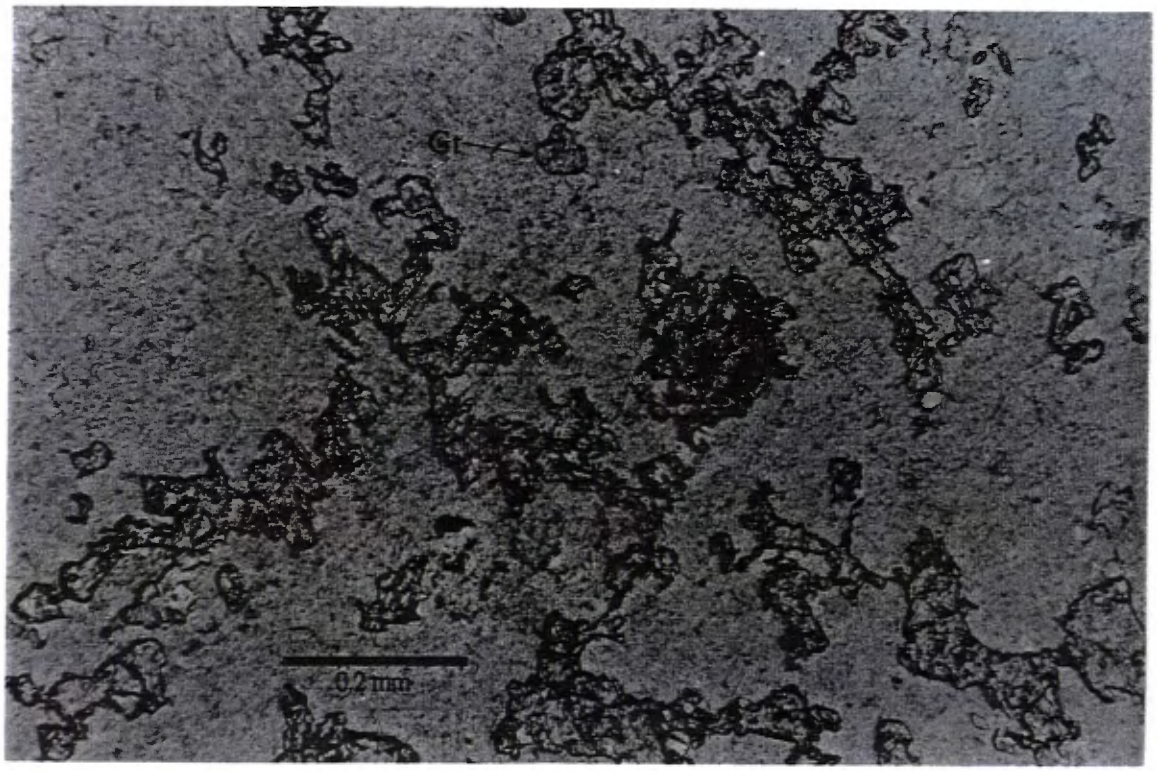


Figure 51. Photomicrograph of anhedral garnet from trondhjemite. Gt = garnet. Sample 93-116. Transmitted plane light, 100X.

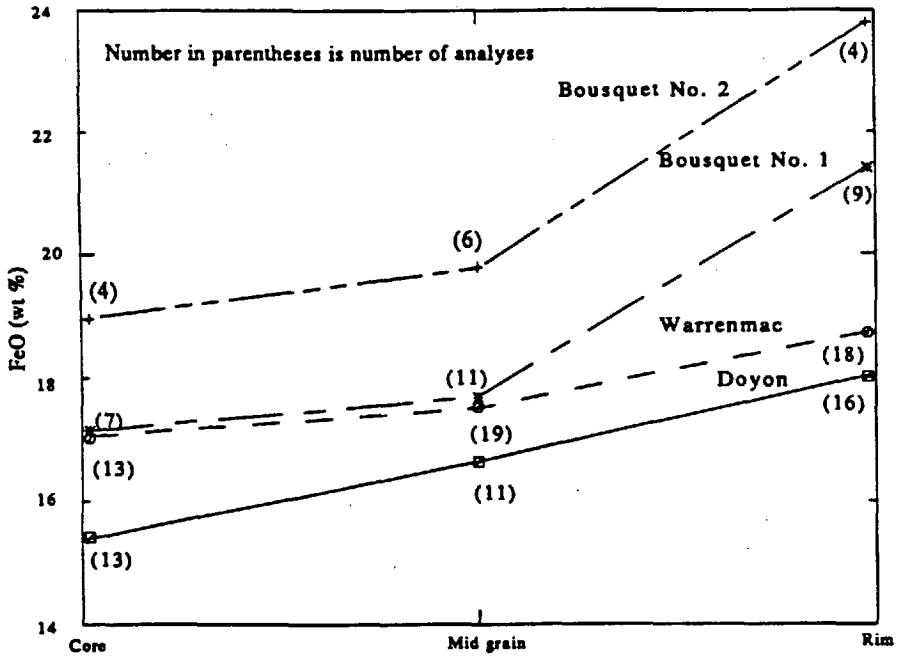


Figure 52. Average FeO variation of Garnet grains.

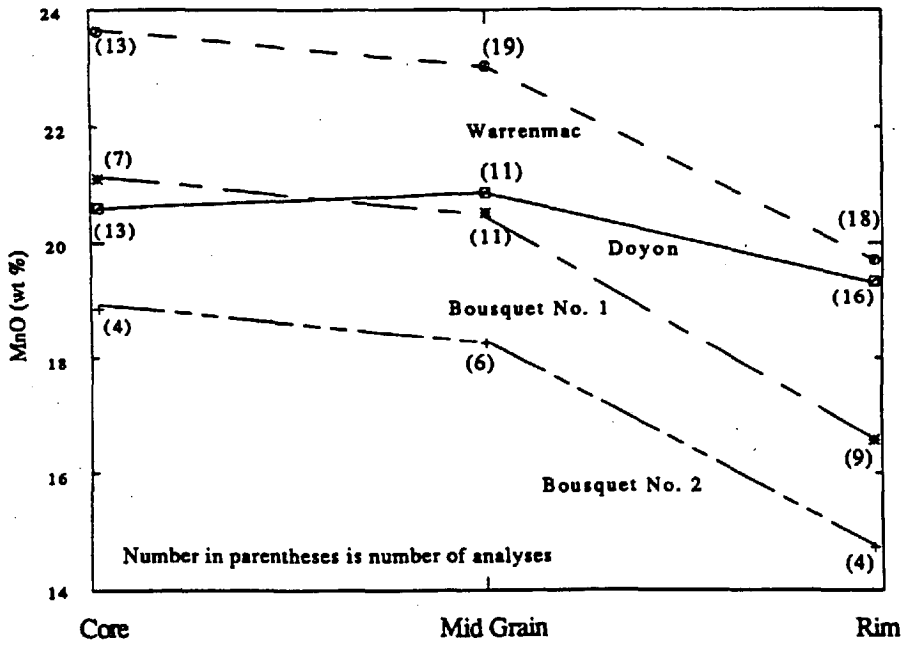


Figure 53. Average MnO variation of Garnet grains.

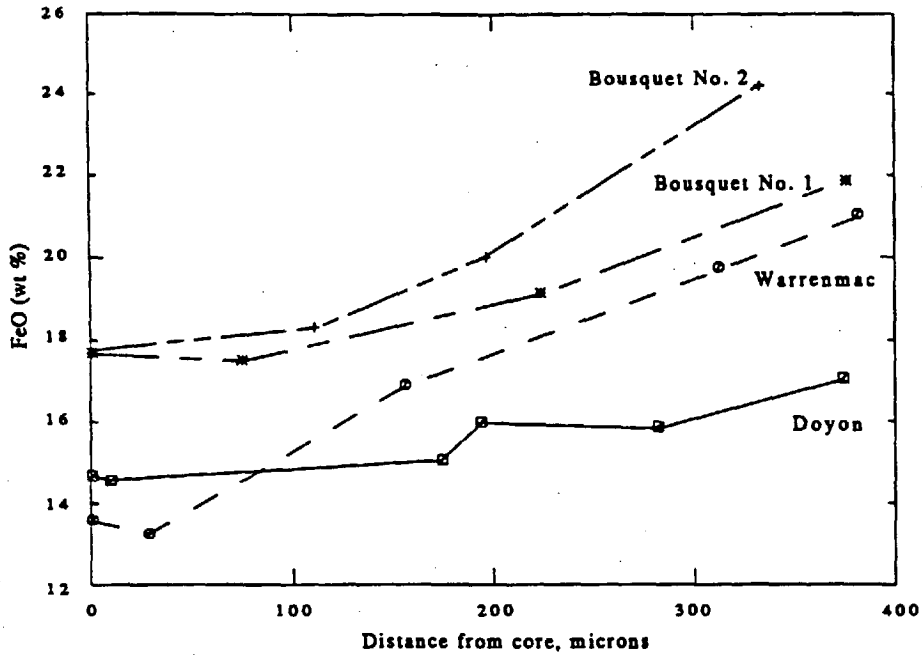


Figure 54. FeO variation in garnet grains with 400 micron radii.

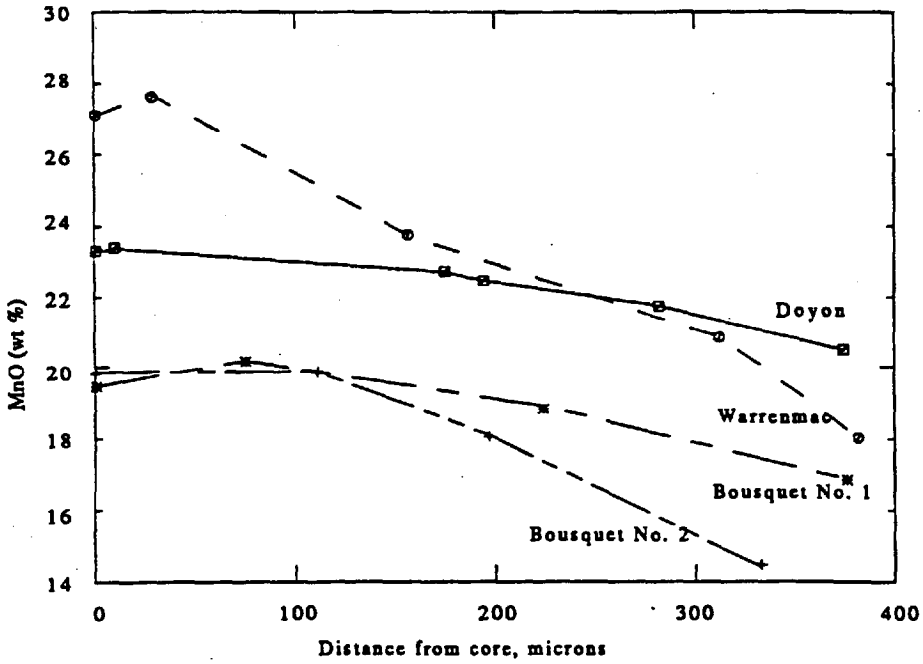


Figure 55. MnO variation in garnet grains with 400 micron radii.

Diffusion is not considered to have played an important role in the distribution of Fe and Mn because of the slow rate of diffusion below 500° C (Spear, 1993). Manganese content in garnets is highest at the Warrenmac occurrence and lowest in the footwall rocks of the Bousquet No. 2 deposit. Manganese content and grain zonation of garnets from the Mooshla intrusion are similar to those from rocks of the Blake River Group, however garnet grains from the Blake River Group volcanic rocks exhibit typical bell-shaped zonation patterns for manganese values away from the core whereas this pattern is less pronounced for garnets of the Mooshla intrusion of the Doyon Mine (Figures 50, 51, 52, 53).

5.3 Alteration of Felsic Volcanic Host Rock

The main and No. 1 zones at the Doyon Mine, the # 3, # 2 and # 1 zones at the Bousquet No. 1 Mine, and the massive and fringe zones at the Bousquet No. 2 Mine are all hosted within altered felsic volcanic rocks. Hydrothermal alteration that accompanied the mineralizing events has modified the original rock mineralogy to either a quartz-sericite assemblage or an andalusite-quartz-muscovite assemblage. Regional metamorphism has also caused weak sericitization of felsic volcanic rocks in areas distant from the gold occurrences but this alteration is less pervasive and usually fracture-controlled. Altered felsic volcanic rocks differ from the mafic rocks in that they lack chlorite and garnet, and are not anomalous in manganese content (Stone, 1988).

5.3.1 Quartz-Sericite

The felsic volcanic rocks of unit 4 at the Doyon Mine host the main zone and, in part, the # 1 zone. Hydrothermal alteration of these felsic volcanic rocks resulted in a quartz-sericite schist. The sericite schist is fine-to very fine-grained, and light grey to buff. The rock is yellow to orange in surface exposures because of the oxidation of pyrite. The rock is essentially 50 to 70 percent recrystallized quartz and lepidoblastic

muscovite, with euhedral pyrite. Andalusite is present, but only locally and in trace amounts. Chemically the alteration is characterized by elevated contents of K_2O, Al_2O_3, S, and MgO and depletions of Na_2O and CaO (Savoie et al., 1986).

5.3.2 Andalusite-Muscovite

The # 3, # 2 and # 1 zones at the Bousquet No. 1 Mine, and the massive and fringe zones at the Bousquet No. 2 Mine are all hosted within felsic volcanic rocks of unit 6 that have been altered to an andalusite-quartz-muscovite assemblage. The andalusite rock is both the host and the hanging wall rock to the mineralized zones at both mines. It is concordant to the dominant schistosity, 1 to 3 metres thick at Bousquet No. 1 Mine but exceeds 30 metres at Bousquet No. 2 Mine. The rock is continuous for several hundred metres along strike beyond the termination of the mineralized zones at the Bousquet No. 1 Mine (Bateman, 1984). Throughout the area, the andalusite schist is uniform in composition, consisting of 5 to 40 percent porphyroblasts of andalusite up to 5 mm in diameter and euhedral pyrite grains 1 to 2 mm in maximum dimension in a matrix of quartz grains and fine muscovite. Quartz is recrystallized and crystal growth was apparently limited by the presence of phyllosilicate minerals which caused growth of elongated quartz grains parallel to the foliation. The rock is typically pale to medium grey, well banded and foliated on a mm scale. Most quartz grains display undulose extinction and are strongly fractured, with muscovite filling the fractures. Andalusite grains are poikiloblastic, with parallel inclusions trails of quartz which are oblique to the regional foliation indicating their late- to post-deformational growth. Locally pyrite constitutes 30 percent of the rock volume. Trace amounts of kyanite are present, usually associated with late quartz veins (Marquis et al., 1992; Stone, 1988). The assemblage of andalusite-quartz±kyanite is believed to represent the maximum prograde metamorphic conditions (Marquis et al. 1992). Andalusite exhibits retrograde alteration to diaspore, kaolinite and muscovite (Tourigny et al., 1989a). The rock is characterized by high SiO_2

and Al_2O_3 contents and low K_2O, CaO, MgO and Na_2O contents (Valliant et al. 1983; Bateman 1984).

5.4 Alteration of Intrusive Host Rock

The Mooshla A occurrence and the West zone of the Doyon Mine are both hosted within the trondhjemite of the Mooshla intrusion. The latter consists of quartz veins that have been interpreted to be of metamorphogenic origin, and alteration of the host rocks was not considered to have been an important factor in ore control (Savoie et al., 1990). Alteration associated with the West zone is concentric about a siliceous core within the central part of the trondhjemite body and the assemblages are similar to those associated with porphyry copper and copper-gold deposits (Lowell and Guilbert, 1970; Sillitoe, 1973; Gustafson and Hunt, 1975; Sillitoe, 1988; Richards, 1992). At the Doyon Mine, the alteration assemblages have been metamorphosed to greenschist facies and structurally deformed, but the alteration envelopes are still recognizable. From the centre of the West zone mineralization outwards, three discrete assemblages are identified, a siliceous a core, an inner sericite-quartz-pyrite envelope, and a peripheral chlorite-calcite-epidote envelope. The envelopes have been faulted into east-west trending blocks by a system of anastomosing faults that are sub-parallel to the late foliation.

5.4.1 Siliceous Core

Siliceous alteration is present only below the 4-0 level of the mine (230 metre below surface), but is best developed on the 8-0 level (480 metre below surface) and below. This core is marked by the introduction of secondary quartz with minor biotite. The assemblage is similar to potassic alteration described for diorite-hosted porphyry copper deposits of western North America (Beane and Titley, 1981; Hollister, 1978). No primary igneous structures are preserved and the rock is weakly foliated. Quartz is very fine-grained, re-crystallized, with 120° crystal junctions, and accounts for 70 percent of

the rock volume. Biotite forms phenocrysts that are altered to chlorite. Pyrite is in amount less than 1 percent or as traces. Sericite is interstitial to the quartz and forms fine disseminations (Figure 56). This core of alteration is discontinuous and has gradational contacts with the surrounding phyllic alteration. No mineable ore exists within the siliceous core.

5.4.2 Phyllic Alteration

Phyllic alteration, consisting of sericite-pyrite-quartz rock, is the most prominent alteration assemblage within the Mooshla intrusion. Most of the trondhjemite in the Doyon Mine belongs to this assemblage. The rock consists of 20 to 30 percent recrystallized blueish quartz grains in a matrix of fine-grained white mica and minor sphene. Anhedral garnets are locally present and can amount to 5 percent of the rock. Pyrite constitutes from 3 to 15 percent of the rock and occurs both as euhedral grains 1 to 5 mm in diameter and in veinlets a few mm wide (Figure 57). The rock is light grey to buff in color, without igneous textures, fractured and foliated. Pyrite in the groundmass is recrystallized, stretched and broken into small pull-apart grains that are strung out parallel to the foliation. Pressure shadows of chlorite and calcite are developed around the pyrite grains, and retrograde chlorite with calcite occurs in the veinlets. Gold is very fine-grained, and occurs on pyrite boundaries or in fractures within pyrite. Coarse gold occurs in late tensional fractures perpendicular to the veinlets with calcite and quartz.

5.4.3 Propylitic Alteration

The propylitic assemblage consisting of epidote, chlorite and calcite is peripheral to the phyllic assemblage, and best developed within the porphyritic quartz diorite. The limits of this alteration are difficult to recognize because the assemblage is characterized by the same minerals that resulted from greenschist facies metamorphism of the mafic intrusive rocks. Within the Doyon Mine workings, both the porphyritic quartz diorite and

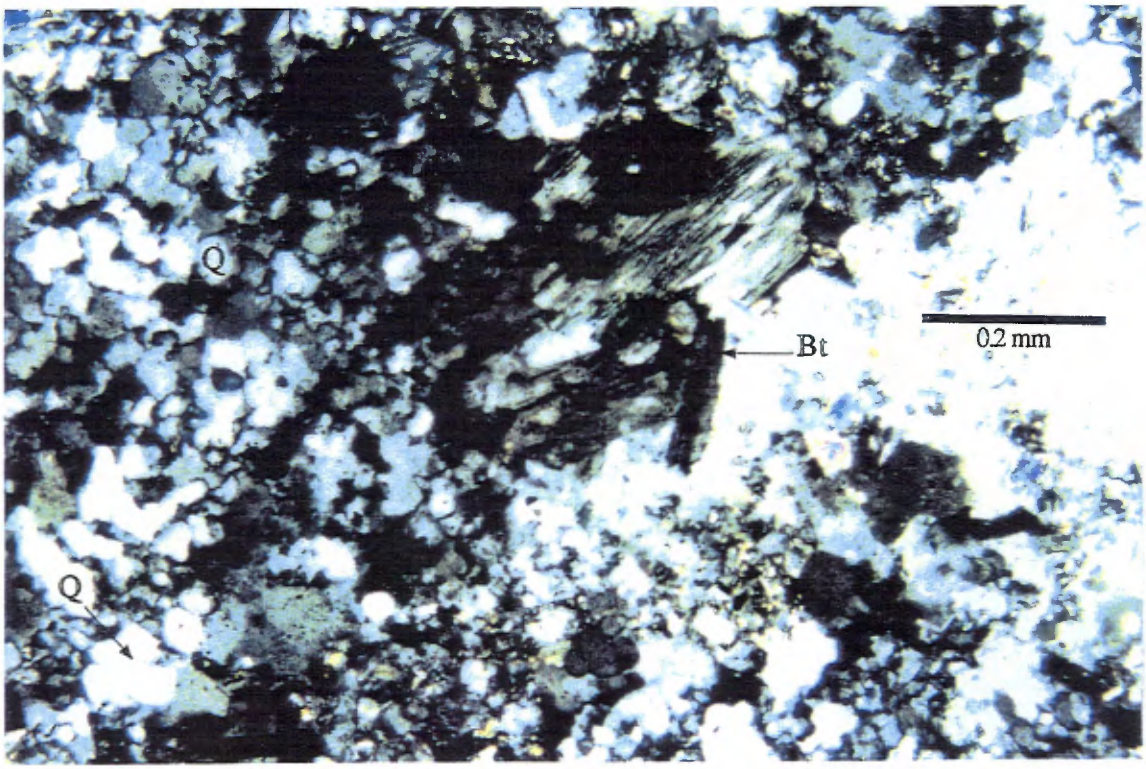


Figure 56. Photomicrograph of rock from siliceous alteration core of trondhjemite. Note fine euhedral quartz grains and minor biotite retrogressively altered to chlorite. Bt = biotite, Q = quartz. Transmitted light, crossed polars, 100X.



Figure 57. Photograph of phyllic alteration with pyrite veinlets. Note secondary silica as blueish quartz grains. Q = quartz.

the quartz diorite have been altered to chlorite-epidote-calcite, obliterating most of the primary igneous crystal structure (Figure 58 A and B). The blocky tuff of unit 3 has also been pervasively altered to chlorite and epidote. The groundmass has been converted to a chlorite-quartz-calcite rock with minor anhydrite, and the fragments have been completely replaced by epidote and clinozoisite. (Savoie et al., 1991, Figure 58).

The propylitic alteration is characterized by the partial to complete replacement of feldspar by epidote and calcite, and by the destruction and substitution of amphibole and biotite by chlorite and oxide minerals. The alteration is pervasive near the Doyon West zone but becomes increasingly fracture-controlled farther away where chlorite, with calcite and sericite are present only in micro-fractures parallel to the foliation, and where the feldspars are weakly saussuritized.

Propylitic alteration of the trondhjemite is difficult to recognize because retrograde alteration has resulted in the development of chlorite and calcite, with minor epidote, in fractures throughout the mine. However, parts of the trondhjemite are altered to a chlorite-sericite-calcite rock which is expressed by a pervasive darkening of the phyllic alteration envelope to a dark green color. The rock has gradational contacts with the earlier phyllic alteration and occurs in irregular pods that are difficult to outline. This propylitic alteration of the trondhjemite is best developed near the contact with the porphyritic quartz diorite, which may indicate that it was formed by the assimilation of quartz diorite fragments and not by hydrothermal fluids.

The propylitic assemblage within the porphyritic quartz diorite has been overprinted by a quartz-sericite assemblage near mineralized quartz veins. These alteration halos are 30 to 50 cm wide and their minerals are similar to those of the phyllic alteration assemblage. Within the alteration halos, the remnant igneous texture is destroyed, and plagioclase grains display reverse zoning with cores of An_{40} and rims of An_{47}, indicating crystallization under rising temperature (Savoie et al., 1990).



Figure 58. Photograph of altered quartz diorite.

a) Propylitic assemblage produced by hydrothermal fluids. Note pervasive replacement of feldspar by chlorite and epidote and partial destruction of igneous texture.

b) Chlorite-epidote assemblage produced by greenschist metamorphism Note good preservation igneous texture.



Figure 59. Photograph of blocky tuff member from unit 3 altered to chlorite and epidote. Note the complete replacement of circled fragment by light green epidote.

5.5 Summary

Alteration associated with gold occurrences in the Blake River Group changes from the base to the top of the volcanic sequence and also from west to east. Occurrences hosted in mafic rocks are characterized by abundant iron and carbonate alteration at the base and manganese rich assemblage near the top. Alteration associated with felsic host rocks changes from a quartz-sericite assemblage near the base of the succession to an andalusite-muscovite assemblage towards the top. The alteration associated with the Mooshla intrusion is concentric about the trondhjemite and similar to that of porphyry copper and copper-gold deposits.

This progressive change in alteration of similar protoliths from the base to the top of the volcanic sequence suggests that the occurrences were probably formed by complex multi-processes rather than by a single process involving a fluid of similar composition and temperature.

Chapter 6
GEOCHEMISTRY OF THE BLAKE RIVER GROUP

6.1 Introduction

In order to interpret the metallogeny of the gold occurrences in rocks of the Blake River Group, it is first necessary to interpret the tectonic setting in which these rocks were deposited. One popular approach to determining the tectonic settings of ancient volcanic successions is to compare their geochemical signatures with those of rocks of modern tectonic settings (Cas and Wright, 1988). However, several problems need to be considered when comparing Archean volcanic successions with modern ones. The applicability of present-day and Phanerozoic plate tectonic settings to those of Archean time is debatable. Many workers advocate that plate tectonics have not changed significantly from Archean time through to the Phanerozoic (Burke et al., 1976; Chown et al., 1992; Blackburn et al., 1985; Easton, 1985; Padgham, 1985; Thurston et al., 1985), but others propose a more unique style of tectonism that involved horizontal or vertical displacement accompanied with buckling and shearing of plates (Condie, 1989; Glikson and Jahn, 1985; Hutchinson, 1981; Jensen, 1985). Furthermore, structural deformation with metamorphism and metasomatism has often obliterated or changed the primary features and original chemical compositions of Archean volcanic rocks (Condie, 1981). In addition, the earth's atmosphere was probably not oxygenated until at least Early Proterozoic time (Cloud, 1972). Studies of cooling models for the earth indicate that the geothermal gradient was probably 3 to 5 times higher in Archean time (Condie, 1989). Mantle convection was probably more vigorous and the crust was likely thinner than today. The higher heat flow was probably dissipated either through faster spreading or greater total ridge length and smaller plate size (Condie, 1989). There is little doubt that

changes in volcanic regimes and mechanisms of plate interactions from Archean time to the present have led to major chemical differences in volcanic rocks through time. Nevertheless, the chemical and physical properties of rocks of Archean volcanic successions share many similarities with volcanic rocks found in modern tectonic settings and these similarities warrant comparative analysis.

6.2 Major Element Analyses

Despite the effects of alteration, major oxides remain a useful criteria in classifying Archean volcanic rocks (Jensen, 1976; Thurston et al., 1985; Gelinas et al, 1983; LaFleche et al., 1992a, b). Analyses of the major elements of the volcanic rocks of the Blake River Group in this study reveal that they represent a bimodal suite (Figure 60). This observation is consistent with analyses of rocks of the Blake River Group in the Noranda region west of the study area (Gelinas et al., 1984). The volcanic rocks consist mainly of basaltic and andesitic flows with some rhyolitic flows and pyroclastic rocks. The rocks belong to the tholeiitic and calc-alkaline magma series. The overall variations in major oxide components of the rocks of the volcanic sequence expressed on stacked Harker diagrams is indicative of crystal fractionation from a common parent magma (Figure 61; Ragland, 1989). However, the comparative quantities of felsic to mafic rocks preclude the possibility of magma differentiation from a simple tholeiitic parent. Gelinas and Ludden (1985) therefore proposed that the effusive rocks of the Blake River Group probably resulted from the differentiation of a large, zoned reservoir consisting of an upper rhyolitic part, underlain by a calc-alkaline, andesitic magma and a primary tholeiitic magma. The tholeiitic magma was generated from partial melting of mantle whereas the calc-alkalic magma was derived from crustal partial melting.

Major oxide variations for rocks of the Mooshla intrusion display a slightly different pattern. Their stacked Harker diagrams exhibit straight line negative correlation of all major oxides with silica (Figure 62). This is not compatible with crystal

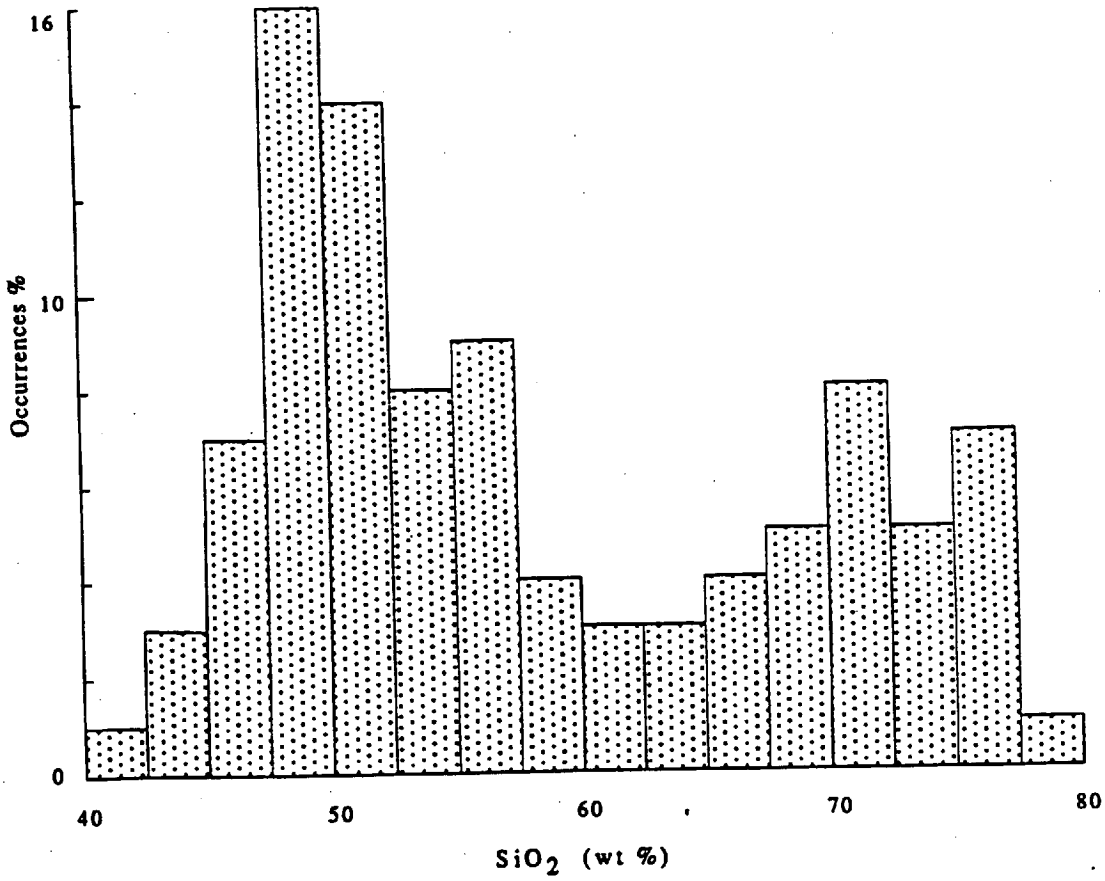


Figure 60. Histogram of silica content of the volcanic rocks of the Blake River Group (total number of samples 246).

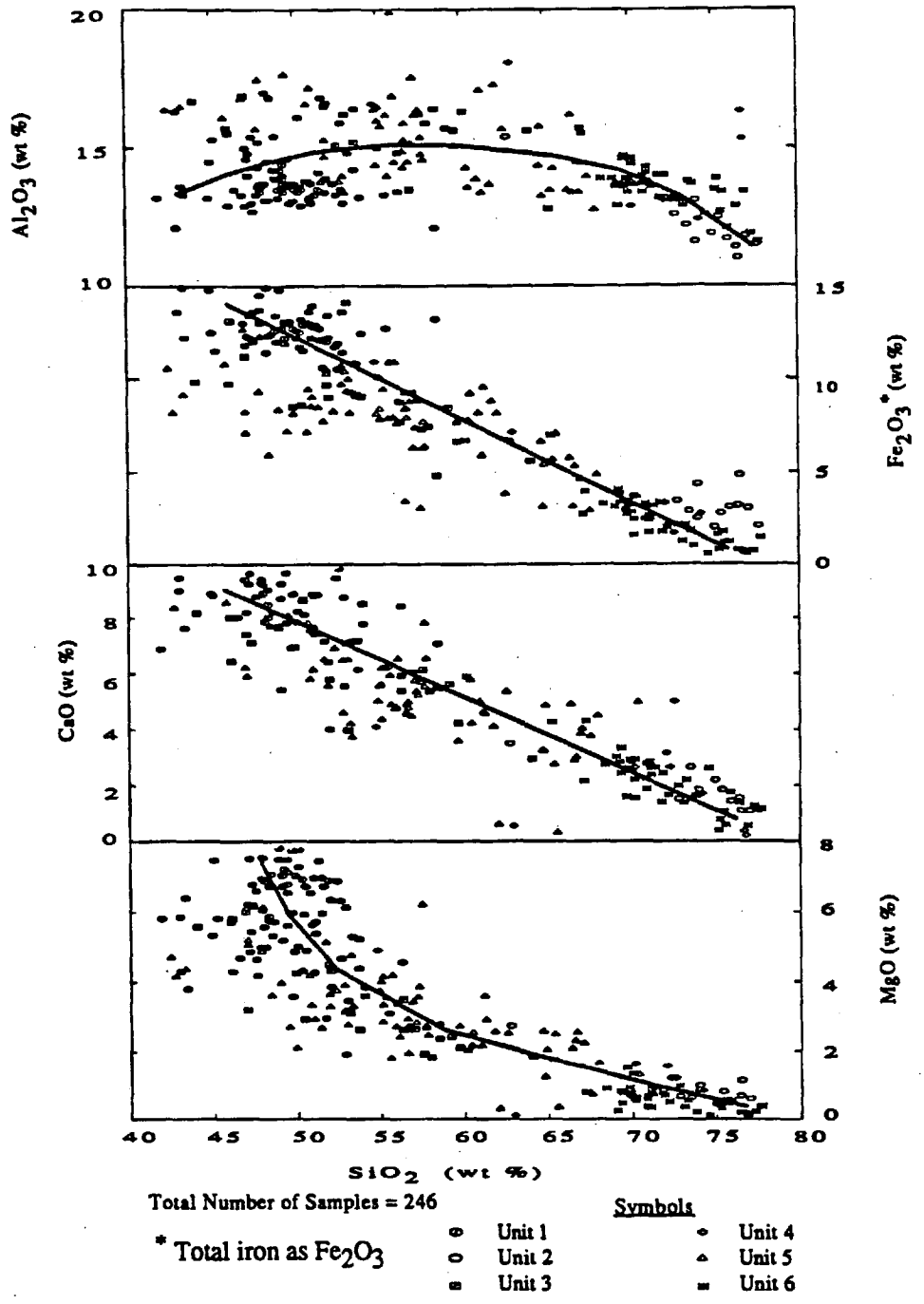


Figure 61. Major oxide variations plotted against silica for the volcanic rocks of the Blake River Group. (recalculated to 100% volatile free, after Harker, 1909).

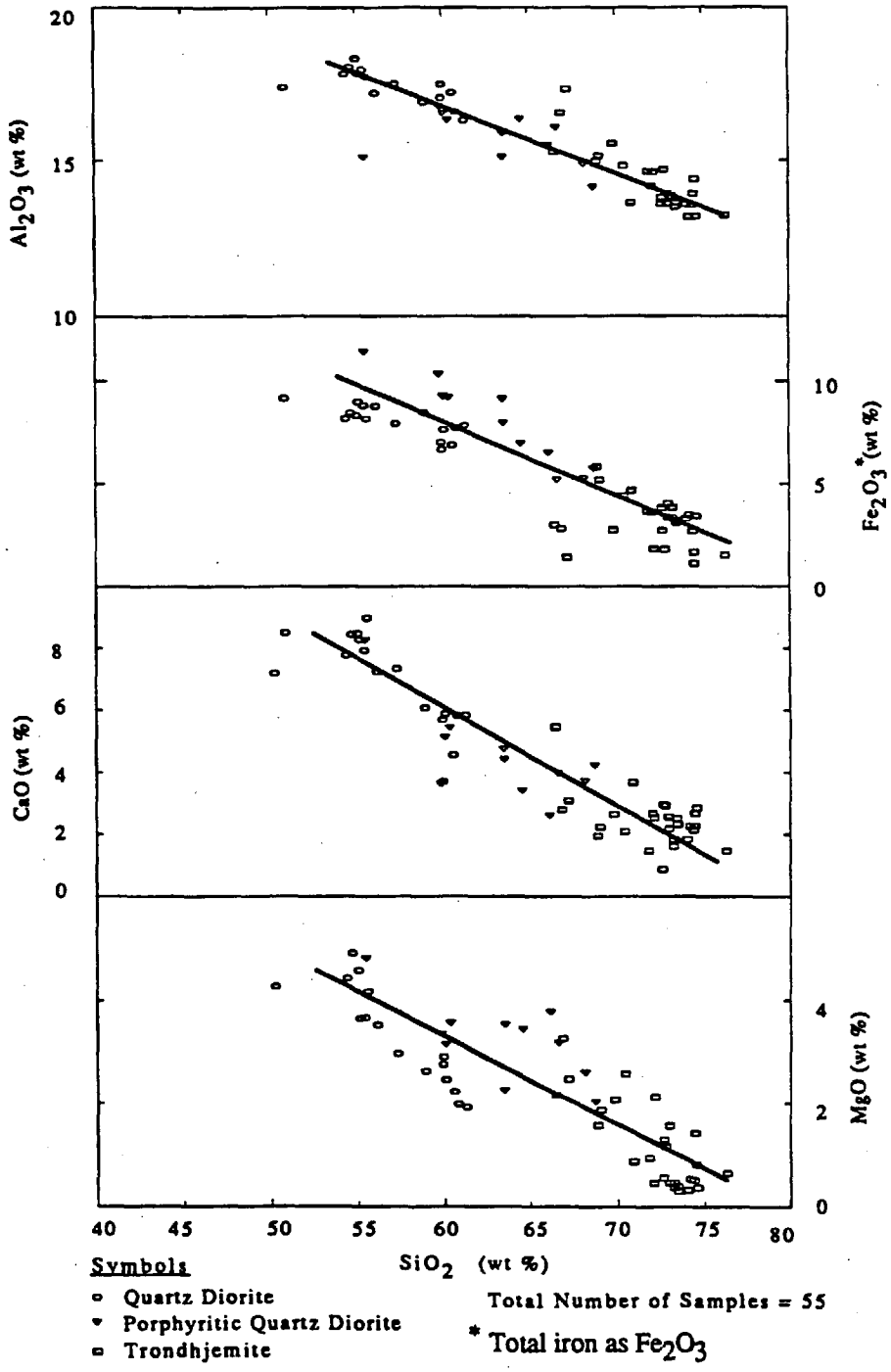


Figure 62. Major oxide variations plotted against silica for the rocks of the Mooshla intrusion (recalculated to 100% volatile free, after Harker 1909).

fractionation as was previously interpreted for the Mooshla complex (Langshur, 1990). Instead, these trends are indicative of magma mixing of quartz dioritic and trondhjemitic end members to produce the porphyritic quartz diorite. Magma mixing is further supported by the ratio-ratio diagrams of four and three oxides (Figures 63, 64). The four oxide ratio diagram displays an hyperbolic trend while the three element plot displays a direct correlation. Both correlations are characteristic of magma mixing (Ragland, 1989). The poor separation of end members and the wide overlap of the three phases on the three element plot, however, suggest that the porphyritic quartz diorite was probably not generated by simple mixing of two end members.

Underground mapping of the porphyritic quartz diorite revealed that large portions of this intrusive rock had been incorporated and digested by the trondhjemite so that a hybrid phase was commonly developed at the contact between the two. Intrusive breccia is also developed at the contact between the trondhjemite and porphyritic quartz diorite indicating that the trondhjemite was emplaced after the porphyritic quartz diorite had, at least in part, solidified. These relationship preclude simple mixing of end member magmas to generate the porphyritic quartz diorite. The apparent mixing indicated by the major oxides trends is not, therefore, interpreted as representing the mixing of quartz dioritic and trondhjemitic magma to yield a melt of porphyritic quartz diorite composition, but rather is interpreted as reflecting the partial melting and incorporation of the porphyritic quartz diorite by the younger trondhjemite to generate a hybrid rock.

6.3 Trace Element Analyses

The use of trace element analyses in conjunction with major oxides as guides to infer the tectonic settings of volcanic successions is also very popular, particularly the use of high field strength elements (HFSE), because they are largely unaffected by hydrothermal alteration (Pearce and Cann, 1973; Hall and Plant, 1992; Wood, 1980;

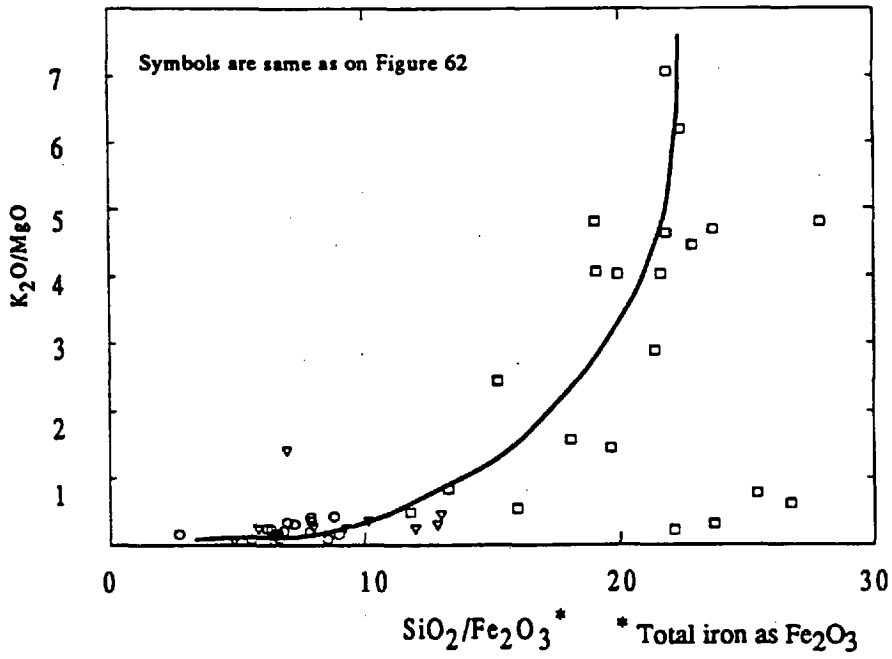


Figure 63. Four oxide ratio-ratio diagram for the rocks of the Mooshla intrusion.

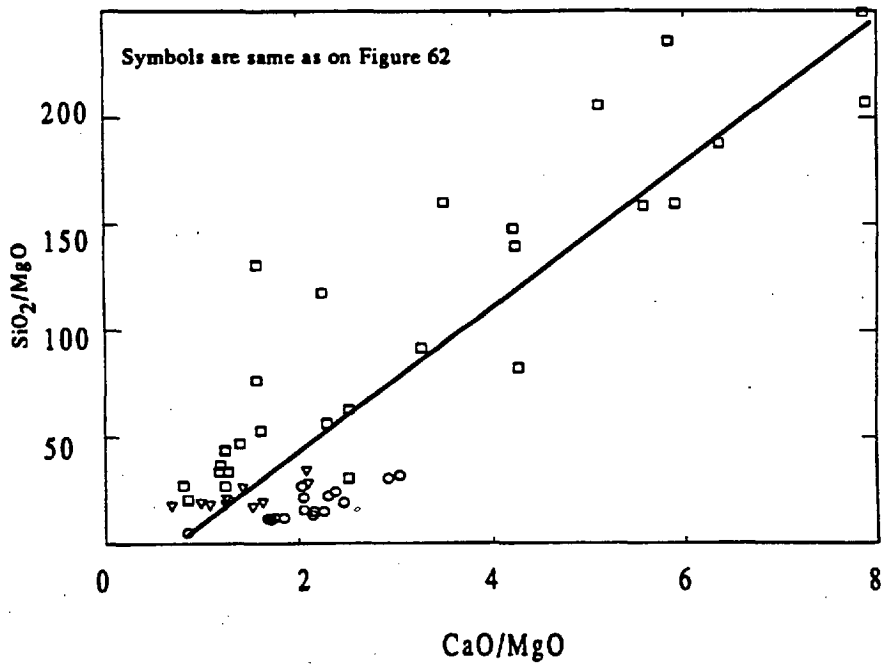


Figure 64. Three oxide ratio-ratio diagram for the rocks of the Mooshla intrusion.

Finlow-Bates and Stumpfl, 1981; Pearce and Norry, 1979; Myers and Breitkopf, 1989; Lafleche et al., 1992b; Smith and Smith, 1976). Problems may arise when using normalized values of certain trace elements because they often are present in concentrations near their detection limits (Hall and Plant, 1992).

Rocks of the Blake River Group were analyzed for Rb, Sr, Y, Zr, Nb, Ba as well as base and precious metals. The base metal and gold analyses were used only for exploration purposes. In order to minimize the problem of analytical errors and assure precision and accuracy, a twenty pound sample was collected and split into six replicates. All replicates were crushed and analyzed separately, each pulp was then re-analyzed. The results indicate that most major and trace elements were determined with reasonable precision with the exceptions of Y and Nb, which display high variance. Accuracy was checked internally by the laboratory using standards with known concentrations of the elements analyzed. The analytical results are displayed in Appendix 2.

In an attempt to assign the volcanic rocks of the Blake River Group to a specific tectonic setting, analyses of basaltic rocks are plotted on Ti-Zr-Y diagram (Figure 65). The diagram displays a wide scatter of points covering all fields with most data points plotting in the fields of ocean floor basalt (OFB) and the within plate basalt (WPB). In order to eliminate the possible analytical errors in analyses of Y, the data were also plotted on a Ti-Zr diagram (Figure 66). These plots appear to show two separate trends, one of which is grouped near the OFB field and the second near the calc-alkalic basalt (CAB) field. Many data points however, fall beyond of the fields outlined by Pearce and Cann (1973).

Rocks of the Blake River Group appear to have elevated titanium contents compared with those of modern tectonic environments. However, the average titanium value for the basaltic rocks of the Blake River Group is 7,830 ppm which is in the range of published data for basaltic rocks (Pearce and Cann, 1973; Condie, 1981; Carmichael et al., 1974). All mafic rocks contain trace amounts of ilmenite which may account for

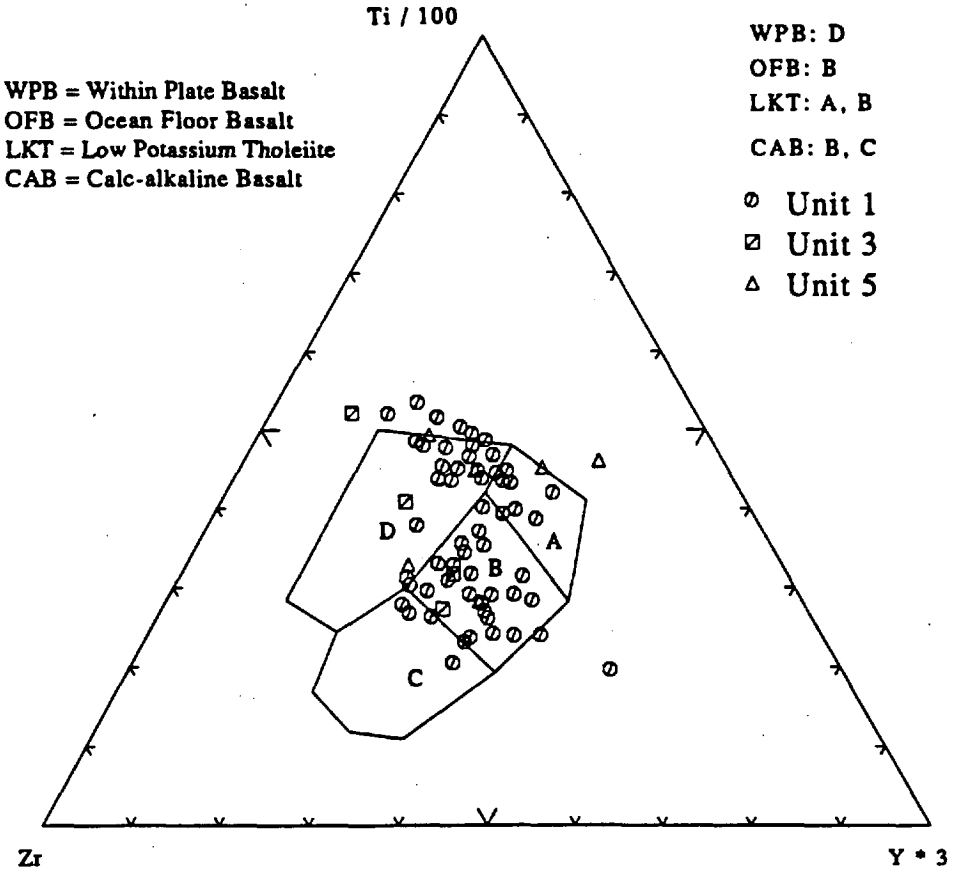


Figure 65. Ti-Y-Zr diagram for basaltic rock of the Blake River Group. Only rocks with CaO+MgO < 20 % and > 12 % were used (after Pearce and Cann, 1973).

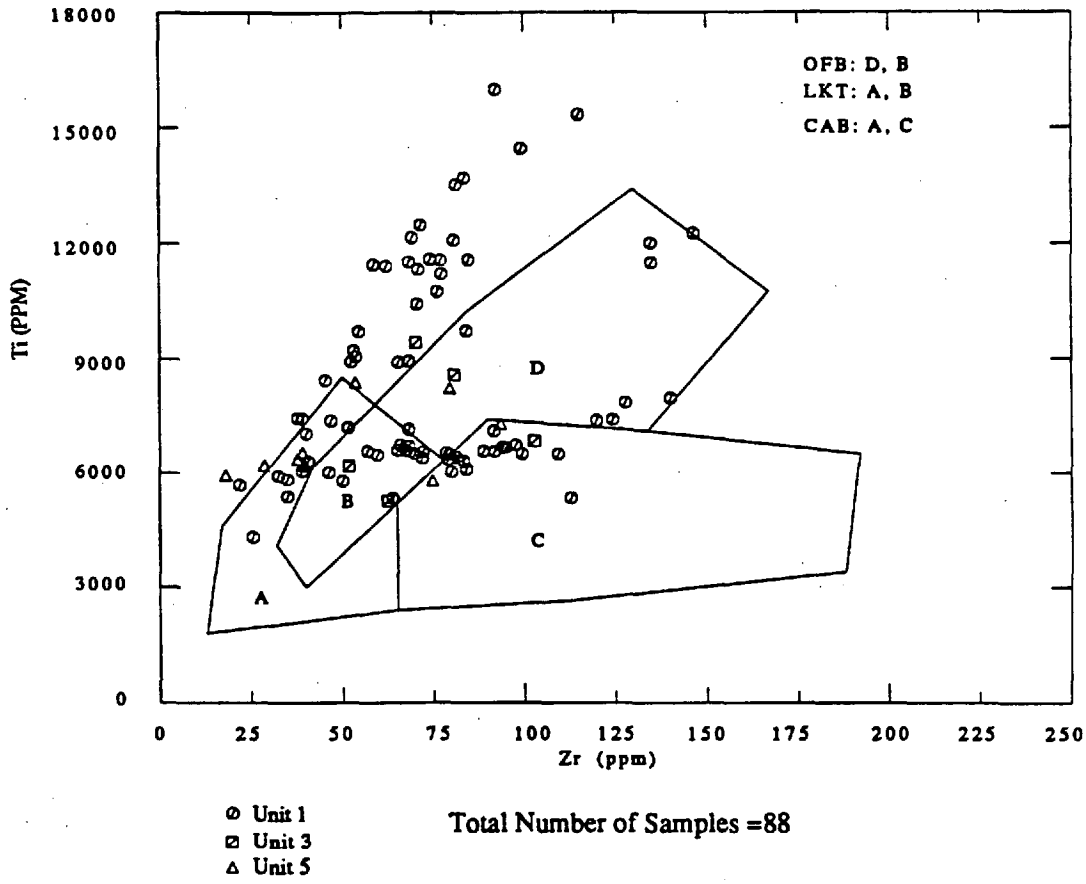


Figure 66. Ti-Zr diagram for basaltic rocks of the Blake River Group (after Pearce and Cann, 1973).

the higher titanium values in some samples and may indicate limited titanium mobility (Van Baalen, 1993). By averaging all points for each rock unit, the wide variation in titanium is eliminated and differences emerge between each unit. With this approach, unit 1 plots within the OFB field, but units 3 and 5 are within the CAB field (Figure 67). The same relationship is expressed on the similarly prepared Ti-Zr diagram (Figure 68).

A common means of identifying different tectonic environments is to display the distribution of the trace elements on a diagram with the values normalized to values for normal mid-ocean ridge basalt (NMORB) in a manner similar to chondrite-normalized plots for the distribution of rare earth elements (REE) (Condie, 1989). The trace elements are arranged in order of increasing incompatibility with a spinel lherzolite (Pearce and Parkinson, 1993; Figure 69). In a plot of this kind, basaltic rocks of the Blake River Group display strong enrichment in large ion lithophile elements (LILE) but have a pattern of high field strength elements (HFSE) similar to that of NMORB values, thus reflecting a similar source mineralogy (Ludden et al., 1982). The LILE enrichment is compatible with an interpretation of contamination of a tholeiitic magma by a continental crustal source. By this treatment, rocks of units 3 and 5 exhibit a higher degree of LILE fraction with respect to NMORB than the rocks of unit 1. The overall pattern of the incompatible elements is similar to that of WPB and CAB from continental margin arcs. However, it should be noted that the deviation from NMORB values is only exhibited by LILE which are the most susceptible to alteration and metamorphism (Pearce, 1983; Ludden and Gelinas, 1982).

Trace elements in igneous rocks often vary significantly between rocks with approximately the same overall major oxide composition, and for this reason, trace elements are a useful tool in differentiating rocks of similar bulk composition and appearance. The similar physical and major elemental characteristics of rocks of units 2 and 6 of the Blake River Group in Bousquet Township have been used to indicate that these two units were lateral equivalents, but on opposite limbs of a major syncline within

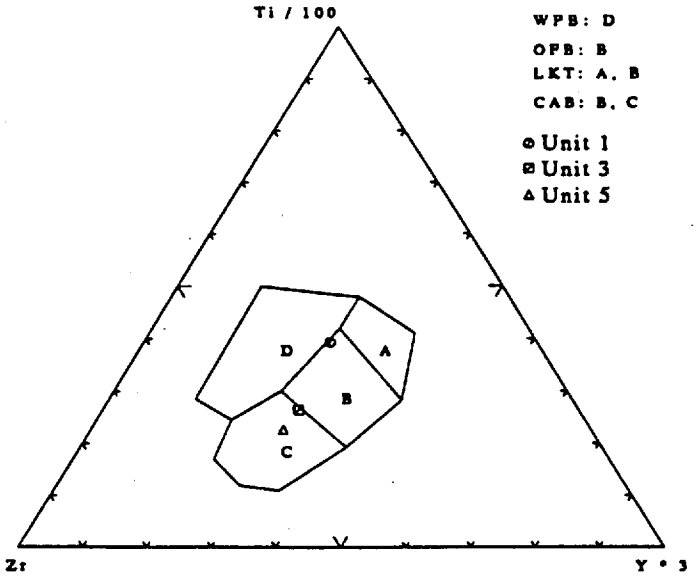


Figure 67. Ti-Y-Zr diagram of average values for basaltic rocks of the Blake River Group (after Pearce and Cann, 1973).

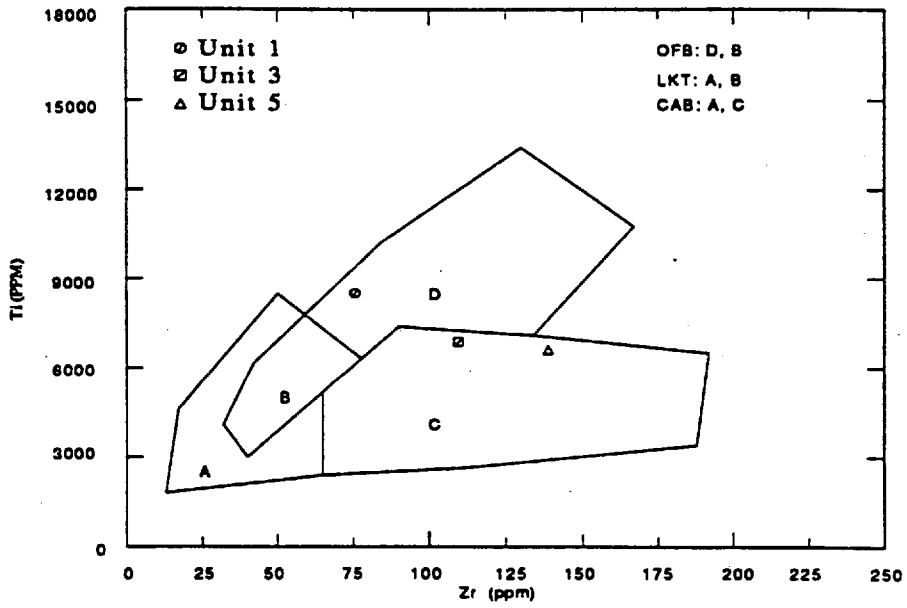


Figure 68. Ti-Zr diagram of average values for basaltic rocks of the Blake River Group (after Pearce and Cann, 1973).

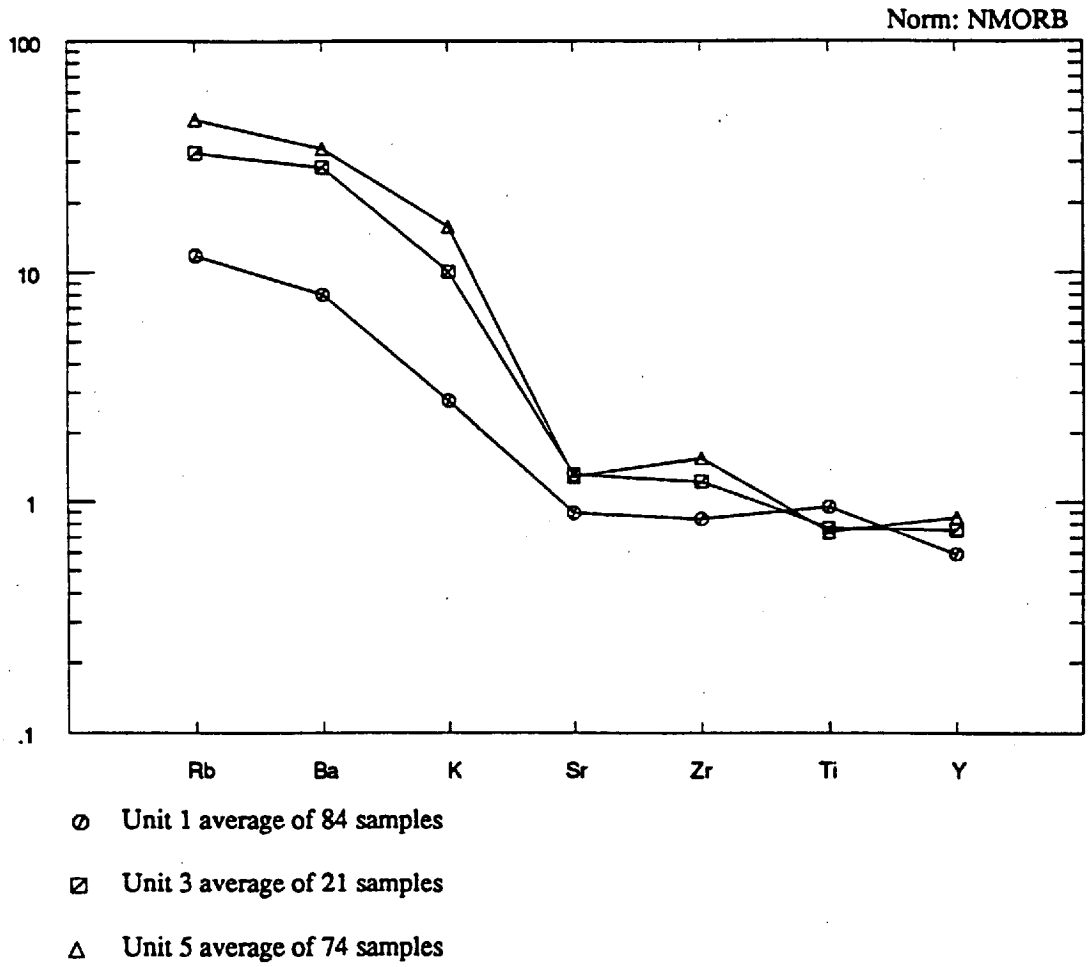


Figure 69. Spidergram of average values for basaltic rocks of the Blake River Group. Normalized to NMORB values (After Condie,1989).

the central portion of the Blake River Group. This evidence was cited for a reversal of younging direction within the volcanic sequence (Bateman, 1984; Eliopoulos, 1983; Hodder et al., 1981). Although the two units have similar major oxide compositions, they have very different (Zr/Y)/Zr and (Zr/Ti)/Ti ratios, and these are not likely to represent lateral continuity of the same volcaniclastic unit on opposite limbs of an isoclinal fold (Figure 70 and 71). The similarities in major element composition between units 2 and 6 are inadequate evidence of folding within the Blake River Group and of a reversal of younging direction.

Trace element analyses of the Mooshla intrusion are in agreement with, and support the interpretation of magma mixing as outlined by plots of the major oxides. The three-element plot of Ti-Sr-Zr yields a straight line with a positive slope and the four element plot yields an hyperbolic curve, both characteristic of mixing (Figures 72 and 73).

A normalized trace element spidergram of the Mooshla intrusion is similar to those of the basaltic rocks except for the enrichment of Zr and Y in the trondhjemite (Figure 74). The similarities between the trace elements of the volcanic and intrusive rocks of the Blake River Group suggest a common parental magma, implying that the Mooshla intrusion is indeed co-magmatic with the rocks of the volcanic succession (Langshur, 1990).

6.4 Rare Earth Element Analyses

The rare earth element signature of a magma is relatively unaffected by metamorphism and alteration so that REE patterns remain nearly constant throughout crystal fractionation (Gromet and Silver, 1983; Ludden and Thompson, 1979). Furthermore, REE contents of basaltic rocks from different tectonic settings exhibit different patterns when normalized to chondritic values (Ludden et al., 1982).

Samples collected for this study were not analyzed for REE, however, data exist from previous studies and warrant brief review here for consideration with the data

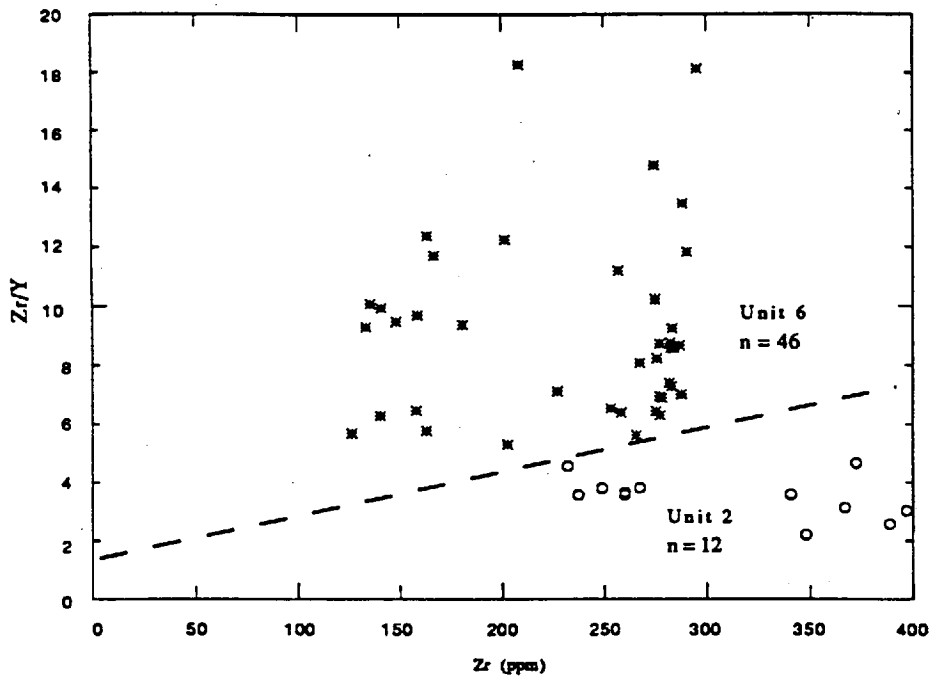


Figure 70. (Zr/Y)/Zr ratio for the felsic volcanic rocks of units 2 and 6.

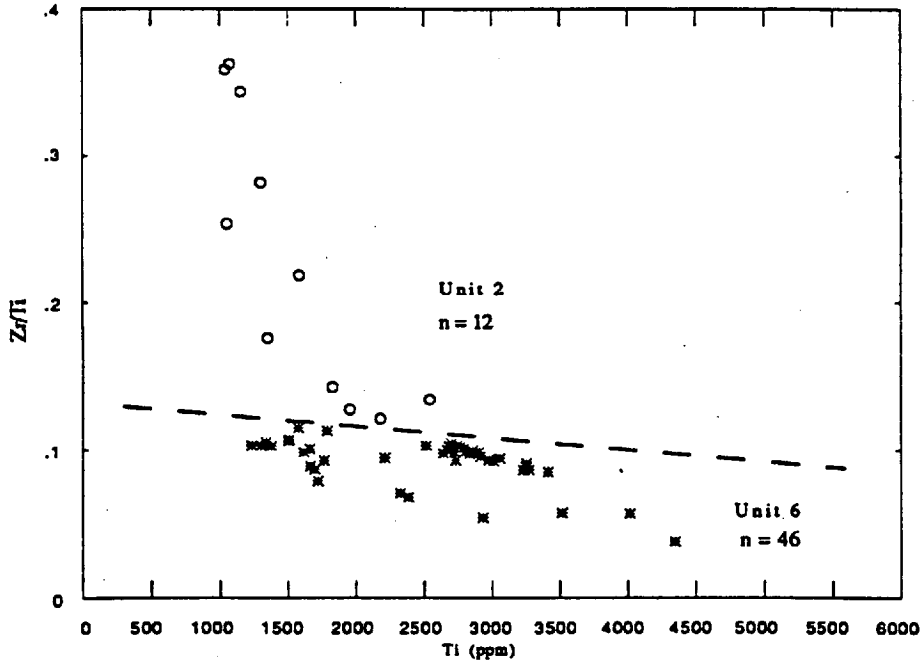


Figure 71. (Zr/Ti)/Ti ratio for the felsic volcanic rocks of units 2 and 6.

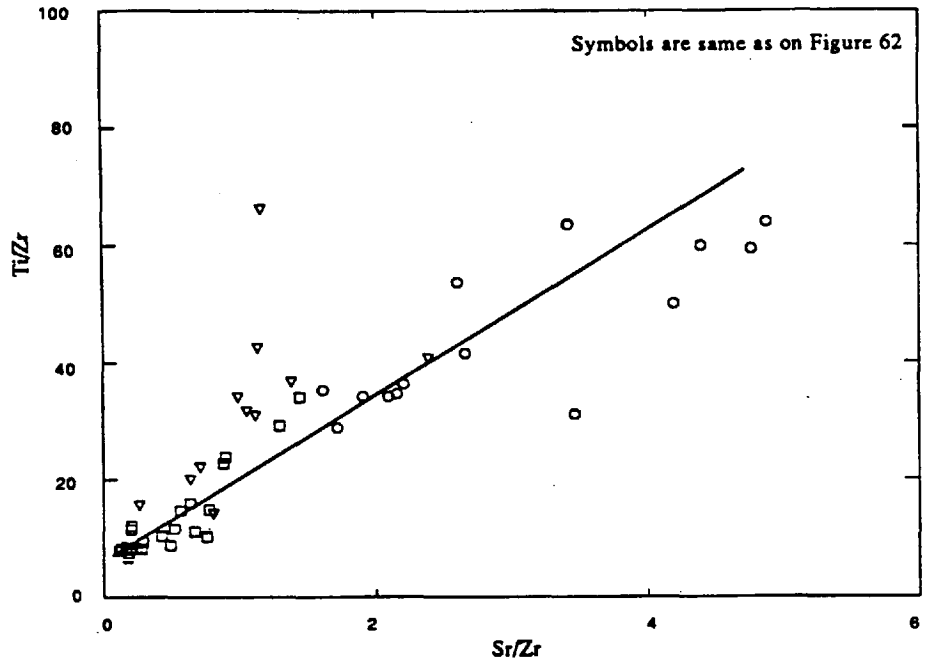


Figure 72. Three element ratio-ratio diagram for the rocks of the Mooshla intrusion.

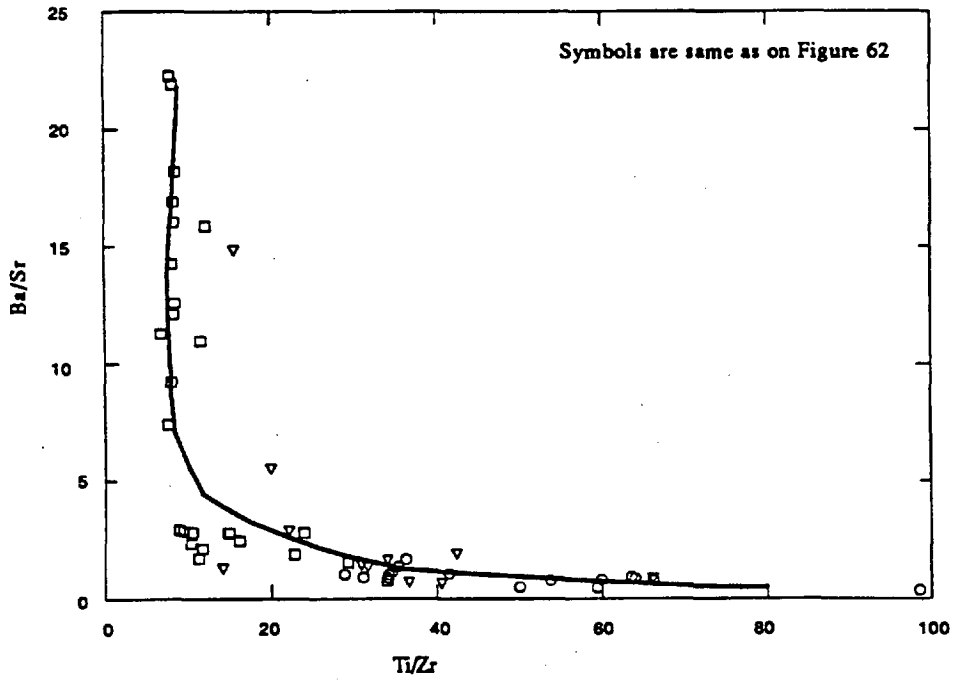


Figure 73. Four element ratio-ratio diagram for the rocks of the Mooshla intrusion.

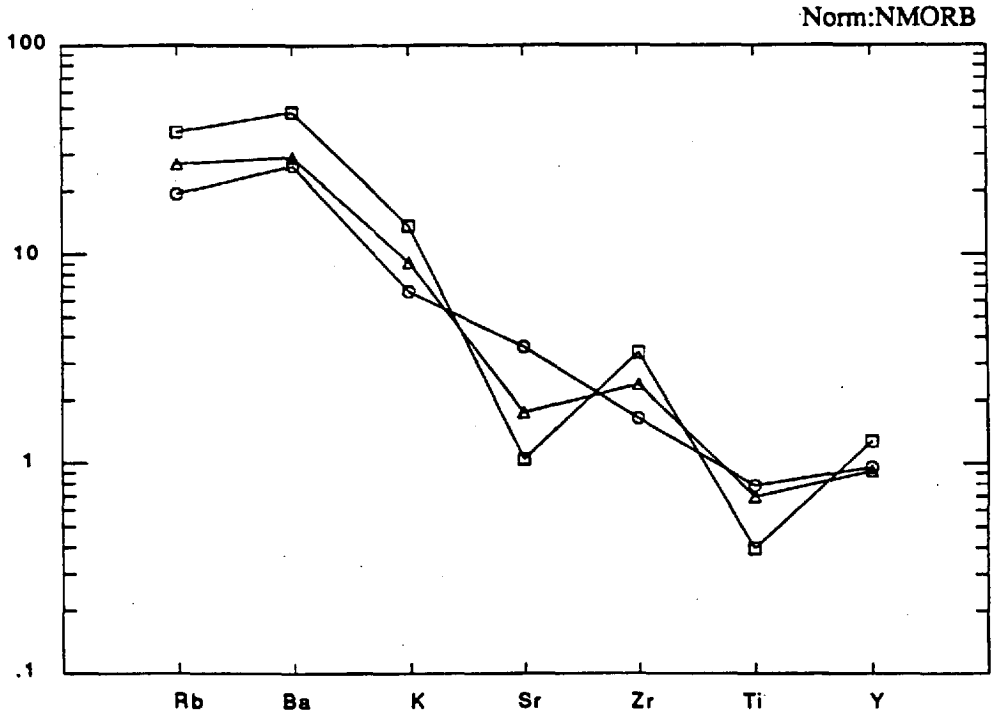


Figure 74. Spidergram normalized to NMORB values for the rocks of the Mooshla intrusion. Number in parenthesis is the number of analysis averaged. Normalized values are from Sun and McDonough (1989).

presented above. The mafic rocks on the Bousquet property display flat REE lines and are slightly depleted in the heavy rare earth elements (HREE) and enriched in light rare earth elements (LREE) (Tourigny et al., 1992). Most samples display a negative Eu anomaly and have an average normalized La/Yb ratio of 2.5 (Figure 75). This pattern is not in agreement with WPB of oceanic crustal origin (Saunders, 1984), but rather is compatible with those of basaltic rocks from back-arc basins from the South Pacific (Eissen et al., 1991).

Comparative analyses of the REE distribution in rocks of the Mooshla intrusion indicate that these rocks are more fractionated in the LREE, and have a higher normalized La/Yb ratio (7.63) than do their volcanic host rocks (Langshur, 1990). The Eu anomaly observed for the volcanic rocks is lacking in the Mooshla intrusive rocks. This pattern is consistent with derivation of the latter by partial melting of basalt at mantle depth, leaving a residue of garnet and clinopyroxene (Hanson, 1978).

6.5 Fluid Inclusion Data

Fluid inclusions can yield information on the temperature and composition of the hydrothermal fluids responsible for the deposition of the inclusion-bearing mineral and associated ore minerals if special care is taken to insure that the trapped inclusions are primary in origin (Goldstein and Reynolds, 1994). Ten samples were selected for fluid inclusion study from the continuous and stockwork veins from the west zone at the Doyon mine in order to discern whether the two veins types were formed by fluids of different temperature, origin and composition, and to compare with the results of previous fluid inclusion studies for the Doyon and Bousquet occurrences (Guha et al., 1982; Savoie et al., 1991; Tourigny et al., 1992). Doubly polished sections were prepared and each section was studied using the methods outlined by Goldstein and Reynolds (1994).

Detailed petrographic study of the samples revealed that at least two generations of quartz are present in all veins. Both generations have similar inclusion populations

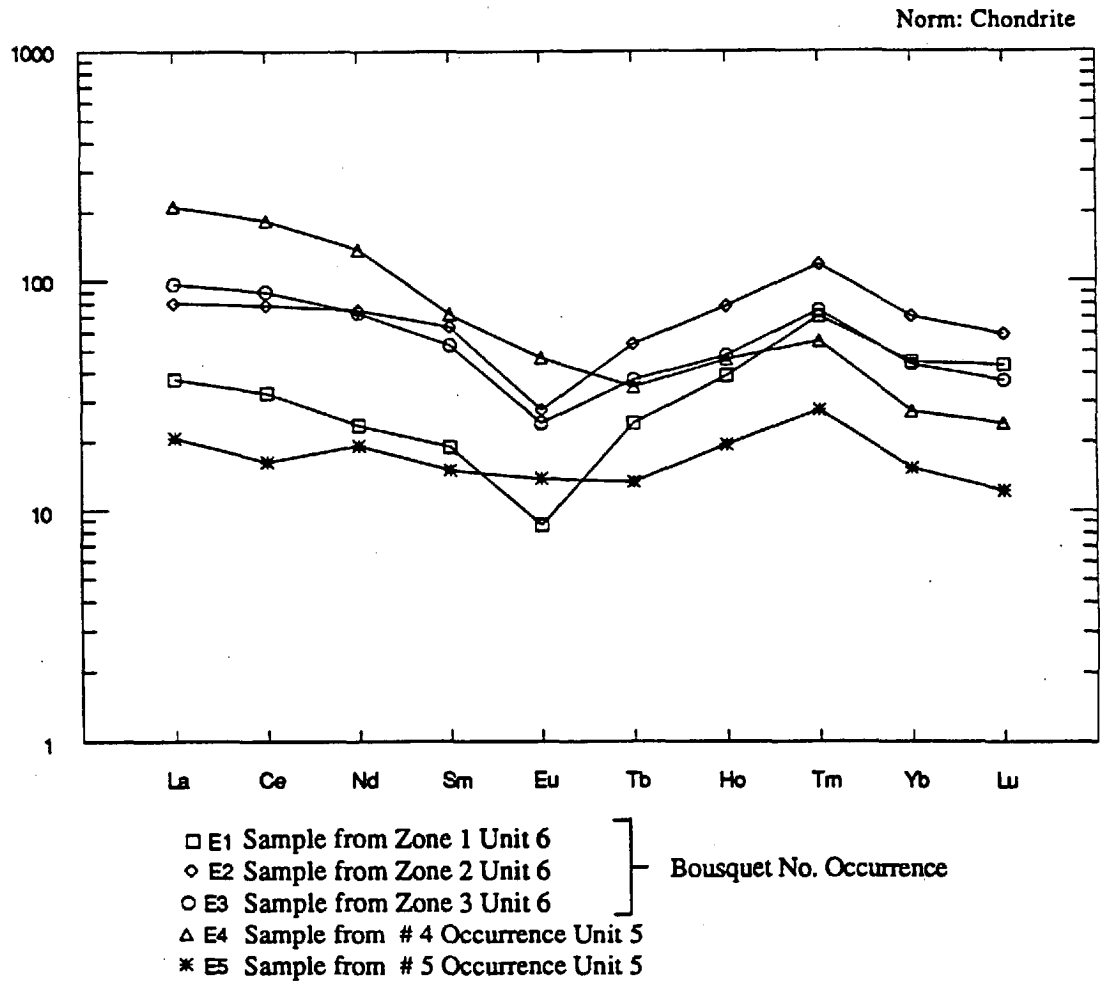


Figure 75. Chondrite normalized REE distribution of the basaltic rocks of the Blake River Group. Normalized values from Sun and McDonough (1989). Data from Tourigny et al., (1992)

which can be grouped into three distinct classes; inclusions with single liquid and vapor phases, inclusions with double liquid and single vapor phases and inclusions with liquid, vapor and solid phases. Most inclusions are 5 to 10 microns in diameter and have been deformed and stretched. The inclusions are on healed fractures and interpreted as secondary, therefore not likely to reveal primary fluid temperatures and compositions (J. Reynolds, pers. comm., 1995). For this reason, no further inclusion work was carried out on the samples. Homogenization and melting temperatures of similar inclusions from the Doyon Mine (Savoie et al., 1991) indicated that the inclusions were formed between 300 and 335° C. Inclusions from veins in the trondhjemite have salinities of 15 weight percent equivalent NaCl, whereas veins in the felsic volcanic rocks of unit 4 (main zone) exhibit salinities of 3.5 percent. The high proportion of CO_2-rich inclusions, greater than 80 percent of total population, suggests that the fluids responsible for the inclusions in both the west and main zones were CO_2- dominated.

Although the gold-bearing zones at Bousquet No. 1 Mine do not for the most part, contain numerous quartz veins, a few cm-wide quartz veins cut across the ore-bearing pyritic zones, and gold is sometimes remobilized within and along these veins (Valliant, 1981). A fluid inclusion study of quartz veins from Bousquet No. 1 was carried out by Tourigny et al., (1992) and their results are summarized below.

Three generations of quartz were recognized but inclusions were present only in two of these. Three types of inclusions exist, CO_2-rich inclusions, two liquid phase inclusions, and inclusions with two liquids and a solid phase. The first of these amount to 90 percent of the inclusions present. Homogenization temperatures of the aqueous-phase inclusions range from 110 to 400° C and their inclusions have salinities ranging from 1 to 2.5 weight percent equivalent NaCl.

6.6 Geochronology

Data on the geochronological evolution of the Blake River Group can assist in the understanding of its metallogeny. However, age determinations for the study area are limited to lead-lead analyses carried out by Valliant (1981) on samples of galena from the Bousquet No. 1 Mine which yielded an average age of 2.7 Ga for the galena. Samples collected by Deloule et al., (1989) from a granitoid rock on the Bousquet property gave similar $^{206}Pb/^{204}Pb$ ratios to those calculated by Valliant (1981) but no isochron was calculated because of the presence of radiogenic lead.

A sample of biotite from the rocks Cadillac Group immediately south of the study area returned an $^{40}Ar/^{39}Ar$ age of 2513±10 Ma (Feng et al., 1992). Age determinations were never carried out on the Doyon property or on the Mooshla Complex.

6.7 Summary

Although Archean plate tectonic models are not entirely compatible with present day analogues, it is likely that some form of plate motion occurred in Archean time. The geochemical character of the rocks of the Blake River Group is a function of their original magma chemistry and tectonic setting. The chemical characteristics of the rocks of the volcanic sequence exhibit many similarities to those of comparable rocks from modern day tectonic environments. Major element analyses of the Blake River Group volcanic rocks indicate bimodal volcanism similar to that associated with tensional tectonic environments, and its trace elemental and REE characteristics are compatible with those of mafic rocks from back-arc basin environments. The wide scatter of points on tectonic discrimination diagrams suggests unknown differences in tectonic regimes and mantle chemistry from Archean time to the present.

Determination of the younging direction of the volcanic sequence is essential in developing a meaningful metallogenic hypothesis for the area studied. Trace element ratio diagrams proved useful in distinguishing subtle differences between rocks of units

2 and 6, therefore discounting the hypothesis of north-facing stratigraphic relationship in the southern part of the Blake River Group and a previously hypothesized major synform.

Fluid inclusion studies indicate that fluids in quartz from veins in the west zone of the Doyon Mine have higher salinity than those in quartz from rare veins at Bousquet No. 1 Mine by about 10 weight percent equivalent NaCl. The inclusions were also trapped at different temperatures, suggesting a somewhat different fluid chemistry for the two occurrences, which is not in agreement with a single metamorphogenic origin for all gold mineralization in rocks of the Blake River Group as previously proposed (Marquis et al., 1990). Fluid salinities in quartz from veins of the West zone at Doyon are similar to those in quartz from porphyry copper and copper-gold deposits associated with large plutonic intrusions (Beane and Titley, 1981).

Chapter 7
SYNTHESIS OF THE GENETIC EVOLUTION AND METALLOGENY OF THE BLAKE RIVER GROUP

7.1 Introduction

Gold mineralization occurs in sheared, deformed and metamorphosed mafic and felsic intrusive and volcanic rocks within the study area. This mineralization occurs both as pyritic bodies and as quartz-dominated veins. Although, at first glance, the mineralization might appear to be distributed throughout the sequence, this study shows that certain litho-stratigraphic horizons are more favourable than others, and the extent and character of mineralized horizons vary from the base to the top of the volcanic succession.

Several genetic hypotheses have been proposed to explain the genesis of gold occurrences in the study area. These range from simple exhalative syngenetic hypotheses (Valliant, 1981; Valliant and Barnett, 1982), to simple syn- or post-tectonic metamorphogenic emplacement (Savoie et al., 1986; Marquis et al., 1992). They also include pre-metamorphic epigenetic emplacement and multi-stage processes involving both syngenetic pyritic mineralization with post-tectonic, epigenetic emplacement of gold mineralization (Tourigny et al., 1989). The explanation for such diverse hypotheses is simply that each worker was describing a particular or individual aspect of each occurrence and thereafter broadening the scope of his study by utilizing the resulting observations to postulate a single process that would account for all mineralization. Alternatively, multiple processes acting throughout the evolution of the volcanic pile were perhaps more likely (Hutchinson, 1993).

Each gold occurrence within the Blake River Group is a function of the following

parameters: source rock composition, fluid transport, fluid discharge, deposition and deposit preservation. These factors are fundamental, regardless of whether the deposit was formed by syngenetic or epigenetic processes or by some combination of these. The available source rock and the fluid composition are different depending on the particular genetic processes involved. According to Colvine et al., (1988), most metamorphogenic Archean gold lodes share similar morphology and are quartz vein hosted. Because of the great variability in mineralized zone morphology and the general lack of quartz veining in the occurrences of Bousquet Township, metamorphogenic processes are not considered to be a viable, single mechanism responsible for the formation of all these various gold occurrences. Similarly, simple syngenetic processes are insufficient to explain the attributes of every occurrence, and particularly of the discordant veins. It is therefore, appropriate to discard both these "extreme" genetic hypotheses and seek an explanation that satisfactorily explains all the differing characteristics of these deposits.

To develop such a comprehensive metallogenic hypothesis for gold mineralization the genetic evolution of the volcanic rocks of the Blake River Group and of the Mooshla intrusion must be considered, along with the stratigraphic and structural settings of each occurrence. The effects of post-depositional deformation and metamorphism must also be considered and included in the hypothesis.

7.2 Genetic Evolution of the Blake River Group

The Blake River Group contains the youngest volcanic rocks of the Abitibi belt in northwestern Quebec, which have been radiometrically dated at 2703-2698 Ma (Mortensen, 1987; Jensen, 1985). The volcanic sequence is characterized by subaqueous, differentiated, mafic, calc-alkaline or tholeiitic flows intercalated with felsic pyroclastic rocks. The rocks are intruded by the Mooshla intrusion in the western part of the study area. Within the study area, the volcanic rocks of the Blake River Group are divisible into three separate bi modal volcanic cycles but its base is not exposed. Each cycle is

separated by what was apparently a hiatus in volcanic activity (Jensen, 1985). The volcanic sequence is in fault contact with the sedimentary rocks of the Kewagama Group to the north. The evolution of the Blake River Group volcanic succession is therefore represented by the three eruptive cycles present in Bousquet Township, and the assumption is made here that these rocks rest on the underlying volcanic rocks of the Kinojevis Group (Jensen, 1985; Card, 1990; Lafleche et al.,1992a; Dimroth et al., 1982).

7.2.1 Cycle 1

The first indication of Blake River volcanism consists of unit 1, a thick sequence of laterally continuous, tholeiitic and pillowed basaltic flows. This sequence forms nearly half of the eruptive rocks of the study area. The rocks have major and trace element compositions that are similar to those of ocean floor basalt, and were probably extruded in a tensional environment on the sea floor (Dimroth et al., 1985). Overlying this tholeiitic base are the felsic rocks of unit 2 which represent the termination of volcanism of cycle 1. Hydrothermal fluids passing through and reacting with the rocks of the thick pillowed sequence would have been strongly reduced and high in sulphur content permitting generation of bisulfide complexes (Hutchinson, 1993). These reduced fluids were capable of mobilizing Si, Fe, Ca, Mg and minor amounts of gold, all of which are present in elevated amounts in the # 6 occurrence. The pillow lavas were porous, permeable and readily penetrated by the reduced hydrothermal fluids which were discharged passively on the sea floor over broad unfocused fumarolic fields (Hutchinson, 1993). The lack of vesiculation in the pillows of the basalts of unit 1 is indicative of deep water. If water depth was in the order of 3,000 metres or greater, the confining water pressure would have prevented explosive fragmentation of the felsic rocks of unit 2 (Cas and Wright, 1988). Unit 2 therefore, was probably a very massive and uniform flow lacking good porosity. The lack of sedimentary strata at the close of cycle 1 volcanism, and the low porosity of unit 2 may have resulted in considerable loss of the

discharged fluids, to sea water at the sea floor.

Recent studies of exhalative deposits forming on the sea floor indicate that for preservation of ore, sea floor exhalation must be either isolated from sea water by a siliceous cap or an Fe-Mn crust (Fouquet et al., 1993; Goodfellow and Franklin, 1993) or by a layer of water of high salinity and density compared with the overlying sea water (Degens and Ross, 1969). These factors may in part explain why the # 6 occurrence is hosted within the basal tuffaceous rocks of the second volcanic cycle. As cycle 2 volcanism began, exhalative activity generated from the rocks of cycle one beneath probably continued for some time. The tuffaceous rocks of cycle 2 then acted as a permeable layer for the rising hydrothermal solution, permitting the preservation of its precipitated sulfide minerals. In other words, hydrothermal activity initiated from, and marking the termination of extrusive activity of cycle 1, was interrupted and sealed off by the onset of cycle 2 volcanism.

7.2.2 Cycle 2

Cycle 2 volcanism began with more explosive eruptions and deposition of thin layers of mafic tuffaceous rock, followed by extrusion of calc-alkaline, pillowed flows. Because basaltic lavas have effusive rates that are a few orders of magnitude greater than those of felsic lavas or intermediate pyroclastic flows (Cas and Wright, 1988), the hydrothermal system was probably overwhelmed by the mafic lavas but not by the mafic tuffaceous deposits. Estimated effusive rates for fissure-erupted basaltic lavas are as high as 10,000 m^3 per second for each kilometre of fissure whereas silicic eruptions have effusive rates in the order of 1 to 10 m^3 per second (Walker, 1973). It is therefore suggested that hydrothermal activity was re-initiated following basaltic volcanism when effusive rates were less and a thick pile of "hot" lavas had accumulated on the sea floor. Capping the basaltic lavas of cycle 2, on the Bousquet property, is a pyroclastic flow of intermediate composition and, on the Dumagami and Doyon properties, both east and west

of the Bousquet property, is a similar but felsic pyroclastic rock.

Hydrothermal fluids rising from the underlying volcanic sequence at the end of cycle 2 would have been similar to the earlier ones from cycle 1 on the Bousquet property because the volcanic rocks below were predominantly mafic in composition. On the Doyon and Dumagami properties hydrothermal solutions could have been precipitated, and the sulfide minerals could have been preserved within a porous, unconsolidated felsic detritus on the sea floor. Fluids on the Bousquet property were, however, discharged on top of the basaltic flows, directly on the sea floor, and lacked means of preservation until the onset of volcanism of cycle 3 when unconsolidated mafic tuffaceous material was erupted, and the sulfides were again deposited in the resulting unconsolidated tuffaceous sediment. This stage of volcanism and related hydrothermal activity led to the formation of the #5 and # 4 occurrences on the Bousquet property, and the B and C zones of the Ellison occurrence.

7.2.3 Cycle 3

Cycle 3 volcanism began with intercalated mafic and intermediate ash flows, followed by extrusion of a thin sequence of basaltic pillowed flows of unit 5. Overlying the latter is a thick sequence of felsic volcaniclastic ash tuff which is then overlain by a rhyolitic pyroclastic breccia. Felsic ash and breccia was probably deposited from the explosive emergence, subsequent collapse of small rhyolitic domes on the Dumagami and Doyon properties to the east and west of the Bousquet property respectively. Brecciation of the felsic rocks is indicative of shallow water environment and the upper portions of these domes may have become sub-aerial (Stone, 1988; Valliant, 1981; Ayres et al., 1985; Dimroth et al., 1982). Once again, at the termination of basaltic magmatism, the hydrothermal system was re-initiated, and, thereafter continued through the end of felsic magmatism of cycle 3.

Hydrothermal fluids passing through the volcanic sequence at the end of cycle 3

were almost certainly different from those of the earlier two cycles. Fluids migrating through the volcanic sequence at the end of cycle 3 volcanism passed through a mixed sequence including both mafic and felsic end members. As well these fluids could have extracted metals from the metalliferous zones associated with the rocks of cycle 2. This "scavenging" of metal from the lower zone, may in part explain why the lower zones are smaller and of lower grade than their counterparts in the upper part of the volcanic sequence.

During the earliest stage of hydrothermal activity, the brecciated flow tops of unit 5 were altered to Fe-Mn hydroxide minerals. The continuing hydrothermal activity leached the alkalic components from the overlying felsic tuffaceous rock enriching the residue in alumina. The thicker felsic pyroclastic strata of unit 6 perhaps permitted the hydrothermal fluids to maintain higher temperature, enabling chloride complexing and transport of both gold and base metals (Hutchinson, 1993). From this fluid, chalcopyrite and pyrite were deposited in stockwork veins along fluid pathways that may have been tensional faults. Auriferous base metals were discharged within the unconsolidated volcaniclastic debris near the sea floor. Sphalerite, with pyrite, was deposited at the stratigraphically higher sea water- volcaniclastic interface, and ultimately the fluids vented into sea water through chimneys at the top of the deposit. Original metal enrichment at the Bousquet No. 1 and 2 deposits, the Warrenmac and Ellison A zone probably resulted from similar mechanisms.

7.2.4 Mooshla Intrusion

Timing of emplacement of the Mooshla intrusion is not well determined, but it is believed to be co-magmatic with the Blake River Group (Langshur, 1990; Valliant and Hutchinson, 1982). The intrusion is multi-phase, the quartz diorite being earlier and the trondhjemite later. Hydrothermal magmatic fluids associated with the cooling stages of the trondhjemite led to the generation of the siliceous stockwork in the central portion of

the Doyon west zone. Meteoric, and/or sea water encroaching on the collapsing magmatic system led to development of propylitic and phyllic alterations, and to the quartz veins in the porphyritic quartz diorite and the felsic rocks of unit 4 (Beane and Titley, 1981). The veins were emplaced parallel to the minimum stress field, which at the time was parallel to the foliation (i.e. volcanic stratigraphy) of the volcanic rocks and, along fractures, perpendicular to the intrusive contact for the porphyritic quartz diorite. Convection of acidic hydrothermal fluids through the overlying cap rocks of unit 4 of the Blake River Group resulted in extensive leaching of alkali-cations, and in the formation of a broad pyritic-argillic alteration halo above the intrusion. The primary gold enrichment of # 1 zone at the Doyon mine, produced during hydrothermal activity associated with cycle 2, may have been remobilized by the circulation of the waters associated with the argillic alteration of units 4 and 5.

7.2.5 Metamorphism

Metamorphism of the volcanic sequence began immediately after burial and diagenesis (Hutchinson, 1993). In Bousquet Township, peak metamorphism reached temperatures of 450 °C and pressures of 3.8 kbar (Stone, 1988; Marquis et al., 1992). Because prograde metamorphic reactions involve dehydration, considerable fluid pressures must be associated with prograde metamorphism (Spear, 1993; Etheridge et al., 1983). Metamorphic fluids have been interpreted as possible mobilizing agents for gold in Archean terrains (Colvine, 1988; Colvine et al., 1988; Burrows and Spooner, 1989; Feng et al., 1992). Metamorphism of the rocks of the Blake River Group has affected all earlier, primary hydrothermally altered zones and metalliferous deposits.

Metamorphic fluids generated by dehydration reaction would migrate towards environments of lower temperature and pressure following paths of least resistance such as permeable horizons, lithological contacts and existing faults. All primary mineral concentrations were affected and re-crystallized by these migrating metamorphic fluids

as a result of elevated temperature under greenschist metamorphism. Some primary mineral enrichments may thus have been partially dissolved, transported and redeposited down metamorphic gradient. Some veins in the porphyritic quartz diorite and in unit 4 at Doyon may have resulted from such metamorphic remobilization. Gold in cross-cutting veins at Bousquet No. 1 Mine may also be metamorphogenic in origin. Metamorphism of the hydrothermally altered rocks at Bousquet No. 1 and 2 occurrences resulted in the manganiferous garnet-rock in the rocks of the footwall, and also in the andalusite schist of the hanging wall. Metamorphic reactions converted the rocks of the pyritic argillic alteration envelope in unit 4 at Doyon to a quartz-sericite schist rock.

Late-stage, retrograde metamorphic reactions to lower greenschist rank resulted in the breakdown of porphyroblasts of andalusite to pyrophyllite, kaolinite and quartz.

7.2.6 Deformation

Deformation also played an important role in influencing the present morphology and structural setting of the gold occurrences of the area. All mineralized zones display some evidence of brittle-ductile deformation. Shearing or faulting is locally associated with all the gold and base metal occurrences. Deformation has obliterated all geopetal fabric of units 3 to 5, and only the primary texture of the breccia of unit 6 is preserved. After the termination of volcanism, the rocks of the Blake River Group were tilted by folding in a single, south-facing homocline. Most major lithological contacts display evidence of faulting parallel to the contacts. On the Bousquet property, faulting parallel to regional foliation resulted in reverse displacement with a late dextral strike-slip movement (Tourigny et al., 1988; Tourigny et al., 1993). Although deformation was intense, most of it was focused along anastomosing faults which developed along or near the contacts of major but differing rock units, particularly where these contacts separated rocks of very different competency. Total displacement is unknown but late dextral

displacement of Proterozoic diabase dikes is in the order of 500 metres.

Deformation of the Bousquet No. 2 occurrence resulted in large scale flattening, rotation, stretching and transportation of the primary sulfide body (Tourigny, et al., 1993). Gold and copper were remobilized by plastic deformation into fractures in recrystallized pyrite and into triple junction of pyrite grains. Sphalerite was remobilized as pressure shadows around pyrite grains (Tourigny et al., 1993). Plastic deformation of the massive ore resulted in schlieren banding and durchbeweggung texture. Fragments of the host andalusite schist were rafted within the massive ore, resulting in the brecciated massive sulfide. During the final stages of extension associated with dextral, east-west deformation, sub-vertical piercement structures containing sulfide and gold (Maiden et al., 1986; Osterman and Hutchinson, 1994; Teasdale et al., 1995) developed at the contacts between massive sulfide and the andalusite schist. Associated with the same late deformation event, foliation-perpendicular, mm-scale, north-south fractures were developed within the massive pyritic sulfide body. Gold, bornite and tennantite were remobilized into the piercement structures and north-south fractures by plastic flow of more malleable, softer and easily deformed minerals (Stanton, 1972). East-west displacement along strike-slip faults is, in part, responsible for the present location of the fringe ore at Bousquet No. 2 Mine and the mineralized zones of the Bousquet No. 1 mine.

Deformation of the rocks at the Doyon Mine resulted in the shearing within the metamorphosed, argillic alteration, and in east-west displacement of the mineralized veins and of the alteration envelopes associated with the emplacement of the trondhjemite.

Late stage north-east-trending normal faults displaced the volcanic strata, but do not appear to have significantly affected the earlier hydrothermal deposits or contributed to the metallogenic history of the area.

7.3 Modern Analogues

Two broad hypotheses try to explain Archean plate motion. The first calls upon Phanerozoic plate tectonic analogues (Dimroth et al., 1983; Gelinas and Ludden, 1984). The second invokes unique Archean plate interactions involving horizontal subduction and vertical sinking of the Archean volcanic complexes (Jensen, 1985; Hutchinson, 1981). These hypotheses attempt to explain both the similarities but also the major differences between Archean volcanic successions and their modern day analogues. Archean volcanic successions are of two broad types, the oldest successions are characterized by ultramafic komatiite at the base and mostly dominated by mafic tholeiitic rocks with minor felsic components, and the younger ones are characterized by a mafic tholeiitic base and felsic rhyolitic tops with felsic and mafic proportions sometimes present in equal amounts (Jensen, 1985). The rocks of the Blake River Group in Bousquet Township lack komatiite towards the base of the sequence, and the succession is dominated by a large proportion of felsic volcanic rocks. As such, the upper portion of the Blake River Group in Bousquet Township shares more similarities with modern day volcanic island arc terrains than with older Archean successions.

In order to identify modern day analogues, certain criteria must be observed. Because the Archean geothermal gradient was presumably higher than at present (Condie, 1981), the length of spreading ridges were probably greater than those of the present day, and crustal thickness was probably thinner. Continental masses were smaller and the tectonic regime was probably oceanic-dominated. Clastic sedimentation, namely sedimentary rocks of the Kewagama and Cadillac Groups suggest, proximity to continental sources. The tectonic setting of any modern analogue must also constitute a favorable site for deposition of gold and base metals.

The back-arc basins of the South West Pacific, in particular the Lau basin, may represent the best modern analogue of the depositional environment of the Blake River Group. The former is situated between the island chains of Tonga and Fiji. The basin

is interpreted as an active, back-arc spreading basin between the remnant arc of the Lau ridge and the Tonga-Kermadec arc (Ewart et al., 1977). The basin has a triangular shape and is 600 kilometres wide at the north but only 200 kilometres in the south. The Valu Fa ridge is the active spreading center within the Lau basin. The ridge is 2.5 to 5 kilometres wide and rises 500 metres above the surrounding sea floor, and water depth ranges from 1,600 to 2,000 metres (Herzig et al., 1993). The central area of the rift consists of small straight ridges only a few hundred metres wide, with steep slopes covered with volcaniclastic debris (Fouquet et al., 1993).

Recent studies of the Lau basin indicate that volcanic activity includes both mafic pillow flows and intermediate to felsic pyroclastic flows (Frenzel et al., 1990; Ewart and Hawkesworth, 1987; Eissen et al., 1991; Von Rad and Muhe, 1990). The basaltic flows are erupted along spreading ridges and are characterized by LILE and LREE enrichments compared to those in NMORB. All these aspects are similar to the basaltic rocks of the Blake River Group. Rocks of the Lau basin belong to a bimodal suite and the more mafic members are tholeiitic in composition whereas the felsic pyroclastic members are calc-alkaline (Frenzel et al., 1990).

Furthermore, recent dives near the Valu Fa ridge found gold-bearing sulfide deposits forming on the flanks of the ridge (Fouquet et al., 1993; Herzig et al., 1993). Massive copper-iron sulfides are also deposited from hydrothermal springs in porous andesitic tuff at the volcanic/volcaniclastic interface. A large mound of barite-sphalerite caps the massive sulfide deposit on the sea floor. An Fe-Mn crust is formed by the discharge of fluids peripheral to the vent. Minerals recovered form this massive sulfide deposit include pyrite, chalcopyrite, bornite, sphalerite, tennantite and marcasite (Fouquet et al., 1993). Gold contents exceeding 28 ppm have been reported from samples collected from the massive sulfide zone (Herzig et al., 1993).

Although the geological setting and sulfide mineralogy of these rocks and sulfide deposits of the Valu Fa ridge are similar to those of the Blake River Group, some

differences are recognizable. The Archean deposits, with rare exceptions, lack barite whereas the Valu Fa deposits are all associated with barite caps. The lack of barite in Archean deposits may be related to the low oxygen content of the Archean ocean or the high solubility of barite in metamorphogenic fluids above 250 °C (Barnes, 1979).

7.4 Recommendations for Further Work

Although there are those who advocate that the Bousquet - Doyon properties have had their share of scientific studies, much work remains to be carried out. The extension of the geochronological study of the felsic volcanic rocks of the Blake River Group to the west towards the Davidson Creek fault and beyond, would add valuable information to the understanding of the genetic evolution of these rocks in Bousquet Township and in correlating them with those of the Noranda area. A detailed structural analysis of the displacement of the post-ore mafic dikes at Doyon may prove useful in understanding the displacement of quartz veins and mineralized stockworks. Detailed mapping of the structural fabric of the massive ore near the south-bounding fault at Bousquet No. 2 could yield to an improved understanding of the relationship of the ore with the overlying schist, and possibly aid in the discovery of additional ore. An expansion of the litho-geochemical analyses of the rocks of the Blake River Group both to the east and west of the study area would be valuable in testing the proposed hypothesis that the former are chemically similar to those of back-arc basins. This in turn, would assist in an improved understanding of ancient volcanism in Archean and Lower Proterozoic greenstone belts, and in understanding the tectonic regimes in which they were generated.

7.5 Recommendations for Exploration

Late epigenetic gold concentrations in Bousquet Township are spatially associated with faulting and shearing but earlier, syn-depositional gold enrichment was apparently associated with a hiatuses in volcanism between mafic dominated eruptions and felsic

dominated ones. Furthermore, larger occurrences are associated with altered, fine- to medium-grained felsic pyroclastic rocks on the flanks of emerging felsic domes associated with volcanic activity of cycle 3. Exploration should therefore be focused in areas of deformed felsic volcanic rocks near the tops of volcanic cycles or of the volcanic pile. One such area lies west of the Doyon property immediately west of the Mooshla intrusion.

Chapter 8
CONCLUSIONS

Economic gold mineralization in Bousquet Township resulted from multiple processes acting at different times during the prolonged volcanic and tectonic evolution of the volcanic rocks of the Blake River Group. Primary syn-depositional gold mineralization occurred at hiatuses in volcanism that was cyclical. The primary mineral depositions were formed by processes and in environments similar to those in present day, active, back-arc spreading basins. A detailed synthesis of the metallogeny of the Blake River Group in Bousquet Township reveals that the generative hydrothermal system evolved through time along with the volcanic members of a cyclical volcanic succession from a deep water exhalative system of unfocused discharge that was dominated by mafic pillowed flows, to a shallow water system of focused discharge in poorly consolidated, felsic volcaniclastic debris. This hydrothermal system resulted in minor gold and pyrite enrichment in the base of the sequence and in the formation of auriferous massive sulfide deposits at the top. The presence of unconsolidated volcaniclastic debris or sediment at the end of a volcanic cycle was essential for the formation and preservation of sulfide deposits. These tuffaceous horizons at the end of volcanic cycles are useful guides in recognizing new mineral deposits. Progressive and prolonged "leaching" of the occurrences of the lower volcanic cycles by continuing hydrothermal activity may, in part, account for the lower grade and size of these occurrences compared to the ones near the top of the sequence.

Metamorphism and deformation remobilized gold and base metals into cross-cutting auriferous-pyritic veins and in mm-scale fractures that are important in most of the occurrences. Manganiferous garnet- and andalusite-bearing alteration assemblages

associated with gold mineralization on the Bousquet property represent metamorphosed equivalents of prior sea floor alteration of mafic and felsic rocks respectively. Paragenetic sequences at the Bousquet No. 2 occurrence are indicative of plastic deformation and flowage of sulfide minerals under confining stress.

Gold mineralization is also associated with a multi-phase, high-level trondhjemitic intrusion. This gold mineralization occurs as stockwork veinlets in quartz-sericite-pyrite-altered trondhjemite and with larger, more continuous quartz-chalcopyrite-pyrite veins that are peripheral to the former. Gold content of the stockwork veinlets is proportional to the pyrite content of the host rock. Alteration and fluid inclusion temperatures and salinities associated with these intrusive-hosted gold deposits are similar to those described for porphyry copper-gold deposits of continental arc environments.

The geochemical character of the volcanic rocks of the Blake River Group is a function of their original magma chemistry and tectonic setting. The affects of metamorphism and deformation on their major and trace element composition can be minimized and their original petrochemical nature deduced by applying the simple alteration index developed by Ishikawa et al., (1976). Geochemical analyses of these rocks suggest that the various members of this sequence were generated by crystal fractionation of a mixed magma chamber. The chemical characteristics of the rocks of the volcanic sequence share many similarities with those of rocks from modern day tectonic environments. Major element analyses indicate bimodal volcanism associated with tensional tectonic environments, and the trace elements and REE characteristics are like those of mafic rocks from back-arc basin environments. Trace element analyses are useful in distinguishing between rocks that have similar major element components and physical characteristics but are of different overall derivation. The rocks of the Blake River Group form a single homoclinal sequence facing south; no major fold axis exists within the volcanic sequence in Bousquet Township.

Trace element analyses of the rocks of the Mooshla intrusive complex suggest that

the later trondhjemite assimilated a large portion of the earlier porphyritic quartz diorite and resulted in a hybrid phase.

In order to interpret the origin and broad metallogeny of Archean deposits, a comprehensive study including the stratigraphic, structural, and metamorphic processes that governed the deposition of all rocks and mineral deposits alike, must be considered. Some gold occurrences of Bousquet Township were clearly associated with post-tectonic metamorphic processes because these were generated by the latest event that affected earlier, syn-depositional orebodies.

REFERENCES CITED

Bancroft, J. A., 1911, Report on the geology and mineral resources of Kiekkiek and Kewagama Lakes regions: Report on mining operations in the province of Quebec during 1911, p. 160-207.

Barnes, H. L., 1979, Geochemistry of ore deposits. New York, John Wiley & Son. 798p.

Bateman, P. W., 1985, Rock alteration at the Bousquet gold mine, Quebec: Unpubl. M.Sc. thesis Univ. of Western Ontario, 159p.

Beane, R. E., and Titley, S. R., 1981, Porphyry copper deposits, part II, Hydrothermal alteration and mineralization, *in*: Economic Geology Seventy-Fifth Anniv. Vol., Skinner, B.J. ed., p. 235-269.

Blackburn, C. E., Bond, W. D., Breaks, F. W., Davis, D. W., Edwards, G. R., Poulsen, K.H., Trowell, N.F., and Wood, J., 1985, Evolution of Archean volcanic-sedimentary sequences of the Western Wabigoon Subprovince and its margins: a review, *in*: Evolution of Archean Supracrustal Sequences. Edited by Ayres, L.D., Thurston, P. C., Card, K. D., and Weber, W. Geological Association of Canada, Special Paper 28, p. 89-116.

Brosnahan, D. R., 1992, Mineralogical characteristics of Bousquet No. 2 ore in est Malartic mill streams. Unpubl. company report. Lac Minerals Ltd., 23p.

Burke, K., Dewey, J. F., and Kidd, W. S. F., 1976, Precambrian palaeomagnetic results compatible with contemporary Wilson cycle: Tectonophysics, v. 33, p. 287-299.

Burrows, D. R., and Spooner, E. T. C., 1989, Relationships between Archean gold quartz vein-shear zone mineralization and igneous intrusions in the Val D'Or and Timmins areas, Abitibi Subprovince, Canada. *in*: Keays, R. R., Ramsay, W. R. H., and Groves, D. I., eds., The geology of gold deposits: the perspective in 1988. Econ. Geol. Monograph 6, p. 424-444.

Card, K. D., 1990, A review of the Superior Province of the Canadian Shield, a product of Archean accretion: Precambrian Research, v. 48, p. 99-156.

Carmichael. I. S. E., Turner, F. J., and Verhoogen, J., 1974, Igneous petrology. New York: McGraw Hill Publishers, 739p.

Cas, R. A. F., and Wright, J. V., 1988, Volcanic successions, modern and ancient. London: Chapman & Hall Publishers,528p.

Chown, E. H., Daigneault, R., Mueller, W., Mortensen, J. K. 1992, Tectonic evolution of the Northern Volcanic Zone, Abitibi belt Quebec: Canadian Jour. of Earth Sci., v. 29, p. 2211-2225.

Cloud, P., A., 1972, A working model of the primitive earth: Am. Jour. of Sci., v. 272, p. 537-548.

Colvine, A. C., 1988, An empirical model for the formation of Archean gold deposits: products of final cratonization of the Superior Province, Canada. *in*: Keays, R. R., Ramsay, W. R. H., and Groves, D. I., eds., The geology of gold deposits: the perspective in 1988. Econ. Geol. Monograph 6, p. 37-53.

Colvine, A. C., Fyon, J. A., Heather. K. B., Marmont, S., Smith, P. M., and Troop, D. G., 1988, Archean lode gold deposits in Ontario: Ont. Geol. Survey, Misc. Paper, 139, 136p.

Condie, K. C., 1981, Archean greenstone belts. Amsterdam, Elsevier Scientific Publishing. 434p.

Condie, K. C., 1989, Plate tectonics & crustal evolution. Oxford, Pergamon Press Publisher. 492p.

Corfu, F., Krogh, T. E., Kwok, Y. Y., and Jensen, L. S., 1989, U-Pb zircon geochronology in the southwestern Abitibi Greenstone Belt, Superior Province: Canadian Jour. of Earth Sci., v. 26, p. 1747-1763.

Date, J., Watanabe, Y. and Saeki, Y., 1983, Zonal alteration around the Fukazawa Kuroko deposits, Akita Prefecture, Northern Japan: Economic Geology Monograph 5, p. 365-386.

Degens, E. T., and Ross, D. A., eds., 1969, Hot brines and recent heavy metal deposits in the Red Sea. New York, Springer Verlag Publisher, 600p.

Deloule, E., Gariepy, C., and Dupre, B., 1989, Metallogenesis of the Abitibi greenstone belt of Canada: a contribution from the analysis of trace lead in sulfide minerals: Canadian Jour. of Earth Sci., v. 26, p. 2529-2540.

Dimroth, E., Imreth, L., Cousineau, P., Leduc, M., and Sanschagrin, Y., 1985, Paleogeographic analysis of mafic submarine flows and its use in the exploration for massive sulphide deposits. *in*: Ayres, L. D., Thurston, P. C. Card, K. D., and Weber, W., eds., Evolution of Archean supracrustal sequences. Geological Association of Canada Special Paper 28. p 203-222.

Dimroth, E., Imreh, L., and Goulet, N., 1982, Evolution of the South-Central segment of the Archean Abitibi Belt, Quebec. Part I: stratigraphy and paleogeographic model: Canadian Jour. of Earth Sci., v. 19, p. 1729-1758.

Dimroth, E., Imreh, L., and Goulet, N., 1983a, Evolution of the South-Central segment of the Archean Abitibi Belt, Quebec. Part II: Tectonic evolution and geomechanical model: Canadian Jour. of Earth Sci., v. 20, p. 1355-1373.

Dimroth, E., Imreh, L., and Goulet, N., 1983b, Evolution of the South-Central segment of the Archean Abitibi Belt, Quebec. Part III: Plutonic and metamorphic evolution and geotectonic model: Canadian Jour. of Earth Sci., v. 20, p. 1374-1388.

Easton, R. M., 1985, The nature and significance of Pre-Yellowknife Supergroup rocks in the Point Lake Area, Slave Structural Province, Canada, *in*: Ayres, L. D., Thurston, P. C., Card, K. D., and Weber, W., eds., Evolution of Archean Supracrustal Sequences. Geological Association of Canada, Special Paper 28, p. 153-168.

Eissen, J. P., Lefevre, C., Maillet, P., Morvan, G., and Nohara, M., 1991, Petrology and geochemistry of the central North Fiji basin spreading centre (Southwest Pacific) between 16° and 22° S: Marine Geology, v. 98, p. 201-239.

Eliopoulos, D. G., 1983, Geochemistry and origin of the Dumagami pyritic gold deposit, Bousquet Township, Quebec. Unpubl. M.Sc. thesis. University of Western Ontario, 263p.

Etheridge, M. A., Wall, V. J., and Vernon, R. H., 1983, The role of the fluid phase during regional metamorphism and deformation: Journal of metamorphic geology, v. 1, p. 205-226.

Ewart, A., Brothers, R. N., and Mateen, A., 1977, An outline of the geology and geochemistry, and the possible petrogenetic evolution of the volcanic rocks of the Tonga-Kermadec-New Zealand arc: Jour. Volcanol. Geotherm. Res., v. 2, p. 205-250.

Ewart, A., and Hawkesworth, C. J., 1987, The Pleistocene-Recent Tonga-Kermadec arc lavas: interpretation of new isotopic and rare earth data in terms of a depleted mantle source model: Jour. of Petrol., v. 28, p. 495-530.

Feng, R., Kerrich, R., McBride, S., and Farrar, E., 1992, $^{40}Ar/^{39}Ar$ age constraints on the thermal history of the Archean Abitibi greenstone belt and the Pontiac Subprovince: implications for terrane collision, differential uplift, and overprinting of gold deposits: Canadian Jour. of Earth Sci., v. 29, p. 1389-1411.

Filion,M., Vallee, M., and Lavoie, C., 1976, Les gisements d'or de la SOQUEM-Silverstack, Canton de Bousquet, Quebec. Canadian Inst. Mining and Met. Bull., v. 70, p. 159-172.

Finlow-Bates, T., and Stumpfl, E. F., 1981, The behavior of so-called immobile elements in hydrothermally altered rocks associated with volcanogenic submarine-exhalative ore deposits: Mineral. Deposita, v. 16, p. 319-328.

Fouquet, Y., Von Stackelberg, U., Charlou, J. L., Erzinger, J., Herzig, P. M., Muhe, R., and Wieldicke, M., 1993, Metallogenesis in back arc environments: the Lau basin example: Econ. Geol., v. 88, p. 2154-2181.

Frenzel, G., Muhe, R., and Stoffers, P., 1990, Petrology of the volcanic rocks from the Lau basin, Southwest pacific: Geologisches Jahrbuch, v. 92, p. 395-479.

Gauthier, A., 1977, Etude petrographique de section polies, sections minces et sections minces polies du projet Thompson-Bousquet. Company report. Long Lac Mineral Exploration Ltd, 67p.

Gelinas, L., and Ludden, J. N., 1985, Rhyolitic volcanism and the geochemical evolution of an Archean central ring complex: the Blake River Group volcanic of the southern Abitibi Belt, Superior Province: Phys. Earth Planet. Int., v. 35, p. 77-88.

Gelinas, L., Trudel, P., and Hubert, C., 1983, Chemostratigraphic division of the Blake River Group, Rouyn-Noranda area, Abitibi, Quebec: Can. Jour. of Earth Sci., v. 21 p. 220-231.

Glikson, A. Y., and Jahn, B. M., 1985, REE and LIL elements, Eastern Kaapvaal shield, South Africa: Evidence of crustal evolution by 3-stage melting, *in*: Evolution of Archean Supracrustal Sequences. Ayres, L.D., Thurston, P.C., Card, K.D., and Weber, W. eds., Geological Association of Canada, Special Paper 28, p. 303-324.

Goldstein, R. H., and Reynolds, J. T., 1994, Systematics of fluid inclusions in diagenetic minerals. SEPM Short Course 31, 199p.

Goodfellow, W. D., and Franklin, J. M., 1993, Geology, mineralogy, and chemistry of sediment-hosted clastic massive sulphide in shallow cores, middle valley, Northern Juan de Fuca ridge: Econ. Geol., v. 88, p. 2037-2068.

Gromet, L. P., and Silver, L. T., 1983, Rare earth element distributions among minerals in granodiorite and their petrogenetic implications: Geochem. and Cosmochim. Acta. v. 47, p. 925-939.

Guha, J., Gauthier, A., Vallee, M., Descarraux, J., and Lange-Brad, F., 1982, Gold mineralization patterns at the Doyon Mine (Silverstack), Bousquet, Quebec, *in*: Geology of Canadian gold deposits. R.W. Hodder and W. Petruk eds. Canadian Inst. of Mining and Metallurgy, Special Volume 24, p. 50-57.

Gunning, H. G., 1937, Cadillac area, Quebec: Geol. Survey of Canada, Memoir 206, 80p.

Gunning, H. G., 1941, Bousquet-Joannes area, Quebec: Geol. Survey of Canada. Memoir 231, 110p.

Gustafson, L. B., and Hunt, J. P., 1975, The porphyry copper deposit a El Salvador, Chile: Econ. Geol., v. 70, p. 857-912.

Hall, G. E. M., and Plant, J. A., 1992, Analytical errors in the determination of high field strength elements and their implications in tectonic studies: Chemical Geology, v. 95, p. 141-156.

Hanson, G. N., 1978, The application of trace elements to the petrogenesis of igneous rocks of granitic composition, *in*: Trace elements in igneous petrology, Allegre, C. J., and Hart, S. R., eds., Amsterdam, Elsevier Scientific Publishing, p. 26-43.

Harker, A., 1909, The natural history of igneous rocks. New York, MacMillan, 384p.

Hashiguchi, H., Yamada, R., and Inoue, T., 1983, Practical application of low Na_2O anomalies in footwall acid lava for delimiting promising areas around the Kosaka and Fukazawa Kuroko deposits, Akita Prefectural, Japan: Economic Geology Monograph 5, p. 387-394.

Hemley, J. J., Montoya, J. W., Marinenko, J. W., and Luce. R. W., 1980, Equilibria in the system Al_2O_3-SiO_2-H_2O and some general implications for alteration/mineralization processes: Econ. Geol., v. 75, p. 210-228.

Herzig, P. M., Hannington, M. D., Fouquet, Y., Von Stackelberg, U., and Petersen, S., 1993, Gold-rich polymetallic sulfides from the Lau back arc and implications for the geochemistry of gold in sea-floor hydrothermal systems of the Southwest Pacific: Econ. Geol, v. 88, p. 2182-2209.

Holdaway, M. J., 1971, Stability of andalusite and the aluminum silicate phase diagram: American Journal of Science, v. 271, p. 97-131.

Hollister, V. F., 1978, Geology of the porphyry copper deposits of the Western Hemisphere: AIME, New York, 219p.

Hubert, C., Trudel, P. and Gelinas, L., 1985, Archean wrench fault tectonics and structural evolution of the Blake River Group, Abitibi Belt, Quebec: Canadian Jour. of Earth Sci., v. 21, p. 1024-1032.

Hutchinson. R. W., 1981, Mineral deposits as guide to supracrustal evolution, *in*: Evolution of the Earth. O'Connell, R.J. and Fyfe, W.S., eds., A.G.U.-G.S.A. Geodynamics Series, v. 5, p. 120-140.

Hutchinson, R. W., 1993, A multi-stage, multi-process genetic hypothesis for greenstone-hosted gold lodes: Ore Geology Reviews, v. 8 p. 349-382.

Imreh, L., 1976, Nouvelle lithostratigraphie a l'ouest de Val d'Or et son incidence gitologique: Ministere des Richesses Naturelles du Quebec, DPV-349.

Irvine, T. N. and Baragar, W. R. A., 1971, A guide to the chemical classification of the common volcanic rocks: Canadian Jour. of Earth Sci., v. 8, p. 523-548.

Ishikawa, Y., Sawaguchi, T., Iwaya, S., and Horiuchi, M., 1976, Delineation of prospecting targets for Kuroko deposits based on modes of volcanism of underlying dacite and alteration haloes: Mining Geology, v. 26, p. 105-117.

Jensen, L. S., 1976, A new cation plot for classifying subalkalic volcanic rocks: Ontario Geological Survey. Misc. paper 66, 22p.

Jensen, L. S., 1985, Stratigraphy and petrogenesis of Archean metavolcanic sequences, Southwestern Abitibi Subprovince, Ontario, *in*: Evolution of Archean Supracrustal Sequences. Ayres, L. D., Thurston, P. C., Card, K. D., and Weber, W. eds., Geological Association of Canada, Special Paper 28, p. 153-168.

Jolly, W. T., 1978, Metamorphic history of the Archean Abitibi Belt. *in*: Metamorphism of the Canadian Shield. Edited by Fraser, I.A., and Heywood, W.W. Geol. Survey of Canada, Paper 78-10, p. 63-78.

Lac Minerals Limited, Annual report to shareholders, 1993. 72p.

Langshur, A., 1990, The geology, geochemistry and structure of the Mooshla Intrusion, Bousquet mining centre, Quebec: Unpubl. MSc. thesis. University of Ottawa, 172p.

LaFleche, M. R., Dupuy, C. and Bougault, H., 1992a, Geochemistry and petrogenesis of Archean mafic volcanic rocks of the southern Abitibi belt, Quebec: Precambrian Research, v. 57, p. 207-241.

LaFleche, M. R., Dupuy, C., and Dostal, J., 1992b, Tholeiitic volcanic rocks of the late Archean Blake River Group, southern Abitibi greenstone belt: origin and geodynamic implications: Canadian Jour. of Earth Sci., v. 29, p. 1448-1458.

LeBas, M. J., LeMaitre, R. W., Streckeisen, J. and Zanettin, B., 1986, A chemical classification of volcanic rocks based on the total alkali-silica diagram: Jour. of Petrology, v. 27, p. 745-750.

Lowell, J. D., and Guilbert, J. M., 1970, Lateral and vertical alteration-mineralization zoning in porphyry ore deposits: Econ. Geol., v. 65, p. 373-408.

Ludden, J. N., and Hubert, C., 1986, Geologic evolution of the late Archean abitibi greenstone belt of Canada: Geology, v. 14, p. 707-711.

Ludden, J. N., and Thompson, G., 1978, Behavior of rare Earth elements during submarine weathering of sea-floor basalt: Earth and Planet. Sci. Letters, v. 43, p. 85-92.

Ludden, J. N., Gelinas, L., and Trudel, P., 1982, Archean metavolcanics from the Rouyn-Noranda district, Abitibi greenstone belt, Quebec. 2. Mobility of trace elements and petrogenetic constraints: Canadian Jour. of Earth Sci., v. 19, p. 2276-2287.

Ludden, J. N., Hubert, C., and Gariepy, C., 1986, The tectonic evolution of the Abitibi greenstone belt of Canada: Geological Magazine, v. 123, p. 153-156.

Marquis, P., 1990, Metallogenie des gisements archeens d'Au-Ag-Cu de la mine Donald J. LaRonde (Dumagami), Cadillac, Abitibi, Quebec: Unpubl. Ph.D. thesis, Univ. Montreal, 139p.

Marquis, P., Hubert, C., Brown, A. C., and Rigg, D. M., 1990, Overprinting of early, redistributed Fe and Pb-Zn mineralization by late-stage Au-Ag-Cu deposition at the Dumagami mine, Bousquet district, Abitibi, Quebec: Canadian Jour. of Earth Sci., v.27, p. 1651-1671.

Marquis, P., Hubert, C., Brown, A. C., Trudel, P., and Hoy, L. D., 1992, Geologie de la mine Donald J. LaRonde (Abitibi): Ministere de L'Energie et des Resources du Quebec, Bull. ET89-06, 106p.

Maruyama, S., Suzuki, K., and Liou, J. G., 1983, Greenschist-amphibolite transition equilibria at low pressures: Journal of Petrology, v. 24, p. 583-604.

Mortensen, J. K. 1987, Preliminary U-Pb zircon ages for volcanic and plutonic rocks of the Noranda-Lac Abitibi area, Abitibi Subprovince, Quebec. *in*: Current Research, Part A, Geol. Survey of Canada, Paper 87-1a, p. 581-590.

Myers, R. E., and Breitkopf, J. H., 1989, Basalt geochemistry and tectonic setting: a new approach to relate tectonic and magmatic processes: Lithos, v. 23, p. 53-62.

Osterman, C., and Hutchinson, R. W., 1994, Sulfide piercement structures in the Selebi-Phikwe nickel-copper deposit, Botswana: Exploration and Mining Geology, v. 3, No. 3, p. 285-296.

Padgham, W. A., 1985, Observation and Speculation on Supracrustal Successions in the Slave Structural Province, *in*: Ayres, L.D., Thurston, P.C., Card, K.D., and Weber, W., eds., Evolution of Archean Supracrustal Sequences. Geological Association of Canada, Special Paper 28, p. 133-152.

Pearce, J. A., 1983, Role of the subcontinental lithosphere in magma genesis at active continental margins, *in*: Continental basalts and mantle xenoliths, Hawkesworth, C. J., and Norry, M. J., eds., Nantwich, U.K., Shiva Press, p. 230-272.

Pearce, J. A., and Cann, J. R., 1973, Tectonic setting of basic volcanic rocks determined using trace element analyses: Earth and Planet. Sci. Letters, v. 19, p. 290-300.

Pearce, J. A., and Norry, M. J., 1979, Petrogenetic implications of Ti, Zr, Y, Nb variations in volcanic rocks: Contrib. Mineral. and Petrol., v. 19, p. 290-300.

Pearce, J. A., and Parkinson, I. J., 1993, Trace element models for mantle melting: application to volcanic arc petrogenesis, *in*: Magmatic processes and plate tectonics. Geological Society Special Publication No. 76, Prichard, H. M., Alabaster, T., Harris, N. B. W., and Neary, C. R., eds. London, Geological Society Publishers. p. 373-403.

Ragland, P. C., 1989, Basic analytical petrology. New York, Oxford University Press. 369p.

Richards, J. P., 1992, Magmatic-epithermal transitions in alkalic systems: Porgera gold deposit, Papua New Guinea: Geology, v. 20, p. 547-550.

Saunders, A. D., 1984, The rare earth element characteristics of igneous rocks from the ocean basins, *in*: Rare earth element geochemistry, Henderson. P., ed. Amsterdam, Elsevier Scientific Publishing, 510p.

Savoie, A., Perrault, G. and Filion, G., 1986, Geological setting of the Doyon gold deposit, Bousquet, Abitibi, Quebec, Canada: Proceedings of Gold 86 symposium, Toronto, p. 97-107.

Savoie, A., Trudel, P., Sauve, P., Hoy, L. and Lao, K., 1991, Geologie de la mine Doyon: Ministere de L'Energie et des Resources du Quebec, Bull. ET90-05, 80p.

Savoie, A., Trudel, P., Sauve, P., Perrault, G., 1990, Geologie de la mine Doyon, Cadillac, Quebec: The Northwestern Quebec polymetallic belt, *in*: a summary of 60 years of mining exploration. Rive, M., Verpaelst, P., Gagnon, Y., Lulin, J.M., Riverin, G., and Simard, A., eds., Canadian Inst. Mining Metallurgy. Special vol., 43, p. 402-411.

Sillitoe, R. H., 1973, The tops and bottoms of porphyry copper deposits: econ. Geol., v. 68, p. 799-815.

Sillitoe, R. H., 1988, Gold and silver deposits in porphyry systems, *in*: Bulk minable precious metal deposits of the western United States, R.W. Schafer, J.J. Cooper, and P.G. Vikre eds., Geol. Soc. Nevada, Reno, p. 233-257.

Smith, R. E., and Smith, S. E., 1976, Comments on the use of Ri, Zr, Y, Sr, K, P, and Nb in classification of basaltic magmas: Earth Planet. Sci. Letters, v. 32, p. 114-120.

Spear, F. S., 1980, NaSi <-> CaAl exchange equilibrium between plagioclase and amphibole: Contributions to Mineralogy and Petrology, v. 72, p. 33-41.

Spear, F. S., 1993, Metamorphic phase equilibria and pressure-temperature-time path: Mineralogical Society of America Monograph, 799p.

Spry, P. G. and Wonder, J. D., 1989, Manganese-rich garnet rocks associated with the Broken Hill lead-zinc-silver deposit, New South Wales, Australia: Canadian Mineralogist, v. 27, p. 275-292.

Stanton, R. L., 1972, Ore petrology, New York, McGraw-Hill Publishers, 713p.

Stone, W. E., 1988, The nature and significance of metamorphism in gold concentration, Bousquet Township Abitibi greenstone belt, Northwest Quebec: Unpubl. Ph.D. thesis, Univ. of Western Ontario, 441p.

Streckeisen, A., 1976, To each plutonic rock its proper name: Earth Sci., Review, v. 12 p. 1-33.

Sun, S.-S., and McDonough, W. F., 1989, Chemical and isotopic systematics of oceanic basalts, *in*: Magmatism in the ocean basins, Saunders, A. D. and Norry, M. J. eds., London, Geol. Society Special Publication 42, p. 313-345.

Teasdale, N. I., in progress, Metallogenesis of gold associated with massive pyrite bands of the Blake River Group at the Bousquet No. 2 mine: Unpubl. Ph.D. thesis Ecole Polytechnique de Montreal.

Teasdale. N. I., Brown, A. C., and Tourigny, G., 1995, Geology of the Bousquet #2 Au-Ag-Cu massive sulfide deposit, Abitibi greenstone belt, Quebec, Canada: Littleton, Soc. Mining, Metal. and Exploration, Preprint 95-48. 4p.

The Northern Miner, August 1994, Shaft deepening at Doyon approved: v. 80, no. 26, p.1

Thurston, P. C., Ayres, L. D., Edwards, G. R., Gelinas, L., Ludden, J. N., and Verpaelst, P., 1985, Archean bimodal volcanism, *in*: Ayres, L.D., Thurston, P.C., Card, K.D., and Weber, W., eds., Evolution of Archean Supracrustal Sequences. Geological Association of Canada, Special Paper 28, p. 153-168.

Tourigny, G., 1984, Geologie structurale et metamorphisme des roches Precambriennes du Groupe de Kewagama dans la region de Cadillac-Malartic, Abitibi, Quebec: Unpubl. M.Sc. thesis Univ. of Montreal, 85p.

Tourigny, G., 1988, Geologie structural et mineralisation aurifere a la mine Bousquet, Abitibi, Quebec: Unpubl. Ph.D. thesis Univ. of Montreal, 244p.

Tourigny, G. and Hubert, C., 1986, The Bousquet property, *in*: Excursion Guidebook. Pirie, J., and Downes, M. J. eds. Gold 86, Toronto, p. 91-99.

Tourigny, G., Brown, A.C., Hubert, C., and Crepeau, R., 1989a, Synvolcanic and syntectonic gold mineralization at the Bousquet mine, Abitibi greenstone belt, Quebec: Econ. Geol., v. 84, p. 1875-1890.

Tourigny, G., Doucet, D., and Bourget, A., 1993, Geology of the Bousquet 2 mine: an example of a deformed, gold-bearing, polymetallic sulfide deposit: Econ. Geol., v. 88, p. 1578-1597.

Tourigny, G. Hubert, C., Brown, A.C. and Crepeau, R., 1988, Structural geology of the Blake River Group at the Bousquet mine, Abitibi, Quebec: Canadian Jour. Earth Sci., v. 25, p. 581-592.

Tourigny, G., Hubert, C., Brown, A. C., and Crepeau, R., 1989b, Structural control of gold mineralization at the Bousquet mine, Abitibi, Quebec: Canadian Jour. of Earth Sci., v. 26, p. 157-175.

Tourigny, G. Hubert, C., Brown, A. C. and Crepeau, R., Trudel, P., Hoy, L. and Kheang, L., 1992, Geologie de la mine Bousquet: Ministere de L'Energie et des Resources du Quebec, Bull, ET89-09.

Tracy, R. C., Jaffe, H. W., and Robinson, P., 1976, Garnet composition and zoning in the determination of temperature of metamorphism, central Massachusetts: American Mineralogist, v. 61, p. 762-775.

Valliant, R. I., 1981, The geology, stratigraphic relationships and genesis of the Bousquet gold deposit, Northwest Quebec: Unpubl. Ph.D. thesis Univ. of Western Ontario, 323p.

Valliant, R. I. and Barnett, R. L., 1982, Manganiferous garnet underlying the Bousquet gold orebody, Quebec: metamorphosed manganese sediments as a guide to gold ore: Canadian Jour. Earth Sci., v. 19, p. 993-1010.

Valliant, R. I., Barnett, R. L., and Hodder, R. W., 1983, Aluminous rocks and its relation to gold mineralization, Bousquet mine, Quebec: Canadian Inst. Mining Met. Bull., 76, p. 811-819.

Valliant, R. I. and Hutchinson, R. W., 1982, Stratigraphic distribution and genesis of gold deposits, Bousquet region, northwestern Quebec, *in*: Geology of Canadian gold deposits. R. W. Hodder and W. Petruk eds. Canadian Inst. of Mining and Metallurgy, Special vol. 24, p. 27-40.

Valliant, R. I., Mongeau, C., and Doucet, R., 1982, The Bousquet pyritic gold deposit, Bousquet region, Quebec: descriptive geology and preliminary interpretation on genesis, *in*: Geology of Canadian gold deposits. R. W. Hodder and W. Petruk eds. Canadian Inst. of Mining and Met., Special v. 24, p. 41-49.

Van Baalen, M. R., 1993, Titanium mobility in metamorphic systems: a review: Chemical Geology, v. 110, p. 233-249.

Von Rad, U., and Muhe, R., 1990, Mineralogy, chemical composition and origin of ash layers and pumice in sediments from the Lau and North Fiji basins (SW Pacific, SO-35 cruise): Geologisches Jahrbuch, v. 92 p. 279-339.

Walker, G. P. L., 1973, Length of lava flows: Phil. Trans. Royal Soc. London, v. 274, p. 107-118.

Wilson, M. E., 1913, Kewagama Lake map area, Quebec. Geol. Survey of Canada Memoir 39, 134 p.

Wonder, J. D., Spry, P. G., and Windom, K. E., 1988, Geochemistry and origin of manganese-rich rocks related to iron-formation and sulphide deposits, western Georgia: Econ. Geol., v. 83, p. 1070-1081.

Wood, D. A., 1980, The application of a Th-Hf-Ta diagram to problems of tectonomagmatic classification and to establishing the nature of crustal contamination of basaltic lavas of the British Tertiary volcanic province: Earth Planet. Sci. Letters, v. 50, p. 11-30.

Yardley, B. W. D., 1977, An empirical study of diffusion in garnet: American Mineralogist, v. 62, p. 793-800.

APPENDIX 1

Major Element Analyses of the Rocks of the Blake River Group

All major and trace elements were analyzed at X-Ral Laboratories in Toronto. Primary sample preparations were carried-out at Rouyn-Noranda using the following procedures:

Primary reduction was achieved by a two stage crushing facility which employed a 15 X 20 cm jaw crusher for the first stage followed by a smaller crusher as second stage. Primary crushing resulted in 45 percent minus 3 mm and 99 percent minus 6 mm fractions.

A sub-sample was withdrawn from the crushed product by means of a 15 mm X 20 mm Jones sample splitter. The sub-sample was normally 1/8 of the original. Samples less than 250 grams were not split. Secondary reduction was achieved by means of an oscillatory swing mill which achieved 100 percent minus 200.

The final crushed product was sent to Toronto for analysis by X-Ray fluorescence Spectrometry by the following procedures:

A 2 gram sample, after roasting at 950 degrees for 1 hour to determine L.O.I., was fused with 7.7 grams of lithium tetraborate and the melt was cast into a 40 mm button. The button was analyzed on a Philips PW 1600 simultaneous X-Ray fluorescence spectrometer. The system was calibrated using 40 reference materials. Counting time on major elements was 60 seconds and each of them was analyzed on its own fixed channel. Trace elements were calculated with a scanner as counts were accumulating for the majors elements.

All elements determined were totalled, and sums of less than 98 or greater than 101 percent were automatically repeated. Instrument precision for the major elements was better than 0.5 percent. The detection limits were 0.01 percent for all oxides, and 10 ppm for all the trace elements. Accuracy was determined by analyzing a standard of known composition (standard SY-2). Precession was controlled by analyzing replicate samples.

Sample Codes

Unit 1	1	Unit 6	6
Unit 2	2	Quartz Diorite	11
Unit 3	3	Porphyritic Quartz Diorite	12
Unit 4 Felsic volcanic	4F	Trondhjemite	13
Unit 4 Sericite Schist	4S	Mafic Dyke	22
Unit 5	5		

Sample	Unit	SiO_2	Al_2O_3	Na_2O	MgO	K_2O	CaO	Fe_2O_3	MnO	P_2O_5	TiO_2	Cr_2O_3	LOI	Total	A.I.
5504	1	53.7	14.2	2.49	5.21	0.19	10.40	9.18	0.18	0.07	0.859	0.02	1.65	98.2	29.52
5505	1	53.3	14.8	4.20	5.28	0.17	7.14	9.26	0.20	0.10	1.180	0.03	2.60	98.3	32.46
5506	1	56.3	13.4	3.84	4.57	0.14	8.43	8.74	0.17	0.09	1.070	0.03	1.70	98.5	27.74
5507	1	48.3	13.1	2.55	5.76	0.25	8.50	15.60	0.19	0.14	1.830	0.01	3.00	99.3	35.23
5508	1	47.6	12.7	2.01	4.17	0.27	8.78	17.80	0.24	0.23	2.570	0.00	1.95	98.4	29.15
5509	1	49.4	13.7	1.09	5.61	0.11	7.83	15.40	0.25	0.24	1.830	0.28	4.00	99.9	39.07
5510	1	47.5	15.4	1.58	6.59	0.05	11.80	12.00	0.18	0.07	1.010	0.04	2.60	98.8	33.17
5514	1	49.9	13.7	0.57	7.02	0.04	11.80	12.70	0.18	0.08	1.060	0.03	2.25	99.4	36.34
5515	1	49.4	14.4	1.59	6.78	0.18	11.40	12.20	0.18	0.06	0.872	0.04	2.10	99.2	34.89
5516	1	47.5	13.0	1.35	4.64	0.24	11.40	13.60	0.20	0.12	1.390	0.03	6.35	99.9	27.68
5517	1	49.8	13.0	2.04	4.86	0.18	8.86	16.40	0.22	0.10	1.570	0.00	1.85	98.9	31.62
5518	1	48.4	14.5	1.07	7.07	0.03	10.20	12.30	0.21	0.05	0.956	0.04	3.75	98.6	38.65
5519	1	48.5	13.1	1.33	5.33	0.17	10.10	16.30	0.23	0.17	1.830	0.02	2.35	99.5	32.49
5520	1	50.4	13.6	0.77	5.92	0.04	11.20	13.20	0.18	0.08	1.060	0.04	2.20	98.7	33.24
5521	1	50.5	13.5	1.09	6.72	0.08	10.90	12.90	0.19	0.08	1.050	0.03	2.15	99.2	36.19
5522	1	49.1	13.9	0.87	5.19	0.22	5.43	16.50	0.15	0.08	1.160	0.05	6.40	99.1	46.20
5523	1	46.5	13.5	0.73	4.68	0.07	8.03	18.40	0.29	0.15	2.280	0.01	3.75	98.4	35.16
5524	1	51.1	13.7	1.72	5.72	0.04	10.10	12.80	0.19	0.08	1.150	0.04	3.25	99.9	32.76
5525	1	49.2	14.2	2.10	7.21	0.07	10.40	12.70	0.18	0.06	0.943	0.04	2.15	99.3	36.80
5526	1	45.0	14.5	2.97	7.46	0.10	8.82	12.50	0.18	0.09	1.150	0.03	5.95	98.8	39.07
5527	1	48.9	13.9	2.95	7.49	0.09	7.71	13.40	0.20	0.12	1.430	0.03	2.40	98.6	41.56
5528	1	47.9	14.3	2.12	7.54	0.09	9.40	13.70	0.22	0.11	1.360	0.06	2.90	99.7	39.84
5533	1	50.3	13.4	1.37	6.91	0.06	10.80	12.50	0.18	0.08	1.060	0.04	2.20	98.9	36.42
5534	1	51.0	13.2	3.08	6.96	0.30	8.85	12.20	0.18	0.08	1.060	0.03	2.20	99.2	37.83
5547	1	51.0	13.1	3.91	4.27	0.26	7.68	16.00	0.28	0.18	1.880	0.02	1.30	99.9	28.10
5548	1	47.1	15.0	2.00	7.51	0.25	10.00	12.30	0.18	0.05	0.902	0.04	2.15	97.5	39.27
5549	1	47.2	14.6	2.23	5.43	0.25	9.62	17.20	0.27	0.19	2.060	0.02	1.30	100.4	32.40
5550	1	49.7	13.7	4.11	3.57	0.26	6.94	18.30	0.26	0.13	1.990	0.00	1.20	100.2	25.74
5551	1	48.1	13.6	1.98	4.98	0.14	7.86	17.70	0.26	0.18	1.960	0.02	2.30	99.1	34.22
5552	1	54.0	13.2	2.71	3.85	0.11	7.80	12.40	0.27	0.11	1.670	0.00	3.40	99.6	27.37
5553	1	51.5	13.5	1.72	5.96	0.06	10.60	12.70	0.20	0.06	0.975	0.03	2.00	99.3	32.82
5554	1	50.9	13.8	3.44	5.64	0.34	7.55	13.60	0.21	0.08	1.080	0.03	1.90	98.6	35.24
5555	1	52.0	13.9	1.93	6.33	0.26	10.70	12.20	0.23	0.08	1.050	0.04	1.10	99.9	34.29
5556	1	52.4	13.7	3.04	6.86	0.41	9.45	11.70	0.21	0.09	1.100	0.03	0.75	99.8	36.79
5557	1	48.6	16.8	3.00	5.72	0.46	8.23	12.40	0.21	0.08	1.160	0.03	3.00	99.7	35.50
5558	1	50.8	13.8	1.28	6.52	0.18	11.30	13.00	0.20	0.08	1.080	0.04	2.00	100.3	34.75
5559	1	48.8	14.2	2.09	8.56	0.12	10.20	12.60	0.18	0.06	0.944	0.03	2.30	100.1	41.39
5560	1	43.4	13.3	2.48	3.80	0.53	11.80	12.20	0.25	0.25	2.310	0.00	7.30	97.7	23.27
5561	1	50.3	16.1	2.01	4.32	0.18	10.20	11.70	0.19	0.10	1.440	0.02	3.55	100.2	26.93
5562	1	58.5	12.1	3.56	2.78	0.22	7.08	13.20	0.28	0.14	2.130	0.00	0.05	100.1	21.99
5563	1	55.5	13.3	4.13	3.09	0.30	6.25	12.70	0.19	0.15	2.300	0.00	0.55	98.5	24.62
5671	1	49.4	13.9	2.74	6.54	0.10	9.96	11.90	0.21	0.08	1.040	0.03	3.40	99.3	34.33
5672	1	47.9	13.6	2.57	6.93	0.14	9.29	14.50	0.21	0.13	1.460	0.02	3.55	100.3	37.35
5673	1	51.3	13.3	2.54	7.44	0.08	8.85	12.90	0.20	0.09	1.090	0.03	2.40	100.3	39.77
5674	1	46.9	13.3	1.70	5.99	0.37	9.41	13.00	0.23	0.07	1.140	0.02	7.80	100.0	36.41
5680	1	52.9	15.9	1.53	1.91	2.41	5.55	11.40	0.11	0.20	1.290	0.00	3.30	96.6	37.89
5683	1	51.7	16.8	2.46	2.96	1.19	7.16	10.60	0.20	0.27	1.290	0.00	5.10	99.8	30.14
5735	1	50.1	13.5	2.02	7.76	0.20	10.00	12.60	0.19	0.07	0.990	0.03	1.90	99.4	39.84
5751	1	43.0	16.3	0.35	4.28	2.43	9.00	13.60	0.31	0.21	1.020	0.00	9.60	100.2	41.78
5752	1	47.0	16.9	2.39	6.22	0.61	8.22	11.80	0.21	0.23	1.260	0.02	4.00	98.9	39.16
5753	1	48.3	17.0	2.46	5.88	0.67	8.03	11.40	0.20	0.24	1.250	0.02	3.90	99.4	38.44
5755	1	43.0	12.1	1.32	5.86	0.18	9.45	16.30	0.24	0.20	2.070	0.02	8.65	99.4	35.93
5756	1	50.5	12.9	2.97	4.89	0.27	8.12	11.50	0.19	0.26	1.870	0.01	5.15	98.7	31.75
5757	1	45.2	15.3	2.07	5.81	0.21	10.70	11.50	0.20	0.08	1.080	0.03	8.10	100.3	32.04
5758	1	43.3	13.6	2.61	6.39	0.03	7.66	14.90	0.20	0.13	1.620	0.03	9.00	99.5	38.47
5759	1	51.1	13.0	3.47	5.39	0.07	7.45	13.90	0.22	0.28	1.980	0.00	2.40	99.3	33.33
5760	1	47.3	14.8	2.25	6.77	0.11	10.40	12.20	0.25	0.06	0.939	0.04	4.85	100.0	35.23
5761	1	47.1	12.9	1.71	4.86	0.19	9.24	16.10	0.26	0.15	1.760	0.01	5.30	99.6	31.56
5762	1	47.9	15.2	1.88	6.05	0.14	10.40	13.00	0.21	0.08	1.180	0.03	4.05	100.2	33.51

Sample	Unit	SiO_2	Al_2O_3	Na_2O	MgO	K_2O	CaO	Fe_2O_3	MnO	P_2O_5	TiO_2	Cr_2O_3	LOI	Total	A.I.
5763	1	46.1	12.9	1.48	4.30	0.10	12.10	15.20	0.24	0.14	1.820	0.01	5.95	100.4	24.47
5764	1	44.9	13.2	2.26	5.33	0.13	8.90	14.80	0.24	0.16	1.770	0.02	8.05	99.8	32.85
5776	1	50.0	13.1	3.40	5.01	0.43	7.87	17.00	0.28	0.15	2.240	0.01	0.10	99.6	32.56
5777	1	51.5	13.5	1.46	6.96	0.21	10.50	12.10	0.20	0.08	0.981	0.03	1.75	99.3	37.48
5781	1	48.9	15.4	2.16	7.82	0.29	10.50	12.00	0.18	0.04	0.705	0.05	2.20	100.3	39.05
5782	1	52.6	13.3	2.09	6.30	0.21	10.10	11.90	0.17	0.09	1.060	0.03	1.05	98.9	34.81
5785	1	53.7	16.4	2.54	4.39	1.19	6.16	10.80	0.17	0.30	1.200	0.00	2.30	99.2	39.08
5788	1	52.6	15.1	2.81	4.66	0.15	9.78	10.50	0.15	0.21	1.150	0.02	1.60	98.8	27.64
5789	1	51.6	14.1	1.55	6.72	0.12	11.10	12.10	0.17	0.10	1.070	0.03	1.75	100.5	35.09
5790	1	48.0	13.7	1.87	6.87	0.17	9.22	16.00	0.24	0.12	1.500	0.03	2.65	100.4	38.83
5791	1	52.9	13.5	1.83	6.12	0.18	8.75	13.60	0.20	0.11	1.210	0.02	1.75	100.2	37.32
5792	1	51.9	13.4	2.43	6.88	0.14	10.10	12.00	0.17	0.09	1.050	0.03	1.40	99.6	35.91
5793	1	48.0	13.4	1.51	5.56	0.25	8.91	16.10	0.23	0.18	1.850	0.01	2.25	98.3	35.80
5794	1	53.0	13.0	2.47	3.45	0.43	3.97	17.90	0.13	0.18	2.050	0.00	2.25	98.9	37.60
5795	1	41.9	13.2	0.82	5.81	1.24	6.90	22.80	0.42	0.09	0.836	0.01	2.95	97.0	47.73
5796	1	49.7	13.6	1.38	7.74	0.07	10.50	13.00	0.19	0.08	1.050	0.04	1.95	99.3	39.66
5798	1	52.0	16.6	2.52	3.85	1.79	4.02	13.40	0.18	0.36	1.280	0.00	3.15	99.3	46.31
5799	1	50.1	13.7	2.67	7.27	0.26	8.25	12.20	0.18	0.09	1.050	0.03	2.50	98.3	40.81
5801	1	49.4	14.0	1.98	7.48	0.21	10.00	13.10	0.20	0.08	1.030	0.03	1.65	99.2	39.10
5802	1	49.1	13.2	1.19	7.03	0.11	8.72	14.80	0.17	0.09	1.040	0.03	2.70	98.2	41.88
5803	1	49.4	13.4	1.98	7.13	0.17	9.64	13.00	0.20	0.08	1.010	0.03	2.20	98.3	38.58
5804	1	49.1	13.5	1.04	6.72	0.13	9.26	15.10	0.19	0.09	1.080	0.03	2.50	98.8	39.94
5805	1	48.3	13.7	2.60	6.72	0.27	9.04	14.90	0.20	0.13	1.580	0.02	1.70	99.2	37.52
5809	1	49.7	14.6	1.35	5.98	0.04	10.90	13.10	0.18	0.08	1.090	0.04	1.75	98.8	32.95
5810	1	47.8	13.3	1.70	4.98	0.12	10.00	16.20	0.25	0.18	1.850	0.02	2.10	98.5	30.36
Maximum		58.50	17.00	4.20	8.56	2.43	12.10	22.80	0.42	0.36	2.57	0.28	9.60	100.50	47.73
Minimum		41.90	12.10	0.35	1.91	0.03	3.97	8.74	0.11	0.04	0.71	0.00	0.05	96.60	21.99
Average		49.47	13.99	2.13	5.80	0.30	9.11	13.58	0.21	0.13	1.36	0.03	3.10	99.26	35.10
Deviation		2.94	1.10	0.84	1.34	0.43	1.68	2.32	0.04	0.07	0.43	0.03	2.04	0.79	5.05

Sample	Unit	SiO_2	Al_2O_3	Na_2O	MgO	K_2O	CaO	Fe_2O_3	MnO	P_2O_5	TiO_2	Cr_2O_3	LOI	Total	A.I.
5665	2	62.8	15.4	3.26	2.73	1.23	3.51	6.68	0.17	0.27	0.859	0.00	3.05	100.1	36.91
5676	2	73.5	12.2	4.07	0.62	1.26	2.65	2.89	0.08	0.05	0.318	0.01	1.40	99.2	21.86
5677	2	75.4	12.5	3.53	0.80	1.56	1.85	2.77	0.06	0.05	0.301	0.00	0.85	99.8	30.49
5729	2	74.2	12.4	4.40	0.84	1.27	1.71	2.73	0.05	0.05	0.327	0.02	1.05	99.2	25.67
5732	2	75.0	11.9	3.01	0.44	1.90	2.20	2.02	0.08	0.05	0.256	0.01	1.40	98.4	30.99
5734	2	77.6	11.5	3.17	0.36	1.58	1.14	2.10	0.03	0.03	0.220	0.01	1.05	98.9	31.04
5738	2	74.0	13.1	3.85	0.86	1.83	1.68	2.50	0.05	0.06	0.343	0.02	1.15	99.6	32.73
5772	2	75.9	11.7	4.64	0.47	1.23	1.44	3.10	0.05	0.03	0.190	0.02	1.40	100.3	21.85
5774	2	74.0	11.6	2.51	0.99	1.68	1.86	4.34	0.07	0.05	0.211	0.01	1.25	98.7	37.93
5775	2	76.5	11.0	2.93	1.13	1.06	1.10	4.82	0.05	0.03	0.171	0.02	1.00	99.9	35.21
5779	2	77.0	11.8	5.48	0.59	0.61	1.10	3.05	0.04	0.03	0.175	0.02	0.50	100.5	15.42
5780	2	76.4	11.4	4.65	0.68	0.92	1.55	3.19	0.04	0.03	0.177	0.02	0.60	99.8	20.51
5797	2	72.8	12.6	4.49	0.65	1.68	1.52	3.45	0.04	0.11	0.414	0.01	0.30	98.2	27.94
Maximum		77.60	15.40	5.48	2.73	1.90	3.51	6.68	0.17	0.27	0.86	0.02	3.05	100.50	37.93
Minimum		62.80	11.00	2.51	0.36	0.61	1.10	2.02	0.03	0.03	0.17	0.00	0.30	98.20	15.42
Average		74.24	12.24	3.85	0.86	1.37	1.79	3.36	0.06	0.06	0.30	0.01	1.15	99.43	28.35
Deviation		3.58	1.07	0.83	0.58	0.36	0.65	1.22	0.03	0.06	0.18	0.01	0.64	0.70	6.62

Sample	Unit	SiO_2	Al_2O_3	Na_2O	MgO	K_2O	CaO	Fe_2O_3	MnO	P_2O_5	TiO_2	Cr_2O_3	LOI	Total	A.I.
5633	3	59.9	15.7	1.79	5.10	1.84	2.06	6.87	0.20	0.25	0.954	0.00	3.80	98.6	64.32
5639	3	57.0	13.5	2.02	2.64	1.09	6.05	9.24	0.21	0.37	1.110	0.00	5.70	99.0	31.61
5640	3	47.0	16.9	3.23	3.19	1.27	7.42	11.20	0.24	0.27	0.964	0.00	4.40	96.2	29.52
5647	3	53.7	15.2	1.63	2.62	1.89	7.19	9.05	0.18	0.37	1.240	0.00	6.20	99.4	33.83
5648	3	58.0	15.9	3.82	1.82	1.31	5.38	7.42	0.17	0.21	1.090	0.00	3.90	99.1	25.39
5653	3	52.0	18.3	3.39	4.32	1.17	5.79	8.97	0.23	0.21	0.886	0.00	3.65	99.0	37.42
5656	3	44.0	16.7	1.34	5.58	1.75	8.20	9.83	0.40	0.16	0.916	0.00	8.32	97.3	43.45
5664	3	46.0	15.7	2.25	5.71	0.91	8.02	9.69	0.22	0.17	0.785	0.02	8.50	98.0	39.19
5669	3	46.1	15.5	1.01	5.81	0.44	6.44	13.10	0.22	0.26	1.290	0.00	5.22	95.4	45.62
5675	3	49.9	18.3	2.78	4.24	1.20	6.96	8.47	0.20	0.26	1.200	0.00	6.15	99.7	35.84
5681	3	47.3	14.0	0.73	6.18	0.31	7.13	13.40	0.30	0.24	1.430	0.00	7.70	98.8	45.23
5730	3	56.3	14.8	3.68	2.62	0.83	5.95	8.74	0.21	0.28	0.985	0.00	3.65	98.1	26.38
5731	3	59.7	15.6	3.96	2.11	1.53	4.24	6.61	0.16	0.32	1.000	0.00	2.90	98.3	30.74
5737	3	57.6	16.2	3.57	1.93	0.94	6.14	7.30	0.15	0.18	0.936	0.00	3.35	98.4	22.81
5745	3	56.3	17.9	3.06	3.50	0.67	5.40	7.67	0.14	0.34	1.100	0.00	2.80	98.9	33.02
5746	3	51.9	16.5	3.67	4.49	1.02	6.41	9.66	0.13	0.23	1.030	0.00	3.80	98.9	35.34
5747	3	64.1	15.6	5.34	1.86	1.08	2.96	5.57	0.09	0.25	0.837	0.00	1.50	99.3	26.16
5771	3	50.4	17.9	3.64	2.92	1.08	8.66	8.57	0.13	0.14	0.840	0.02	5.45	99.8	24.54
5773	3	54.0	17.8	3.91	3.60	0.87	8.53	9.03	0.14	0.13	1.130	0.05	0.75	100.0	26.43
5783	3	59.2	15.7	4.23	2.42	0.87	5.62	8.42	0.09	0.54	1.230	0.00	1.40	99.8	25.04
5825	3	58.5	16.4	6.10	2.36	0.31	5.50	4.81	0.06	0.38	1.190	0.00	2.20	97.9	18.71
5826	3	53.1	16.2	2.50	3.10	2.34	3.97	14.10	0.07	0.24	1.530	0.00	1.60	98.8	45.68
5850	3	55.1	20.6	2.59	5.34	1.86	3.61	5.60	0.06	0.19	1.120	0.00	3.35	99.5	53.73

Maximum	64.1	20.60	6.10	6.18	2.34	8.66	14.10	0.40	0.54	1.53	0.05	8.50	100.00	64.32
Minimum	44.00	13.50	0.73	1.82	0.31	2.06	4.81	0.06	0.13	0.79	0.00	0.75	95.40	18.71
Average	53.78	16.39	3.05	3.63	1.16	5.98	8.84	0.17	0.26	1.08	0.00	4.19	98.62	34.78
Deviation	5.211	1.53	1.29	1.40	0.51	1.71	2.35	0.08	0.09	0.18	0.01	2.13	1.10	10.72

Sample	Unit	SiO_2	Al_2O_3	Na_2O	MgO	K_2O	CaO	Fe_2O_3	MnO	P_2O_5	TiO_2	Cr_2O_3	LOI	Total	A.I.
5570	4F	63.0	14.9	0.81	4.73	2.61	0.98	6.77	0.07	0.23	0.801	0.01	5.25	100.4	80.39
5572	4F	58.5	14.3	0.63	5.24	2.25	1.60	9.06	0.07	0.13	0.826	0.02	5.40	98.2	77.06
5573	4F	62.9	15.0	0.42	3.38	3.32	0.49	7.71	0.05	0.25	0.826	0.00	5.65	100.2	88.04
5576	4F	55.2	13.1	0.21	3.85	2.58	1.28	15.10	0.10	0.20	1.360	0.02	7.40	100.5	81.19
5577	4F	52.0	14.9	0.59	6.09	1.93	1.17	13.50	0.13	0.22	1.540	0.00	6.35	98.5	82.00
5578	4F	71.5	13.9	0.36	1.25	3.54	1.00	4.44	0.05	0.11	0.535	0.01	3.45	100.3	77.89
5615	4F	70.2	12.9	3.56	1.63	1.04	2.65	3.74	0.07	0.09	0.482	0.02	1.70	98.2	30.07
5727	4F	72.1	13.1	3.07	1.56	0.80	3.16	3.33	0.05	0.10	0.563	0.01	1.80	99.7	27.47
5744	4F	57.3	14.9	0.98	2.88	2.88	3.48	8.15	0.19	0.32	0.918	0.00	5.70	97.9	56.36
5819	4F	71.1	14.6	1.47	1.57	3.40	1.04	2.96	0.06	0.16	0.619	0.01	2.65	99.8	66.44
5820	4F	72.3	13.2	2.71	1.19	2.33	2.66	2.22	0.04	0.10	0.558	0.02	2.50	100.0	39.60
5823	4F	48.9	16.6	0.37	8.07	2.24	0.53	12.60	0.05	0.27	1.390	0.01	9.50	100.6	91.97
5824	4F	72.0	14.3	1.86	1.05	3.05	2.05	2.07	0.11	0.11	0.554	0.02	1.65	98.9	51.19
5835	4F	58.0	17.1	0.96	2.68	2.57	1.99	8.93	0.05	0.42	1.130	0.01	6.40	100.4	64.02
5836	4F	68.5	12.2	0.40	0.82	3.36	1.25	7.28	0.03	0.08	0.476	0.02	5.10	99.7	71.70
5859	4F	72.4	12.7	1.46	1.75	2.24	0.89	3.89	0.02	0.10	0.529	0.03	3.95	100.1	62.93
5860	4F	54.8	16.6	2.77	4.90	1.17	4.10	10.90	0.15	0.30	1.140	0.00	2.35	99.3	46.91
5864	4F	72.6	13.1	2.51	1.19	0.98	5.00	1.71	0.03	0.09	0.490	0.03	2.25	100.1	22.42
5871	4F	72.0	14.1	0.49	0.96	3.69	2.69	2.66	0.08	0.10	0.508	0.02	2.00	99.4	59.39
5894	4F	73.4	14.0	0.65	1.97	2.75	0.47	2.04	0.02	0.16	0.640	0.01	3.25	99.5	80.82
67909	4F	69.2	14.1	1.93	1.38	2.99	1.30	5.12	0.06	0.18	0.750	0.02	2.18	99.2	57.50

Maximum	73.40	17.10	3.56	8.07	3.69	5.00	15.10	0.19	0.42	1.54	0.03	9.50	100.60	91.97
Minimum	48.90	12.20	0.21	0.82	0.80	0.47	1.71	0.02	0.08	0.48	0.00	1.65	97.90	22.42
Average	65.14	14.27	1.34	2.77	2.46	1.89	6.39	0.07	0.18	0.79	0.01	4.12	99.57	62.64
Deviation	7.89	1.29	1.01	1.96	0.85	1.22	4.00	0.04	0.09	0.32	0.01	2.15	0.80	19.89

Sample	Unit	SiO_2	Al_2O_3	Na_2O	MgO	K_2O	CaO	Fe_2O_3	MnO	P_2O_5	TiO_2	Cr_2O_3	LOI	Total	A.I.
5571	4S	73.8	14.1	0.52	0.28	3.51	0.23	3.36	0.01	0.10	0.559	0.03	3.55	100.2	83.48
5574	4S	75.2	12.0	0.39	0.42	3.25	0.22	4.40	0.02	0.06	0.468	0.02	3.60	100.3	85.75
5575	4S	72.2	13.5	0.42	0.41	3.56	0.45	4.26	0.04	0.08	0.496	0.02	3.70	99.4	82.02
5579	4S	71.5	14.9	1.63	0.20	1.96	0.14	4.60	0.01	0.05	0.608	0.04	4.40	100.2	54.96
5858	4S	77.1	14.5	0.32	0.14	1.41	0.08	1.85	0.01	0.10	0.534	0.02	3.55	99.7	79.49
5862	4S	63.0	18.1	0.32	0.11	0.53	0.56	7.12	0.01	0.50	1.560	0.02	8.00	99.9	42.11
5863	4S	66.9	14.9	1.58	0.95	1.86	0.53	6.82	0.03	0.17	0.798	0.55	4.75	100.1	57.11
5869	4S	72.0	11.4	0.31	0.28	3.00	0.10	7.48	0.01	0.07	0.406	0.02	4.90	100.1	88.89
5870	4S	76.7	16.3	1.34	0.19	0.97	0.36	0.60	0.02	0.14	0.692	0.04	2.62	100.1	40.56
5883	4S	55.9	15.7	1.18	4.19	0.54	0.61	10.90	0.03	0.41	1.220	0.01	9.30	100.1	72.55
5887	4S	76.8	15.3	0.16	0.09	0.05	0.19	0.71	0.02	0.14	0.628	0.03	5.25	99.4	28.57

Maximum	77.10	18.10	1.63	4.19	3.56	0.61	10.90	0.04	0.50	1.56	0.55	9.30	100.30	88.89
Minimum	55.90	11.40	0.16	0.09	0.05	0.08	0.60	0.01	0.05	0.41	0.01	2.62	99.40	28.57
Average	71.01	14.61	0.74	0.66	1.88	0.32	4.74	0.02	0.17	0.72	0.07	4.87	99.95	65.04
Deviation	6.33	1.80	0.54	1.14	1.23	0.19	3.01	0.01	0.14	0.34	0.15	1.94	0.30	20.25

Sample	Unit	SiO_2	Al_2O_3	Na_2O	MgO	K_2O	CaO	Fe_2O_3	MnO	P_2O_5	TiO_2	Cr_2O_3	LOI	Total	A.I.
5564	5	48.0	15.0	0.51	2.99	2.95	4.59	15.00	0.67	0.37	0.794	0.00	7.55	98.5	53.80
5565	5	67.1	13.4	0.88	2.25	2.28	4.07	4.70	0.28	0.21	0.765	0.00	3.40	99.4	47.78
5566	5	74.1	10.3	0.41	0.25	2.13	0.33	7.15	0.14	0.07	0.414	0.01	4.65	100.0	76.28
5567	5	60.8	12.3	0.17	4.43	1.15	1.99	12.00	1.34	0.33	0.936	0.00	3.70	99.2	72.09
5585	5	51.0	17.2	1.02	2.93	2.73	6.15	9.01	0.51	0.31	0.902	0.00	7.45	99.3	44.12
5586	5	53.1	13.4	0.80	3.22	2.42	6.52	9.34	0.34	0.33	1.080	0.00	8.80	99.4	43.52
5587	5	53.6	16.3	0.46	1.13	3.71	0.50	14.30	0.34	0.28	0.877	0.00	6.80	98.4	83.45
5588	5	54.6	15.4	0.74	3.15	2.48	4.59	10.20	0.30	0.40	1.410	0.00	5.60	99.0	51.37
5589	5	57.8	14.6	1.32	2.49	2.07	6.58	6.41	0.16	0.34	0.924	0.00	7.15	100.0	36.60
5590	5	51.0	18.8	0.83	2.93	3.08	6.17	8.52	0.33	0.36	0.983	0.00	7.30	100.4	46.20
5591	5	49.5	17.7	1.89	2.72	2.26	8.12	7.20	0.19	0.31	0.899	0.00	9.05	99.9	33.22
5592	5	52.8	19.5	0.83	1.43	3.90	0.94	12.80	0.55	0.35	1.040	0.00	4.65	98.9	75.07
5597	5	56.7	15.9	1.60	2.74	2.08	4.80	7.94	0.26	0.57	1.420	0.00	5.10	99.2	42.96
5598	5	61.8	13.7	1.54	2.59	1.27	4.15	8.82	0.18	0.40	1.170	0.00	4.15	99.9	40.42
5599	5	53.7	15.3	0.72	3.68	2.69	4.42	9.00	0.35	0.41	1.280	0.00	6.60	98.3	55.34
5603	5	57.7	14.8	1.04	2.75	2.32	7.86	7.71	0.25	0.39	0.940	0.01	2.45	98.3	36.29
5604	5	47.9	17.5	2.21	6.15	0.91	8.84	12.30	0.19	0.16	1.060	0.01	2.05	99.3	38.98
5605	5	64.7	14.4	2.39	2.60	1.73	3.29	6.67	0.18	0.21	0.794	0.01	1.95	99.0	43.26
5606	5	52.3	19.9	1.84	3.76	1.43	6.95	8.28	0.24	0.16	0.830	0.01	2.90	98.7	37.12
5609	5	50.8	16.6	2.12	3.36	1.68	5.82	9.43	0.11	0.31	1.040	0.00	4.75	96.1	38.83
5612	5	50.7	19.3	1.50	4.19	2.70	7.85	7.16	0.56	0.19	1.310	0.02	3.00	98.6	42.43

Sample	Unit	SiO_2	Al_2O_3	Na_2O	MgO	K_2O	CaO	Fe_2O_3	MnO	P_2O_5	TiO_2	Cr_2O_3	LOI	Total	A.I.
5613	5	46.9	16.8	1.77	6.12	0.77	6.24	12.70	0.26	0.33	1.130	0.00	4.00	97.1	46.24
5614	5	55.3	15.8	1.13	3.57	1.33	6.22	9.44	0.25	0.43	1.090	0.00	4.40	99.0	40.00
5619	5	60.4	14.3	0.89	2.18	2.76	5.81	7.79	0.26	0.31	0.946	0.00	4.65	100.4	42.44
5620	5	51.9	16.3	1.73	4.57	2.19	3.74	12.00	0.25	0.30	1.110	0.00	4.90	99.1	55.27
5621	5	57.2	17.6	1.23	3.58	2.21	5.40	7.40	0.26	0.14	0.826	0.00	2.40	98.4	46.62
5624	5	49.9	21.6	2.68	2.13	1.11	8.93	8.15	0.18	0.22	1.430	0.03	2.25	98.7	21.82
5625	5	62.8	13.8	0.80	2.84	3.22	4.62	4.89	0.30	0.14	0.541	0.00	4.25	98.3	52.79
5630	5	65.4	18.1	2.26	0.82	4.52	0.92	3.17	0.02	0.36	1.050	0.00	2.60	99.4	62.68
5631	5	55.7	14.0	4.99	4.20	0.89	4.92	10.90	0.34	0.39	1.410	0.00	1.40	99.2	33.93
5632	5	60.5	13.6	2.03	2.55	1.62	4.25	9.23	0.26	0.39	1.110	0.00	4.20	99.8	39.90
5636	5	66.6	16.2	2.87	2.33	1.51	2.94	3.17	0.09	0.35	0.974	0.00	2.10	99.3	39.79
5637	5	53.0	14.0	0.93	2.77	1.79	7.10	10.40	0.26	0.39	1.390	0.00	6.75	98.9	36.22
5638	5	47.1	19.3	0.97	3.76	3.01	4.46	11.10	0.75	0.15	1.250	0.02	5.25	97.2	55.49
5641	5	51.9	15.3	4.44	3.31	0.31	5.58	10.50	0.17	0.20	1.330	0.00	5.20	98.3	26.54
5644	5	56.6	23.0	2.27	1.98	2.27	4.64	3.48	0.05	0.22	1.480	0.02	2.80	98.9	38.08
5645	5	56.6	14.9	1.85	2.74	1.87	4.93	8.39	0.16	0.39	1.210	0.00	5.05	98.2	40.47
5646	5	55.9	19.9	2.36	2.75	1.42	4.76	7.95	0.27	0.16	1.280	0.02	2.80	99.7	36.94
5652	5	47.8	15.7	1.73	4.88	0.89	10.50	9.33	0.20	0.22	0.891	0.00	7.75	100.0	32.06
5655	5	52.8	13.8	2.15	3.17	1.05	6.50	10.70	0.24	0.38	1.370	0.00	6.05	98.3	32.79
5661	5	46.8	15.6	0.58	7.98	2.43	2.42	14.20	0.22	0.19	0.928	0.02	7.40	98.8	77.63
5662	5	58.0	18.5	1.76	1.86	4.20	1.69	7.10	0.13	0.31	1.250	0.01	4.20	99.2	63.72
5663	5	53.3	19.1	6.28	3.31	1.33	3.76	8.18	0.27	0.34	0.948	0.00	2.10	99.0	31.61
5668	5	56.1	14.5	1.34	2.44	1.93	6.55	7.61	0.20	0.36	1.110	0.00	7.25	99.5	35.64
5678	5	55.1	16.5	1.67	4.16	1.10	5.65	7.85	0.12	0.50	1.090	0.00	4.90	98.8	41.81
5679	5	57.3	16.2	1.43	3.88	0.94	5.26	8.86	0.13	0.27	1.020	0.00	3.80	99.2	41.88
5682	5	57.2	16.1	2.44	5.38	1.19	2.98	8.93	0.20	0.36	1.260	0.00	3.55	99.7	54.80
5685	5	54.8	15.2	1.23	3.96	2.23	4.55	10.20	0.27	0.36	1.240	0.00	4.10	98.2	51.71
5686	5	67.6	13.0	0.41	2.09	2.61	3.74	3.66	0.14	0.11	0.467	0.00	4.60	98.5	53.11
5688	5	67.6	14.0	2.32	0.74	2.97	3.79	2.98	0.09	0.17	0.570	0.00	3.15	98.6	37.78
5689	5	63.4	14.7	0.79	1.97	3.17	3.43	4.87	0.25	0.23	0.727	0.00	4.30	98.0	54.91
5690	5	66.7	13.4	1.12	2.57	1.20	3.06	5.34	0.09	0.19	0.731	0.00	4.55	99.1	47.42
5692	5	47.0	19.1	0.93	5.21	0.89	9.92	8.25	0.24	0.18	1.300	0.02	5.25	98.3	35.99
5693	5	63.5	14.7	0.76	1.76	3.32	3.17	5.66	0.33	0.12	0.573	0.00	3.10	97.1	56.38
5694	5	56.6	14.3	1.71	2.96	1.62	4.58	9.28	0.25	0.41	1.220	0.00	4.55	97.6	42.13
5696	5	65.6	15.6	1.04	1.68	2.98	2.44	4.43	0.40	0.18	0.869	0.00	2.90	98.2	57.25
5697	5	61.0	13.9	1.16	2.19	2.05	5.02	8.19	0.23	0.40	1.100	0.00	3.35	98.7	40.69
5698	5	54.6	14.8	1.13	4.62	1.02	4.40	11.30	0.27	0.41	1.520	0.00	4.85	99.0	50.49
5699	5	66.9	14.6	0.89	0.80	3.12	1.59	6.03	0.33	0.23	0.810	0.00	4.25	99.9	61.25
5702	5	62.6	15.7	0.80	2.54	2.77	5.40	3.88	0.19	0.22	0.708	0.00	3.70	98.6	46.13
5703	5	55.0	14.4	1.78	4.02	1.21	5.60	10.10	0.21	0.41	1.440	0.00	6.00	100.3	41.48
5705	5	48.4	19.8	1.50	3.63	2.40	7.75	5.93	0.42	0.18	1.380	0.02	6.95	98.4	39.46
5706	5	52.8	15.8	0.69	3.67	3.22	5.37	7.23	0.38	0.46	1.090	0.00	7.25	98.1	53.20
5707	5	55.1	16.0	2.06	3.36	1.29	4.39	10.10	0.23	0.36	1.270	0.00	4.00	98.2	41.89
5711	5	65.4	14.5	0.40	1.35	3.90	2.54	4.82	0.38	0.19	0.636	0.00	3.05	97.3	64.10
5712	5	58.4	14.8	0.56	4.10	2.10	3.16	9.33	0.21	0.40	1.210	0.00	4.00	98.4	62.50
5713	5	42.7	19.4	1.54	4.16	1.94	8.41	8.20	0.13	0.19	0.929	0.00	4.35	92.0	38.01
5715	5	51.4	20.3	1.08	2.70	1.58	7.48	8.49	0.72	0.20	1.410	0.03	2.90	98.4	33.33
5716	5	51.9	14.7	1.11	3.65	1.94	5.61	10.30	0.39	0.41	1.340	0.00	4.60	96.1	45.41
5717	5	65.4	13.5	2.25	2.51	1.64	2.80	5.72	0.13	0.17	0.682	0.00	3.25	98.2	45.11
5719	5	64.8	15.8	3.81	1.25	2.77	3.27	3.18	0.08	0.22	0.670	0.00	2.30	98.3	36.22
5720	5	55.1	15.0	0.98	2.86	2.81	6.22	8.40	0.34	0.41	1.210	0.00	6.40	99.8	44.06
5721	5	62.5	15.1	1.37	1.85	2.38	1.50	7.74	0.07	0.37	1.080	0.00	5.55	99.6	59.58
5722	5	51.7	13.8	0.68	5.15	2.03	6.54	7.75	0.14	0.26	0.753	0.03	6.35	95.3	49.86
5725	5	62.5	14.3	0.46	3.08	3.11	3.14	5.59	0.44	0.25	0.771	0.02	3.85	97.6	63.23
5726	5	57.3	15.5	1.21	4.55	1.20	3.21	9.28	0.21	0.43	1.170	0.00	4.90	99.1	56.54
5728	5	53.2	18.3	2.98	4.77	1.09	4.23	10.00	0.15	0.23	1.050	0.00	2.90	99.1	44.84
5742	5	66.6	12.3	0.30	1.81	2.60	4.07	4.68	0.25	0.18	0.669	0.00	4.60	98.1	50.23
5743	5	56.9	14.5	2.14	3.44	1.35	4.51	8.78	0.21	0.44	1.220	0.00	4.35	97.9	41.87
5748	5	53.8	16.4	1.62	5.71	0.97	3.76	9.53	0.12	0.48	1.240	0.00	5.15	98.9	55.39
5749	5	52.8	18.0	2.20	3.91	1.04	4.62	9.71	0.09	0.42	1.170	0.00	5.35	99.4	42.06
5806	5	54.9	16.4	1.95	3.76	1.63	5.05	8.13	0.25	0.40	1.080	0.00	5.35	99.0	43.50
5807	5	60.4	15.2	0.75	3.44	1.35	0.75	9.23	0.03	0.37	1.170	0.01	7.60	100.4	76.15
5808	5	62.1	17.3	1.23	0.33	0.68	0.66	8.17	0.02	0.39	1.320	0.03	7.75	100.1	34.83
5816	5	67.0	14.5	1.15	1.57	2.44	3.88	4.65	0.13	0.22	0.802	0.00	2.70	99.1	44.36
5817	5	72.0	16.3	0.88	0.10	3.11	0.38	2.07	0.01	0.32	1.510	0.02	3.20	100.0	71.81
5818	5	46.6	15.6	0.38	6.41	2.73	0.55	16.00	0.06	0.18	0.749	0.04	10.80	100.2	90.76
5821	5	64.9	13.3	0.98	2.06	1.79	4.88	5.45	0.18	0.21	0.746	0.00	4.65	99.2	39.65
5822	5	58.3	16.0	0.97	4.67	2.10	0.61	8.95	0.09	0.42	1.080	0.01	6.90	100.2	81.08
5830	5	55.6	16.2	1.63	1.82	2.35	5.96	7.87	0.23	0.38	0.986	0.00	4.05	97.2	35.46
5831	5	53.7	18.1	0.31	7.25	2.46	1.02	9.75	0.11	0.25	0.953	0.02	6.05	100.1	87.95
5832	5	55.0	17.4	2.26	8.27	2.49	3.62	6.03	0.12	0.19	1.150	0.01	2.85	99.5	64.66
5833	5	57.5	16.4	5.13	6.23	0.94	5.72	3.09	0.04	0.51	1.020	0.01	1.80	98.5	39.79
5834	5	56.7	15.3	1.32	2.62	2.47	5.02	8.43	0.18	0.33	1.020	0.00	4.45	97.9	44.53
5837	5	61.2	17.1	2.57	3.61	1.24	4.64	5.91	0.09	0.24	0.905	0.01	2.30	99.9	40.22
5842	5	68.0	12.8	1.00	1.68	1.75	4.52	4.91	0.13	0.20	0.720	0.00	3.75	99.5	38.32
5855	5	66.4	13.5	1.09	2.11	1.92	4.92	5.77	0.17	0.24	0.762	0.00	2.65	99.6	40.14
5856	5	61.3	16.1	0.55	0.22	0.88	0.47	10.10	0.01	0.46	1.330	0.02	8.60	100.2	51.89
5857	5	61.8	15.3	0.82	3.37	1.89	3.42	7.83	0.26	0.34	0.954	0.00	3.40	99.5	55.37
5865	5	56.0	16.9	2.79	3.39	0.93	4.80	10.90	0.10	0.28	1.140	0.00	1.90	99.2	36.27
5868	5	54.4	16.8	1.26	4.56	1.72	0.73	10.80	0.07	0.42	1.050	0.02	8.35	100.3	75.94

Sample	Unit	SiO_2	Al_2O_3	Na_2O	MgO	K_2O	CaO	Fe_2O_3	MnO	P_2O_5	TiO_2	Cr_2O_3	LOI	Total	A.I.
5876	5	42.4	16.4	1.39	4.72	0.57	13.20	10.60	0.18	0.12	0.937	0.02	8.10	98.7	26.61
5878	5	43.3	16.5	2.29	4.37	0.10	13.80	9.15	0.20	0.12	0.938	0.02	7.25	98.1	21.74
5879	5	45.8	16.1	2.00	8.83	0.28	8.59	10.80	0.15	0.12	0.927	0.03	4.80	98.5	46.24
5880	5	59.7	15.1	2.15	2.74	1.38	3.63	7.69	0.14	0.41	1.160	0.00	5.70	99.9	41.62
5881	5	47.0	18.3	3.51	5.08	2.11	5.93	7.14	0.20	0.13	1.120	0.03	8.00	98.7	43.24
5882	5	70.4	13.7	2.19	1.31	1.40	5.00	3.73	0.09	0.09	0.458	0.00	1.85	100.4	27.37
5884	5	61.3	13.4	1.82	2.93	0.93	4.60	9.54	0.20	0.37	1.080	0.00	3.25	99.5	37.55
5886	5	49.0	19.4	4.32	3.98	0.46	7.67	8.37	0.14	0.14	1.160	0.03	3.55	98.3	27.02
67911	5	57.7	15.4	0.54	2.70	3.22	5.57	6.32	0.42	0.36	0.920	0.01	5.05	98.2	49.21
67912	5	65.2	16.9	0.34	1.56	3.53	0.83	6.68	0.26	0.41	1.050	0.01	2.89	99.7	81.31
67913	5	62.3	13.3	0.40	0.13	3.63	0.35	11.54	0.01	0.13	0.840	0.03	7.17	99.8	83.37
67914	5	57.1	15.2	0.48	2.85	3.40	5.78	6.34	0.44	0.33	0.920	0.01	5.44	98.2	49.96
67915	5	65.6	14.3	31.00	0.37	3.94	0.34	7.10	0.01	0.16	0.630	0.02	5.29	98.1	12.09
67916	5	63.8	13.5	0.33	0.35	3.59	0.33	9.56	0.01	0.14	0.630	0.03	6.31	98.5	85.65
67917	5	65.0	11.2	0.45	0.43	2.29	0.33	12.30	0.01	0.02	0.390	0.03	7.10	99.5	77.71
67918	5	57.7	14.9	0.38	0.25	4.01	0.62	12.69	0.01	0.24	0.970	0.02	7.85	99.7	80.99
67919	5	49.6	17.5	1.74	0.08	2.64	0.37	14.39	0.01	0.09	0.630	0.02	9.67	96.8	56.31
67920	5	63.5	18.2	2.23	2.43	2.96	1.53	4.01	0.04	0.11	0.640	0.02	3.07	98.7	58.91
67922	5	70.9	13.5	0.83	0.15	2.71	0.39	5.67	0.01	0.13	0.480	0.01	4.36	99.1	70.10
67923	5	75.0	10.3	0.30	0.44	2.47	0.34	5.99	0.01	0.09	0.340	0.02	4.24	99.6	81.97
Maximum		75.00	23.00	31.00	8.83	4.52	13.80	16.00	1.34	0.57	1.52	0.04	10.80	100.40	90.76
Minimum		42.40	10.30	0.17	0.08	0.10	0.33	2.07	0.01	0.02	0.34	0.00	1.40	92.00	12.09
Average		57.48	15.76	1.75	3.05	2.07	4.37	8.18	0.22	0.28	1.00	0.01	4.81	98.83	49.27
Deviation		6.94	2.18	2.87	1.73	0.94	2.63	2.78	0.18	0.12	0.27	0.01	1.95	1.13	15.78

Sample	Unit	SiO_2	Al_2O_3	Na_2O	MgO	K_2O	CaO	Fe_2O_3	MnO	P_2O_5	TiO_2	Cr_2O_3	LOI	Total	A.I.
5501	6	65.3	12.8	1.76	1.76	1.73	4.27	6.97	0.14	0.22	0.693	0.01	4.62	100.4	36.66
5502	6	75.2	13.5	4.64	0.41	2.37	0.40	1.62	0.04	0.09	0.532	0.00	1.25	100.2	35.55
5503	6	70.9	14.0	2.92	0.36	4.15	1.87	2.47	0.07	0.09	0.483	0.00	2.60	100.2	48.49
5546	6	71.4	13.6	2.92	0.93	2.94	2.65	3.16	0.08	0.09	0.445	0.00	2.15	100.5	41.00
5568	6	75.5	12.7	3.13	0.45	3.62	1.08	1.78	0.06	0.05	0.226	0.01	0.95	99.7	49.15
5569	6	75.6	12.2	1.70	0.39	4.38	1.65	1.46	0.08	0.04	0.218	0.00	1.30	99.2	58.74
5602	6	75.4	11.2	0.31	0.19	3.08	0.02	5.31	0.02	0.04	0.249	0.02	3.75	99.7	90.83
5607	6	60.2	16.3	1.85	2.03	2.11	5.90	6.68	0.16	0.39	0.977	0.00	2.75	99.5	34.82
5618	6	71.3	15.7	0.86	0.98	2.26	1.22	3.70	0.21	0.16	0.650	0.01	2.60	99.8	60.90
5623	6	69.9	13.9	3.45	0.74	3.04	2.53	3.33	0.08	0.09	0.454	0.01	1.50	99.2	38.73
5626	6	77.3	11.9	5.62	0.22	0.96	1.28	0.72	0.03	0.05	0.219	0.02	1.25	99.7	14.60
5627	6	75.3	13.9	4.83	0.31	1.99	0.78	0.79	0.02	0.05	0.272	0.02	0.95	99.4	29.08
5629	6	77.7	11.6	4.98	0.37	1.21	1.18	1.47	0.05	0.04	0.203	0.02	1.10	100.0	20.41
5634	6	72.8	13.2	3.36	0.97	2.08	1.99	2.14	0.05	0.06	0.285	0.00	1.75	98.8	36.31
5635	6	75.6	13.4	6.92	0.55	0.73	0.59	1.21	0.04	0.06	0.250	0.01	0.80	100.3	14.56
5642	6	76.9	13.4	6.26	0.14	1.11	0.54	0.58	0.02	0.06	0.249	0.02	0.45	99.9	15.53
5643	6	75.9	12.1	2.74	0.53	2.82	1.76	1.20	0.04	0.04	0.211	0.01	2.25	99.8	42.68
5649	6	73.6	13.8	4.44	0.71	2.24	1.50	1.84	0.06	0.05	0.259	0.00	1.40	100.1	33.18
5650	6	70.2	14.4	1.70	0.64	3.92	2.94	1.60	0.06	0.05	0.266	0.00	2.50	98.4	49.57
5651	6	70.3	13.8	0.85	1.31	2.60	1.84	3.80	0.68	0.08	0.457	0.01	2.80	98.6	59.24
5654	6	74.7	12.0	0.52	1.15	2.48	0.69	3.32	0.88	0.05	0.218	0.00	2.30	98.4	75.00
5657	6	69.7	14.6	4.89	1.50	2.14	1.61	3.00	0.08	0.15	0.480	0.01	0.90	99.2	35.90
5658	6	73.3	12.9	4.58	0.52	1.62	2.20	2.14	0.07	0.06	0.263	0.01	1.85	99.7	23.99
5659	6	74.6	12.2	1.45	0.74	3.47	1.86	1.31	0.04	0.05	0.193	0.00	2.15	98.2	55.98
5660	6	67.3	15.5	1.41	0.79	2.56	4.30	3.97	0.11	0.20	0.648	0.00	1.20	98.2	36.98
5666	6	67.2	15.7	3.51	0.79	3.72	2.17	2.73	0.07	0.08	0.355	0.00	2.55	99.1	44.26
5667	6	71.9	13.2	3.45	0.68	2.37	2.45	1.78	0.06	0.11	0.383	0.02	1.85	98.4	34.08
5684	6	72.2	14.0	2.45	0.49	3.27	1.67	2.01	0.05	0.05	0.273	0.00	1.75	98.4	47.72
5687	6	69.4	13.7	2.26	0.77	3.29	2.45	3.86	0.10	0.09	0.459	0.00	2.60	99.2	46.29
5691	6	70.2	13.7	3.10	0.59	2.83	2.22	3.65	0.08	0.09	0.443	0.00	2.10	99.2	39.13
5695	6	70.1	13.9	2.60	0.59	3.32	2.55	2.85	0.08	0.10	0.468	0.00	2.50	99.2	43.16
5700	6	71.1	13.8	4.13	0.33	3.03	2.62	1.75	0.06	0.09	0.473	0.00	1.85	99.4	33.23
5701	6	69.8	14.1	2.02	1.01	3.34	2.10	3.32	0.06	0.11	0.500	0.00	2.25	98.8	51.36
5704	6	70.9	13.7	2.33	0.67	2.96	2.24	3.29	0.09	0.09	0.457	0.00	2.30	99.2	44.27
5708	6	73.1	13.1	3.03	0.34	4.05	1.38	1.25	0.04	0.05	0.277	0.00	1.05	97.8	49.89
5709	6	71.8	14.0	3.14	0.77	2.89	1.42	3.35	0.08	0.09	0.458	0.00	1.40	99.6	44.53
5710	6	69.1	13.9	4.66	0.25	1.90	3.04	3.13	0.20	0.17	0.568	0.00	2.25	99.4	21.83
5714	6	69.4	12.9	2.88	0.46	2.64	3.34	3.40	0.11	0.09	0.421	0.00	2.80	98.6	33.26
5718	6	68.9	13.8	1.62	0.76	3.80	2.20	3.87	0.07	0.09	0.450	0.00	2.55	98.3	54.42
5723	6	69.9	13.7	2.03	0.66	3.57	2.62	3.30	0.11	0.09	0.438	0.00	2.55	99.2	47.64
5724	6	76.4	12.9	4.61	0.20	1.92	1.38	0.78	0.02	0.09	0.414	0.01	1.10	100.0	26.14
5740	6	69.2	13.3	2.41	1.69	2.85	1.90	3.91	0.06	0.09	0.478	0.00	2.85	98.9	51.30
5741	6	70.9	13.8	2.63	1.48	2.91	1.09	3.38	0.06	0.09	0.477	0.00	2.25	99.2	54.13
5815	6	69.9	13.9	3.86	0.77	2.54	2.92	3.39	0.10	0.09	0.446	0.00	1.55	99.6	32.80
5841	6	70.2	14.6	3.32	0.52	3.94	1.56	2.45	0.07	0.10	0.496	0.00	1.55	99.0	47.75
5843	6	68.0	13.9	2.18	0.45	4.04	2.17	2.39	0.05	0.10	0.522	0.01	1.50	95.5	50.79
5844	6	69.8	13.6	3.18	0.93	3.10	2.63	3.01	0.08	0.09	0.433	0.00	1.55	98.6	40.96
5845	6	71.2	13.8	3.26	0.71	3.12	2.39	2.50	0.06	0.10	0.556	0.00	1.15	99.0	40.40
5846	6	68.4	13.9	3.17	0.90	3.10	2.75	3.31	0.12	0.09	0.525	0.00	1.90	98.3	40.32
5847	6	70.0	13.4	2.50	1.32	3.16	2.83	3.23	0.08	0.09	0.432	0.00	2.30	99.5	45.67
5848	6	71.1	14.3	3.56	0.96	2.79	2.84	2.39	0.06	0.12	0.382	0.00	0.85	99.5	36.95

Sample	Unit	SiO_2	Al_2O_3	Na_2O	MgO	K_2O	CaO	Fe_2O_3	MnO	P_2O_5	TiO_2	Cr_2O_3	LOI	Total	A.I.
5849	6	69.8	14.7	4.12	0.71	2.74	2.59	2.74	0.06	0.10	0.532	0.01	1.35	99.6	33.96
5853	6	73.8	13.7	4.29	0.20	2.56	1.63	1.00	0.04	0.09	0.451	0.01	0.90	98.8	31.80
5854	6	70.9	13.4	2.29	0.57	3.22	2.78	3.07	0.08	0.09	0.436	0.00	3.15	100.1	42.78
5861	6	69.3	13.6	3.29	0.83	2.76	2.85	4.07	0.08	0.09	0.489	0.63	1.80	100.1	36.90
5874	6	71.1	14.1	3.47	0.79	2.60	2.72	2.66	0.04	0.11	0.532	0.01	1.70	100.0	35.39
5875	6	67.6	14.3	0.56	1.58	3.33	3.75	4.25	0.10	0.17	0.585	0.01	2.25	98.6	53.25
67921	6	74.6	12.6	6.10	0.11	0.28	2.62	0.57	0.02	0.08	0.290	0.02	1.28	98.5	4.28
Maximum		77.70	16.30	6.92	2.03	4.38	5.90	6.97	0.88	0.39	0.98	0.63	4.62	100.50	90.83
Minimum		60.20	11.20	0.31	0.11	0.28	0.02	0.57	0.02	0.04	0.19	0.00	0.45	95.50	4.28
Average		71.43	13.61	3.11	0.73	2.75	2.15	2.73	0.10	0.09	0.42	0.02	1.90	99.20	41.01
Deviation		3.18	0.95	1.43	0.42	0.86	1.01	1.32	0.14	0.05	0.15	0.08	0.77	0.81	14.21

Sample	Unit	SiO_2	Al_2O_3	Na_2O	MgO	K_2O	CaO	Fe_2O_3	MnO	P_2O_5	TiO_2	Cr_2O_3	LOI	Total	A.I.
5511	11	60.5	16.1	4.79	1.89	0.38	5.76	7.72	0.07	0.41	1.090	0.01	1.75	100.6	17.71
5512	11	58.6	16.0	4.65	1.91	0.68	5.60	7.42	0.09	0.39	1.030	0.01	3.70	100.2	20.17
5513	11	58.4	16.6	5.74	2.16	0.92	4.40	6.64	0.08	0.40	1.060	0.00	3.35	99.9	23.30
5532	11	53.9	17.2	3.06	4.04	0.85	8.69	7.93	0.12	0.30	0.850	0.01	1.80	98.9	29.39
5535	11	58.3	17.0	6.81	2.83	0.46	3.61	6.49	0.11	0.46	1.140	0.00	1.60	98.9	24.00
5765	11	52.7	17.4	3.63	4.73	0.32	8.12	8.15	0.14	0.29	0.852	0.00	3.35	99.8	30.06
5766	11	54.0	17.5	3.68	3.57	0.86	7.72	8.56	0.11	0.45	0.971	0.01	2.45	100.0	27.98
5767	11	49.9	13.3	2.89	4.24	0.70	7.14	18.50	0.22	0.15	2.270	0.00	0.85	100.2	33.00
5768	11	53.8	17.4	3.50	3.56	0.87	8.05	8.74	0.15	0.46	1.010	0.00	2.05	99.7	27.72
5769	11	56.3	17.2	4.17	2.92	0.92	7.21	7.79	0.13	0.49	1.130	0.01	1.70	100.1	25.23
5770	11	58.2	16.7	4.38	2.60	0.89	6.00	8.37	0.10	0.44	1.080	0.00	1.60	100.5	25.16
5784	11	47.1	16.1	2.32	9.20	0.77	7.86	8.46	0.13	0.07	0.530	0.03	7.55	100.2	49.48
5786	11	58.3	16.2	4.43	2.40	0.99	5.71	7.40	0.09	0.42	1.060	0.01	3.15	100.3	25.06
5787	11	58.7	16.7	5.62	2.71	0.24	5.57	6.87	0.08	0.42	1.030	0.00	1.75	99.8	20.86
5811	11	53.2	17.7	3.34	4.41	0.70	8.17	8.04	0.12	0.30	0.643	0.00	2.50	99.2	30.75
5812	11	53.7	17.6	5.53	4.37	0.41	7.67	8.07	0.12	0.30	0.954	0.00	1.50	100.3	26.59
5813	11	55.5	17.0	4.77	3.48	0.55	7.16	8.67	0.13	0.47	1.110	0.00	1.20	100.2	25.25
Maximum		60.50	17.70	6.81	9.20	0.99	8.69	18.50	0.22	0.49	2.27	0.03	7.55	100.60	49.48
Minimum		47.10	13.30	2.32	1.89	0.24	3.61	6.49	0.07	0.07	0.53	0.00	0.85	98.90	17.71
Average		55.36	16.69	4.31	3.59	0.68	6.73	8.46	0.12	0.37	1.05	0.01	2.46	99.93	27.16
Deviation		3.45	1.00	1.14	1.66	0.23	1.41	2.60	0.03	0.11	0.35	0.01	1.50	0.49	6.77

Sample	Unit	SiO_2	Al_2O_3	Na_2O	MgO	K_2O	CaO	Fe_2O_3	MnO	P_2O_5	TiO_2	Cr_2O_3	LOI	Total	A.I.
5536	12	45.9	16.1	2.85	4.76	1.67	7.96	14.10	0.21	0.47	2.360	0.00	1.85	98.4	37.30
5580	12	61.2	15.3	2.21	3.40	0.85	4.25	7.67	0.06	0.34	1.040	0.02	3.95	100.4	39.68
5581	12	60.1	14.3	1.19	2.14	3.00	4.50	8.62	0.08	0.13	0.592	0.02	5.30	100.1	47.46
5582	12	58.1	16.3	3.56	3.26	0.76	3.53	10.00	0.07	0.40	1.120	0.00	2.85	100.0	36.18
5583	12	62.4	15.8	2.96	3.32	0.78	3.29	6.73	0.03	0.33	1.000	0.01	3.10	99.8	39.61
5596	12	63.8	15.4	2.48	3.04	0.88	3.81	4.97	0.04	0.31	1.020	0.01	2.75	98.6	38.39
5838	12	59.1	16.7	1.82	4.26	2.02	3.16	6.46	0.06	0.39	1.090	0.01	3.80	99.0	55.77
5866	12	57.6	14.9	0.95	3.22	2.53	4.04	9.05	0.07	0.31	0.949	0.02	5.15	98.9	53.54
5867	12	62.8	14.7	2.77	3.58	1.23	2.46	6.19	0.04	0.27	0.841	0.01	3.15	98.2	47.91
Maximum		63.80	16.70	3.56	4.76	3.00	7.96	14.10	0.21	0.47	2.36	0.02	5.30	100.40	55.77
Minimum		45.90	14.30	0.95	2.14	0.76	2.46	4.97	0.03	0.13	0.59	0.00	1.85	98.20	36.18
Average		59.00	15.50	2.31	3.44	1.52	4.11	8.20	0.07	0.33	1.11	0.01	3.54	99.27	43.98
Deviation		5.05	0.75	0.81	0.70	0.79	1.48	2.56	0.05	0.09	0.47	0.01	1.07	0.77	6.93

Sample	Unit	SiO_2	Al_2O_3	Na_2O	MgO	K_2O	CaO	Fe_2O_3	MnO	P_2O_5	TiO_2	Cr_2O_3	LOI	Total	A.I.
5531	13	72.7	12.9	4.19	0.52	1.50	2.21	3.40	0.07	0.06	0.404	0.02	1.90	100.0	23.99
5537	13	69.2	13.3	3.24	0.84	2.05	3.59	4.55	0.11	0.10	0.577	0.00	2.55	100.3	29.73
5538	13	71.3	13.1	4.49	0.38	1.78	2.42	3.01	0.08	0.07	0.425	0.02	2.00	99.2	23.81
5539	13	71.2	14.5	5.39	0.93	1.35	1.46	3.62	0.05	0.10	0.515	0.02	1.20	100.5	24.97
5540	13	72.5	13.2	3.62	0.49	2.35	2.07	2.60	0.07	0.07	0.450	0.02	2.45	100.1	33.29
5541	13	72.0	13.6	4.76	0.35	1.42	1.79	3.77	0.05	0.07	0.446	0.02	1.55	100.0	21.27
5542	13	72.5	12.8	2.43	0.35	2.47	2.76	3.31	0.08	0.06	0.385	0.02	1.95	99.3	35.21
5543	13	72.3	13.4	5.10	0.29	1.29	2.28	3.16	0.09	0.07	0.387	0.01	1.45	100.0	17.63
5544	13	73.1	13.4	4.34	0.31	1.92	1.81	3.26	0.08	0.07	0.411	0.02	1.40	100.3	26.61
5545	13	72.1	13.5	5.24	0.55	2.64	0.87	3.79	0.07	0.07	0.419	0.02	1.20	100.7	34.30
5839	13	67.0	14.6	3.11	2.56	1.14	3.65	5.16	0.07	0.23	0.737	0.02	1.65	100.1	35.37
5840	13	71.8	13.7	2.04	1.53	2.41	2.14	3.97	0.07	0.10	0.580	0.02	1.80	100.3	48.52
5851	13	68.2	14.0	3.84	2.01	0.47	4.19	5.69	0.04	0.13	0.617	0.02	0.85	100.2	23.60
5852	13	71.6	13.6	5.11	1.27	0.78	2.92	2.68	0.04	0.08	0.455	0.02	0.75	99.4	20.34
5872	13	67.5	14.2	3.26	2.47	1.32	2.00	4.23	0.02	0.19	0.595	0.02	4.05	100.0	41.88
5873	13	66.1	14.5	3.72	1.79	1.49	2.14	4.98	0.02	0.19	0.765	0.03	3.55	99.4	35.89

Sample	Unit	SiO_2	Al_2O_3	Na_2O	MgO	K_2O	CaO	Fe_2O_3	MnO	P_2O_5	TiO_2	Cr_2O_3	LOI	Total	A.I.
5888	13	70.2	13.8	4.46	0.44	1.77	2.60	3.52	0.08	0.08	0.418	0.01	0.75	98.3	23.84
5889	13	64.4	14.8	5.31	2.10	0.47	5.29	2.91	0.04	0.43	1.090	0.02	2.10	99.1	19.51
5890	13	72.1	13.6	4.77	0.45	2.08	1.58	3.30	0.03	0.07	0.427	0.01	1.00	99.6	28.49
5891	13	71.4	13.3	4.50	0.45	1.81	2.51	3.30	0.05	0.08	0.408	0.02	2.10	100.1	24.38
5892	13	65.9	17.0	6.19	2.44	0.67	3.03	1.38	0.04	0.35	1.040	0.01	1.80	100.0	25.22
5893	13	65.4	16.2	5.49	3.19	0.98	2.73	2.76	0.04	0.19	0.800	0.02	1.85	99.7	33.66
5895	13	65.8	14.3	4.71	1.50	0.73	1.87	5.58	0.03	0.18	0.760	0.02	4.20	99.8	25.31
5896	13	58.8	15.9	2.94	3.47	0.58	5.30	8.93	0.06	0.37	1.070	0.00	2.80	100.3	32.95
5897	13	67.8	15.1	4.20	2.01	1.55	2.56	2.67	0.04	0.27	0.846	0.02	1.40	98.6	34.50
5898	13	58.8	16.2	3.88	3.08	0.38	5.03	9.04	0.04	0.40	1.050	0.01	1.95	100.0	27.97
5899	13	72.3	14.6	5.10	1.15	0.79	2.91	1.78	0.04	0.13	0.535	0.02	1.00	100.5	19.50
5900	13	53.7	14.6	3.07	4.65	0.26	7.96	11.00	0.15	0.22	1.170	0.01	1.80	98.6	30.80
67901	13	72.6	14.0	4.58	0.79	1.07	2.59	1.07	0.05	0.11	0.550	0.03	1.75	99.2	20.60
67903	13	70.7	11.6	0.19	0.36	3.76	0.16	7.07	0.01	0.01	0.320	0.02	4.59	98.8	92.17
67904	13	60.5	8.3	0.19	0.28	2.66	1.19	15.84	0.10	0.03	0.220	0.03	8.89	98.2	68.06
67905	13	70.6	14.3	5.07	2.09	0.77	2.47	1.77	0.02	0.13	0.620	0.02	1.09	98.9	27.50
67906	13	69.4	12.1	0.13	0.56	4.12	0.14	7.13	0.02	0.02	0.330	0.03	4.62	98.6	94.55
67908	13	71.8	13.4	4.41	1.35	1.11	2.18	1.58	0.04	0.03	0.480	0.03	2.03	98.5	27.18
67910	13	74.4	12.9	4.73	0.63	1.49	1.42	1.48	0.03	0.04	0.390	0.03	1.16	98.7	25.63
Maximum		74.40	17.00	6.19	4.65	4.12	7.96	15.84	0.15	0.43	1.17	0.03	8.89	100.70	94.55
Minimum		53.70	8.30	0.13	0.28	0.26	0.14	1.07	0.01	0.01	0.22	0.00	0.75	98.20	17.63
Average		68.79	13.84	3.94	1.36	1.53	2.62	4.38	0.05	0.14	0.59	0.02	2.21	99.58	33.09
Deviation		4.71	1.46	1.46	1.09	0.89	1.50	2.98	0.03	0.11	0.25	0.01	1.54	0.71	17.51

Sample	Unit	SiO_2	Al_2O_3	Na_2O	MgO	K_2O	CaO	Fe_2O_3	MnO	P_2O_5	TiO_2	Cr_2O_3	LOI	Total	A.I.
67902	22	52.1	12.5	2.00	6.62	0.98	7.87	6.52	0.22	0.37	0.670	0.05	9.06	99.1	43.50
67907	22	53.5	13.2	3.11	6.38	0.84	6.85	6.54	0.10	0.36	0.670	0.05	7.57	99.5	42.03
Maximum		53.50	13.20	3.11	6.62	0.98	7.87	6.54	0.22	0.37	0.67	0.05	9.06	99.50	43.50
Minimum		52.10	12.50	2.00	6.38	0.84	6.85	6.52	0.10	0.36	0.67	0.05	7.57	99.10	42.03
Average		52.80	12.85	2.56	6.50	0.91	7.36	6.53	0.16	0.37	0.67	0.05	8.32	99.30	42.77
Deviation		0.70	0.35	0.55	0.12	0.07	0.51	0.01	0.06	0.00	0.00	0.00	0.74	0.20	0.73

Analyses of replicate samples

Samples are all of the same composite prepared in the field. Analyses were carried out twice by taking two 2 gram samples of the same plup.

Sample	SiO_2		Al_2O_3		Na_2O		MgO		K_2O		CaO		Cr_2O_3	
	1	2	1	2	1	2	1	2	1	2	1	2	1	2
5503	70.90	71.40	14.00	14.30	2.92	2.95	0.36	0.54	4.15	4.14	1.87	1.90	0.01	0.01
5584	72.80	72.10	14.00	13.90	2.99	3.02	0.47	0.50	3.87	3.93	1.57	1.56	0.01	0.01
5600	71.30	71.10	14.40	14.50	2.93	2.87	0.49	0.56	4.18	4.09	1.20	1.23	0.01	0.01
5628	71.80	72.30	13.80	13.80	3.06	2.96	0.41	0.48	3.96	3.92	1.57	1.58	0.01	0.01
5736	71.50	71.80	13.70	13.80	2.73	2.70	0.45	0.56	4.07	3.97	1.44	1.46	0.01	0.01
5814	70.00	70.40	14.20	14.20	3.10	3.06	0.45	0.51	4.10	4.00	2.14	2.17	0.01	0.01
5877	71.90	71.90	14.00	14.10	3.03	3.03	0.48	0.54	4.05	4.03	1.36	1.39	0.01	0.01
Avg.	71.30	71.60	14.00	14.10	2.98	2.94	0.44	0.53	4.05	4.01	1.54	1.61	0.01	
Std.	0.88	0.66	0.23	0.27	0.17	0.12	0.05	0.03	0.06	0.08	0.36	0.32	0.00	

Sample	Cr_2O_3	Fe_2O_3		MnO		P_2O_5		TiO_2		LOI		Total	
	2	1	2	1	2	1	2	1	2	1	2	1	2
5503	0.01	2.47	2.34	0.07	0.07	0.09	0.09	0.48	0.49	2.60	1.90	100.20	100.50
5584	0.01	2.28	2.21	0.07	0.06	0.10	0.09	0.48	0.47	1.00	1.60	99.90	100.40
5600	0.01	2.26	2.46	0.06	0.06	0.10	0.10	0.53	0.49	1.70	1.45	99.50	99.70
5628	0.01	2.10	2.15	0.06	0.06	0.09	0.09	0.45	0.45	1.65	1.20	99.20	99.20
5736	0.01	2.19	2.27	0.06	0.06	0.09	0.09	0.45	0.45	1.10	1.05	98.10	99.20
5814	0.01	2.21	2.20	0.07	0.07	0.09	0.09	0.45	0.46	1.75	1.45	98.80	98.50
5877	0.01	2.30	2.28	0.06	0.06	0.09	0.09	0.47	0.48	1.45	1.30	99.40	98.90
Avg.	0.01	2.20	2.27	0.06	0.06	0.09	0.09	0.48	0.47	1.61	1.42	98.90	99.50
Std.	0.00	0.08	0.10	0.01	0.00	0.00	0.00	0.03	0.02	0.53	0.28	0.57	0.75

APPENDIX 2

Trace Element Analyses of the Rocks of the Blake River Group

Trace elements Rb, Ba, Sr, Zr, Y, and Nb were analyzed by X-Ray Fluorescence by the methods described in Appendix 1. Au, Ag, Cu, Zn, and Pb were determined by atomic absorption. All results are in parts per million with the exception of Au which is reported in parts per billion. Detection limits are 10 ppm for most trace element and 5 ppb for gold. Values that were below the detection limits were converted to half the detection limit for calculation purpose.

Sample	unit	Rb	Sr	Y	Zr	Nb	Ba	Au	Cu	Zn	Pb
5504	1	5	129	30	109	13	104	6	84	25	7
5505	1	15	98	36	119	26	155	6	84	41	10
5506	1	12	91	20	105	22	89	7	55	29	9
5507	1	5	53	16	60	15	62	18	100	65	15
5508	1	5	133	15	89	23	136	2	55	57	13
5509	1	10	100	31	129	574	81	5	74	84	16
5510	1	11	84	0	39	24	62	2	70	32	9
5514	1	5	72	28	70	26	0	196	50	27	11
5515	1	5	74	11	34	16	69	9	93	32	11
5516	1	5	109	20	49	25	93	5	31	47	14
5517	1	5	92	21	53	32	89	2	86	46	10
5518	1	5	69	18	37	25	54	7	130	48	12
5519	1	11	82	0	69	28	88	5	68	35	11
5520	1	5	78	13	65	27	0	10	140	26	9
5521	1	25	82	0	77	13	0	7	65	32	10
5522	1	14	67	15	59	34	114	26	463	36	16
5523	1	5	144	18	94	28	102	2	92	112	15
5524	1	5	94	28	66	31	0	9	110	43	13
5525	1	5	99	0	34	14	69	11	100	36	9
5526	1	5	111	20	35	14	82	12	91	52	17
5527	1	5	70	16	63	28	58	12	102	34	12
5528	1	5	110	13	44	44	64	12	75	50	12
5533	1	5	91	0	55	21	62	16	76	30	10
5534	1	5	80	30	89	0	117	14	55	28	11
5547	1	5	234	0	58	0	143	18	58	42	10
5548	1	5	205	0	21	12	78	16	106	33	9
5549	1	5	136	15	71	23	83	13	60	73	10
5550	1	13	135	10	80	23	114	26	150	31	10
5551	1	5	39	20	67	22	62	20	11	42	12
5552	1	5	78	18	68	22	88	6	54	62	12
5553	1	5	78	0	45	24	0	7	120	40	9
5554	1	5	168	19	66	19	126	44	81	20	11
5555	1	12	201	19	71	0	72	12	83	20	7
5556	1	5	296	19	94	29	149	11	73	18	8
5557	1	12	111	19	50	21	146	8	99	54	12
5558	1	12	102	0	64	0	55	7	126	32	6
5559	1	5	85	0	49	0	74	62	62	28	7
5560	1	5	64	34	104	17	167	2	46	89	17
5561	1	5	198	15	66	31	187	6	66	64	10
5562	1	5	61	32	92	29	86	6	45	25	6
5563	1	5	88	35	89	27	137	14	185	23	6
5671	1	17	100	30	67	19	0	7	100	43	12
5672	1	5	67	0	52	15	69	12	98	50	14
5673	1	5	93	21	92	30	73	9	81	41	12
5674	1	5	49	12	36	0	94	13	128	73	20
5680	1	92	77	0	45	14	521	10	129	30	15
5683	1	32	207	15	58	21	392	14	96	80	14
5735	1	13	81	16	82	13	74	6	100	36	11
5751	1	60	96	0	44	24	301	14	110	64	21
5752	1	27	234	39	133	16	222	22	58	67	13

Sample	unit	Rb	Sr	Y	Zr	Nb	Ba	Au	Cu	Zn	Pb
5753	1	20	254	29	122	0	218	20	53	64	12
5755	1	5	128	22	76	26	102	20	83	84	18
5756	1	5	90	38	126	18	166	29	70	83	14
5757	1	19	90	0	37	20	89	10	109	57	15
5758	1	20	45	16	69	30	61	16	73	75	18
5759	1	5	85	49	142	18	73	14	61	56	10
5760	1	5	109	11	31	19	89	15	107	46	11
5761	1	5	103	13	73	18	87	11	91	70	14
5762	1	13	110	14	45	20	72	18	103	52	11
5763	1	12	89	0	80	0	0	15	74	63	16
5764	1	12	41	16	68	0	63	24	93	82	18
5776	1	5	83	31	81	22	124	17	38	15	9
5777	1	5	62	54	78	17	87	18	75	21	9
5781	1	24	103	0	25	0	117	23	6	21	10
5782	1	14	107	22	107	15	82	46	60	18	9
5785	1	50	197	0	61	22	250	11	13	37	14
5788	1	5	133	29	89	30	89	23	110	23	11
5789	1	5	124	34	98	24	97	32	71	26	9
5790	1	23	76	0	52	18	79	23	58	32	13
5791	1	23	106	23	118	33	84	13	49	61	11
5792	1	26	107	24	80	15	80	20	97	21	9
5793	1	5	134	31	74	12	124	19	48	38	13
5794	1	33	48	162	114	33	164	137	677	39	16
5795	1	53	34	0	60	0	252	273	152	60	17
5796	1	5	94	19	58	15	0	17	89	31	11
5798	1	68	143	25	108	21	680	18	108	39	16
5799	1	5	72	28	85	20	110	14	65	30	13
5801	1	5	90	20	77	30	85	25	86	30	9
5802	1	5	51	0	75	41	73	50	201	28	11
5803	1	5	59	37	80	32	93	54	79	33	9
5804	1	5	62	37	94	19	98	62	237	31	12
5805	1	5	90	26	82	25	95	25	123	38	8
5809	1	5	89	18	64	0	0	67	91	28	8
5810	1	5	77	24	66	16	59	22	68	44	10
Maximum		92	296	162	142	574	680	273	677	112	21
Minimum		5	34	0	21	0	0	2	6	15	6
Average		13	105	20	73	26	110	24	98	44	12
Deviation		15	50	20	26	61	101	38	84	20	3

Sample	unit	Rb	Sr	Y	Zr	Nb	Ba	Au	Cu	Zn	Pb
5665	2	48	100	69	252	37	335	17	24	112	14
5676	2	37	59	64	243	31	440	6	4	26	8
5677	2	46	98	72	257	16	443	2	9	26	7
5729	2	32	75	60	237	26	808	2	17	14	8
5732	2	60	42	153	337	33	495	26	58	14	7
5734	2	41	45	65	232	30	450	2	3	13	6
5738	2	43	56	50	228	24	633	9	15	19	7
5772	2	43	121	129	392	41	634	15	58	42	8
5774	2	73	45	114	357	37	394	21	67	13	8
5775	2	37	43	79	368	42	320	19	78	18	11
5779	2	12	56	70	267	31	413	12	14	12	6
5780	2	42	58	149	385	29	159	15	7	12	8
5797	2	41	105	93	333	34	576	38	28	16	8
Maximum		73	121	153	392	42	808	38	78	112	14
Minimum		12	42	50	228	16	159	2	3	12	6
Average		43	69	90	299	32	469	14	29	26	8
Deviation		14	26	34	61	7	159	10	25	26	2

Sample	unit	Rb	Sr	Y	Zr	Nb	Ba	Au	Cu	Zn	Pb
5633	3	48	61	35	206	21	505	18	52	135	13
5639	3	27	170	39	125	19	397	8	50	86	17
5640	3	58	155	11	56	29	431	39	160	48	14
5647	3	68	74	34	129	25	520	8	65	80	16
5648	3	39	123	19	134	23	488	6	22	50	12
5653	3	23	174	0	45	22	424	9	110	84	13
5656	3	56	61	0	46	29	442	30	102	510	20
5664	3	36	110	15	56	19	342	36	70	86	21
5669	3	12	145	13	73	33	188	12	208	99	19
5675	3	28	102	18	61	18	426	24	80	71	15
5681	3	22	120	5	64	19	139	17	156	95	23
5730	3	26	173	30	121	25	303	2	44	95	16
5731	3	40	156	44	210	28	706	16	28	67	13
5737	3	22	177	29	131	20	387	10	111	42	15
5745	3	24	147	28	97	12	280	13	74	34	12

Sample	unit	Rb	Sr	Y	Zr	Nb	Ba	Au	Cu	Zn	Pb
5746	3	11	156	23	83	14	478	14	195	29	16
5747	3	38	157	66	256	20	407	19	95	38	12
5771	3	41	250	28	80	17	307	11	22	18	7
5773	3	36	139	26	102	18	255	19	157	24	8
5783	3	37	295	46	144	30	435	47	17	22	10
5825	3	5	184	45	127	0	223	15	73	13	10
5826	3	75	119	0	44	0	461	26	192	23	10
5850	3	59	165	5	52	5	681	12	5	12	9
Maximum		75	295	66	256	33	706	47	208	510	23
Minimum		5	61	0	44	0	139	2	5	12	7
Average		36	148	24	106	19	401	18	91	77	14
Deviation		18	52	17	56	9	135	11	60	98	4

Sample	unit	Rb	Sr	Y	Zr	Nb	Ba	Au	Cu	Zn	Pb
5570	4F	62	76	79	256	36	1480	43	16	52	8
5572	4F	53	28	13	127	20	839	393	444	92	12
5573	4F	75	41	75	268	34	1480	0	343	28	6
5576	4F	52	13	5	45	22	595	0	581	46	12
5577	4F	50	22	13	67	20	460	245	66	41	15
5578	4F	105	19	53	275	33	873	78	15	23	5
5615	4F	39	147	45	216	13	507	13	13	14	10
5727	4F	22	163	27	218	24	365	11	4	12	10
5744	4F	66	57	54	215	23	1420	30	23	76	16
5819	4F	110	79	31	265	13	781	770	517	33	7
5820	4F	65	121	12	284	36	630	8	4	5	8
5823	4F	35	62	26	119	24	374	840	29	30	10
5824	4F	78	41	42	287	5	599	70	76	36	7
5835	4F	59	162	43	191	34	755	10	22	40	11
5836	4F	74	22	35	244	31	1400	46	8	6	7
5859	4F	44	65	37	221	23	826	7	4	4	7
5860	4F	40	74	26	100	34	316	18	105	37	10
5864	4F	27	161	47	210	22	394	8	5	5	7
5871	4F	104	31	43	281	30	701	180	45	18	9
5894	4F	52	101	31	208	13	813	5	3	3	5
67909	4F	0	85	37	228	0	343	6	7	87	0
Maximum		110	163	79	287	36	1480	840	581	92	16
Minimum		0	13	5	45	0	316	0	3	3	0
Average		58	75	37	206	23	760	132	111	33	9
Deviation		27	49	19	71	10	375	238	181	26	3

Sample	unit	Rb	Sr	Y	Zr	Nb	Ba	Au	Cu	Zn	Pb
5571	4S	81	167	38	284	37	1080	26	14	10	3
5574	4S	62	72	35	259	15	1450	21	14	10	4
5575	4S	64	57	67	234	42	1780	83	15	15	5
5579	4S	36	336	44	279	35	445	33	8	11	3
5858	4S	19	82	67	232	24	538	6	4	4	4
5862	4S	15	438	60	199	10	175	15	52	3	6
5863	4S	31	199	46	239	983	501	13	17	12	4
5869	4S	68	44	49	198	28	839	144	6	3	5
5870	4S	34	385	29	280	31	325	9	3	7	3
5883	4S	20	126	46	179	5	241	11	46	12	8
5887	4S	14	118	46	272	34	146	16	6	2	5
Maximum		81	438	67	284	983	1780	144	52	15	8
Minimum		14	44	29	179	5	146	6	3	2	3
Average		40	184	48	241	113	684	34	17	8	5
Deviation		23	133	12	35	275	518	40	16	4	1

Sample	unit	Rb	Sr	Y	Zr	Nb	Ba	Au	Cu	Zn	Pb
5564	5	72	44	5	76	29	615	91	130	740	32
5565	5	73	52	43	144	22	451	9	43	65	18
5566	5	66	28	5	170	29	197	30	57	490	15
5567	5	32	20	22	149	25	376	26	178	200	16
5585	5	73	72	0	90	0	759	16	65	294	24
5586	5	55	61	0	96	15	454	14	50	93	14
5587	5	88	37	19	77	21	668	80	111	4000	30
5588	5	70	52	21	144	30	595	22	87	400	15
5589	5	71	152	22	177	17	667	13	8	78	15
5590	5	110	94	20	96	20	722	14	45	105	17
5591	5	71	127	11	86	17	611	14	17	64	15
5592	5	117	56	12	109	23	707	15	137	3070	29
5597	5	59	116	26	182	21	452	20	36	194	21

Sample	unit	Rb	Sr	Y	Zr	Nb	Ba	Au	Cu	Zn	Pb
5598	5	24	138	58	215	21	386	15	46	161	16
5599	5	67	74	42	162	37	628	12	43	220	19
5603	5	57	124	47	164	33	468	35	25	67	25
5604	5	35	178	0	38	0	187	56	194	46	16
5605	5	55	162	24	134	25	382	8	74	42	15
5606	5	44	158	0	67	25	353	9	298	55	16
5609	5	53	260	22	59	20	347	12	60	30	16
5612	5	80	162	0	76	13	472	30	60	147	66
5613	5	42	232	17	87	22	164	15	40	65	32
5614	5	30	139	22	135	25	388	36	60	95	28
5619	5	59	69	42	203	25	538	22	14	52	20
5620	5	56	166	20	75	21	783	72	105	160	23
5621	5	73	109	16	131	28	661	14	65	43	18
5624	5	33	292	14	44	24	248	90	96	70	11
5625	5	91	11	20	167	27	763	10	26	54	22
5630	5	141	94	48	214	20	748	21	42	11	7
5631	5	32	78	27	136	12	282	22	40	36	10
5632	5	64	66	41	209	28	417	10	22	70	14
5636	5	78	280	56	237	25	436	7	17	44	12
5637	5	62	63	37	132	11	521	7	50	119	18
5638	5	75	44	19	62	24	556	10	108	144	40
5641	5	20	100	12	57	25	153	8	125	90	14
5644	5	83	228	17	64	17	371	45	147	31	12
5645	5	56	74	23	129	16	487	9	35	113	15
5646	5	61	234	0	45	0	429	10	95	66	17
5652	5	31	236	22	69	21	250	20	75	71	20
5655	5	32	112	37	112	21	407	22	7	146	16
5661	5	95	33	21	54	16	401	42	11	52	19
5662	5	120	108	37	143	21	796	56	72	378	17
5663	5	59	183	17	91	0	503	55	8	57	16
5668	5	65	141	35	165	18	579	11	48	67	20
5678	5	12	218	37	160	38	958	13	8	40	16
5679	5	12	139	33	135	17	368	57	103	32	13
5682	5	42	74	36	151	28	405	17	60	82	17
5685	5	72	75	11	119	31	536	60	60	91	15
5686	5	79	41	24	198	19	287	9	21	34	17
5688	5	81	183	36	191	16	1100	2	31	44	110
5689	5	111	27	38	228	29	611	15	22	62	32
5690	5	43	200	78	256	18	567	7	5	25	14
5692	5	34	98	10	50	19	174	16	86	122	39
5693	5	100	38	40	184	20	571	246	57	310	50
5694	5	40	117	36	155	25	361	56	74	50	17
5696	5	80	94	43	209	23	577	18	10	113	61
5697	5	58	119	45	207	12	706	20	40	38	18
5698	5	40	160	25	138	31	258	16	140	56	18
5699	5	90	91	45	228	31	2210	88	73	44	13
5702	5	86	51	28	148	5	518	22	20	182	40
5703	5	50	91	37	142	32	438	13	70	102	16
5705	5	80	115	5	56	12	435	13	82	145	42
5706	5	100	32	40	178	34	537	15	31	100	34
5707	5	40	142	35	111	14	337	45	83	108	16
5711	5	118	19	37	153	18	728	35	36	92	40
5712	5	75	72	43	191	18	571	20	40	54	20
5713	5	51	229	0	33	14	428	17	6	29	17
5715	5	71	121	10	59	0	281	16	89	172	33
5716	5	66	98	32	127	32	506	21	56	115	26
5717	5	44	102	63	264	25	531	9	10	28	14
5719	5	114	202	24	230	25	1120	8	31	46	16
5720	5	102	77	26	161	24	597	10	12	117	18
5721	5	66	120	53	209	21	691	31	38	28	10
5722	5	54	84	31	132	29	648	12	61	37	20
5725	5	89	13	20	173	38	406	27	31	72	37
5726	5	41	109	43	195	37	363	11	80	64	16
5728	5	29	107	10	62	23	1210	10	125	33	14
5742	5	74	36	30	137	11	297	7	35	46	16
5743	5	43	137	56	185	13	331	10	57	45	18
5748	5	37	165	21	133	25	381	37	58	35	15
5749	5	32	227	29	124	18	326	50	24	21	15
5806	5	45	162	37	183	20	367	71	38	102	16
5807	5	19	135	53	197	23	765	26	23	8	6
5808	5	5	314	28	232	19	545	40	29	6	5
5816	5	84	88	26	147	28	374	5	28	35	10
5817	5	74	158	5	164	25	467	22	18	6	4
5818	5	65	41	11	40	29	470	435	8	13	13
5821	5	41	72	34	140	20	276	7	28	44	10
5822	5	49	72	22	161	24	878	8	26	36	10
5830	5	67	160	21	116	25	689	11	48	63	20
5831	5	54	31	5	133	27	710	65	91	30	11
5832	5	108	125	19	131	31	492	36	10	58	13
5833	5	47	286	60	128	33	208	9	16	9	11

Sample	unit	Rb	Sr	Y	Zr	Nb	Ba	Au	Cu	Zn	Pb
5834	5	61	127	21	98	35	561	10	48	100	23
5837	5	40	147	43	202	27	277	77	152	20	10
5842	5	55	78	31	142	16	336	7	29	40	9
5855	5	51	64	28	161	22	314	20	40	47	11
5856	5	17	381	39	220	18	314	9	13	7	5
5857	5	30	89	53	217	27	679	16	21	70	10
5865	5	25	176	17	58	25	315	42	119	29	9
5868	5	28	121	17	145	25	791	11	52	18	9
5876	5	5	108	11	36	26	153	10	72	51	15
5878	5	5	352	14	26	14	61	11	90	45	14
5879	5	5	318	16	17	19	114	10	81	35	12
5880	5	12	189	48	195	16	487	16	108	63	11
5881	5	51	114	32	29	26	625	26	116	40	13
5882	5	54	390	33	278	20	447	5	29	27	11
5884	5	25	150	58	208	27	359	18	70	78	14
5886	5	5	152	0	51	25	112	15	94	46	13
67911	5	0	56	43	203	0	603	7	22	150	0
67912	5	0	37	4	223	0	663	10	25	70	0
67913	5	0	39	38	172	0	608	795	18	16	0
67914	5	0	63	42	194	0	722	2	15	120	0
67915	5	0	33	46	260	0	684	49	12	21	0
67916	5	0	30	44	244	0	212	871	18	9	0
67917	5	0	75	16	181	0	214	611	1260	11	0
67918	5	0	49	39	149	0	823	1930	7280	125	0
67919	5	0	170	22	207	0	713	904	211	200000	0
67920	5	0	165	19	226	0	1149	24	56	100	0
67922	5	0	93	28	166	0	727	81	29	259	0
67923	5	0	54	15	125	0	806	486	91	104	0
Maximum		141	390	78	278	38	2210	1930	7280	200000	110
Minimum		0	11	0	17	0	61	2	5	6	0
Average		52	122	28	143	20	519	75	128	1798	18
Deviation		32	79	16	61	10	270	227	664	18099	14

Sample	unit	Rb	Sr	Y	Zr	Nb	Ba	Au	Cu	Zn	Pb
5501	6	38	106	27	156	39	898	5	28	70	13
5502	6	76	159	40	275	35	986	2	15	14	7
5503	6	118	254	43	270	21	1550	2	35	10	12
5546	6	94	184	33	271	22	443	22	50	32	13
5568	6	95	200	14	139	23	751	18	11	18	5
5569	6	91	77	5	123	36	1060	5	8	14	5
5602	6	93	5	16	147	23	514	840	16	120	13
5607	6	84	312	37	196	26	631	5	34	54	14
5618	6	76	82	16	173	25	531	13	12	44	12
5623	6	100	230	38	276	17	924	10	28	32	13
5626	6	16	124	22	138	30	621	5	9	31	8
5627	6	57	144	14	164	28	1180	8	7	23	6
5629	6	39	213	22	125	30	543	5	9	10	6
5634	6	68	181	0	158	28	906	6	6	19	7
5635	6	31	131	0	160	17	511	8	7	13	5
5642	6	31	139	0	158	20	727	5	9	23	5
5643	6	85	91	14	130	24	957	6	6	9	6
5649	6	73	144	19	178	19	918	13	6	22	7
5650	6	113	162	15	142	22	1040	18	12	11	10
5651	6	71	90	23	190	23	547	75	47	237	286
5654	6	75	25	5	121	20	502	42	52	1070	113
5657	6	54	117	24	155	15	692	12	17	20	9
5658	6	47	146	16	155	19	836	15	13	26	10
5659	6	95	138	16	96	20	753	9	6	20	8
5660	6	75	312	31	220	37	1090	18	20	27	9
5666	6	110	158	11	201	29	1110	19	8	32	12
5667	6	73	254	0	155	28	675	21	8	19	10
5684	6	93	155	0	142	31	1100	2	13	15	25
5687	6	88	184	32	274	21	878	2	33	17	13
5691	6	95	259	32	274	21	863	7	28	28	16
5695	6	101	180	32	277	41	799	9	35	15	12
5700	6	87	173	39	270	13	773	5	38	25	15
5701	6	113	91	36	270	19	840	15	19	22	17
5704	6	101	140	26	266	17	704	13	42	31	18
5708	6	86	93	13	131	23	774	15	6	7	11
5709	6	97	129	42	270	27	743	14	32	26	14
5710	6	50	213	57	194	23	1120	10	15	15	12
5714	6	99	205	22	246	22	979	10	25	24	17
5718	6	133	134	22	282	18	929	12	30	27	17
5723	6	104	188	32	258	18	1030	7	31	21	15
5724	6	50	189	40	255	0	1180	7	25	6	30
5740	6	82	63	18	259	26	716	8	28	17	10
5741	6	74	119	38	280	20	898	6	41	16	11

Sample	unit	Rb	Sr	Y	Zr	Nb	Ba	Au	Cu	Zn	Pb
5815	6	83	219	38	248	0	742	11	48	26	17
5841	6	123	176	40	280	28	1220	8	40	14	13
5843	6	110	122	25	296	27	1010	9	33	14	12
5844	6	112	169	18	266	29	851	6	34	26	14
5845	6	86	164	24	284	20	949	22	27	17	10
5846	6	100	258	31	272	34	805	5	26	23	11
5847	6	119	157	46	258	16	747	8	27	28	13
5848	6	108	266	13	161	23	814	11	10	20	7
5849	6	99	195	21	283	15	800	9	36	31	10
5853	6	64	135	30	277	28	909	8	24	6	11
5854	6	88	156	37	273	28	732	11	31	15	12
5861	6	89	138	31	270	998	782	7	30	19	8
5874	6	83	162	16	290	27	1030	10	26	16	14
5875	6	105	68	31	224	10	492	7	22	28	13
67921	6	0	110	16	196	0	256	20	6	65	0
Maximum		133	312	57	296	998	1550	840	52	1070	286
Minimum		0	5	0	96	0	256	2	6	6	0
Average		83	158	24	215	40	834	26	23	46	18
Deviation		27	63	13	60	127	225	108	13	139	38

Sample	unit	Rb	Sr	Y	Zr	Nb	Ba	Au	Cu	Zn	Pb
5511	11	24	365	27	191	22	361	6	28	17	11
5512	11	5	368	39	214	23	372	6	11	23	14
5513	11	37	291	24	180	31	383	225	430	21	13
5532	11	10	446	30	77	0	340	19	59	30	10
5535	11	5	331	40	127	27	250	16	30	18	8
5765	11	17	428	23	102	21	211	18	43	31	10
5766	11	39	444	23	91	13	373	20	50	25	11
5767	11	15	82	23	92	17	190	17	15	30	10
5768	11	24	444	26	101	21	346	20	12	22	10
5769	11	13	434	45	163	14	449	15	20	19	10
5770	11	35	404	28	187	19	447	19	21	29	13
5784	11	29	171	0	50	15	155	10	14	36	16
5786	11	27	387	58	175	14	633	16	6	19	12
5787	11	20	380	33	181	13	325	42	193	15	17
5811	11	18	430	11	124	28	378	36	36	31	9
5812	11	5	700	19	58	22	238	21	13	23	7
5813	11	5	534	45	112	22	247	24	17	14	7
Maximum		39	700	58	214	31	633	225	430	36	17
Minimum		5	82	0	50	0	155	6	6	14	7
Average		19	391	29	131	19	335	31	59	24	11
Deviation		11	130	13	49	7	113	49	102	6	3

Sample	unit	Rb	Sr	Y	Zr	Nb	Ba	Au	Cu	Zn	Pb
5536	12	42	311	26	212	56	711	14	37	116	18
5580	12	32	181	25	183	27	288	44	18	17	9
5581	12	71	60	34	227	0	890	2	377	27	12
5582	12	21	179	33	158	21	332	21	25	24	11
5583	12	34	217	39	194	28	303	37	9	28	9
5596	12	22	203	34	193	24	264	14	8	17	6
5838	12	45	119	31	185	17	572	25	7	19	16
5866	12	56	84	47	192	5	699	295	16	25	12
5867	12	37	162	42	228	19	458	68	5	13	10
Maximum		71	311	47	228	56	890	295	377	116	18
Minimum		21	60	25	158	0	264	2	5	13	6
Average		40	168	35	197	22	502	58	56	32	11
Deviation		15	71	7	21	15	214	86	114	30	3

Sample	unit	Rb	Sr	Y	Zr	Nb	Ba	Au	Cu	Zn	Pb
5531	13	47	58	33	302	23	535	69	70	47	9
5537	13	62	59	35	285	28	936	106	126	47	10
5538	13	59	64	36	302	16	808	28	24	28	13
5539	13	41	226	50	299	20	523	55	122	15	8
5540	13	100	52	31	316	21	946	2	10	18	9
5541	13	33	68	47	320	24	1090	31	11	16	8
5542	13	80	35	38	291	35	973	42	82	17	7
5543	13	38	61	51	343	30	689	36	28	16	8
5544	13	69	39	27	309	21	867	170	41	15	8
5545	13	53	85	61	302	26	1030	266	16	14	8
5839	13	32	141	18	221	17	777	23	9	135	15
5840	13	69	60	23	301	33	659	50	104	16	9
5851	13	5	210	18	261	34	261	16	21	9	9

Sample	unit	Rb	Sr	Y	Zr	Nb	Ba	Au	Cu	Zn	Pb
5852	13	17	151	42	307	16	435	19	5	10	8
5872	13	16	185	42	239	29	510	17	4	4	6
5873	13	33	181	61	285	30	438	12	3	14	7
5888	13	67	40	45	302	12	875	64	64	14	10
5889	13	17	277	54	192	0	204	15	5	8	10
5890	13	60	74	38	307	25	1250	122	58	6	7
5891	13	52	84	52	299	21	1200	310	5	9	7
5892	13	14	276	44	213	13	416	5	2	7	7
5893	13	47	185	25	210	18	340	18	3	6	10
5895	13	22	174	58	308	31	480	54	4	5	8
5896	13	26	242	38	175	13	163	62	4	10	21
5897	13	54	190	42	212	22	522	228	6	19	8
5898	13	11	370	27	155	30	234	6	2	6	8
5899	13	47	190	49	285	13	319	8	7	16	8
5900	13	5	123	0	106	18	101	66	326	25	10
67901	13	0	136	44	316	0	377	2	3	36	0
67903	13	0	38	20	286	0	949	866	597	418	0
67904	13	0	18	26	181	0	607	10000	17353	588	0
67905	13	0	164	29	317	0	342	1248	118	24	0
67906	13	0	12	25	297	0	993	1106	88	20	0
67908	13	0	89	22	307	0	253	108	163	55	0
67910	13	0	59	31	308	0	438	208	27	21	0
Maximum		100	370	61	343	35	1250	10000	17353	588	21
Minimum		0	12	0	106	0	101	2	2	4	0
Average		34	126	37	270	18	615	441	557	49	7
Deviation		27	86	14	56	11	314	1665	2883	116	4

Sample	unit	Rb	Sr	Y	Zr	Nb	Ba	Au	Cu	Zn	Pb
67902	22		787	18	146	0	305	46	4	293	0
67907	22		892	18	145	0	508	73	33	115	0
Maximum			892	18	146	0	508	73	33	293	0
Minimum			787	18	145	0	305	46	4	115	0
Average			839.5	18	145.5	0	407	60	19	204	0
Deviation			52.5	0	0.5	0	102	14	15	89	0

Analyses of replicate samples

Samples are all of the same composite prepared in the field. Analyses were carried out twice by taking two 2 gram samples of the same pulp.

Sample	Rb		Sr		Y		Zr		Nb		Ba	
	1	2	1	2	1	2	1	2	1	2	1	2
5503	118	98	254	249	43	27	270	280	21	30	1550	1560
5584	104	96	240	252	39	37	277	276	29	33	1530	1490
5600	108	106	230	250	23	31	280	283	18	18	1500	1540
5628	124	113	234	232	15	34	266	280	29	15	1480	1470
5736	109	98	234	221	32	32	259	287	28	30	1520	1500
5814	111	108	307	283	55	26	265	275	25	26	1560	1550
5877	112	96	261	228	32	35	264	275	28	33	1570	1610
Avg.	112	102	251	245	34	32	269	279	25	26	1530	1531
Std.	6.70	6.79	27.03	20.69	13.15	4.07	7.48	4.50	4.35	7.23	32.66	48.11

APPENDIX 3

Electron Microprobe Analyses of Garnets from the Blake River Group

Analyses of garnet grains were carried out at the University of Colorado in Boulder using a JOEL JXA 8600 Superprobe equipped with four spectrometers, and data reductions were carried out, on line, using the Bence-Albee reduction program. Garnet compositions were calculated both on the basis of 24 oxygens and 16 cations.

The analyses were carried out with an excitation voltage of 15 KV, a sample current of 15.0 nanoamps, and a beam diameter of 1 to 2 microns. The standards utilized to calibrate the instrument were:

- Garnet P130 from California Institute of Technology was used to calibrate for Si, Al, Fe, and Mn.
- Apatite from the National History Museum was used to calibrate for Ca.
- Ilmenite from the National History Museum was used to calibrate for Ti.
- Olivine 225 from National History Museum was used to calibrate for Mg .

Sample	gr	dist to core	FeO	MnO	Al_2O_3	MgO	CaO	SiO_2	TiO_2	Total	Andr+Gros	Spes	Almd
A93-80	GR1	0.0	19.23	20.91	20.29	0.73	1.12	38.24	0.14	100.68	2.71	50.68	46.61
A93-80	GR1	5.0	18.40	21.76	20.14	0.72	1.28	38.50	0.12	100.85	3.09	52.51	44.40
A93-80	GR1	7.0	20.11	19.44	20.48	0.84	1.18	37.95	0.08	100.10	2.90	47.73	49.37
A93-80	GR2	0	17.66	21.91	21.70	0.67	1.50	37.76	0.20	101.42	3.65	53.35	43.00
A93-80	GR2	24	17.95	21.81	21.58	0.62	1.45	37.47	0.25	101.16	3.52	52.92	43.56
A93-80	GR2	55	15.42	23.68	21.53	0.51	1.33	37.30	0.18	99.98	3.29	58.57	38.14
A93-80	GR2	84	17.34	23.01	21.68	0.65	1.39	38.15	0.29	102.55	3.33	55.13	41.54
A93-80	GR2	87	15.58	24.28	20.97	0.54	1.44	36.56	0.11	99.51	3.49	58.79	37.72
A93-80	GR2	107	16.18	24.21	21.03	0.57	1.47	36.55	0.14	100.19	3.51	57.84	38.65
A93-80	GR2	124	16.98	22.97	20.99	0.60	1.34	36.77	0.14	99.81	3.25	55.63	41.12
A93-80	GR2	146	18.45	21.91	20.68	0.68	1.11	37.13	0.06	100.04	2.68	52.83	44.49
A93-80	GR2	176	21.57	17.10	21.26	0.87	2.25	38.30	0.07	101.45	5.50	41.79	52.71
A93-80	GR2	191	21.06	17.16	21.06	0.83	2.28	36.63	0.07	99.12	5.63	42.37	52.00
A93-80	GR2	0	17.66	21.91	21.70	0.67	1.50	37.76	0.20	101.42	3.65	53.35	43.00
A93-80	GR2	25	17.27	23.02	20.71	0.60	1.43	37.21	0.20	100.47	3.43	55.18	41.40
A93-80	GR2	55	17.69	23.09	20.82	0.60	1.19	37.18	0.15	100.74	2.84	55.02	42.15
A93-80	GR2	88	17.68	22.70	20.49	0.62	1.12	37.11	0.14	99.98	2.70	54.70	42.60
A93-80	GR2	115	17.21	22.52	20.59	0.54	0.98	35.82	0.07	97.75	2.41	55.32	42.27
A93-80	GR3	24	18.17	22.76	20.28	0.55	1.03	36.02	0.11	98.95	2.45	54.24	43.30
A93-80	GR3	29	17.61	21.87	21.98	0.59	1.10	33.11	0.10	96.39	2.71	53.89	43.40
A93-80	GR3	80	19.56	21.69	20.77	0.65	1.08	34.97	0.11	98.86	2.55	51.24	46.21
A93-80	GR3	117	21.05	18.74	20.97	0.74	2.37	34.68	0.11	98.69	5.62	44.45	49.93
A93-80	GR4	0	15.29	24.05	21.93	0.64	1.66	36.52	0.11	100.23	4.05	58.66	37.29
A93-80	GR4	19	17.68	23.89	21.52	0.63	1.48	37.00	0.12	102.35	3.44	55.49	41.07
A93-80	GR4	40	18.45	22.78	21.21	0.63	1.28	37.33	0.12	101.83	3.01	53.59	43.40
A93-80	GR4	74	20.14	21.51	20.70	0.77	1.05	35.43	0.11	99.74	2.46	50.37	47.17
A93-80	GR4	105	21.74	18.33	22.02	0.81	2.10	37.69	0.03	102.74	4.98	43.47	51.55
A93-80	GR4	0	15.29	24.05	21.93	0.64	1.66	36.52	0.11	100.23	4.05	58.66	37.29
A93-80	GR4	20	16.05	24.04	22.08	0.65	1.52	38.06	0.10	102.53	3.65	57.77	38.57
A93-80	GR4	45	16.71	23.63	21.87	0.63	1.40	38.11	0.11	102.48	3.35	56.61	40.03
A93-80	GR4	85	19.93	21.62	21.74	0.76	1.03	38.27	0.12	103.50	2.42	50.78	46.81
A93-80	GR4	112	21.46	17.60	22.05	0.80	2.14	37.66	0.02	101.77	5.19	42.72	52.09

Sample	gr	dist to core	FeO	MnO	Al_2O_3	MgO	CaO	SiO_2	TiO_2	Total	Andr+Gros	Spes	Almd
A93-80	GR5	0	17.13	23.65	20.98	0.58	1.00	36.53	0.19	100.08	2.39	56.61	41.00
A93-80	GR5	53	15.97	24.26	21.00	0.47	1.10	37.33	0.32	100.50	2.66	58.70	38.64
A93-80	GR5	293	18.59	23.10	21.42	0.60	1.10	37.88	0.18	102.90	2.57	53.98	43.44
A93-80	GR5	418	21.07	17.33	21.42	0.82	3.09	37.26	0.30	101.32	7.45	41.77	50.78
A93-80	GR5	0	17.13	23.65	20.98	0.58	1.00	36.53	0.19	100.08	2.39	56.61	41.00
A93-80	GR5	87	16.29	24.64	21.04	0.51	1.06	36.55	0.07	100.19	2.52	58.68	38.79
A93-80	GR5	174	18.18	22.23	20.77	0.71	0.82	36.77	0.10	99.61	1.99	53.92	44.09
A93-80	GR6	0	17.87	23.33	20.81	0.56	1.07	37.25	0.08	100.99	2.53	55.19	42.28
A93-80	GR6	0	17.06	23.20	20.83	0.65	1.06	37.07	0.07	99.96	2.57	56.15	41.29
A93-80	GR6	4	17.88	23.24	20.32	0.61	1.01	37.02	0.10	100.21	2.40	55.16	42.44
A93-80	GR6	5	17.49	23.04	20.60	0.60	0.98	36.19	0.10	99.04	2.36	55.50	42.13
A93-80	GR6	11	17.87	23.74	21.35	0.58	0.99	37.73	0.10	102.39	2.32	55.73	41.95
A93-80	GR6	133	19.14	21.70	20.74	0.60	1.56	37.70	0.06	101.54	3.68	51.18	45.14
A93-80	GR7	0	13.61	27.11	20.46	0.61	1.89	36.91	0.15	100.74	4.44	63.62	31.94
A93-80	GR7	29	13.26	27.61	20.46	0.56	1.99	36.40	0.24	100.53	4.64	64.42	30.94
A93-80	GR7	156	16.92	23.75	20.37	0.66	1.29	37.17	0.09	100.25	3.07	56.60	40.32
A93-80	GR7	312	19.76	20.85	20.48	0.81	1.30	36.38	0.08	99.67	3.10	49.75	47.15
A93-80	GR7	382	21.06	18.03	20.29	0.88	2.91	36.09	0.04	99.31	6.93	42.93	50.14
A93-80	GR8	0	17.42	23.60	21.45	0.62	0.89	35.36	0.15	99.48	2.12	56.31	41.57
A93-80	GR8	48	18.94	23.30	20.97	0.70	1.04	36.94	0.23	102.12	2.40	53.84	43.76
A93-80	GR8	199	20.64	18.69	21.09	0.89	2.41	37.20	0.09	101.00	5.77	44.78	49.45
A93-80	GR9	0	19.54	21.81	20.23	0.76	1.17	36.11	0.21	99.84	2.75	51.29	45.95
A93-80	GR9	194	20.62	17.85	20.69	0.87	3.26	36.90	0.08	100.27	7.81	42.77	49.41
A93-80	GR9	0	19.54	21.81	20.23	0.76	1.17	36.11	0.21	99.84	2.75	51.29	45.95
A93-80	GR9	149	20.64	18.04	20.51	0.89	3.02	36.11	0.15	99.35	7.24	43.26	49.50
A94-25	GR1	0	20.09	16.09	20.65	1.26	4.79	37.67	0.03	100.60	11.69	39.27	49.04
A94-25	GR1	74	20.93	15.56	21.32	1.31	4.95	38.85	0.02	102.97	11.94	37.55	50.51
A94-25	GR1	25	20.61	15.55	21.53	1.25	5.07	38.14	0.05	102.23	12.30	37.72	49.99
A94-25	GR1	119	21.14	15.85	21.81	1.22	4.04	38.53	0.01	102.62	9.85	38.63	51.52
A94-25	GR2	0	17.19	18.45	21.96	1.30	4.43	39.05	0.05	102.47	11.06	46.04	42.90
A94-25	GR2	281	16.65	18.83	21.83	1.20	5.37	38.55	0.15	102.62	13.15	46.10	40.76
A94-25	GR2	452	17.07	19.01	21.48	0.94	5.44	38.40	0.13	102.51	13.10	45.79	41.11
A94-25	GR2	954	20.65	15.15	20.91	1.18	4.34	37.74	0.05	100.04	10.81	37.74	51.44
A94-25	GR3	0	15.35	20.18	21.81	0.85	5.33	38.21	0.09	101.85	13.04	49.39	37.57
A94-25	GR4	0	17.01	20.16	19.91	0.99	5.21	36.26	0.12	99.66	12.29	47.57	40.14
A94-25	GR4	156	16.83	20.14	19.97	1.00	5.02	36.45	0.03	99.44	11.96	47.96	40.08
A94-25	GR4	381	17.58	19.45	19.92	1.05	5.26	36.42	0.15	99.83	12.44	45.99	41.57
A94-25	GR4	466	20.67	16.30	19.89	1.35	4.66	36.21	0.00	99.07	11.19	39.15	49.65
A94-25	GR5	0	16.00	20.68	19.67	1.03	4.95	36.63	0.01	99.12	11.89	49.68	38.43
A94-25	GR5	286	15.29	19.80	20.43	1.00	5.02	36.32	0.13	97.99	12.52	49.36	38.12
A94-25	GR5	755	16.39	20.51	19.52	0.93	5.54	36.60	0.04	99.53	13.05	48.33	38.62
A94-25	GR5	113	16.58	20.10	19.79	0.95	5.24	36.56	0.06	99.30	12.50	47.95	39.55
A94-25	GR5	309	19.95	17.09	19.90	1.24	4.69	36.90	0.06	99.84	11.24	40.95	47.81
A94-55	GR1	0	17.97	19.95	19.57	1.45	4.30	36.11	0.19	99.55	10.18	47.25	42.56
A94-55	GR1	102	19.37	17.63	19.69	1.54	4.33	36.79	0.08	99.43	10.48	42.66	46.87
A94-55	GR1	125	21.29	16.97	19.91	1.44	3.59	36.36	0.13	99.70	8.58	40.55	50.87
A94-55	GR1 s	0	17.51	19.04	19.87	1.39	5.52	36.05	0.23	99.61	13.12	45.26	41.62
A94-55	GR1 s	45	17.99	19.09	19.69	1.38	5.17	36.36	0.18	99.87	12.24	45.18	42.58
A94-55	GR1 s	76	18.52	19.46	19.99	1.51	4.15	36.45	0.11	100.19	9.85	46.19	43.96
A94-55	GR1 s	88	18.46	19.19	19.82	1.54	4.17	36.16	0.16	99.50	9.97	45.89	44.14
A94-55	GR2	0	17.70	19.47	19.49	1.42	4.36	36.40	0.21	99.04	10.50	46.88	42.62
A94-55	GR2	75	17.52	20.17	19.85	1.40	3.89	36.60	0.21	99.64	9.36	48.51	42.14
A94-55	GR2	224	19.15	18.85	19.81	1.57	4.35	35.95	0.16	99.82	10.27	44.51	45.22
A94-55	GR2	376	21.86	16.85	19.95	1.40	3.41	35.99	0.09	99.56	8.10	40.00	51.90
A94-55	GR3	0	18.93	18.96	19.77	1.52	4.03	37.22	0.18	100.61	9.61	45.23	45.16
A94-55	GR3	98	18.65	19.03	19.77	1.57	4.22	36.67	0.22	100.13	10.07	45.42	44.51
A94-55	GR3	185	19.39	18.15	19.81	1.56	4.36	37.16	0.19	100.62	10.41	43.32	46.28
A94-55	GR3	232	21.29	16.79	19.72	1.19	3.70	36.38	0.11	99.19	8.86	40.19	50.96
A94-55	GR3	232	21.09	16.56	19.73	1.32	3.75	37.03	0.07	99.55	9.06	40.00	50.94
A94-76	GR1	0	15.60	24.46	19.50	0.77	2.82	36.94	0.05	100.14	6.58	57.04	36.38
A94-76	GR1	199	14.98	24.41	19.73	0.57	3.19	36.45	0.20	99.53	7.49	57.33	35.18
A94-76	GR1	317	14.49	25.00	19.68	0.58	3.50	37.02	0.07	100.33	8.14	58.15	33.71
A94-76	GR1	524	14.91	24.83	19.77	0.58	3.60	36.55	0.03	100.28	8.31	57.29	34.40
A94-76	GR1	764	21.41	16.29	19.86	1.18	4.77	36.73	0.05	100.29	11.23	38.36	50.41
A94-76	GR2	0	15.01	24.90	19.68	0.61	3.18	36.65	0.07	100.11	7.38	57.79	34.83
A94-76	GR2	157	18.36	21.03	19.65	0.96	3.48	36.75	0.22	100.49	8.12	49.06	42.83
A94-76	GR2	489	24.43	13.05	20.18	1.31	3.50	37.14	0.00	99.61	8.54	31.84	59.61
A94-76	GR3	0	17.32	20.98	19.75	0.74	4.50	36.77	0.13	100.20	10.51	49.02	40.47
A94-76	GR3	255	19.71	17.70	19.80	1.03	5.01	37.01	0.13	100.39	11.81	41.73	46.46
A94-76	GR3	523	24.27	13.96	20.10	1.10	3.32	37.38	0.00	100.14	7.99	33.60	58.41
A94-09	GR1	0	15.62	22.00	20.03	1.31	4.55	37.43	0.19	101.13	10.79	52.17	37.04
A94-09	GR1	177	16.17	22.40	20.34	1.39	4.10	37.13	0.10	101.62	9.61	52.50	37.90
A94-09	GR1	300	15.82	22.49	20.32	1.31	4.32	37.32	0.13	101.71	10.13	52.76	37.11
A94-09	GR1	460	17.91	20.43	20.14	1.28	4.06	35.15	0.05	101.02	9.58	48.18	42.24
A94-09	GR2	0	16.11	21.65	20.10	1.43	4.74	37.46	0.12	101.60	11.15	50.94	37.91
A94-09	GR2	77	16.36	21.40	20.29	1.39	4.63	37.44	0.11	101.62	10.92	50.48	38.59
A94-09	GR2	187	16.08	22.35	20.36	1.38	4.19	37.08	0.00	101.44	9.83	52.44	37.73
A94-09	GR2	277	16.71	21.59	20.14	1.44	4.09	36.73	0.13	101.84	9.65	50.93	39.42
A94-09	GR2	343	17.30	20.91	20.07	1.18	3.99	36.74	0.00	100.19	9.45	49.55	41.00

Sample	gr	dist to core	FeO	MnO	Al_2O_3	MgO	CaO	SiO_2	TiO_2	Total	Andr+Gros	Spes	Almd
A94-09	GR3	0	16.30	20.16	19.09	1.11	5.33	34.58	3.66	100.23	12.75	48.24	39.00
A94-09	GR3	279	16.82	21.82	20.12	1.28	3.54	36.70	0.33	100.61	8.39	51.73	39.88
A94-09	GR3	301	16.33	21.79	20.23	1.40	3.98	36.81	0.08	100.63	9.45	51.76	38.79
A94-09	GR3	309	17.37	20.51	20.19	1.18	3.85	36.66	0.13	99.88	9.23	49.15	41.62
A94-09	GR4	0	15.78	21.44	20.12	1.33	4.48	37.03	0.12	100.30	10.74	51.41	37.84
A94-09	GR4	77	15.68	22.18	20.09	1.37	4.50	36.79	0.12	100.73	10.62	52.36	37.02
A94-09	GR4	182	15.73	21.74	20.18	1.41	4.05	36.92	0.11	100.13	9.75	52.36	37.89
A94-09	GR4	222	17.01	20.54	19.95	1.28	4.00	36.59	0.03	99.41	9.63	49.43	40.94
A94-09	GR5	0	14.69	23.30	20.08	1.25	4.01	36.40	0.22	99.94	9.55	55.48	34.98
A94-09	GR5	10	14.58	23.40	20.01	1.26	3.97	36.84	0.10	100.17	9.46	55.78	34.76
A94-09	GR5	175	15.07	22.73	20.24	1.31	4.25	36.58	0.12	100.30	10.11	54.05	35.84
A94-09	GR5	194	15.99	22.47	20.03	1.27	4.19	36.54	0.12	100.59	9.82	52.68	37.49
A94-09	GR5	282	15.88	21.75	20.17	1.28	4.44	36.69	0.13	100.34	10.55	51.70	37.75
A94-09	GR5	375	17.06	20.51	20.04	1.15	4.11	36.55	0.05	99.47	9.86	49.21	40.93
A94-51	GR1	0	7.35	20.22	20.61	1.42	4.42	36.73	0.17	100.90	13.82	63.21	22.98
A94-51	GR1	112	19.59	18.30	20.36	1.56	4.19	36.54	0.43	100.96	9.96	43.49	46.55
A94-51	GR1	220	19.28	18.35	20.53	1.63	3.85	36.19	0.15	99.98	9.28	44.24	46.48
A94-51	GR1	324	23.66	14.60	20.65	1.68	2.49	37.14	0.03	100.25	6.11	35.83	58.06
A94-51	GR2	0	17.69	19.82	20.53	1.49	4.05	36.66	0.25	100.48	9.74	47.69	42.56
A94-51	GR2	111	18.32	19.88	20.77	1.50	3.78	37.14	0.18	101.58	9.00	47.36	43.64
A94-51	GR2	197	20.02	18.07	20.59	1.68	3.26	36.74	0.15	100.50	7.88	43.70	48.42
A94-51	GR2	333	24.21	14.47	20.73	1.58	2.39	36.03	0.09	99.49	5.82	35.23	58.95
A94-51	GR2	0	17.69	19.82	20.53	1.49	4.05	36.66	0.25	100.48	9.74	47.69	42.56
A94-51	GR2	244	23.40	15.15	20.37	2.05	2.56	35.90	0.06	99.48	6.23	36.85	56.92
A94-51	GR3	0	23.10	15.55	20.79	2.22	2.59	36.44	0.10	100.79	6.28	37.71	56.01
A94-51	GR3	276	18.84	19.14	20.61	1.52	3.59	36.84	0.18	100.73	8.64	46.04	45.32
A94-51	GR3	453	22.67	15.87	21.01	2.09	2.58	36.91	0.09	101.21	6.27	38.59	55.13
A94-51	GR3	526	23.90	14.72	20.98	1.77	2.56	37.00	0.03	100.96	6.22	35.75	58.04

Centre de documentation du MER
QER A 080 841